High pressure–low temperature induced structures in dairy foams and protein model systems

Vorgelegt von

Diplom-Ingenieur

Marcus Volkert

von der Fakultät III – Prozesswissenschaften
der Technischen Universität Berlin

zur Erlangung des akademischen Grades
Doktor der Ingenieurwissenschaften
-Dr.-Ing-
genehmigte Dissertation

Promotionsausschuss:
Vorsitzender: Prof. Dr. Dipl.-Ing. Frank-Jürgen Methner
1. Berichter: Prof. Dr. Dipl.-Ing. Dietrich Knorr
2. Berichter: Dr. Max Puaud
Tag der wissenschaftlichen Aussprache: 30.04.2009

Berlin 2009
D-83

Sooner or later God'll cut you down.
- Johnny Cash

Für Bianca und Béla

My special thanks go to my supervisor, Prof. Dr. Dietrich Knorr, for encouraging me to focus on the field of HPLT processing, for his excellent scientific guidance, his consistent confidence and support. I want to express my special gratitude to Dr. Max Puaud, for his outstanding supervision, knowledgeable advises and for being a constant source of help, motivation and inspiration to me. Merci beaucoup Max! Thanks a lot to Prof. Dr. Frank-Jürgen Methner for taking the time to be the chairman of my thesis defence.

I wish to thank the staff from the Néstle PTC in Beauvais and the NRC in Lausanne, who contributed in so many aspects to this work, for their reliable support. I want to express my gratitude to Pierre-Yves Fosseux for his engagement and support in the last period of my work, Dr. Hans-Jürgen Wille for many open discussions, Alina Barniol, Paola Olmos, Béatrice Beilleul, Sylvie Penet and Martine Rouvet for their analytic support and Françoise Peron, who was abundantly helpful in the literature search.

Thanks to the students Ricardo Limp and Nanna Molnit Orum who made a contribution to my work. Particular thanks to Daniel Künzel, for being an extraordinary master student and a trusted co-worker for a long time during this project. Thanks Dän!

I also benefited greatly from all my colleagues and the pleasant working atmosphere at the Department of Food Biotechnology and Food Process Engineering in Dahlem, during my working time and beyond it. Special thank you for encouragement and supportive discussions up from the very beginning to the “high pressure group”, to Dr. Gabriel Urrutia Benet, Dr. Alexander Mathys, Dr. Oliver Schlüter and my long time room mate Dr. Cornelius Luscher. Thank you to Sophie Uhlig, highly supportive in administrative affairs and always in a good temper. Thanks a lot to the permanent technical staff, Irene Hemmerich, Martin Bunzeit and Gisela Martens. I was particularly fortunate to have Stefan Boguslawski for constant assistance and support in all technical issues and as a laid back room mate in the final period of writing this thesis. And of course, thank you to all the other colleagues and students at this institute that are to numerous to be mentioned individually.

This entire work would not have been possible were it not for my friends and my loving family. My sincere gratitude goes to my parents Renate and Konrad Volkert, for their endless trust and for backing me all the way. Thanks to my brother Carsten for being a good friend and someone I could look up to over all the years.
I dearly thank my wife Bianca and my son Béla. Thank you, Bianca, for your love, patience and endless trust, which gave me the fortitude and motivation to finish this work. And thanks to you Béla, for being the most precious gift to me and for always reminding me what’s really important in my life.

List of figures

List of tables

Table of acronyms and symbols

Acronyms

DSC	Differential scanning calorimetry
FPD	Freezing point depression
HP	High pressure
HPLT	High pressure-low temperature
OR	Overrun
PAF	Pressure assisted freezing
PAGE	Polyacrylamide gel electrophoresis
PIC	Pressure induced crystallization
PSF	Pressure shift freezing
PTM	Pressure transmitting medium
SEM	Scanning electron microscopy
SD	Standard deviation
SDS	sodium dodecylsulfate polyacrylamide
SMP	Skim milk powder
TPA	Texture profile analysis
TS	Total solids
TUB	Technische Universitaet Berlin
WP	Whey powder
WPI	Whey protein isolate

Symbols

A	area	$[m^2]$
c_p	specific heat capacity	$[kJ\ kg^{-1}\ K^{-1}]$
E	energy	[J]
F	force	[N]
G	Gibb's free energy	[J]
G´	storage modul	[Pa]
G´´	loss modul	[Pa]
h	specific enthalpy	$[kJ\ kg^{-1}]$
H	enthalpy	[J]
k_H	Henry's Law constant	$[L\ atm\ mol^{-1}]$
k	reaction rate constant	$[s^{-1}]$
K	equilibrium constant	-
L	latent heat	$[J\ kg^{-1}]$
l	length	[m]
m	mass	[kg]
p	pressure	[MPa]
r	radius	[m]
R	universal gas constant	$8.314J\ mol^{-1}\ K^{-1}$
s	thickness	[m]
S	entropy	$[J\ K^{-1}]$
t	time	[s]
T	temperature	[K]
V	volume	$[m^3]$
v	specific volume	$[m^3\ kg^{-1}]$
$V^{\ddagger}$	Activation volume	$[m^3]$
Z	mass fraction	[%]

Greek symbols

α	thermal expansion factor	$[K^{-1}]$
β	isothermal compressibility	$[Pa^{-1}]$
ρ	density	$[kg\ m^{-3}]$
η*	complex viscosity	[Pa s]
σ,γ	surface tension	$[N\ m^{-1}]$
υ	phase transition temperature	[°C]

Zusammenfassung

Schäume sind Bestandteil einer Vielzahl von Lebensmitteln und rücken zunehmend in das Interesse der Lebensmittelindustrie. Bekannte Beispiele für aufgeschäumte Produkte sind Schlag- und Sprühsahne, Eiscreme und Luftschokolade. Die Qualität vieler gefrorener Produkte wird maßgeblich von Größe und Form der während des Verarbeitungsprozesses gebildeten Eiskristalle bestimmt. Neben der Texturzerstörung durch Eiskristallwachstum und damit verbundenen Qualitätsverlusten in pflanzlichen und tierischen Tiefkühlprodukten, wirken sich große Eiskristalle negativ auf die Sensorik von Produkten aus, die im gefrorenen Zustand verzehrt werden. Ein Beispiel hierfür ist die Beeinträchtigung von Sensorik und Textur von Eiscreme. Darüber hinaus beeinflussen Luftblasen in Lebensmittelschäumen die Produktqualität und spielen nicht nur in sensorischer Hinsicht eine wichtige Rolle, sondern tragen maßgeblich zu strukturellen Eigenschaften bei.

In den letzten Jahren zeigt sich ein zunehmender Trend im Verzehr fettreduzierter Lebensmittel. Diesem Trend gerecht zu werden stellt hohe Anforderungen an die Lebensmittelindustrie, da Fette und Öle wichtige qualitätsgebende Inhaltsstoffe für viele hochwertige Produkte darstellen. So tragen sie maßgeblich zur Strukturbildung und Stabilisierung in gefrorenen Lebensmittelschäumen (z.B. Eiscreme) bei. Viele Verbraucher assoziieren mit reduziertem Fettgehalt oft auch reduzierten Geschmack. Dementsprechend ergibt sich die Notwendigkeit verbesserter Produktqualität in diesem Sektor um wachsenden Ansprüchen der Verbraucher gerecht zu werden. Ein wichtiges Ziel in der Entwicklung neuer Produkte ist es demnach Lebensmittelsysteme zu verbessern und neu zu entwickeln, die hohe Ansprüche an Qualität und Textur besser erfüllen.

Hochdruck-Niedertemperatur (HPLT) Behandlungen umfassen Hochdruckprozesse im Niedertemperaturbereich die abhängig von der Prozessführung einen Phasenübergang des Wassers im behandelten Produkt herbeführen können. Entsprechend den von Knorr und Urrutia eingeführten Definitionen, sind die HPLT-Gefrierprozesse das Pressure Shift Freezing (PSF), Pressure Assisted Freezing (PAF) und Pressure induced Crystallization (PIC).

Wissenschaftliche Arbeiten im Bereich der Hochdruck-Niedertemperatur Behandlungen konzentrierten sich bisher weitgehend auf die Entwicklung schonender Gefrierverfahren und auf die Inaktivierung von Mikroorganismen und Enzymen. Durch HPLT Gefrier-Prozesse können Strukturzerstörungen nachweislich vermindert werden und darüber hinaus ermöglichen Hochdruckverfahren die Induzierung neuer funktioneller Eigenschaften in Proteinsystemen. In der Industrie angewendete Hochdruckprozesse beschränken sich bis heute jedoch auf die Pasteurisation und Sterilisation. Gaseinschlüsse in entsprechenden Produkten werden vermieden um Volumenänderungen während der Behandlung so gering wie möglich zu halten.

Ziel dieser Arbeit ist die Untersuchung der Einflüsse verschiedener Prozess- und Produktparameter auf HPLT induzierte Strukturen in aufgeschäumten Emulsionen und Milchprotein Modellsystemen. Von besonderem Interesse war hierbei das Aufzeigen verschiedener Mechanismen und deren Abhängigkeit von Prozessparametern wie Druck, Entspannungsrate und dem Einfluss der sich unter Druck und während der Entspannung bildenden Eiskristalle. Grundlegende Zusammenhänge im Bezug auf funktionelle Inhaltsstoffe wurden Untersucht. Spezielles Interesse galt der Fraktion der Michlproteine. Verschiedene HPLT Verfahren wurden hinsichtlich ihres Potentials untersucht, Eigenschaften von Eiskristallen und funktionellen Inhaltsstoffen zu induzieren, die zur Stabilisierung und Texturierung von milchbasierten Lebensmittelschäumen beitragen. In diesem Zusammenhang wurde eine grundlegende Bewertung von HPLT Prozessen als diskontinuierliches oder kontinuierliche Herstellungsverfahren für gefrorene Lebensmittelschäume vorgenommen und darüber hinaus das Potential von HPLT vorbehandelten Milchproteinen als Inhaltsstoff in konventionell hergestellten Produkten untersucht.

Chapter I Scope and outline

A diverse range of foods are foams and even if not entirely understood, obtain increasing importance as manufacturers seek to exploit the novelty of bubbles as food ingredients (Campbell & Mougeot, 1999). Dairy foams may be defined as products that contain a gaseous phase stabilized in a matrix where a significant proportion of the principal components are of milk origin (Anderson & Brooker, 1988). Well known examples are whipped cream, spray cream, ice cream or foamed chocolates. The quality of many frozen products is highly influenced by the size and shape of the ice crystals formed during the production process (Fennema, 1966; Sanz, de Elvira, Martino, Zaritzky, Otero & Carrasco, 1999). Besides textural damage due to ice crystal growth and resulting quality loss in plant and animal tissue, the presence of large crystals in products that are consumed in the frozen state negatively affects sensory properties. A well known example is the negative impact of large ice crystals on the sensory properties and texture of ice cream and frozen desserts (Marshall, Goff & Hartel, 2003; Clarke, 2004; Drewett & Hartel, 2007). Furthermore the incorporated air cells essentially affect product quality and make a significant contribution to the sensory and structural properties of frozen foams (Marshall et al., 2003; Eisener, Wildmoser & Windhalb, 2005).

For the last decade, there is a growing trend towards increased consumption of reduced-fat products (Robb, Reynolds & Abdel-Ghany, 2007). This trend is highly challenging for the food industry, as fat is an important ingredient to high quality dairy products and plays a key role in the stabilization of frozen dairy foams (Goff, Verespej & Smith, 1999). The general consumer perception is that products labelled as “low fat” or “no fat” do not taste good (Wolfe, 1998). It has been suggested that improvements in product quality for lower fat dairy products are required to deliver the quality expected by consumers (Aime, Arntfield, Malcolmson & Ryland, 2001). In this respect, one of the goals in modifying and developing new products is to provide improvements in the products physical structure to deliver desirable texture.

The field of High Pressure-Low Temperature (HPLT) processing embraces high pressure processes with and without water phase transitions in the subzero temperature domain. According to (Urrutia Benet, Schlüter & Knorr, 2004) and (Knorr, Schlüter & Heinz, 1998) the relevant processes that include liquid to solid water phase transitions under pressure can be summarized as Pressure Shift Freezing (PSF), Pressure Assisted Freezing (PAF) and Pressure induced Crystallization (PIC).

Scientific research in the field of HPLT treatment so far is mostly focused on inactivation of microorganisms and the development of gentile freezing processes to minimize textural damage in plant and animal tissue (Urrutia Benet, 2005; Buggenhout, Grauwet, Loey & Hendrickx, 2007). However, the HPLT technology has proven its potential to positively affect the product texture in the freezing step and moreover, high pressure treatments induce new functional properties in protein systems (Merel-Rausch, Kulozik & Hinrichs, 2007; Urrutia Benet, Arabas, Autio, Brul, Hendrickx, Kakolewski et al., 2007). Today, industrial high pressure processes aim on food pasteurization and sterilization, covering a variety of products with low gas content to minimize volume changes during the process (Mathys, 2008).

The focus of this work was to study the influence of different process and product parameters on high pressure-low temperature induced structures in dairy foams and protein model systems. A profound understanding of the mechanisms induced by different process parameters, such as pressure level, pressure release rate and ice formation under pressure was of central concern. The basic impact on functionally relevant ingredients was investigated, with special respect to the milk protein fraction. The HPLT technology was evaluated regarding its potential to induce and affect properties of ice crystals and functional ingredients of dairy emulsions, which are involved in the stabilization of air cells and the development of

unique product texture. In this respect, HPLT induced functional and textural changes in emulsified aerated and non aerated model systems were investigated and a basic evaluation of the HPLT technology concerning its applicability as a batch or continuous process in frozen food foam processing was performed. Moreover the potential of HPLT treated milk proteins as ingredients for conventionally processed foods was investigated.

[1]Aime, D. B., Arntfield, S. D., Malcolmson, L. J. & Ryland, D. (2001). Textural analysis of fat reduced vanilla ice cream products. *Food Research International*, *34*, 237-246.

[2]Anderson, M. & Brooker, B. E. (1988). Dairy foam. In E. Dickinson & G. Stainsby. *Advances in food emulsions and foams* (pp. 221-255). Elsevier Applied Science, New York.

[3]Buggenhout, S. V., Grauwet, T., Loey, A. V. & Hendrickx, M. (2007). Effect of high-pressure induced ice I/ice III-transition on the texture and microstructure of fresh and pretreated carrots and strawberries. *Food Research International*, *40*, 1276-1285.

[4]Campbell, G. M. & Mougeot, E. (1999). Creation and characterisation of aerated food products. *Trends in Food Science & Technology*, *10*(9), 283-296.

[5]Clarke, C. (2004). *The Science of Ice Cream*. The Royal Society of Chemistry, Cambridge.

[6]Drewett, E. M. & Hartel, R. W. (2007). Ice crystallization in a scraped surface freezer. *Journal of Food Engineering*, *78*, 1060-1066.

[7]Eisener, M. D., Wildmoser, H. & Windhalb, E. J. (2005). Air cell microstructuring in a high viscous ice cream matrix. *Colloids and Surfaces A: Physicochemical and Engineering Aspects*, *263*, 390-399.

[8]Fennema, O. (1966). An over-all view of low temperature food preservation. *Cryobiology*, *3*(3), 197-213.

[9]Goff, H. D., Verespej, E. & Smith, A. K. (1999). A study of fat and air structures in ice cream. *International Dairy Journal*, *9*(11), 817-829.

[10]Knorr, D., Schlüter, O. & Heinz, V. (1998). Impact of high hydrostatic pressure on phase transitions of foods. *Food Technology*, *52*(9), 42-45.

[11]Marshall, R. T., Goff, H. D. & Hartel, R. W. (2003). *Ice Cream*. Kluwer Academic / Plenum Publishers, New York.

[12]Mathys, A. (2008). *Inactivation mechanisms of Geobacillus and Bacillus spores during high pressure thermal sterilization*. PhD thesis, Berlin, Berlin University of Technology, 162.

[13]Merel-Rausch, E., Kulozik, U. & Hinrichs, J. (2007). Influence of pressure release rate and protein concentration on the formation of pressure-induced casein structures. *Journal of Dairy Research*, *74*(03), 283-289.

[14]Robb, C. A., Reynolds, L. M. & Abdel-Ghany, M. (2007). Consumer Preference Among Fluid Milks: Low-Fat vs. High-Fat Milk Consumption in the United States. *International Journal of Consumer Studies*, *31*(1), 90-94.

[15]Sanz, P. D., de Elvira, C., Martino, M., Zaritzky, N., Otero, L. & Carrasco, J. A. (1999). Freezing rate simulation as an aid to reducing crystallization damage in foods. *Meat Science*, *52*(3), 275-278.

[16]Urrutia Benet, G., Schlüter, O. & Knorr, D. (2004). High pressure–low temperature processing. Suggested definitions and terminology. *Innovative Food Science and Emerging Technologies*, *5*(4), 413-427.

[17]Urrutia Benet, G. (2005). *High Pressure Low temperature Processing of Foods: Impact of Metastable Phases on Process and Quality Parameters*. PhD, Berlin University of Technology, 196.

[18]Urrutia Benet, G., Arabas, J., Autio, K., Brul, S., Hendrickx, M., Kakolewski, A., Knorr, D., Le Bail, A., Lille, M., Molina-García, A. D., Ousegui, A., Sanz, P. D., Shen, T. & Van Buggenhout, S. (2007). SAFE ICE: Low-temperature pressure processing of foods: Safety and quality aspects, process parameters and consumer acceptance. *Journal of Food Engineering*, *83*, 293-315.

[19]Wolfe, K. (1998). Consumer Preferences and Low-fat and No-fat Food, Agricultural Development Center.

Chapter II General introduction

1 HP processing in the food industry

1.1 Historical review

Fundamentally, the history of the high pressure technology goes back to the 14th century, when the German monk Berthold Schwarz invented the first known cannon (Kendall, 2000). For several centuries this was the only significant application of high pressure in which the pressure, if only for a short time, is contained in a vessel. During this period the high pressure technology was not truly a technology as we define it today and its progress mostly driven by military interests. In the 19th century the foundation of high pressure vessel design was established as a result of the research activities of Lamé and Clapeyron, who developed the equations for the elastic stress in a thick walled cylinder subjected to internal pressure (Bernard, 1986). Perkins was the first scientist, who conducted research on the compressibility of water and other fluids (Perkins, 1820; 1826). In the late 1890s high pressure equipment was reasonable high developed and first findings about the inactivation of microorganisms in milk were published by Hite, showing extended shelf life of bovine milk after high pressure treatment. 1914 Bridgman reported the coagulation of egg albumin by high pressure and reported different product properties as compared to gels obtained by heat coagulation. Furthermore he presented an extensive data set for the phase diagram of pure water (Bridgman, 1912). Since the early 1980s, high hydrostatic pressure treatment has been evaluated as a food processing alternative to classical heat treatment technologies (Knorr et al., 1998). Decisive for the emerging research effort in this field was the growing consumer demand for minimally processed, fresh-like, safe, high quality food products (Hendrickx & Knorr, 2001).

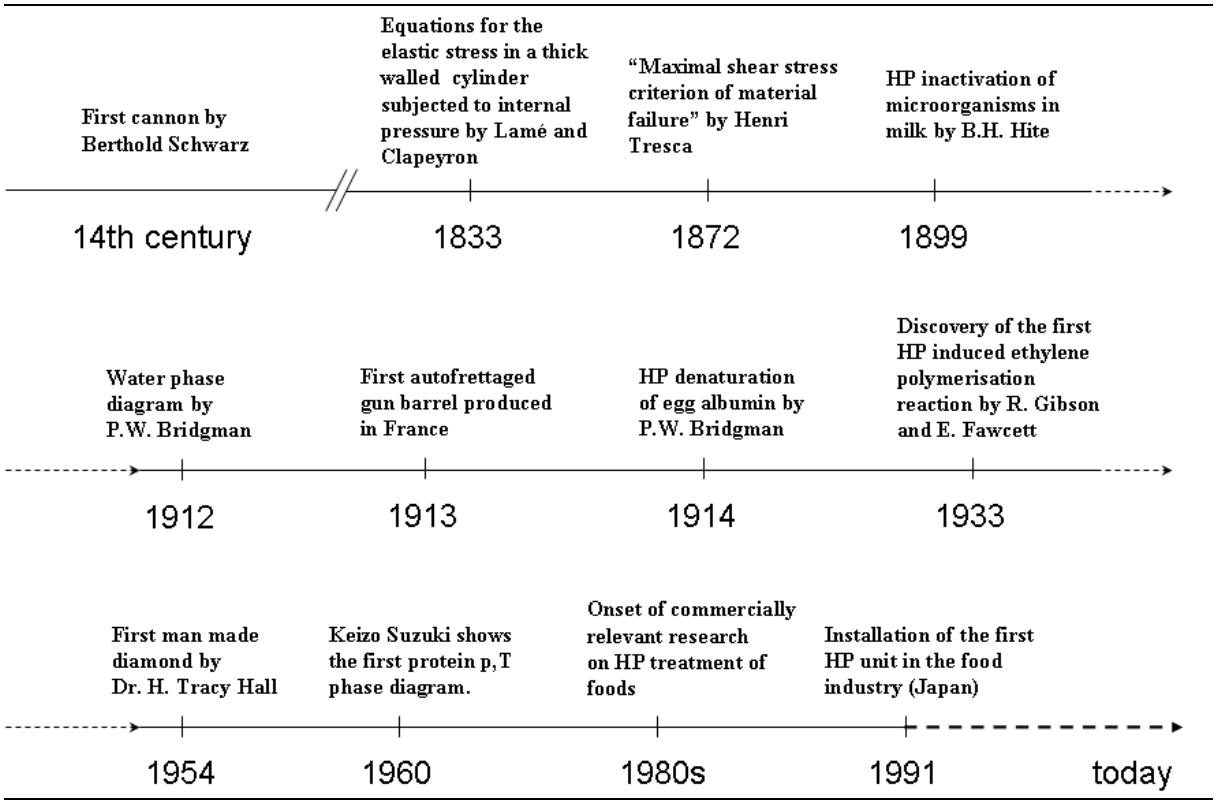

Figure II-1: Milestones in the development of the high pressure technology for the food industry.

Japan was the first country that commenced research of food related high pressure applications with focus on food preservation at moderate temperatures (microbiology, effect on enzymes, texture and colour stability of fruits, vegetables and meat) (Michel, Leser, Syrbe, Clerc, Bauwens, Bovetto et al., 2001). The first HP application in the food industry was installed in 1991 in Japan (Yaldagard, Mortazavi & Tabatabaie, 2008). Figure II-1 gives an overview about the milestones in the development of the high pressure technology. Since the early 1990s, food industry and related research institutes have extensively explored this field and introduced the high pressure technology to a broad range of products. In the late 1990s high-pressure treatment was identified as a potential technology for food texture engineering by specifically influencing food ingredient properties (Michel et al., 2001). Important process goals of high pressure treatment in the food industry today are inactivation of microorganisms and enzymes, quality retention and increasingly the modification of biopolymers and changes in product functionality (Knorr, 1993; Yaldagard et al., 2008). Conventionally, HP processing of foods and food ingredients is applied at mild temperatures to exploit the synergistic effects of pressure and temperature treatments. Extending the field of HP processing into the subzero temperature domain introduced the novel technology of high pressure-low temperature (HPLT) processing, which covers a wide range of process alternatives to conventional freezing and thawing methods (Urrutia Benet, 2005).

1.2 High pressure effects on biomaterials

As for inorganic systems, such as water and air, the state and stability of biomaterials is regulated by an interaction between internal and external parameters. Changing a single parameter in on direction or the other potentially disequilibriates the system and changes its phase or state. Pressure as a basic thermodynamic parameter affects biomolecules and can change the state of molecular organisation (e.g. crystallization of fat or phase changes of phospholipids) (Macdonald, 1992). In food systems this changes can either be positive (e.g. inactivation of microorganisms, gel formation) or negative (texture defects). High Pressure effects are governed by three general principles:

1. *Le Châtelier`s principle*, which states that at equilibrium a system tends to minimize the effect of any external factor by which it is perturbed. Any phenomenon (phase transition, change in molecular configuration, chemical reaction) accompanied by a decrease in volume is enhanced by pressure (and vice versa) (Cheftel, 1995). Consequently an increase in pressure favours reduction of the volume of a system (Mozhaev, Heremans, Frank, Masson & Balny, 1996). In the case of a reaction, pressure will shift equilibrium toward the system with the lowest volume. Moreover, when the activation volume $\Delta V^{\ddagger} < 0$ (partial molar volume, in cm^3 mol-~), that is, when the volume of the activated complex is smaller than that of the initial reactants, a pressure increase and a temperature decrease will increase the reaction rate constant $k_{kinetic}$ and therefore also the reaction rate according to equation I-1:

$$\ln K_{kinetic} = \ln k_0 - \Delta V^{\ddagger} \cdot \frac{p}{R \cdot T} \qquad \textbf{(II-1)}$$

   However, an increase in temperature also increases the rate of reaction according to Arrhenius' law (Cheftel, 1995).

2. *Microscopic ordering principle*: at constant temperature, an increase in pressure increases the degree of ordering of the molecules of a substance (Urrutia Benet, 2005).

3. *Isostatic principle*: pressure is transmitted in a uniform and instantaneous manner independent of the size and geometry throughout the whole biological sample (Balny & Masson, 1993; Cheftel, 1995). Therefore, in contrast to thermal processing, the pressurization process time is independent of sample volume.

The primary source of the dynamical behaviour of biomolecules is the free volume of a system, and this may be expected to decrease with increasing pressure (Heremans, 2001). The following equation describes the Gibbs free energy of transition and holds for a general equilibrium process from A ↔ B:

$$\Delta G = -RT \cdot \ln K = \Delta H - T \cdot \Delta S \qquad \textbf{(II-2)}$$

In a simple manner a general rule of thumb is: "Every system seeks to achieve a minimum of free energy". Accordingly, changes in ΔG effect a reaction as follows:
ΔG < 0 : favored reaction (spontaneous)
ΔG = 0 : System in equilibrium, neither forward nor reverse reaction prevails.
ΔG > 0 : disfavored reaction (non-spontaneous)
As a consequence of structural changes on a molecular level and therefore changes in the functionality of biopolymers, complex biological systems (e.g. microorganisms) are affected in their stability as well.

1.2.1 Microorganisms and Spores

The most important criterion a food has to fulfil is its safety. One important aspect of food safety is microbiological hazards. Foodborne illness caused by microorganisms is a large and growing public health problem (WHO, 2002). As a consequence and to find an alternative to conventional thermal processing, intensive research on the HP inactivation of microorganisms and spores has been carried out in the past. However, in high pressure applications thermal effects can not be fully ruled out and high pressure inactivation of vegetative microorganisms is almost always connected to a thermal treatment (Smelt, Hellemons & Patterson, 2001). The specific effects and damages of pressure on vegetative microorganisms are complex and cannot be evaluated detached from heat effects (Luscher, 2008). Primarily, the lethal effects of high pressure on vegetative microorganisms are attributed to enzyme inactivation and cell membrane rupture (Ardia, 2004; Ananta, 2005). In the course of finding mechanisms behind this inactivation, it was shown that flow cytometry is a potent tool to gain insights in the states and mechanisms of cell damage of pressure treated microorganisms (Ananta, Heinz & Knorr, 2004). But pressure treatments are not necessarily weakening biological cells. At low pressure levels fortification of microbial cells was observed and pressure induced thermo tolerance of lactic acid bacteria occurs after HP treatment between 100 and 200 MPa (Ananta & Knorr, 2003). As a result of this phenomenon, pressure induced stress response was found to offer promising processing options, such as pre-treatment of lactic acid bacteria before drying or freezing for the purpose of starter culture production. Microbial inactivation of more that 5 log cycles in food products is reported by several authors to occur at pressures between 300 - 800 MPa (Hendrickx & Knorr, 2001; Ardia, 2004; Li, Zhang, Balasubramaniam, Lee, Bomser, Schwartz et al., 2006). According to Smelt et al, the HP induced effects, that result in vegetative cell death can be summarized as follows (Smelt et al., 2001):

Proteins and enzymes: High pressure induces unfolding of globular proteins. It is assumed that the combined, complete or partial inactivation of numerous enzymes and metabolic pathways leads to the inability to proliferate and cell death, respectively (Bunthof, 2002).
Membranes: Besides the inactivation of enzymes, membrane damage is considered as one of the key events related to microbial cell death. Membranes undergo phase transitions and

solidify under pressure and perturbations are promoted (Schlüter, 2004). In addition pressure leads to the detachment and inactivation of membrane proteins (Ulmer, Herberhold, Fahsel, Gänzle, Winter & Vogel, 2002).
Ribosomes: The disintegration of ribosomes in their subunits is promoted by pressure and may be related to cell death (Niven, Miles & Mackey, 1999).
pH: The maintenance of intracellular pH is crucial for the survival of cells. Some authors related cell death predominantly to intracellular pH changes, which are related to inactivation of enzymes controlling the acidity and membrane damages (Luscher, 2008).
Bacterial spores have a higher barotolerance than vegetative bacteria and may survive pressures above 1200 MPa (Ananta, Heinz, Schlüter & Knorr, 2001; Gao, Ju & Jiang, 2006). Early approaches towards spore inactivation aimed on the germination at moderate pressure. However, combination processes with spore germination at pressures below 200 MPa and an additional moderate heat treatment could not guarantee sufficient inactivation since small population of spores could not be germinated (Mathys, 2008). The HP inactivation of bacterial spores is not yet fully understood and still of high relevance in today's HP sterilization research activities. A detailed discussion of HP related spore inactivation mechanisms is given by Mathys (Mathys, 2008).

1.2.2 Protein structures

It has been known for a long time that proteins unfold at high pressure (Heremans & Smeller, 1998). While temperature effects are relatively well understood and the change in heat capacity upon unfolding has been reasonably well parameterized, the state of understanding pressure effects is much less advanced (Royer, 2005). The state and linked to it the functionality of proteins and enzymes is thermodynamically governed by the present pressure and temperature conditions. Pressure denaturation of proteins is a complex phenomenon that depends on a number of factors, such as the protein structure, the pressure range and other external parameters, e.g. temperature, pH and solvent composition (Masson, 1992). Based on the assumption that there are only two distinct states of proteins (native and denaturated), Hawley calculated the Gibbs free energy difference (ΔG) for the denatured and the native state of chymotrypsinogen and ribonuclease. On the basis of ΔG as a function of temperature and pressure he developed the theory of the elliptical phase diagram of proteins (Hawley, 1971). The Gibbs free energy difference between the native and denaturated states is defined as:

$$\Delta G = G_{denaturated} - G_{native} \qquad \textbf{(II-3)}$$

The elliptical shape of the phase diagram, based on the calculations for chymotrypsinogen, is shown in Figure II-2. The second order transition line in this phase diagram is defined by $\Delta G=0$. Crossing the boundaries of this region towards $\Delta G<0$, the native conformation looses its stability and the protein unfolds (Hawley, 1971; Smeller, 2002). The stable native state ($\Delta G>0$) exists only in a closed p-T range. It has to be noted, that this theory is a phenomenological one and based on the assumption of only two possible states a protein can exist in. Detailed discussion on the limitations of Hawley`s theory is given by L. Smeller (Smeller, 2002). Based on the phase diagram of proteins, different denaturation mechanisms can be derived. According to the driving force behind the denaturation the different modes of action can be classified as heat, cold and pressure denaturation, as illustrated in Figure II-3.
Changes in protein conformation are often referred to as denaturation. Induced loss of solubility and enzymatic activity were taken as indicators of protein denaturation (Dubois, Hovanessian & Bensaude, 1991). Denaturation of monomeric proteins can often be regarded as a two state transition. Effectively, the conformational changes in oligomeric protein structures during the denaturation process are more complex and involve more or less stable

intermediates (Privalov, 1982). This progressive effect leads to denaturation at the point of complete unfolding of the polypeptide chains (Masson, 1992).
Functional properties of food proteins strongly depend on their conformation and can be classified into the following three groups (Galazka, Dickinson & Ledward, 2000):

1. *Hydration properties*: dependent on protein – water interactions that affect swelling, adhesion, dispersibility, solubility, viscosity, water absorption and water holding.
2. *Interfacial properties*: including surface tension, emulsification and foaming characteristics.
3. *Aggregation and gelation properties*: Properties related to protein – protein interactions (e.g. gel formation).

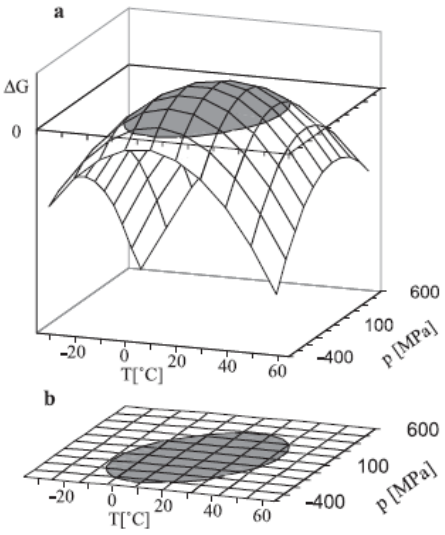

Figure II-2: (a) ΔG as a function of temperature and pressure for chymotrypsinogen, using the parameters determined by Hawley.
(b) The elliptical phase diagram shown as the horizontal projection of the above function. The grey area shows the region where the native state is more stable (Smeller, 2002).

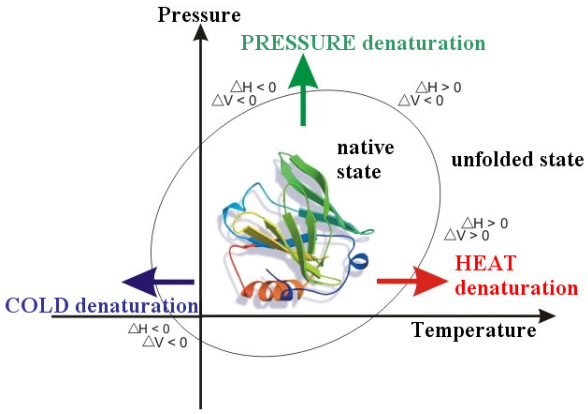

Figure II-3: Schematic heat, cold and pressure denaturation of proteins, including changes in enthalpy and volume, redrawn from (Heremans, 2001).

The effects of high pressure on the structure of globular proteins in aqueous solution have been extensively investigated over the last 20 years (Silva & Weber, 1993; Cruz-Romero, Smiddy, Hill, Kerry & Kelly, 2004). Structural rearrangements taking place in the proteins under pressure are attributed to Le Châtelier´s principle, which states that processes associated with a negative ΔV are encouraged by pressure increases, whereas processs involving positive ΔV are inhibited by pressure increases (Hendrickx, Ludikhuyze, Van den Broeck & Weemaes, 1998). Electrostatic and hydrophobic interactions are sensitive to high pressure, as they are accompanied by positive ΔV (Masson, 1992; Heremans, 2001). Hydrogen bonds are almost pressure insensitive and are reported to even stabilize under high pressure (Mozhaev et al., 1996). High pressure induced changes in conformation, structure and hydration properties are related to deprotonation of charged groups, cleavage of salt bridges and hydrophobic interactions. The native protein folds into three-dimensional structures which are made of up to four distinct sub structures, as schematically shown in Figure II-4. Due to different forms of molecular bonds, the four structure levels are differently affected by high pressure treatment:

Quaternary structure: The quaternary structure is held together by noncovalent hydrophobic interactions and is sensitive to high pressure (Hendrickx et al., 1998). Moderate pressures (<150 – 200 MPa) were found to favour the dissociation of oligomeric proteins, a phenomenon always accompanied with negative and sometimes very large volume changes. Dissociation can be followed by subunit aggregation or by precipitation (Masson, 1992; Mozhaev et al., 1996; Balny, 2004).
Tertiary structure: Significant changes in the tertiary structure can be observed above 200 MPa (Hendrickx et al., 1998). Denaturation affecting the tertiary structure is a complex process sometimes involving intermediate states such as the molten globule state, leading to multiple denatured forms (Balny, 2004).
Secondary structure: In general, secondary structure changes occur at a very high pressure, above 300–700 MPa and lead to irreversible denaturation (Hendrickx et al., 1998). The effect depends on the applied pressure and on the extent of the secondary structure rearrangements (Masson, 1992; Balny, 2004).
Primary structure: The ΔV values for exchanges in covalent bonds are nearly zero. As a consequence, covalent bonds participating in the protein primary structure are pressure insensitive at last up to pressure values of 1000–1500 MPa (Hendrickx et al., 1998; Balny, 2004).

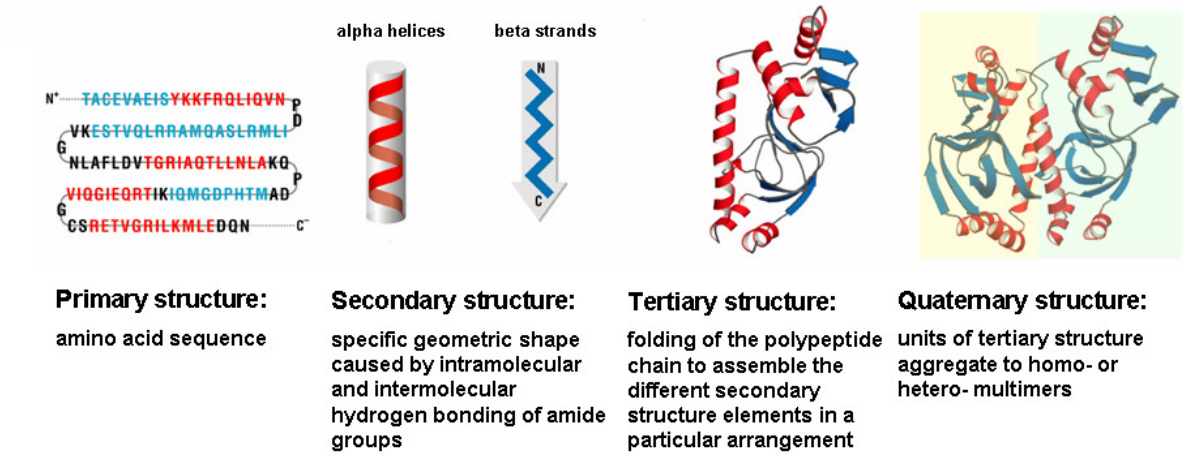

Figure II-4: The four levels of protein structure.

High hydrostatic pressure induces either local or global changes in protein structures that may lead to denaturation. The pressure stability of proteins is very specific and among others liked to the size of the protein. In general, oligomeric proteins are dissociated at pressures below 200 MPa, whereas monomeric proteins usually unfold between 400 and 800 MPa (Masson, 1992; Mozhaev et al., 1996). Pressure induced unfolding and denaturation can be reversible and after pressure release the protein conformation shifts back to the native folded state. Due to chemical modifications, e.g. aggregation reactions, pressure induced denaturation can be irreversible (Masson, 1992). Lower denaturation pressure at decreased temperature (cold denaturation) has been observed (Kunugi & Tanaka, 2002). The only general comment one can make about the effect of pressure on protein structure is that it tends to favour protein conformations that occupy smaller specific volumes (Royer, 2005). Which conformation a protein will adopt under particular conditions of temperature, pressure and solution compositions depends on the protein and the conditions under which the pressure has been applied.

1.2.3 Polysaccharides

Effects of high pressure on polysaccharides have been investigated product specifically by several research groups in the last years. It shows that pressure affects the properties of various homo- and hetero-polysaccharides. Gelation of crystalline starch in presence of water was observed showing highly specific gelation properties of starches from different plants (Oh, Pinder, Hemar, Anema & Wong, 2008). Starch gelation at 20°C occurs at pressures from 100 – 600 MPa, depending on the raw material and concentration (Stolt, Oinonen & Autio, 2000; Oh et al., 2008). High pressure induced gelation in biopolymer mixtures, such as pectin-whey protein mixtures, has been investigated, showing high potential for controlled structure engineering in food systems (Dickinson & James, 2000; Hendrickx & Knorr, 2001; Michel et al., 2001). Structure formation in pure pectin solutions and an almost 10fold increase in viscosity was found after pressure treatment at 400 MPa (Michel & Autio, 2001). Studies on the influence of high pressure on gel forming maltodextrines indicate denser structures and an increased mechanical and thermal stability of treated powders (Schuricht, Schierbaum & Fleischer, 1998).

1.2.4 Fat

High pressure treatment of fat is often linked to crystallization effects. Compared with proteins, relatively little attention has been paid to HP-induced changes in fat globules (Huppertz, Fox, de Kruif & Kelly, 2006). Crystallization of milk fat in cream is induced by HP treatment at 100-400 MPa (Buchheim & Abou El-Nour, 1992). Different from thermal treatments, the HP treatment allows crystallization of the inner phase of o/w emulsions independently from the fat globule size. In addition, shorter treatment times are required and crystallization can be induced at temperatures that would not allow a phase change at atmospheric pressure (Buchheim, 1994). In presence of proteins, rheological properties of HP treated emulsions can differ from the native state. However, this effect is not due to changes in the fat structure itself but attributed to protein-fat interactions that occur under pressure. The exact mechanism behind this phenomenon remains to be elucidated (Huppertz et al., 2006).

1.3 Industrial HP applications

High hydrostatic pressure has been successfully implemented in the food industry since the early 1990s. The use of high pressure in food processing is an extension of a technology that is commonly employed in many other industrial processes, notably in the manufacturing of ceramics, diamonds, super-alloys, and sheet metal forming. Pressure-treated food products were first available in Japan and were introduced in the US and European market few years later. The application of high pressure in food technology lies mostly on pasteurisation of juices, marmalades, and other fruit and vegetable products, to achieve a better quality of products after processing, as compared to conventional thermal processes (Cheftel, 1995). HP treated meat products, e.g. sliced ham, are commercially available as well. The use of pressure as an alternative to thermal processing leads to lower temperature levels during processing, thus lower influence on the properties of the raw materials occurs. A detailed summary of research work related to HP applications in the food industry is given by Urrutia (Urrutia Benet, 2005).

1.4 High Pressure-Low Temperature treatment

1.4.1 Process definitions

Analogous to the standard High Pressure processing, the field of “High Pressure-Low Temperature” (HPLT) processing embraces high pressure processes in the subzero temperature domain. Outgoing from the initial state of the water in the sample material at

atmospheric pressure, HPLT processes can be classified according to the process aim as schematically shown in Figure II-5. The majority of HPLT processes are freezing or thawing processes. According to the schematic definition in Figure II-5, the only process that does not include a water phase transition is the sub zero cooling (Urrutia Benet et al., 2004). This treatment allows liquid storage at sub zero temperatures without ice formation in the sample. Processes that comprise a phase transition of water are freezing or thawing under pressure. Water phase transitions under pressure can be either pressure assisted, pressure induced or induced by a pressure shift (Urrutia Benet et al., 2004). Pressure assisted freezing (PAF) is a freezing process at elevated pressure that allows direct freezing to different ice modifications (ice I, ice III or ice V). During high pressure shift freezing (PSF) a liquid sample is cooled well below its freezing point at atmospheric pressure without ice formation. Freezing is triggered by a sudden pressure release that induces homogeneous nucleation throughout the product. During pressure release instant ice formation occurs (Otero & Sanz, 2000; 2006a). Pressure induced freezing (PIF) is defined as a process that induces a water phase change (freezing) by pressure increase (Urrutia Benet, 2005). Strictly speaking, it is a PSF process, since the phase transition is induced by a pressure shift. Even if the Δp that causes nucleation in this process is positive. As for the freezing, the same rules of nomenclature are valid for thawing processes. Depending on the Δp, the thawing process is either pressure induced or assisted. Concerning the pressure induced thawing (PIT) process the same note as for PIF has to be made.

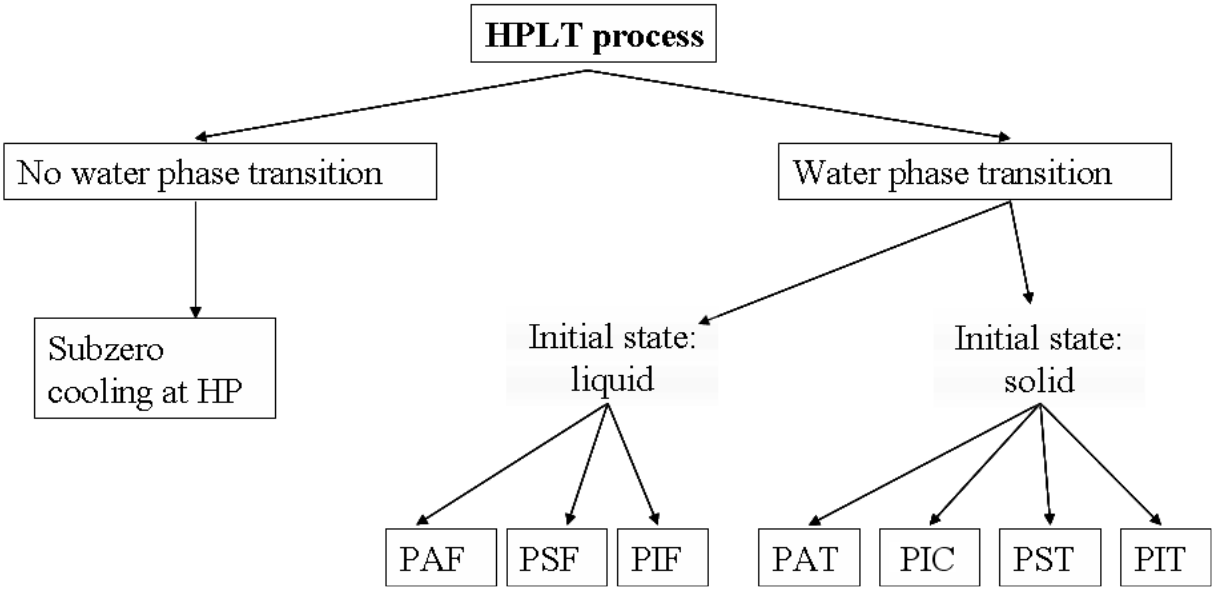

Figure II-5: Definition of different processes in the HPLT domain. (PAF: pressure assisted freezing; PSF (HPSF): (high) pressure shift freezing; PIF: pressure induced freezing; PAT: pressure assisted thawing; PST: pressure shift thawing; PIT: pressure induced thawing). Redrawn from (Urrutia Benet, 2005).

1.4.2 Water at low temperatures under pressure

Water is the major constituent of most living organisms and plant or animal related food products. Therefore it is of special interest when considering the impact of high pressure on biological materials. The thermodynamic properties of water are well documented and available e.g. in software databases such as NIST/ASME Steam Properties. According to this data, the viscosity and heat capacity as two relevant parameters in the context of this study are shown in Figure II-6 as a function of pressure and temperature. In addition to the specific thermodynamic parameters of water, the most relevant property of water is its aggregate state. Today, sixteen crystalline phases and three amorphous (non-crystalline) phases are known (Zheligovskaya & Malenkov, 2006; Chaplin, 2008). All crystalline phases of ice involve the water molecules being hydrogen bonded to four neighbouring water molecules. The sectional

enlargement of the water phase diagram in Figure II-7 is the very base for process planning in the HPLT region. Of special interest for HPLT processes are the water ice modifications I, III and V as they exist at temperatures below the atmospheric freezing point of water and their phase boundaries separate them from the liquid state.

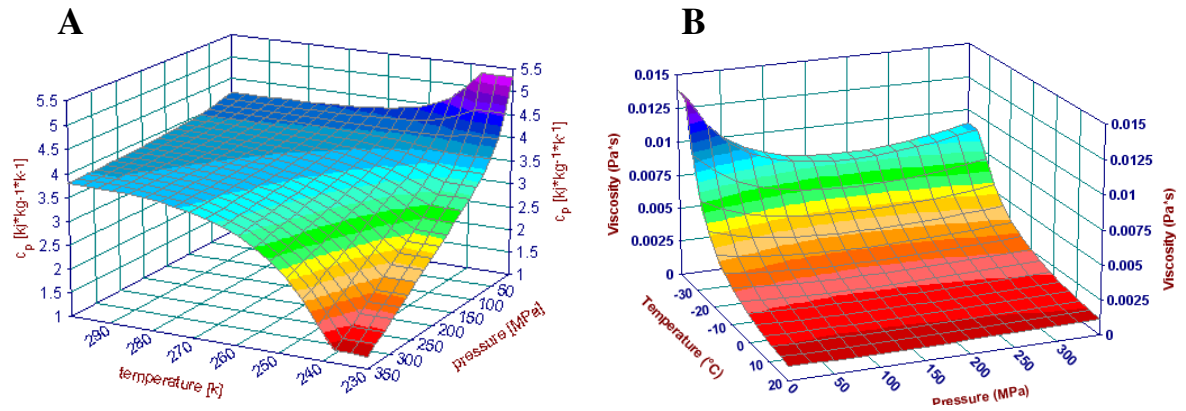

Figure II-6: Heat capacity (A) and viscosity (B) of water as functions of temperature and pressure according to the NIST/ASME software database.

The Clausius-Clapeyron relation is one way of characterizing the phase transition between two phases of matter, such as solid and liquid:

$$\frac{dp}{dT} = \frac{L}{T \cdot \Delta V} \qquad \textbf{(II-4)}$$

Where dp/dT characterises the slope of the melting line, L is the latent heat, T is the temperature, and ΔV is the volume change of the phase transition.

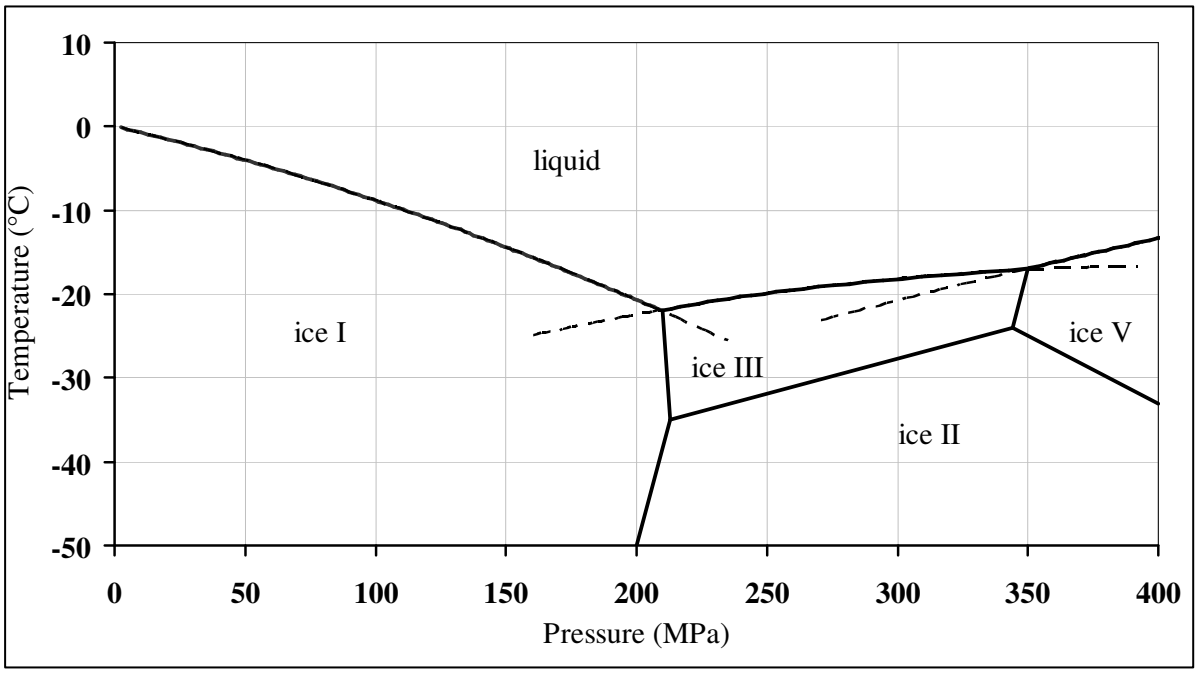

Figure II-7: Sectional enlargement of the water phase diagram after Bridgman (Bridgman, 1912). Dotted lines show the trend of the extended melting lines of ice I, ice III and ice V.

1.4.3 HPLT processing of food systems

HPLT is not yet an industrially applied technology. Nevertheless, intensive applied research on the impact of HPLT treatment on various food systems and microorganisms has been carried out (Schlüter, 2004; Fernández, Otero, Guignon & Sanz, 2006; Buggenhout et al., 2007). In the focus of these studies were predominantly two aspects. First, the idea of exploiting the freezing point depression of water under pressure and using the HPLT technology as an alternative to conventional freezing and thawing processes for plant and animal related food products. Shorter phase transition times and small ice crystals, which reduce textural damages during freezing, are the practical benefit in this context. The different HPLT processes can be ranked according to their potential of food industrial applicability as follows (Schlüter, 2004):
pressure induced thawing > pressure assisted thawing > pressure shift freezing > subzero storage > pressure assisted freezing to ice III/ice V > pressure assisted freezing to ice I.
The second effect that motivates research in this area so far is the potential of HPLT treatment to inactivate microorganisms in already frozen foods by changing the water ice phase from ice I to ice III and back to ice I. Microbial inactivation of up to 7 log cycles are induced by the high volume changes that occur during this kind of treatment (Luscher, Balasa, Frohling, Ananta & Knorr, 2004).
Another aspect, that was not of central concern in HPLT research so far and is of special interest in this work, is the modification of proteins and other biomolecules by HPLT treatment to improve the properties of already established substances or create new ingredients for the food industry.

2 Food foams

2.1 Foam properties

Foams are concentrated dispersions of gas in a liquid or solid matrix. According on the state of the continuous phase they can either be classified as liquid or solid foams. Most of the solid foams have a liquid foam as precursor, so that solid foams are usually processed liquid foams (Weaire, Cox & Brakke, 2006). Furthermore, foams are classified according to the quantity of the liquid fraction as wet or dry foams. In this respect, wet foams show relatively high values of the liquid fraction, whereas in dry foams the volume of the liquid (continuous) phase is rather low. The amount of liquid in foams governs the bubble arrangement, wet and dry foams relevant to food processing can be defined by their macroscopic structure (Niranjan, 1999; Murray, 2007):

Polyhedral foams have a honeycombed structure and a higher gas fraction, greater that 85% (e.g. froth on a pint of beer). In these cellular foams the geometry of the packed lamellae is a large determinant of foam stability.
Spherical foams (“bubbly foams”) consist of spherical bubbles and relatively low gas fractions ranging between 50 and 70% (e.g. ice creams). The bubbles in this type of foam are not as closely packed and the foam lamellae between the bubbles do not occupy nearly as much of the bubble surface area as in polyhedral foams.

Figure II-8 shows the typical structures of dry (polyhedral) and wet (spherical) foams.

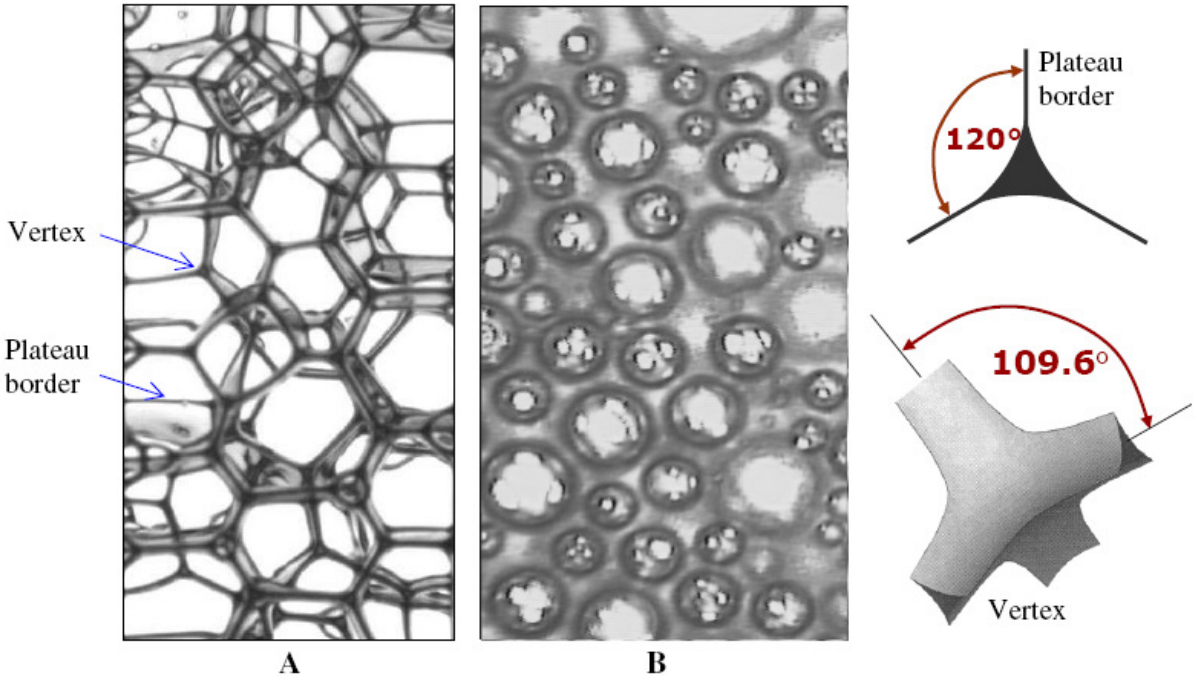

Figure II-8: Typical structures of dry/polyhedral foam (A) and wet/spherical foam (B); redrawn from (Hoehler & Cohen-Addad, 2005).

The Belgian scientist Joseph Plateau made intense observations of soap film behaviour in wire frames. From these observations he developed a set of rules which govern the equilibrium of liquid films and foams. Plateaus equilibrium rules apply to dry foam at equilibrium:

- Three films meet at angles of 120 degrees.
- The films form a curved triangular channel, the so called "Plateau borders".
- Four Plateau borders meet at angles of 109.6 degrees to form a "vertex".

The air cell size in foams can differ largely from 10 µm to several millimetres, accordingly the density may range from nearly zero to about 700 g/L, beyond which gas emulsions rather than foams are found (Hoehler & Cohen-Addad, 2005). The amount of air incorporated into aerated products is commonly expressed as percent overrun (OR). The overrun is the increase in volume of the foam over the volume of the liquid phase. It is expressed as percent of the volume of the continuous phase:

$$overrun = \frac{V_{foam} - V_{liquid}}{V_{liquid}} \cdot 100\% \qquad \textbf{(II-5)}$$

Foam properties depend primarily on the chemical composition. The properties of the adsorbed films are affected by numerous factors such as the extend of adsorption from solution at the liquid/gas surface, the surface rheology, diffusion of gas out of and into foam cells, size and distribution of the cells, surface tension of the liquid and external pressure and temperature (Ross & Morrison, 2002). The rheological behaviour of foams is usually examined under the following assumptions:

- Foams are highly viscous
- Foams exhibit shear thinning
- Foams exhibit yield point
- Foams appear to slip at solid boundaries.

The relationship between internal and external pressure and the size of a single bubble with one interface and given surface tension is described by LaPlace`s Law:

$$p_b = p_0 + \frac{4\sigma}{r} \quad \textbf{(II-6)}$$

With p_b the internal pressure of the bubble, p_0 the pressure of the surrounding medium and σ the surface tension.

The solubility of gases is related to pressure: gases are more soluble at higher pressures. Henrys Law states that: "*At constant temperature, the amount of a given gas dissolved in a given type and volume of liquid is directly proportional to the partial pressure of that gas in equilibrium with that liquid.*" According to this, Henry`s Law introduced the Henry's Law constant k_H. A larger k_H corresponds to a les soluble gas:

$$p = k_H \cdot c \quad \textbf{(II-7)}$$

where p is the partial pressure of the solute, c is the concentration of the solute and k_H the Henry's Law constant.

2.1.1 Foam formation

Foaming is a complex multi time scale processes involving multiple aspects that have to be considered in the production of a stable aerated product. The foam formation begins with the bubble creation or gas bubble brake up, which happens within 10^{-3} to 0.1 seconds. In order to stabilize the created foam bubbles, surface active material has to adsorb to the newly created bubble surfaces. The rate of surface stabilization is subjected to the properties of available surfactants and the properties of the continuous phase. The formation of adsorption layers on the bubble surfaces can start in milliseconds but may continue for days or even month. The foam films and plateau borders, i.e. the general macroscopic foam structure, is usually created within the first minute after bubble creation (Michel, 2006).
Foam formation can be induced by mixing or agitation (draught beer, whipped cream or sea foam), evolution of dissolved gas (canned beer, soft drinks, shaving foam and hair mousse) or simple bubbling gas through liquid (widget in canned Guinness beer). It is not possible to get pure liquid water to foam. Surfactants are necessary even to create weak foams (Joseph, 1997; Indrawati, Wang, Narsimhan & Gonzalez, 2008). Foaming properties can be characterized by foamability and foam stability. The foamability is defined as the capacity of the continuous phase to entrap gas, and foam stability as the ability to retain the gas over time. The foaming properties of protein foams depend on many intrinsic factors (size, structure of protein, hydrophobicity, surface potential, charge, etc.) and environmental and processing factors (protein concentration, pH, temperature, addition of other ingredients, etc.) (Indrawati et al., 2008).

2.1.2 Stabilization and destabilization mechanisms

Stabilization and destabilization mechanisms of foams are highly complex and intensive research in this field is carried out by scientists of diverse scientific disciplines. The following section gives an basic overview about the principles behind some food foam relevant effects.
Foams are affected by destabilization effects from the moment they are created. Unless the continuous phase is completely solidified, foams are thermodynamically unstable systems that will break down eventually (Indrawati et al., 2008). The stability of foams is determined by a number of conditions, in particular the nature and amount of surfactants that stabilize the stationary phase interfaces and other ingredients that affect the viscosity of the continuous phase. An increase in the surfactant content limits the rate of descending liquid flow and increases the liquid efflux time, thus reduces drainage effects. This is conventionally

explained by the enhanced interaction between adsorption layers, growing mechanical strength of the walls, and increasing viscosity (Pakharukov & Shevnina, 2001). Apart from gravitational destabilization (i.e. drainage and creaming) coalescence and Ostwald ripening are mechanisms that promote foam collapse. Hence, three relevant mechanisms of foam destabilization can be summarized as follows:

Drainage: Gravitational drainage describes the descending flow of liquid out of the foam. In wet foam, this phenomenon is accompanied by creaming of the bubbles in the opposite direction. Drainage is decisively governed by the viscosity of the continuous phase and the air to liquid ratio (Clarke, 2004). Drainage in spherical foams eventually leads to the formation of a polyhedral foam structure. Thin liquid films form and end in plateau boarders at the contact point of more than two bubbles.

Coalescence: The merge of two bubbles after contact and film rupture. The risk of coalescence in polyhedral foams is strongly determined by the properties of the adsorption layers of the bubbles. Gravitational drainage supports coalescence due to film thinning. In addition the lower pressure in the plateau boarders promotes the liquid flow towards the boarders and out of the foam films.

Ostwald ripening: Gas has the ability to diffuse through a liquid matrix, between the bubbles and into the gas phase that surrounds the foam (Jang, Nikolov & Wasan, 2006). When this is manifested in the growth of larger bubbles at the expense of smaller bubbles, as a consequence of differences in the Laplace pressure, the phenomenon is referred to as disproportionation or Ostwald ripening (Dickinson, Ettelaie, Murray & Du, 2002). Different from coalescence the air bubbles surfaces do not need to be in physical contact to be affected by such disproportionation effect. Even when the viscosity of the continuous phase is very high (e.g. ice cream) disproportionation occurs. Ostwald ripening is slowed down when the gas phase has a poor solubility in the continuous phase, so for aqueous systems nitrogen gives more stable foams than carbon dioxide. Also, a homogeneous bubble size distribution limits disproportionation effects because of lower pressure gradients between the individual air cells. Ostwald ripening as a destabilization mechanism in aerated food products has been discussed in detail in several publications (Dickinson et al., 2002; Dutta, Chengara, Nikolov, Wasan, Chen & Campbell, 2004). The three destabilization mechanisms are schematically shown in Figure II-9.

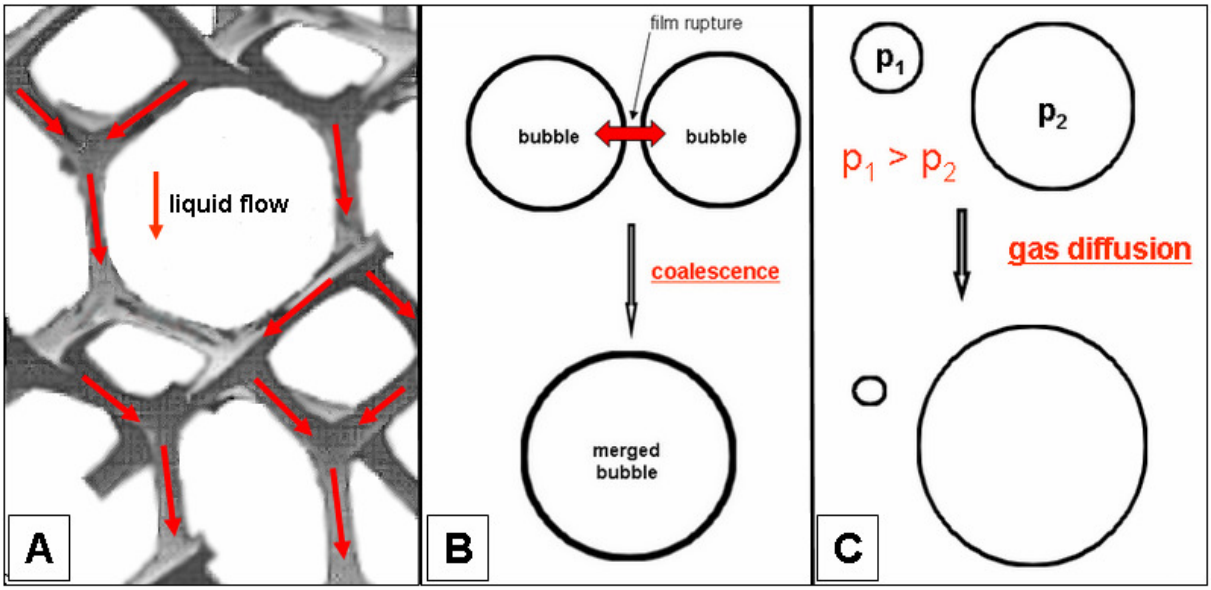

Figure II-9: Destabilization mechanisms of foams (highly schematic). Gravitational Drainage (A)**, Coalescence** (B)**, Ostwald ripening (Disproportionation)** (C)**.**

2.2 Characterisation of aerated food products

A diverse range of foods are aerated and even if poorly understood, obtain increasing importance as manufacturers seek to exploit the novelty of bubbles as food ingredients (Campbell & Mougeot, 1999). Well known examples of foamed food products are whipped cream, spray cream, ice cream or foamed chocolates. The results of food product aeration are versatile. In general, food aeration leads to:

- Reduced density of the product
- Changes in texture and rheology, giving different sensory properties
- Enhanced ability to soak up liquid products (e.g. sauces)
- Possibly reduces shelf life due to the chance of enhanced oxidation reactions
- Change in flavour intensity

The positive effects of aeration are primarily texture effects (Campbell & Mougeot, 1999). Liquid products obtain higher smoothness and tingling mouthfeel (Dessirier, O´Mahony, Sieffermann & Carstens, 1999) and solid products gain lightness, crispiness or creaminess. Furthermore, aerated products are easier to chew.
Aeration processes in the food industry are numerous. A rough classification into three groups according to the basic principle of aeration can be made:

1. Processes in which the liquid is actively (mechanically) forced around external gases (e.g. whipping, shaking)
2. Processes in which gas is actively forced through the liquid (e.g. gas injection)
3. *In situ* generation of gas cells (biological or chemical, steam formation by heat or gas evaporation upon pressure release).

As food systems in general, food foam stabilization is very complex and many different stabilizing mechanisms can be found. Depending on the manufacturing process and the composition of the product, bubbles in food can be stabilized by surfactants (surface active agents), such as proteins, fat and polysaccharides. A rather indirect way of stabilization is found when the viscosity of the continuous phase is increased or the continuous phase is semi solid (e.g. by ice crystal formation in ice cream or baking of bread dough). Important to mention is, that in the majority of products not one single stabilization mechanism is responsible for the foam structure but a co-action of different mechanisms occurs. A detailed overview about different stabilization mechanisms occurring in aerated food products is given by Campbell and Mougeot (Campbell & Mougeot, 1999).

2.3 Frozen food foams

A variety of foods are frozen products. Freezing is an established process for food preservation that allows extending the shelf life of previously manufactured products. Hence, the fresh character of foods is maintained by freezing after production. But freezing can also be part of the manufacturing process itself in the production of foods that are consumed in the frozen state, such as ice cream and frozen deserts. This group of products is especially interesting in terms of foam formation and stabilization, since the foam formation in ice cream and frozen deserts takes place during the freezing step at subzero temperatures. The foam structures in aerated products that are frozen for storage reasons only and thawed before eating (e.g. frozen cakes, bread dough) usually develop at temperatures above the freezing point. While the dynamic freezing process in ice cream manufacturing is generally associated with the formation of the ice phase, aeration and agitation during this process are also responsible for the formation of colloidal aspects of structure, i.e. the formation of air bubbles and the partial coalescence of fat into a major structural element (Marshall et al., 2003).

Ice cream has a relatively low gas volume and the bubbles are not in contact and therefore are spherical. Under ambient conditions, this type o foam would be highly unstable and sensible to destabilization effects as described above. However, provided it is frozen, the foam structure in ice cream is stable over month and creaming and drainage are very slow (Clarke, 2004). During the freezing stage the ice cream mix emulsion is foamed. Both, the air bubbles and the ice crystals form a dispersed phase in the unfrozen matrix. In addition, partially crystalline fat undergoes partial coalescence during the concomitant whipping and freezing process. The resulting solid like structure is created by a network of agglomerated fat that surrounds the air cells.

3 References

[1]Ananta, E., Heinz, V., Schlüter, O. & Knorr, D. (2001). Kinetic studies on high-pressure inactivation of Bacillus stearothermophilus spores suspended in food matrices. *Innovative Food Science & Emerging Technologies*, *2*(4), 261-272.

[2]Ananta, E. & Knorr, D. (2003). Pressure-induced thermotolerance of Lactobacillus rhamnosus GG. *Food Res. Intl.*, *In press*.

[3]Ananta, E., Heinz, V. & Knorr, D. (2004). Assessment of high pressure induced damage on Lactobacillus rhamnosus GG by flow cytometry. *Food Microbiology*, *21*(5), 567-577.

[4]Ananta, E. (2005). *Impact of enviromental factors on vitality and stability and high pressure pretreatment on stress tolerance of Lactobacillus rhamnosus GG (ATCC 53103) during spray drying*. PhD thesis, Berlin, Berlin University of Technology, 218.

[5]Ardia, A. (2004). *Process Considerations on the Application of High Pressure Treatment at Elevated Temperature Levels for Food Preservation*. PhD Thesis thesis, Berlin, Berlin University of Technology, 94.

[6]Balny, C. & Masson, P. (1993). Effects of High-Pressure on Proteins. *Food Reviews International*, *9*(4), 611-628.

[7]Balny, C. (2004). Pressure effects on weak interactions in biological systems. *Journal of Physics: Condensed Matter*, *16*, S1245-S1253.

[8]Bernard, M. (1986). The paradox of pressure vessel wall thickness calculation. *Physica B+C*, *139-140*, 773-775.

[9]Bridgman, P. W. (1912). Water, in the liquid and five solid forms, under pressure. *Proceedings of the American Academy of Arts and Sciences*, *47*, 441-558.

[10]Buchheim, W. & Abou El-Nour, A. M. (1992). Induction of Milkfat Crystallization in the Emulsified State by High Hydrostatic Pressure. *Fett Wissenschaft Technologie/Fat Science Technology*, *94*(10), 369-373.

[11]Buchheim, W. (1994). *Verfahren zur hydrostatischen Hochdruckbehandlung eines Stoffes*. Germany, patent.

[12]Buggenhout, S. V., Grauwet, T., Loey, A. V. & Hendrickx, M. (2007). Effect of high-pressure induced ice I/ice III-transition on the texture and microstructure of fresh and pretreated carrots and strawberries. *Food Research International*, *40*, 1276-1285.

[13]Bunthof, C. J. (2002). *Flow Cytometry, Fluorescent Probes, and Flashing Bacteria*. Thesis thesis, Wageningen, Wageningen University, 160.

[14]Campbell, G. M. & Mougeot, E. (1999). Creation and characterisation of aerated food products. *Trends in Food Science & Technology*, *10*(9), 283-296.

[15]Chaplin, M. (2008). Water structure and science, http://www.lsbu.ac.uk/.

[16]Cheftel, J. C. (1995). Review : High-pressure, microbial inactivation and food preservation / Revision: Alta-presion, inactivacion microbiologica y conservacion de alimentos. *Food Science and Technology International*, *1*(2-3), 75-90.

[17]Clarke, C. (2004). *The Science of Ice Cream*. The Royal Society of Chemistry, Cambridge.

[18]Cruz-Romero, M., Smiddy, M., Hill, C., Kerry, J. P. & Kelly, A. L. (2004). Effects of high pressure treatment on physicochemical characteristics of fresh oysters (Crassostrea gigas). *Innovative Food Science & Emerging Technologies*, *5*(2), 161-169.

[19]Dessirier, J.-M., O´Mahony, M., Sieffermann, J.-M. & Carstens, E. (1999). What causes the tingle in carbonated drinks. In G. M. Campbell, C. Webb, S. S. Pandiella & K. Niranjan. *Bubbles in Food* (pp. 333-338). Amer Assn of Cereal Chemists, Minnesota.

[20]Dickinson, E. & James, J. D. (2000). Influence of high-pressure treatment on [beta]-lactoglobulin-pectin associations in emulsions and gels. *Food Hydrocolloids*, *14*(4), 365-376.

[21]Dickinson, E., Ettelaie, R., Murray, B. S. & Du, Z. P. (2002). Kinetics of disproportionation of air bubbles beneath a planar air-water interface stabilized by food proteins. *Journal of Colloid and Interface Science*, *252*(1), 202-213.

[22]Dubois, M. F., Hovanessian, A. G. & Bensaude, O. (1991). Heat-Shock-Induced Denaturation of Proteins - Characterization of the Insolubilization of the Interferon-Induced P68 Kinase. *Journal of Biological Chemistry*, *266*(15), 9707-9711.

[23]Dutta, A., Chengara, A., Nikolov, A. D., Wasan, D. T., Chen, K. & Campbell, B. (2004). Destabilization of aerated food products: effects of Ostwald ripening and gas diffusion. *Journal of Food Engineering*, *62*(2), 177-184.

[24]Fernández, P. P., Otero, L., Guignon, B. & Sanz, P. D. (2006). High-pressure shift freezing versus high-pressure assisted freezing: Effects on the microstructure of a food model. *Food Hydrocolloids*, *20*, 510-522.

[25]Galazka, V. B., Dickinson, E. & Ledward, D. A. (2000). Influence of high pressure processing on protein solutions and emulsions. *Current Opinion in Colloid & Interface Science*, *5*(3-4), 182-187.

[26]Gao, Y.-L., Ju, X.-R. & Jiang, H.-H. (2006). Studies on inactivation of Bacillus subtilis spores by high hydrostatic pressure and heat using design of experiments. *Journal of Food Engineering Special Section: CHISA 2004 (pp. 379-471)*, *77*(3), 672-679.

[27]Hawley, S. A. (1971). Reversible pressure-temperature denaturation of chymotrypsinogen. *Biochemistry*, *10*(13), 2436-2442.

[28]Hendrickx, M., Ludikhuyze, L., Van den Broeck, I. & Weemaes, C. (1998). Effects of high pressure on enzymes related to food quality. *Trends in Food Science & Technology*, *9*(5), 197-203.

[29]Hendrickx, M. & Knorr, D. (2001). *Ultra High Pressure Treatments of Foods*. Kluwer Academic, New York.

[30]Heremans, K. & Smeller, L. (1998). Protein structure and dynamics at high pressure. *Biochim Biophys Acta*, *1386*(2), 353-70.

[31]Heremans, K. (2001). The Effects of High Pressure on Biomaterials. In M. Hendrickx & D. Knorr. *Ultra High Pressure Treatments of Foods* (pp. 23-51). Kluwer Academic, New York.

[32]Hoehler, R. & Cohen-Addad, S. (2005). Rheology of liquid foam. *Journal of Physics: Condensed Matter*, *17*, r1041-r1069.

[33]Huppertz, T., Fox, P. F., de Kruif, K. G. & Kelly, A. L. (2006). High pressure-induced changes in bovine milk proteins: A review. *Biochimica et Biophysica Acta (BBA) - Proteins & Proteomics;Proteins Under High Pressure*, *1764*(3), 593-598.

[34]Indrawati, L., Wang, Z., Narsimhan, G. & Gonzalez, J. (2008). Effect of processing parameters on foam formation using a continuous system with a mechanical whipper. *Journal of Food Engineering*, *88*(1), 65-74.

[35]Jang, W., Nikolov, A. & Wasan, D. T. (2006). The destabilization of aerated food products. *Journal of Food Engineering*, *76*(2), 256-260.

[36]Joseph, D. D. (1997). Questions in Fluid Mechanics: Understanding Foams and Foaming. *Journal of Fluids Engineering*, *119*(3), 497-498.

[37]Kendall, D. P. (2000). A Short History of High Pressure Technology From Bridgman to Division 3. *Journal of Pressure Vessel Technology*, *122*(3), 229-233.

[38]Knorr, D. (1993). Effects of High-Hydrostatic-Pressure Processes on Food Safety and Quality. *Food Technology*, *47*(6), 156-&.

[39]Knorr, D., Schlüter, O. & Heinz, V. (1998). Impact of high hydrostatic pressure on phase transitions of foods. *Food Technology*, *52*(9), 42-45.

[40]Kunugi, S. & Tanaka, N. (2002). Cold denaturation of proteins under high pressure. *Biochimica et Biophysica Acta (BBA) - Protein Structure and Molecular Enzymology*, *1595*(1-2), 329-344.

[41]Li, S.-Q., Zhang, H. Q., Balasubramaniam, V. M., et al. (2006). Comparison of Effects of High-Pressure Processing and Heat Treatment on Immunoactivity of Bovine Milk Immunoglobulin G in Enriched Soymilk under Equivalent Microbial Inactivation Levels. *J. Agric. Food Chem.*, *54*(3), 739-746.

[42]Luscher, C., Balasa, A., Frohling, A., Ananta, E. & Knorr, D. (2004). Effect of High-Pressure-Induced Ice I-to-Ice III Phase Transitions on Inactivation of Listeria innocua in Frozen Suspension 10.1128/AEM.70.7.4021-4029.2004. *Appl. Environ. Microbiol.*, *70*(7), 4021-4029.

[43]Luscher, C. M. (2008). *Effect of high pressure - low temperature phase transitions on model systems, foods and microorganisms*. PhD thesis, Berlin, Berlin University of Technology, 158.

[44]Macdonald, A. G. (1992). Effects of high hydrostatic pressure on natural and artificial membranes. In C. Banly, K. Hayashi, K. Heremans & P. Masson. *High Pressure and Biotechnology* (pp. 67-75). Colloque INSERM.

[45]Marshall, R. T., Goff, H. D. & Hartel, R. W. (2003). *Ice Cream*. Kluwer Academic / Plenum Publishers, New York.

[46]Masson, P. (1992). Pressure denaturation of proteins. In C. Banly, K. Hayashi, K. Heremans & P. Masson. *High Pressure and Biotechnology* (pp. 89-99). Colloque INSERM.

[47]Mathys, A. (2008). *Inactivation mechanisms of Geobacillus and Bacillus spores during high pressure thermal sterilization*. PhD thesis, Berlin, Berlin University of Technology, 162.

[48]Michel, M. & Autio, K. (2001). Effects of High Pressure on Protein- and Polysaccharide-Based Structures. In M. Hendrickx & D. Knorr. *Ultra High Pressure Treatments of Foods* (pp. 189-214). Kluwer Academic, New York.

[49]Michel, M., Leser, M. E., Syrbe, A., et al. (2001). Pressure effects on whey protein-pectin mixtures. *Lebensmittel-Wissenschaft Und-Technologie-Food Science and Technology*, *34*(1), 41-52.

[50]Michel, M. (2006). personal communication. Lausanne.

[51]Mozhaev, V. V., Heremans, K., Frank, J., Masson, P. & Balny, C. (1996). High pressure effects on protein structure and function. *Proteins: Structure, Function, and Genetics*, *24*(1), 81-91.

[52]Murray, B. S. (2007). Stabilization of bubbles and foams. *Current Opinion in Colloid & Interface Science*, *12*(4-5), 232-241.

[53]Niranjan, K. (1999). An introduction to bubble mechanics in foods. *Bubbles in Food*, 3-9.

[54]Niven, G. W., Miles, C. A. & Mackey, B. M. (1999). The effects of hydrostatic pressure on ribosome conformation in Escherichia coli : an in vivo study using differential scanning calorimetry. *Microbiology*, *145*(2), 419-425.

[55]Oh, H. E., Pinder, D. N., Hemar, Y., Anema, S. G. & Wong, M. (2008). Effect of high-pressure treatment on various starch-in-water suspensions. *Food Hydrocolloids*
8th International Hydrocolloids Conference, *22*(1), 150-155.

[56]Otero, L. & Sanz, P. D. (2000). High-Pressure Shift Freezing. Part 1. Amount of Ice Instantaneously Formed in the Process. *Biotechnology Progress*, *16*, 1030-1036.

[57]Otero, L. & Sanz, P. D. (2006). High-Pressure-shift freezing: Main factors implied in the phase transition time. *Journal of Food Engineering*, *72*, 354-363.

[58]Pakharukov, Y. V. & Shevnina, T. E. (2001). Foam stabilization by surfactants: A fractal-percolation fracture model. *Technical Physics Letters*, *27*, 127-128.

[59]Perkins, J. (1820). On the Compressibility of Water. *Philosophical Transactions of the Royal Society of London*, *110*, 324-329.

[60]Perkins, J. (1826). On the progressive compression of water by a high degree of force, with trials on the effect of other fluids. *Philosophical Transactions of the Royal Society of London*, *116*, 541-547.

[61]Privalov, P. L. (1982). Stability of proteins: proteins which do not present a single cooperative system. *Adv. Prot. Chem.*, *35*, 1-104.

[62]Ross, S. & Morrison, I. D. (2002). *Colloidal Dispersions: Suspensions, Emulsions, and Foams*. John Wiley & Sons.

[63]Royer, C. A. (2005). Insights into the role of hydration in protein structure and stability obtained through hydrostatic pressure studies. *Brazilian journal of medical and biological research*, *38*, 1167-1173.

[64]Schlüter, O. (2004). *Impact of High Pressure - Low Temperature Processes on Cellular Materials Related to Foods*. PhD thesis, Berlin, Berlin University of Technology, 172.

[65]Schuricht, H., Schierbaum, F. & Fleischer, L.-G. (1998). Hochdruckeinfluß auf gelbildende Maltodextrine Teil 1: Makrostruktur, thermodynamische und fluiddynamische Wirkungen. *Starch - Stärke*, *50*(11-12), 499-511.

[66]Silva, J. L. & Weber, G. (1993). Pressure Stability of Proteins. *Annual Review of Physical Chemistry*, *44*, 89-113.

[67]Smeller, L. (2002). Pressure-temperature phase diagrams of biomolecules. *Biochimica Et Biophysica Acta-Protein Structure and Molecular Enzymology*, *1595*(1-2), 11-29.

[68]Smelt, J. P., Hellemons, J. C. & Patterson, M. (2001). Effects of High Pressure on Vegetative Microorganisms. In M. Hendrickx & D. Knorr. *Ultra High Pressure Treatments of Foods* (pp. 55-76). Kluwer Academic, New York.

[69]Stolt, M., Oinonen, S. & Autio, K. (2000). Effect of high pressure on the physical properties of barley starch. *Innovative Food Science & Emerging Technologies*, *1*(3), 167-175.

[70]Ulmer, H. M., Herberhold, H., Fahsel, S., Gänzle, M. G., Winter, R. & Vogel, R. F. (2002). Effects of pressure-induced membrane phase transitions on inactivation of HorA, an ATP-dependent multidrug resistance transporter, in *Lactobacillus plantarum*. *Appl. Environ. Microbiol.*, *68*, 1088-1095.

[71]Urrutia Benet, G., Schlüter, O. & Knorr, D. (2004). High pressure–low temperature processing. Suggested definitions and terminology. *Innovative Food Science and Emerging Technologies*, *5*(4), 413-427.

[72]Urrutia Benet, G. (2005). *High Pressure Low temperature Processing of Foods: Impact of Metastable Phases on Process and Quality Parameters*. PhD, Berlin University of Technology, 196.

[73]Weaire, D., Cox, S. & Brakke, K. (2006). Liquid Foams - Precursors for Solid Foams. In P. I. P. C. Dr. Michael Scheffler. *Cellular Ceramics* (pp. 18-29.

[74]WHO (2002). WHO Global Strategy for Food Safety: safer food for better health.

[75]Yaldagard, M., Mortazavi, S. A. & Tabatabaie, F. (2008). The principles of ultra high pressure technology and its application in food processing/preservation: A review of microbiological and quality aspects. *African Journal of Biotechnology*, *7*, 2739-2767.

[76]Zheligovskaya, E. A. & Malenkov, G. G. (2006). Crystalline water ices. *Uspekhi Khimii*, *75*(1), 64-85.

Chapter III Technical aspects of High Pressure-Low Temperature freeze-process design and development for aerated products

1 Introduction

In conventional HP applications and HPLT research, the treated products are mostly air-free to avoid volume changes under pressure. Different aspects of temperature measurement, sample packaging and general process setups in the HPLT treatment of aerated dairy based emulsions are discussed in this chapter and basic issues in the batch and continuous process development identified. In this respect the HPLT processes of central concern are HP freeze processes within the HPLT domain that induce crystallization effects at temperatures below the atmospheric freezing point of the product. Accordingly the process pressure range was chosen from 0.1 to 360 MPa at temperatures from 15 to -50°C, which covers the liquid state of water as the starting region for pressure shift freezing (PSF) and pressure assisted freezing (PAF) treatments and the subzero ice modifications that have a phase boundary to the liquid state and are relevant for pressure induced crystallization (PIC). The relevant ice modifications in this area are ice I, ice III and ice V. Generally, the HPLT domain can be defined by the p-T coordinates that describe the liquid or solid states of water at temperatures below the atmospheric freezing point. Figure III-1 shows the p,T region of the HPLT domain according to this definition and the process window relevant for the present study in the water phase diagram. The process-aim of the investigated HPLT freeze processes is a frozen or liquid product at atmospheric pressure, with modified physico-chemical characteristics. The basic cause for this can be high freezing rates, homogeneous ice I nucleation and instant ice formation, recrystallization effects and/or p-T induced modification of functional ingredients.

As discussed in chapter II, several process options arise in the HPLT domain, including freezing-, thawing and liquid subzero storage processes. A number of research groups have conducted profound work, dealing with different HPLT processes in the past but not all of them were using the same terminology, so that processes description in different publications is rather inconsistent. In this work all process description follows the definitions of Urrutia, Schlüter and Knorr, who suggested a clear and detailed terminology for HPLT processes with and without water phase transitions (Urrutia Benet et al., 2004). The criteria for these definitions are based on the aim of the global process, in which the initial and final states of the product are at atmospheric pressure. In the scope of the present work, the definitions of pressure *shift,* pressure *induced* and pressure *assisted* are especially relevant for a clear understanding of cause and effect in HPLT – freeze processes and will be discussed in detail in this chapter.

HPLT processes that include a water phase change from the liquid to the solid phase (crystallization) are pressure assisted freezing (PAF), pressure induced freezing (PIF) and pressure shift freezing (PSF) (Urrutia Benet et al., 2004). However, PIF is not in the focus of the present work, as it does not provide any crystallization effects that are not covered by PSF and PAF in the pressure range from 0.1 to 360 MPa. In addition to the PSF and PAF processes that induce a liquid – solid phase change, the recrystallization effects that occur during solid – solid phase transition were investigated. The recrystallization of ice I to ice III and back to ice I is the process aim of pressure induced crystallization (PIC).

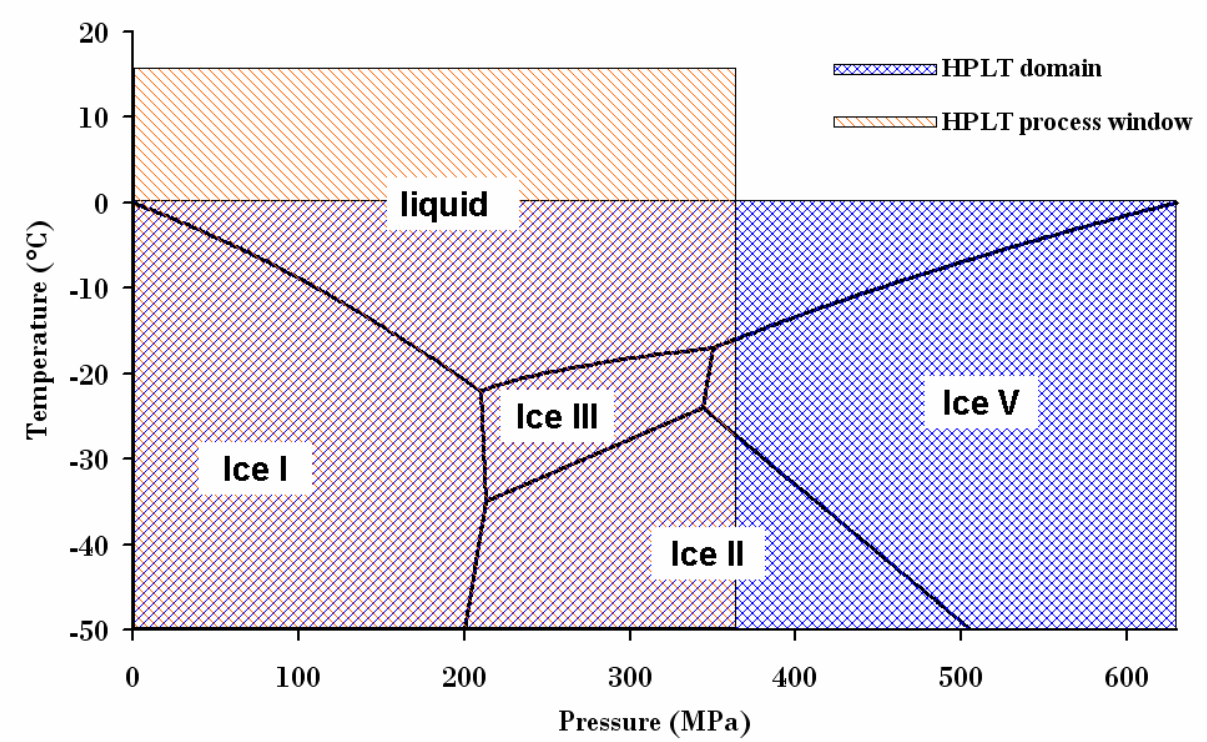

Figure III-1: p-T coordinates of the HPLT domain (0°C to -50°C / 0.1 MPA to 630 MPa) and the relevant HPLT process window covering the liquid state and the subzero ice modifications ice I, ice III and ice V.

An important aspect in the HPLT process control is the detection of phase changes, i.e. water crystallization and recrystallization. Based on differences in density and latent heat of the different ice modifications and the liquid phase, pressure and temperature are potential indicators for crystallization effects. For a temperature based detection of phase changes, a direct measurement of the temperature in the sample material is required. Hence, one or more thermocouples have to be in direct contact to the sample material, which includes penetration of the product packaging in most of the HP units. A major problem in this way of temperature measurement is the risk of contamination of the sample material with the pressure transmitting medium (PTM). This is of special relevance in liquid or paste-like products that mix with PTM upon contamination and changes the physico-chemical properties of the product (e.g. melting point) are induced. High pressure treatment of aerated food samples is always accompanied by high volume changes of the product during the pressurization and pressure release step. As a consequence, in batch processes, pressure build up times are slowed down and the risk of contamination of penetrated samples increases. In the food industry HP processes are designed as batch or semi-batch processes (Yuste, Capellas, Pla, Fung & Mor-Mur, 2001). Continuous processing of liquid foods is possible (Yaldagard et al., 2008) but besides conventional high pressure homogenisation, no continuous system has been introduced so far, even if already established in the chemical industry. A schematic overview about the relevant processes in the HPLT domain in the pressure range from 0.1 to 360 MPa is given in Figure III-2. Adiabatic heating/cooling effects and temperature changes due to crystallization/recrystallization are not considered in this scheme.

2 High Pressure-Low Temperature freeze processes

2.1 Pressure shift freezing (PSF)

During PSF an aqueous matrix is pressurized in the liquid state and cooled under pressure to a temperature well below its atmospheric freezing point without ice formation. Subsequently, freezing is triggered by an instant pressure release (pressure shift), which implicates sudden supercooling. Homogeneous nucleation occurs instantly and results in uniform distribution and a high number of small ice crystals. The ice crystals that grow in this process are small, irregularly shaped and without specific orientation. Experiments with pork meat showed intra- and extracellular ice crystals with a mean diameter <7 µm. In contrast, ice crystals were not uniformly distributed in samples frozen at atmospheric conditions with a mean diameter of 19 µm for freezing in liquid nitrogen and of over 31 µm for air blast freezing (Lévy, Dumay, Kolodziejczyk & Cheftel, 1999). During the PSF the ice crystals form during pressure release and liquid water is instantly frozen to ice I to some extent (Thiebaud, Dumay & Cheftel, 2002; Otero & Sanz, 2006a). The percentage of instantly formed ice depends on the pressure-temperature conditions at the time of pressure release. The higher the pressure and the lower the temperature at which expansion takes place, the higher the percentage of instantaneously formed ice. This assumption goes back to the statement of Otero and Sanz (Otero & Sanz, 2000), pointing out that the amount of ice instantaneously formed in the process can be increased by increasing the pressure before expansion. However, not all water is transformed to ice during pressure release. During subsequent atmospheric freezing latent heat has to be

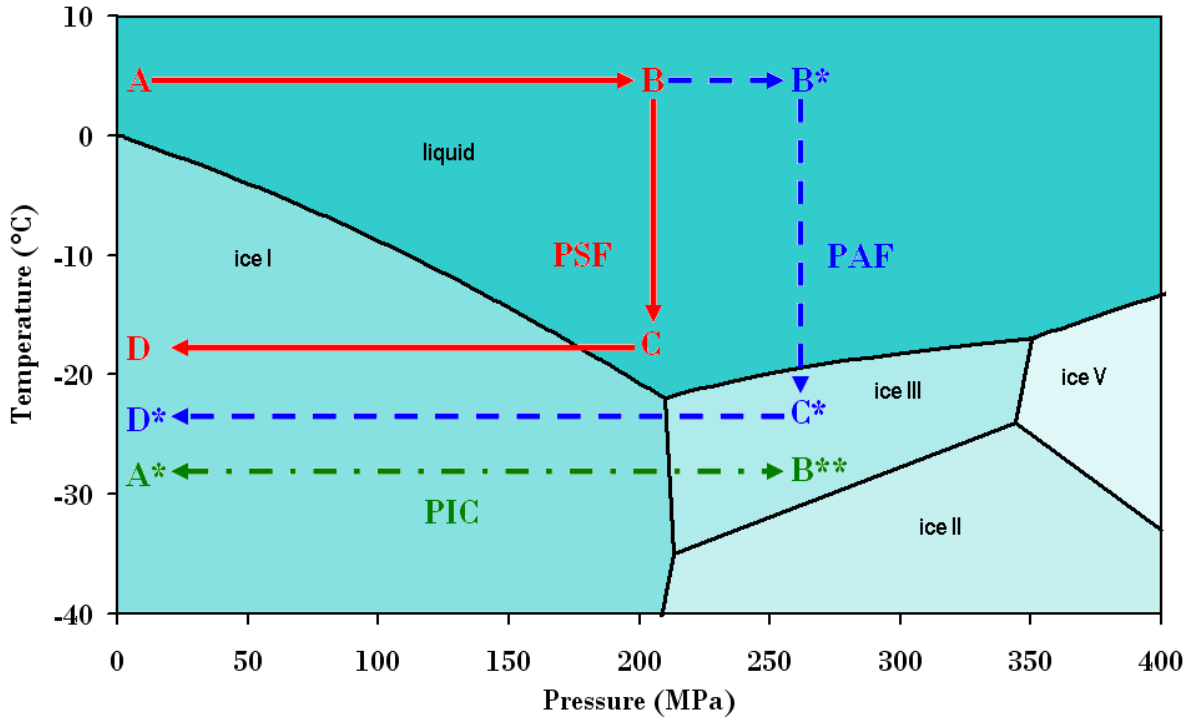

Figure III-2: Schematic process description of: PSF (A-B-C-D), PAF (A-B*-C*-D*) and PIC (A*-B-A*) in the water phase diagram after Bridgman (Bridgman, 1912).**

removed across the matrix surface (Knorr et al., 1998). The formation of ice during pressure release in the PSF process shortens the total water phase transition time compared to conventional freezing (Lévy et al., 1999; Schlüter, 2004). This is because during subsequent atmospheric freezing less water has to be frozen and the total amount of latent heat required for the phase transition is reduced. In addition the heat transfer is improved by the already frozen water fraction at the beginning of atmospheric freezing. The phenomenon of instantaneous ice formation during pressure release is discussed in detail in Chapter IV and

VI. As other freezing methods the PSF treatment potentially inactivates microorganisms but due to high freezing rates and a relatively low maximum pressure the lethal effect on viable cells is rather negligible (Volkert, Ananta, Luscher & Knorr, 2008).

2.2 Pressure assisted freezing (PAF)

During PAF a product is frozen at elevated pressure. In the HPLT area defined in Figure III-1, the resulting ice modifications can be ice I, III or V. Accordingly the processes are referred to as PAF I, PAF III and PAF V. Which ice modification occurs depends on the pressure-temperature conditions. Exploiting the high density of ice III and V, PAF has been in the focus of several research activities that aimed on minimizing the structural damages to foodstuff during freezing and thawing (Cheftel, 1995). PAF involves heterogeneous nucleation and a growing ice-body outgoing from the nucleation site throughout the product. Due to lower latent heat of crystallization at high pressures, water freezing rates are possibly increased with increasing pressure. In practice, however, the freezing temperature decreases with increasing pressure and the cooling medium must be cooled to lower temperatures to maintain a sufficient ΔT. In the pressure range of interest in this study, the relevant ice modifications are ice I, III and V. The scheme in Figure III-2 shows PAF from the liquid phase to ice III. According to the freezing pressure, the process may also induce nucleation to ice I or ice V. Supercooling occurs to a larger extend with increasing pressure and crystallization rates may be reduced at higher pressures (Urrutia Benet et al., 2007; Luscher, 2008). PSF effects can occur in this process, if not all water is frozen before pressure release.

2.3 Pressure induced crystallization (PIC)

Pressure induced crystallization can be regarded as a special form of pressure shift freezing that starts with a frozen or partly frozen product. The general p-T pathways of PSF and PIC are identical, except from the cooling step under pressure, which is not necessarily part of the PIC treatment. The treatment starts at atmospheric pressure with the pressurization of a frozen sample. The pressure is increased beyond the ice I to ice III phase boundary until recrystallization of ice I to iceII. During the subsequent pressure release the ice III fraction recrystallizes back to ice I. Contrary to the conventional PSF, the aim of this treatment is not homogeneous nucleation and rapid crystallization in the first place but recrystallization of ice I to ice III and back to ice I. This solid- solid phase shift induces high density changes in the water phase and is reported to induce inactivation of microorganisms more effectively than the liquid – ice I phase transition in conventional PSF (Luscher, 2008). PIC can also involve recrystallization of higher ice modifications (e.g. ice III to ice V). However, these types of recrystallization are not discussed in the present work.

3 Experimental setup

The following section gives an overview about the aeration system and different HPLT units and process setups that were used in the scope of the present study and investigates several aspects of process monitoring. The experimental HPLT setup includes two batch systems and one continuously operating system. Both batch systems, the laboratory and the pilot scale unit operate with indirect pressurization, meaning the pressure build up is achieved by an external intensifier.

3.1 Aeration system

For the controlled aeration of different dairy emulsions a Minimondo A-05 P13774 (Haas Mondomix, Almere, Netherlands) was used. The liquid product is manually fed into the jacketed hopper. The hopper is connected to the main feed pump which delivers the product to the mixing head whilst air is injected. Pins on both rotor and stator see to it that the mass is aerated under controlled pressure. The mixing head provides axial flow to the product (constant shear force). After aeration the product is delivered to the product outlet. A process diagram of the aeration system is shown in Figure III-3.

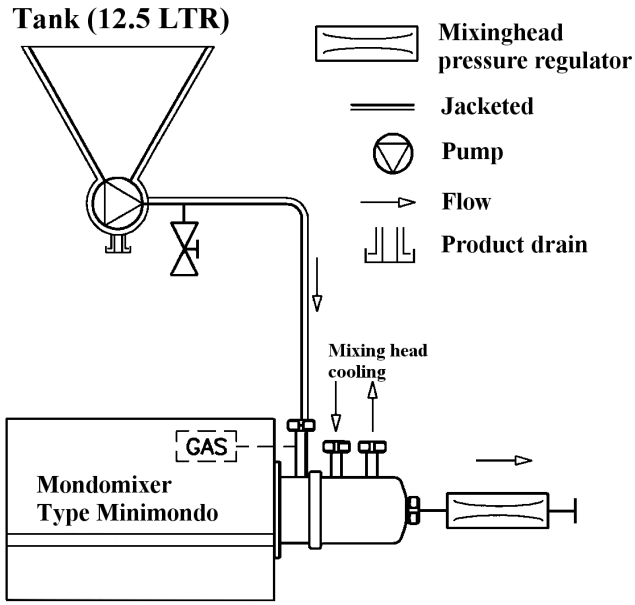

Figure III-3: Schematic description of the Minimondo aeration system (Haas Mondomix, Almere, Netherlands).

3.2 HPLT processing

3.2.1 Batch systems

3.2.1.1 Laboratory scale unit

The lab scale HPLT unit consist of a vertically installed copper-beryllium high pressure vessel (Unipress, Warsaw, Poland), connected to a manually driven pressure intensifier. The unit is operational in a pressure range from 0.1 MPa to 1 GPa at temperatures from -50°C to 150°C and has a 3.7 ml treatment chamber. A schematic drawing of the unit is given in Figure III-4. The unit can be equipped with different type K thermocouples and run with two different chamber designs. In the standard configuration the sample material is placed directly in the treatment chamber, which is filled with the PTM during or before pressurization. To avoid contamination with the PTM, the sample material needs a pressure and temperature resistant packaging in this setup, e.g. a polyethylene bag or a plastic container. To measure the sample temperature in this setup, the sample packaging is penetrated by a thermocouple. The second setup is based on a flexible treatment chamber. For the flexible chamber setup an open metal cylinder, serving as the treatment chamber for the sample material, is screwed to the top plug of the HP vessel. The bottom of the cylinder is sealed by a Teflon plug, which allows compensation of volume changes inside the cylinder by vertical movement. The thermocouples in this setup measure the sample temperature inside the flexible treatment chamber without the risk of contamination due penetration of the sample packaging.

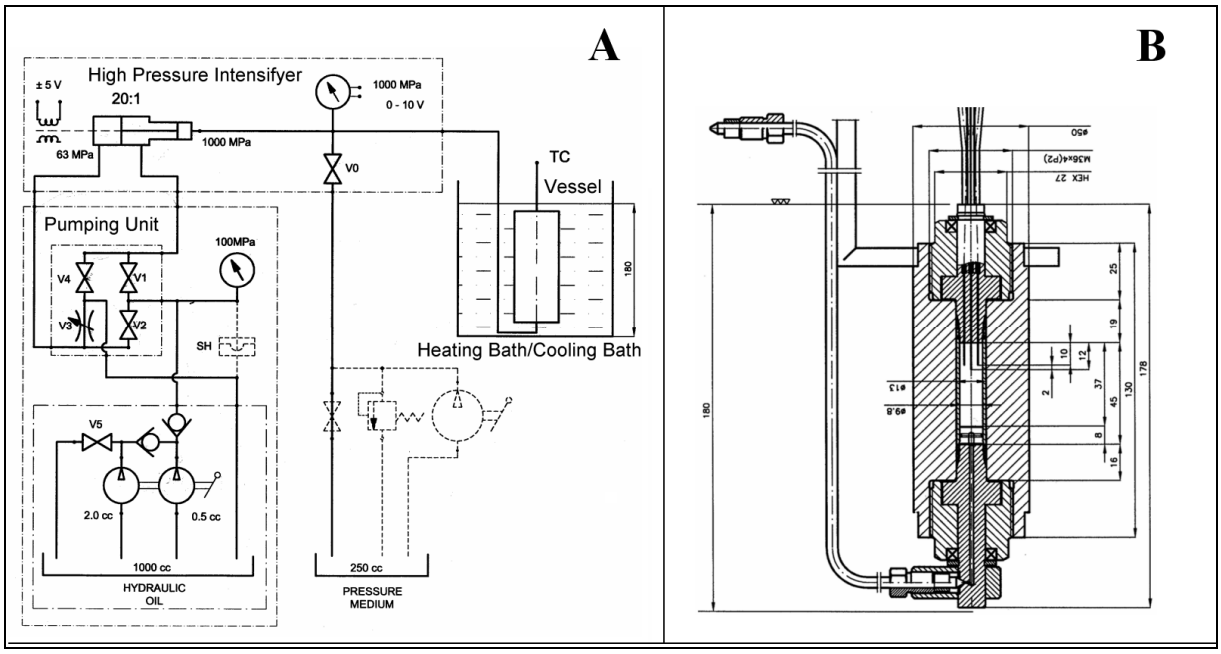

Figure III-4: Schematic drawing of the laboratory scale HPLT unit (A) **and a cross-sectional view of the high pressure vessel with the HP tubing connector (UNIPRESS, Warsaw, Poland)** (B)**.**

The flexible chamber setup allows accurate sample temperature measurement in the treatment of aerated samples. The treatment chamber with the flexible Teflon plug is shown in Figure III-5.

Figure III-5. Flexible treatment chamber (UNIPRESS, Warsaw, Poland) with movable rubber sealed Teflon plug: open chamber with female thread (left), closed treatment chamber with inserted Teflon plug (right).

3.2.1.2 Pilot scale unit

The pilot scale HPLT unit was developed at the Technische Universitaet Berlin (TUB) and is schematically shown in Figure III-6. The unit is based on a vertically installed high pressure vessel (Uhde GmbH, Hagen, Germany) with 1.6 litres internal volume, 55 mm internal diameter and 700 mm height. The vessel is equipped with a cooling jacket and operates in a pressure range from 0.1 to 360 MPa. The process temperature is controlled externally by a cryostat (Ultra-Kryomat RUK 50-D, Lauda, Germany). An 80% (v/v) Ethanol water mixture is used as cooling medium, allowing heating or cooling the treatment chamber from 30°C to -45°C. The pressure transmitting medium (PTM) is also 80% (v/v) ethanol/water (freezing point < -59°C). The medium was chosen because of its non-toxicity, its suitable chemical and thermo-physical properties within the pressure and temperature range used and its industrial applicability. Pressurisation is obtained with an air driven piston pump type DXS HF-602

(Haskel, California, USA). The unit can be equipped with different setups of type K thermocouples, allowing temperature measurement of the samples and/or the PTM. The process pressure is measured with a pressure transducer (Intersonde HP28, Watford, England).

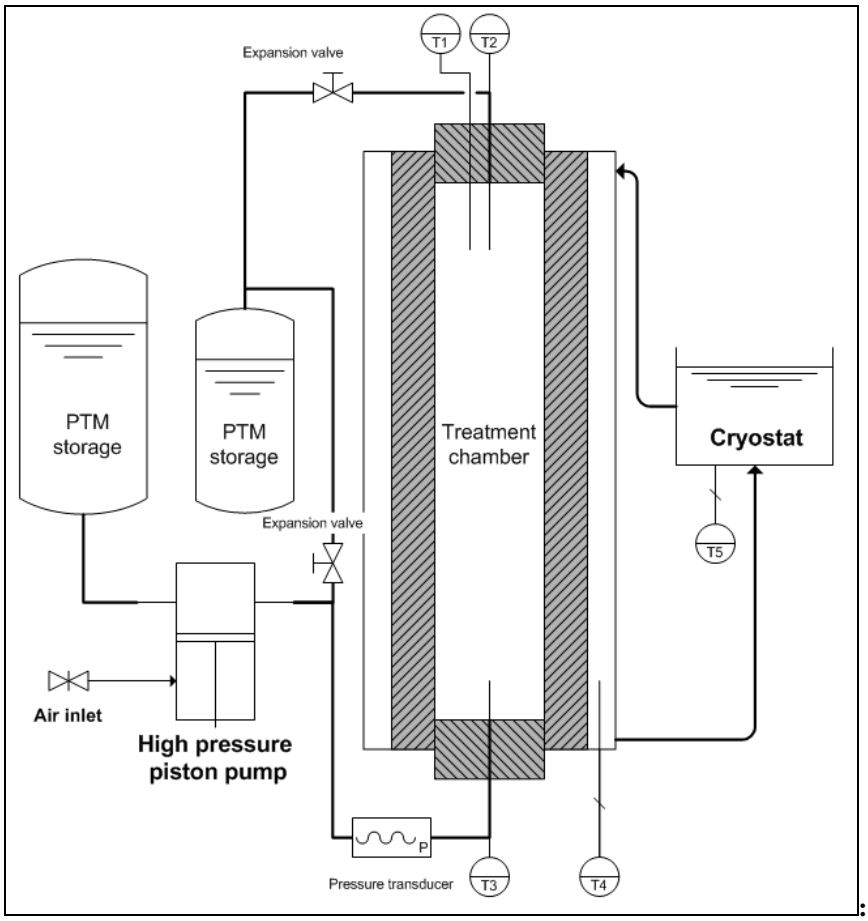

Figure III-6: Schematic drawing of the pilot scale HPLT unit, developed at the TUB.

During the HPLT treatments the following parameters were monitored and recorded: temperature of the PTM (T3, T2 and/or T1), sample temperature (T3, T2 and/or T1), cooling media temperature (T4), cryostat outlet temperature (T5) and the internal pressure, using type K (Ni / Cr-Ni) thermocouples, a KPCI-3101 data acquisition system and TestPoint (Keithley Instruments, Inc., Cleveland, USA). P/T acquisition at 10 Hz allows precise recording of temperature and pressure during the fast pressure release. A picture of the pilot scale unit, which was developed at the Technical University Berlin and further optimized for HPLT applications during the time of this work and a technical drawing of the high pressure vessel are shown in Figure III-7.

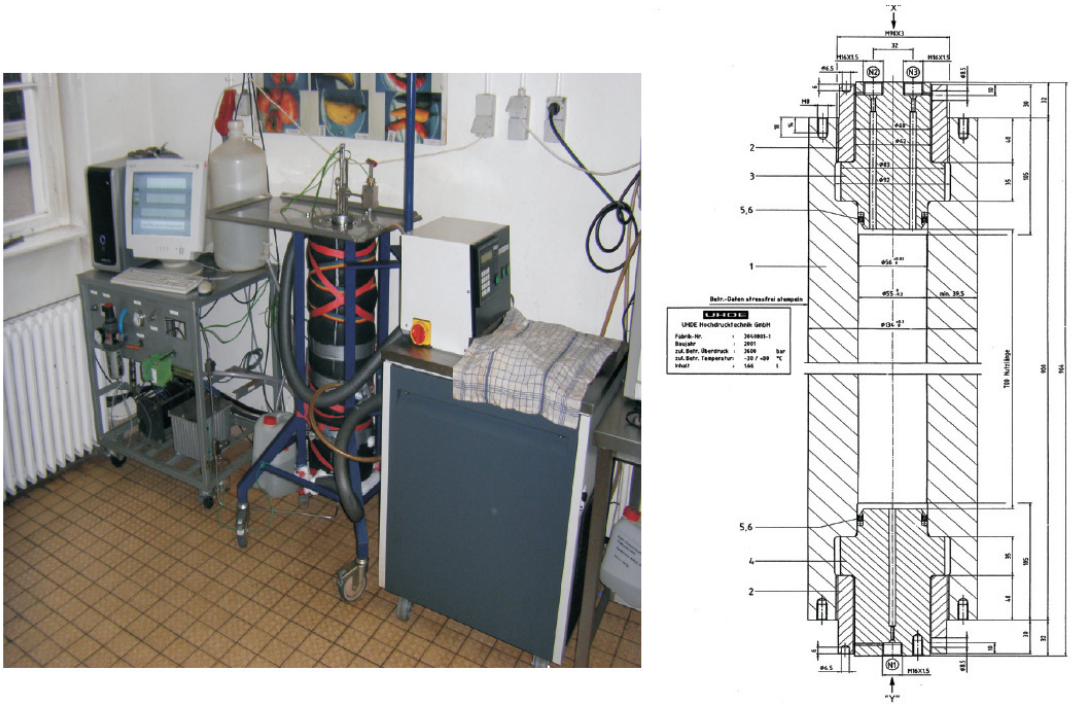

Figure III-7: HPLT pilot unit: equipment with cryostat and data acquisition system (left), technical drawing of the HP vessel (Uhde GmbH, Hagen, Germany) (right)

3.2.1.3 Sample packaging

During HPLT treatment the packaging of aerated products is exposed to high volume changes due to the extreme compressibility of incorporated gases. In this respect, the crucial steps are pressurization and the pressure release, as in this phases the pressure gradient between the sample and the PTM are highest (Figure III-8). In addition to the volume changes due to the compressibility of gas and liquids under pressure, the volume changes caused by ice formation have to be taken into account in the sample packaging design.

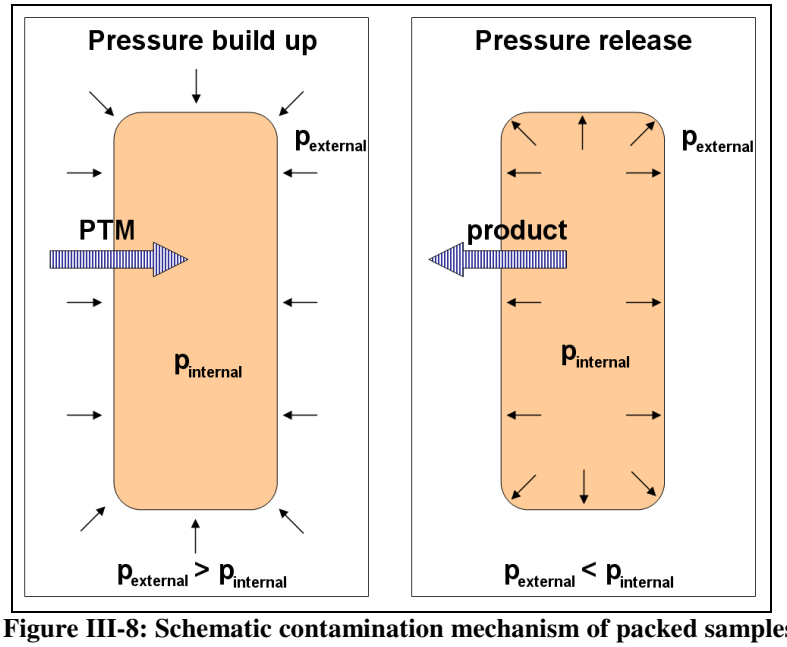

Figure III-8: Schematic contamination mechanism of packed samples during pressure build up and pressure release. The pressure inside the packaging is referred to as $p_{internal}$ and the pressure in the surrounding pressure transmitting medium (PTM) as $p_{external}$. The hatched arrow indicates possible direction of mass transfer.

High flexibility of the sample packaging is required to compensate volume changes of the sample. According to the analytical demands and the design of the treatment chamber, different sample packaging was used. For simple packaging with no internal temperature measurement and for samples that had not to meet special demands on their shape after treatment (e.g. cylindrical shape for texture analyses), simple polyethylene bags (PE) were used. The PE bags were heat sealed after filling and a double packing reduces the risk of contamination. For experiments that required a region of constant shape and volume in the sample (e.g for temperature measurement at the sample surface and in the sample centre), semi flexible packaging were developed for the laboratory- and the pilot scale unit. The flexible treatment chamber (Figure III-5) in the lab-scale unit is not a packaging as such, as it is part of the HP vessel top plug. However, the working principle of the device was transferred to the development of a semi flexible sample packaging for the pilot scale unit. The container consists of a stainless-steel cylinder with a threaded coupling on top and a moveable piston on the bottom side. The metal cylinder has an internal diameter of 53 mm and a total length of 200 mm. Figure III-9 shows the technical drawing of the device. After filling, the container is closed with the threaded lid on the top side. To avoid leakage during movement in the cylinder, the Teflon piston is equipped with 3 rubber seals (o-rings). To minimize the risk of contamination with the PTM, the Teflon piston is designed to compensate volume changes of up to 40% without an overlap of the contact points between the rubber seals and the cylinder wall of the first and last o-ring. At the time of the experiments, no thermocouples were installed in the treatment chamber. Since the container is not exposed to high pressure gradients to the surrounding media in normal function, a simple thermocouple installation through the lid is possible.

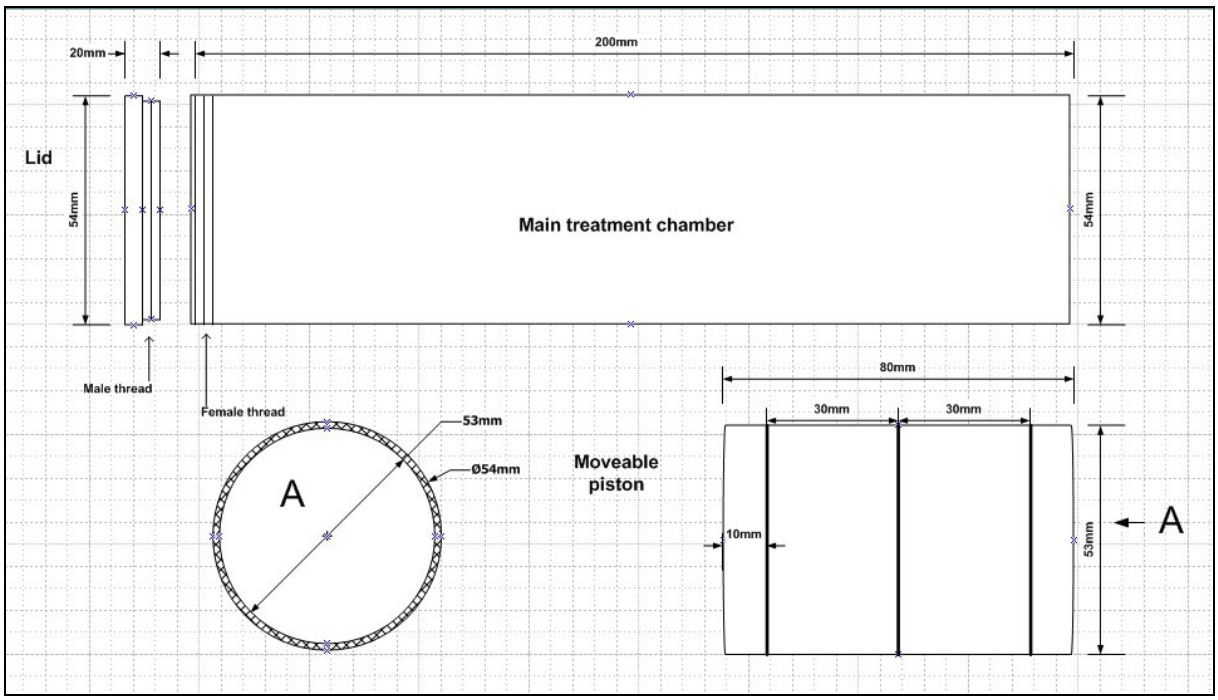

Figure III-9: Technical drawing of the semi-flexible pilot scale HP sample container, developed at the TUB.

The second semi-flexible sample packaging that was used for the production of cylindrical aerated samples is a half open plastic shell which is closed with a flexible PE bag on the bottom side. During compression, the sample material accumulates in the plastic shell, whereas the PE bag serves as a compression zone. Temperature measurement is achieved by penetration of the plastic shell top with type K (Ni / Cr-Ni) thermocouples. Figure III-10 schematically shows the function of the device.

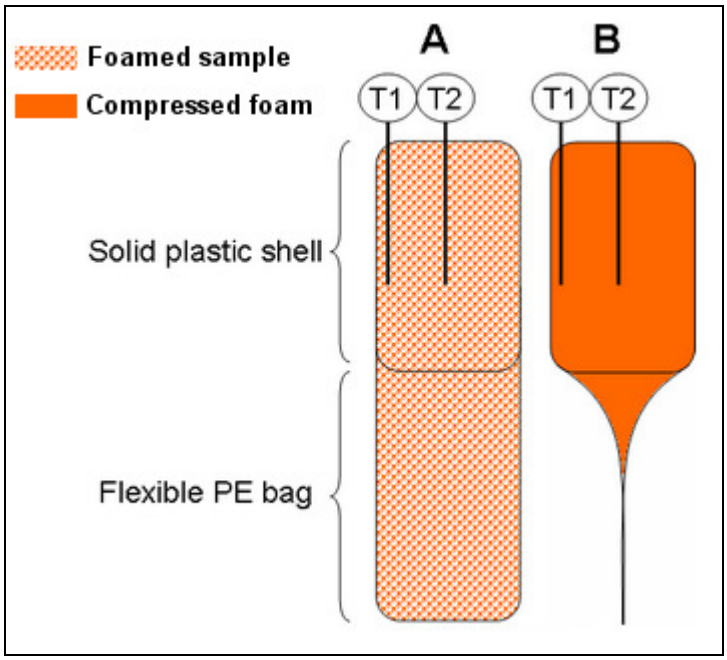

Figure III-10. Schematic drawing of the semi flexible plastic shell packaging for aerated products with thermocouples for surface (T1) and core (T2) temperature measurement at atmospheric pressure in a foamed sample (A) and in the liquid an gas free sample during compression (B).

3.2.2 Continuous process design

Continuous processing describes a method of processing in which materials are added and products removed continuously. In the food industry, most processes are based on this concept. The high efficiency of continuous processes usually makes them economically superior to batch or semi-batch processes. In addition, continuous processing offers advantages in the monitoring of process parameters (i.e. temperature) and eliminates the risk of product contaminations with the PTM. However, high pressure treatments in the food industry are batch or semi batch processes and no continuous system has been industrially introduced so far, except for high pressure homogenisation processes. The latter process involves high pressure treatment of a liquid product but does not cover the directly pressure induced effects but exploits mechanical shear force effects that are driven by the pressure gradient at the homogenizer outlet.

3.2.2.1 Experimental continuous high pressure system

In the experimental continuous HPLT unit that was developed in this work, a liquid or aerated product is cooled or frozen under high pressure to ice I, ice III or ice V, depending on the system pressure and temperature conditions. The unit is operational at temperatures to -45°C in a pressure range from 0.1 to 400 MPa. Different from the batch system, no pressure transmitting media is required. The pressure is build up by direct compression of the product. On the low pressure side, the liquid product is foamed under controlled air volume inlet in a Minimondo aeration system (Haas Mondomix, Almere, Netherlands). An upstream screw pump provides pre-compression (6 bar) of the aerated product and delivers the compressed foam to an air driven high pressure piston pump type DXS HF-602 (Haskel, California, USA). On the high pressure side the product is conveyed through a high pressure tubing coil (internal pipe diameter 2.4 mm) that is immersed into a cryostat controlled cooling bath. In the cooling coil the product can be cooled under pressure to a minimum temperature of -45°C. After passing the coil, the product pressure is released by a manually controlled micro metering backpressure-expansion valve. The valve is scaled and can be adjusted from 100%

(fully open) to 0% (fully closed). The product throughput is controlled by the operating pressure of the piston pump air inlet. Figure III-11 shows the schematic process diagram of the continuous HPLT unit.

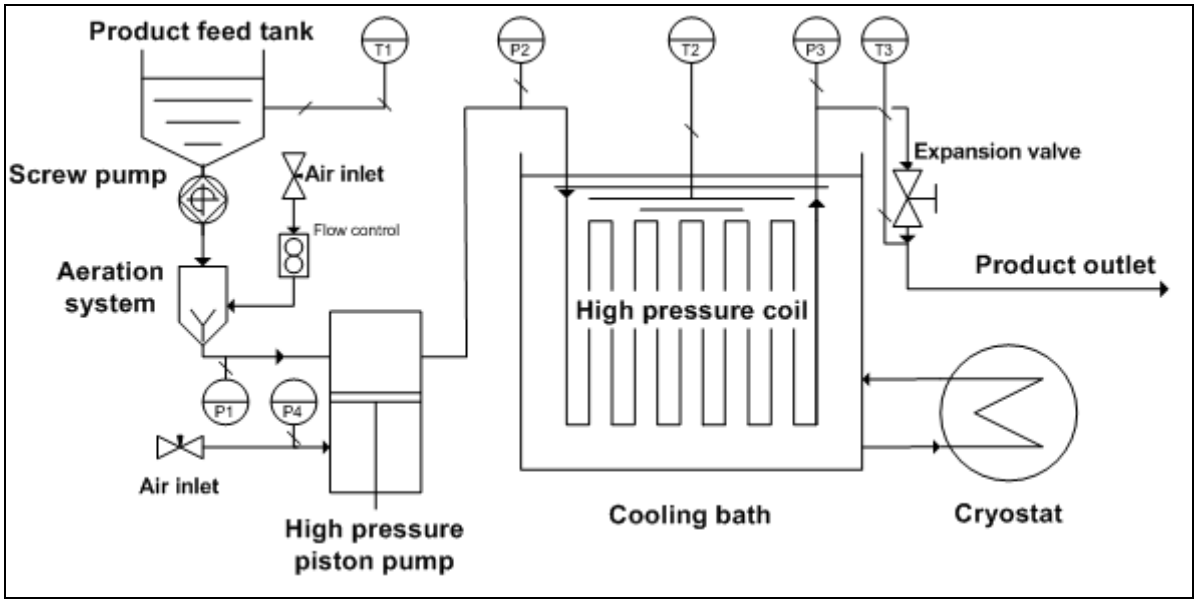

Figure III-11: Flow diagram of the experimental continuous HPLT unit, developed at the TUB.

Type K (Ni / Cr-Ni) thermocouples are installed in the product feed tank (T1), in the cooling bath (T2) and after the expansion valve (T3). The aeration system outlet pressure on the low pressure side (P1) is measured with a pressure gauge. On the high pressure side, pressure is measured with pressure transducers (Intersonde HP28, Watford, England) in the HP tubing before (P2) and after (P3) the cooling coil. The system pressure is controlled by the low pressure air inlet (P4) of the piston pump. Pressure and temperature is monitored and recorded with a KPCI-3101 data acquisition system and TestPoint software (Keithley Instruments, Inc., Cleveland, USA). The P/T acquisition rate is 10 Hz.

3.3 Microbial methods

To evaluate the effect of the HPLT treatment on the microbial safety of the dairy product, samples were taken at the critical points in the process (feed tank, aeration system outlet and after HPLT treatment). 1 ml samples were plated on standard count agar, GSP-agar and VRBD-agar (Merck, Darmstadt, Germany). The cell count was determined in triplicates.

4 Results and discussion

4.1 Batch processing

4.1.1 Temperature and pressure control

Temperature and pressure are closely connected parameters. In closed systems they affect each other following the laws of thermodynamics. Following the first and the second law of thermodynamic and by re-arrangement of the Maxwell equations, the heating during the compression and the cooling during the decompression can be described as a function of thermo-physical properties of the compressible product (Reineke, Mathys & Knorr, 2008). The temperature increase upon compression in adiabatic-isentropic-processes is described by equation III-1. Compressibility β, density ρ and the specific heat c_p are pressure-temperature dependent:

$$\frac{\partial T}{\partial p} = \frac{\beta}{\rho \cdot c_p} \cdot T \qquad \textbf{(III-1)}$$

The ideal adiabatic process does not occur in practical applications. Hence, to approximate this effect, the studied processes are regarded adiabatic and referred to as quasi adiabatic processes in this context.
During high hydrostatic pressure treatments, pressure is instantly transmitted throughout the system, irrespective of size and geometry (Rastogi, Raghavarao, Balasubramaniam, Niranjan & Knorr, 2007). Induced by pressure changes, quasi adiabatic heating or cooling of PTM and the product also occurs instantly. Hence, pressure induced temperature changes are predictable and homogeneous thorough the product, assumed it is homogeneous in its composition. Unlike the latter effects, conventional heating or cooling during the HPLT treatment is based on the laws of thermal conduction. As a consequence, the temperature conditions inside the externally cooled treatment chamber are not homogeneous. Temperature gradients in the PTM and in the product occur. Figure III-12 shows the temperature development in the PTM, the cooling jacket and in the surface and core region of a sample in a HPLT cycle. The sections A and D show temperature changes due to quasi adiabatic heating and cooling, respectively. During the pressure holding time (section B) heat conduction from the cooling jacket to the vessel wall, from the vessel wall to the PTM and from the PTM to the sample governs the temperature development. The same is valid during the atmospheric freezing after expansion (section D). After pressure build up, the system pressure is held constant by the air inlet pressure of the HP pump. The peak in the PTM temperature after 3000 seconds (section B in Figure III-12) is not an adiabatic effect but a temperature increase due to warm pressure medium pumped into the vessel for cooling related pressure drop compensation. The temperature recordings clearly show initial crystallization in the sample core followed by crystallization at the product surface. The nucleation in this case occurred first at the bottom of the sample and crystal growth proceeded from bottom to top. The thermocouple measuring the core temperature was located below the surface temperature thermocouple, therefore the phase transition was detected first in the sample centre (see Figure III-13).

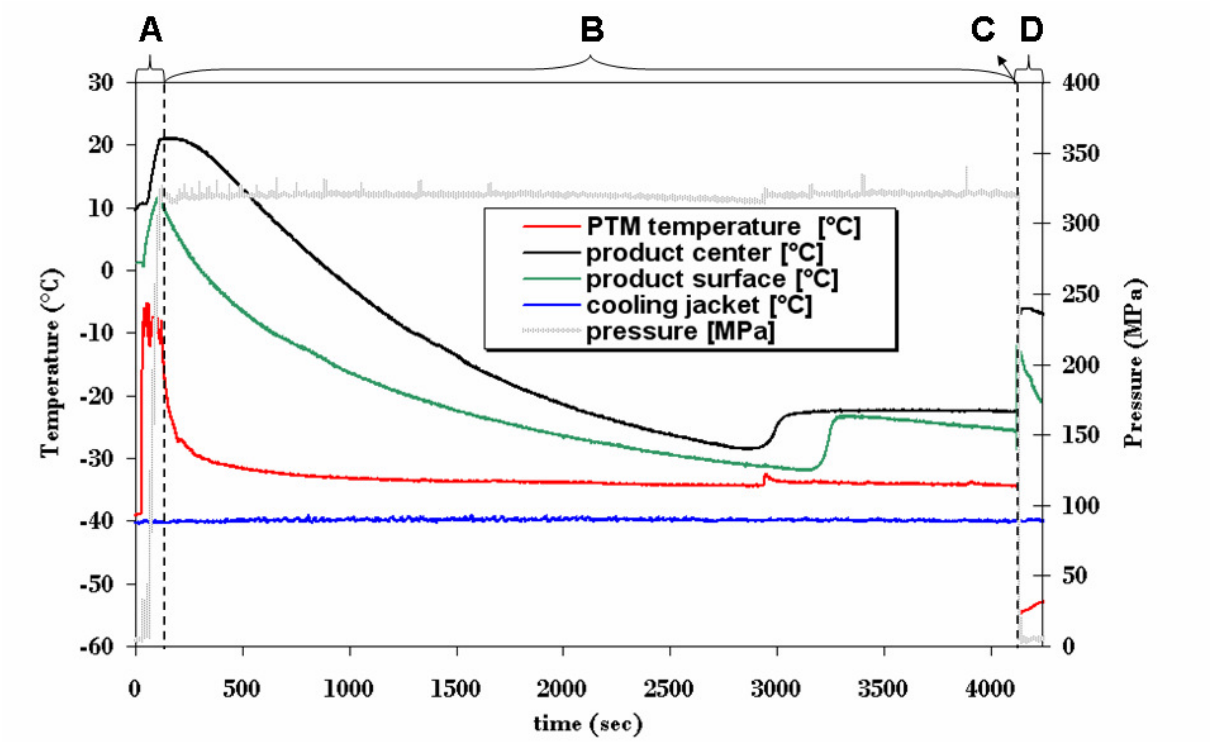

Figure III-12: p,T,t chart of a HPLT cycle with temperature recordings of the cooling jacket, PTM, sample surface and sample centre. The process is divided in sections governed by quasi adiabatic heating/cooling effects (A and C) and sections of heat conduction (B and D).

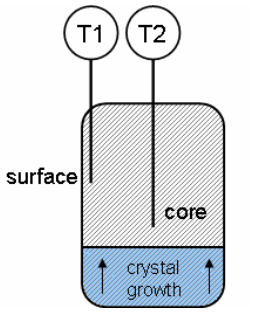

Figure III-13. Schematic drawing of the thermocouple (product core T2 and surface T1) arrangement and the crystal growth from bottom to top in the plastic shell of the flexible packaging during HPLT treatment according to Figure III-12.

In addition to temperature inhomogeneity in the sample packaging, the temperature gradient in the PTM hinders the uniform treatment of sample material in batch vessels. This is of particular importance in temperature sensitive reactions such as protein denaturation. Figure III-14 shows the temperature gradients between top and bottom section of the pilot scale HPLT vessel. Noticeable is the high peak of the bottom temperature, which is caused by the inflow of warm PTM during pressure build up. After pressurization the bottom temperature decreases faster as the top temperature and temperature gradients (ΔT) of 10 K between bottom and top section occur due to the density driven formation of thermal layers. The vessel temperature is equilibrated after 3200 sec. As expected, the same temperature characteristics show after pressure release. However, with respect to the pressure treatment the temperature gradient after expansion is not as critical as it is during pressurization. Basically, the occurrence of different temperature layers in a static cooling process is inevitable when no mechanical mixing of the fluid is involved. One way to minimize such effects is reducing the vessel height. Consequently, a horizontal arrangement of the treatment chamber, as it is increasingly done most industrial HP applications today, should be preferred.

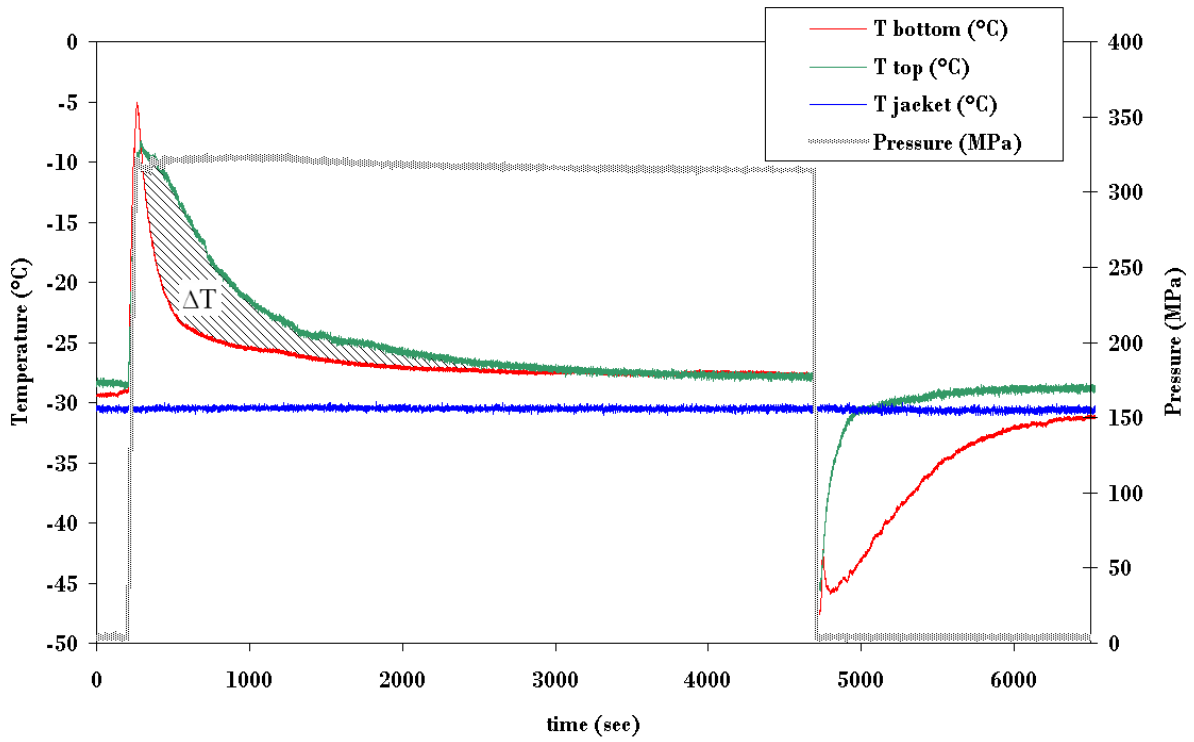

Figure III-14: Temperature gradient in the PTM between bottom and top section in a p,t,T chart of a HPLT cycle in the pilot scale unit with PTM only. The hatched area indicates the temperature difference between bottom and top after pressure build up.

Temperature control in HPLT processes is especially important for two reasons:

1. Temperature serves as an indicator for phase changes in the product.
2. HPLT induced changes in the product (e.g. protein denaturation) mainly depend on the temperature – pressure profile throughout the product.

Water undergoes density changes when changing its phase. Hence phase transitions are always accompanied by internal pressure changes in closed systems. Detecting those pressure changes can serve as an indicator for water phase transitions. In a closed treatment chamber the internal pressure is also affected by the temperature development of the PTM and the sample, as decreasing temperatures during cooling usually result in negative volume changes. Moreover, pressure changes caused by phase transition of a small fraction of the product are rather small and slow phase changes as they occur in the freezing of sugar rich products therefore hard to detect. Consequently, as an indicator for water phase changes the crystallization induced pressure changes are less accurate compared to the temperature based detection. Nevertheless, in small laboratory scale units with a high sample volume to chamber volume ratio and for products with low freezing point depression, pressure can be used as an indicator for water phase changes in the product but pressure changes do not give quantitative information about the temperature conditions during the treatment.

4.1.2 Temperature measurements in aerated samples under pressure

In process monitoring, the location of thermocouples inside the product is of high importance. During batch freezing, high temperature gradients between the surface- and the core-region of a product occur. During HPLT treatment, an aerated product changes its size and shape due to pressure build up and pressure release. In a flexible packaging a thermocouple that was well positioned under atmospheric conditions is possibly dislocated after pressure build up and the obtained data can not be clearly interpreted. To overcome the problem of sample deformation due to the gas fraction compression, two different semi-flexible sample containers were

developed in the scope of this work. The first container is a modification of the laboratory scale flexible chamber (see section 3.11, Figure III-5). The device worked well for aerated products in the lab scale version but did not meet the requirements in the pilot scale version. Major problems were the flexibility of the piston. Loose fit did not ensure leak tightness during sample compression; whereas too tight fit of the piston resulted in deformation of the cylinder during pressure build up. Figure III-15 shows the open cylinder with the rubber sealed Teflon piston and a deformed device after a HPLT cycle with jammed piston.

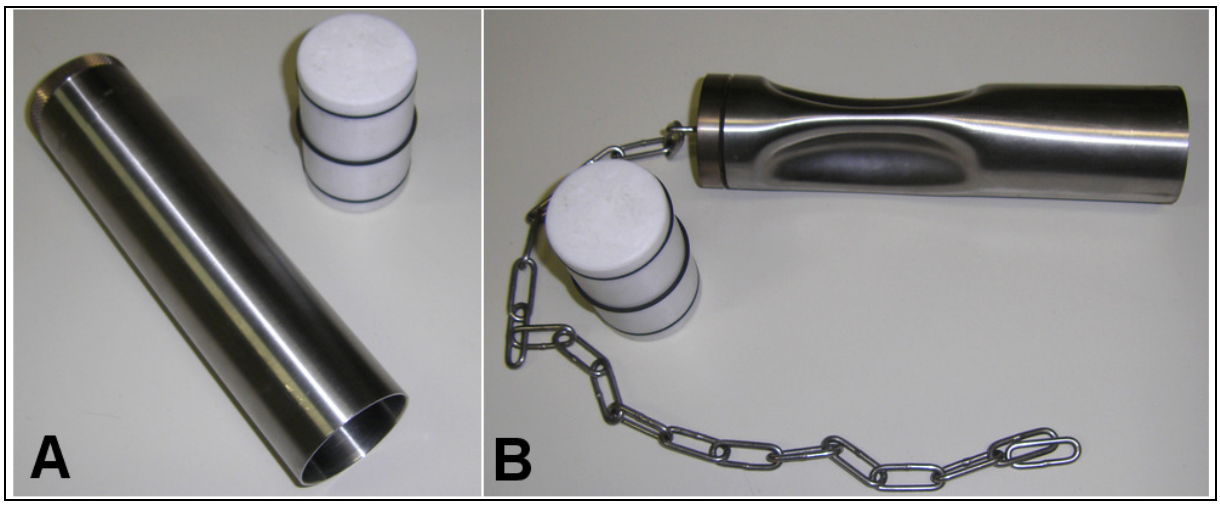

Figure III-15: Semi flexible HP sample container for aerated products developed at the TUB (A) and deformed sample cylinder after HPLT cycle with jammed piston (B).

Compared to the metal device, the semi-flexible plastic shell packaging showed higher reliability and easier handling. Major advantages in this respect are the absence of moving parts and the simple construction. During pressure build up, the air volume fraction in the sample packaging is compressed and due to the high flexibility of the bottom part of the packaging, the sample material accumulates in the plastic shell. High volume changes due to high OR of the product can be compensated by extending the PE-bag section.

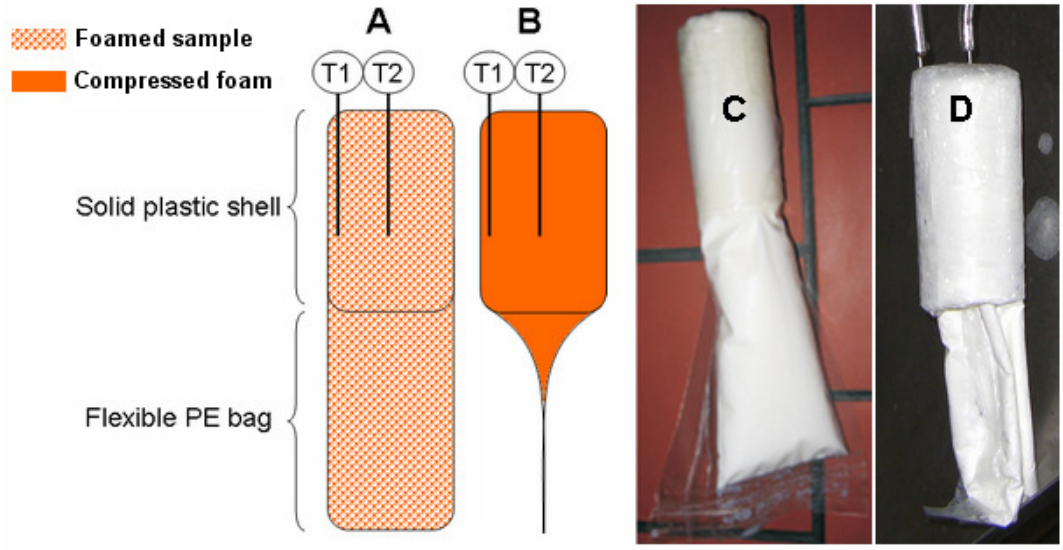

Figure III-16. Schematic drawing of the semi flexible plastic shell packaging with thermocouples for surface (T1) and core (T2) temperature measurement, at atmospheric pressure in a foamed sample (A) and in the sample under pressure (B). Images of the filled packaging before treatment (C) and after HPLT treatment (D) are shown on the right.

Essential for the function of the device is a liquid sample at the time of compression as with increasing hardness of the product the flexible PE-bag loses its function. Since the shape of the plastic shell does not change over the HPLT cycle, the thermocouples stay in place and an accurate temperature measurement is achieved. Surface and core temperature of the sample material are obtained. Furthermore, the cylindrical shape of the sample after treatment meets the requirements of texture analyses and physico-chemical analyses. Figure III-16 shows the schematic function of the sample packaging and the filled device before and after HPLT treatment.

4.1.3 Microbial safety

To evaluate the microbial safety of the batch processes, samples were taken from the feed tank, the aeration system outlet and after HPLT treatment. The results of the microbial analyses are shown in Table III-1

Table III-1: Microbial cell count before and after HPLT treatment

Sample	Standard-agar	GSP-agar	VRBD-agar
Feed tank	3.0E02	1.0E00	2.0E00
Aeration system outlet	5.0E02	6.6E01	7.5E01
After PAF	1.5E02	<1	<1
After PSF	4.5E02	2.0E00	3.0E00

The results show a low cell count in the liquid product before aeration, which is due to the pasteurization step during the emulsion preparation. After passing the aeration system, the cell count increased slightly, probably due to contaminations in the system. After PAF and PSF the cell count is reduced. PSF induces very little inactivation of microorganisms, which is consistent with the results of previous studies (Volkert et al., 2008). However, PAF treatment has a significantly higher lethal effect on the microorganisms. According to Luscher, this effect is due to the water phase change from ice III to ice I, which involves high volume changes and mechanical stress to microorganisms (Luscher, 2008). Internal and external disintegration are the proposed inactivation mechanisms in this respect. In addition mechanical stress to the cells due to the high volume changes in the ice fraction may occur. The lethal effects on microorganisms depend on several parameters, such as growth state and medium composition. Further investigations are required to quantify the inactivation effect of HPLT treatments on the investigated emulsions, but the present results imply that inactivation is induced to some extent and pasteurization prior to treatment may be required at lesser intensities.

4.2 Continuous processing

4.2.1 Process conception

Basically two major problems occur in HPLT batch processing and give the motivation for a continuous process concept: poor heat conduction and inhomogeneous treatment conditions due to the lack of forced convection and resulting temperature gradients in the treatment chamber. In all batch processes the product undergoes a static freezing or cooling step, which is economically unfavourable and always involves an inhomogeneous temperature distribution in the sample material. Measuring the temperature in inhomogeneously cooled samples is rather inaccurate with respect to the actual profile of the sample. Even if core and surface temperatures are recorded, the intermediates can not be fully detected. Continuous processing potentially overcomes both problems due to a continuous product flow that supports the homogeneity of the product. Without the use of a pressure transmitting medium the product is directly pressurized and pumped through a high pressure tubing that can be equipped with thermocouples at the desired control points. The product is mixed and

temperature can be monitored online. In addition to the heat transfer improvement by the continuously agitated product, the HP tubing can be convection-cooled with cooling media. In batch HPLT systems the cooling media that is in direct contact to the product surface is the PTM, which does not provide any convection current as it is largely stagnant in the treatment chamber and mixed only by thermal effects. In contrast, immersing the HP tubing of a continuous system in a cooling bath with turbulent flow improves heat transfer. Depending on the desired HPLT treatment the cooling coil fulfils different functions. In continuous PSF, the coil functions as a supercooling section, that delivers the liquid product under constant pressure to the expansion valve without ice formation under pressure. For PAF treatments, the cooling section is followed by a freezing section. In this part of the coil ice formation takes place and the viscosity increases further with the residence time area.

4.2.2 Temperature and pressure control during continuous pressure assisted freezing and pressure shift freezing

As discussed in section 3.2, the liquid foam is directly pressurized without the use of a PTM. As the HP piston pump is not a self-priming system and designed for liquid products, high air content in the product disturbs a constant product flow and eventually causes flow interruption. To reduce the air volume and make the aerated emulsion suitable for pumping, the gas fraction in the foam was pre-compressed by the upstream screw pump of the aeration system at 6 bar to ~20% of its initial volume. The obtained compression was sufficient for further compression by the HP intensifier. For the experiments the product flow was in the range of 5 to 10 L/h. The system pressure was controlled by the backpressure valve at the cooling coil outlet. The two pressures that were monitored during the treatments are the inlet pressure (before the cooling coil) and the outlet pressure (between the cooling coil outlet and the backpressure valve). The inlet pressure results from the delivery rate of the piston pump and was finally controlled by the adjustment of the backpressure micro metering valve. The outlet pressure could not be directly controlled as it results from the internal friction which is linked to the viscosity and density of the product and the design of the HP pipe. The pressure at the coil outlet was measured in all trials but not recorded with the data acquisition system and therefore not displayed in the p,t,T-charts. Due to the small diameter of the cooling coil and the long residence time of the product, it is assumed that the product temperature in the coil reaches values close to the temperature of the cooling bath. At the time of experiments the unit was not equipped with a thermocouple inside the tubing of the cooling coil.

4.2.2.1 Continuous pressure assisted freezing to higher ice modifications

Continuous freezing requires continuous conveying of a progressively freezing product. Due to the freeze concentration in the aerated emulsion, the ice content and linked to it the viscosity of the product increases over the freezing time. The continuous system developed in this study is designed to convey a semi frozen product with relatively low ice content. When exceeding a certain ice content, the product is no longer suitable for pumping and the freezing coil gets clogged with the solid ice matrix. To ensure constant product flow, the first section of the coil serves as a cooling zone without ice formation but supercooling to the nucleation temperature of the product. Nucleation and subsequent ice formation is intended to occur in the second section of the coil, close to the product outlet.

Continuous freezing of the aerated emulsion to ice III or ice V (PAF III / PAF V) with subsequent recrystallization to ice I at the freezer outlet was not reproducible achieved in this work. For trials aiming on PAF III or PAF V, the cooling bath was set to -45°C which is well in the nucleation temperature range temperature of the product (about -38 to -44°C at 320 MPa). To maintain the product flow of about 5 to 10 L/h the expansion valve was open to 90%. The challenge in freezing to higher ice modifications under pressure was to maintain a sufficient pressure level in the coil that excludes nucleation to Ice I and allows constant

product flow through the coil. Ice formation in the supercooling section of the coil was not intended, since high ice contents caused increased viscosity and internal friction that eventually resulted in jamming of the coil. In addition the pressure drop between inlet and outlet of the coil increases and the pressure in the freezing section shifts to the ice I region. The formation of ice I during PAF III / PAF V treatment conditions results in extension of the freezing section and rapid ice crystal growth. The pump resistance increases and jamming of the coil is promoted. Figure III-17 schematically illustrates the freezing process over time in the treatment coil and indicates the problems of ice I formation in the PAF III/V treatment.

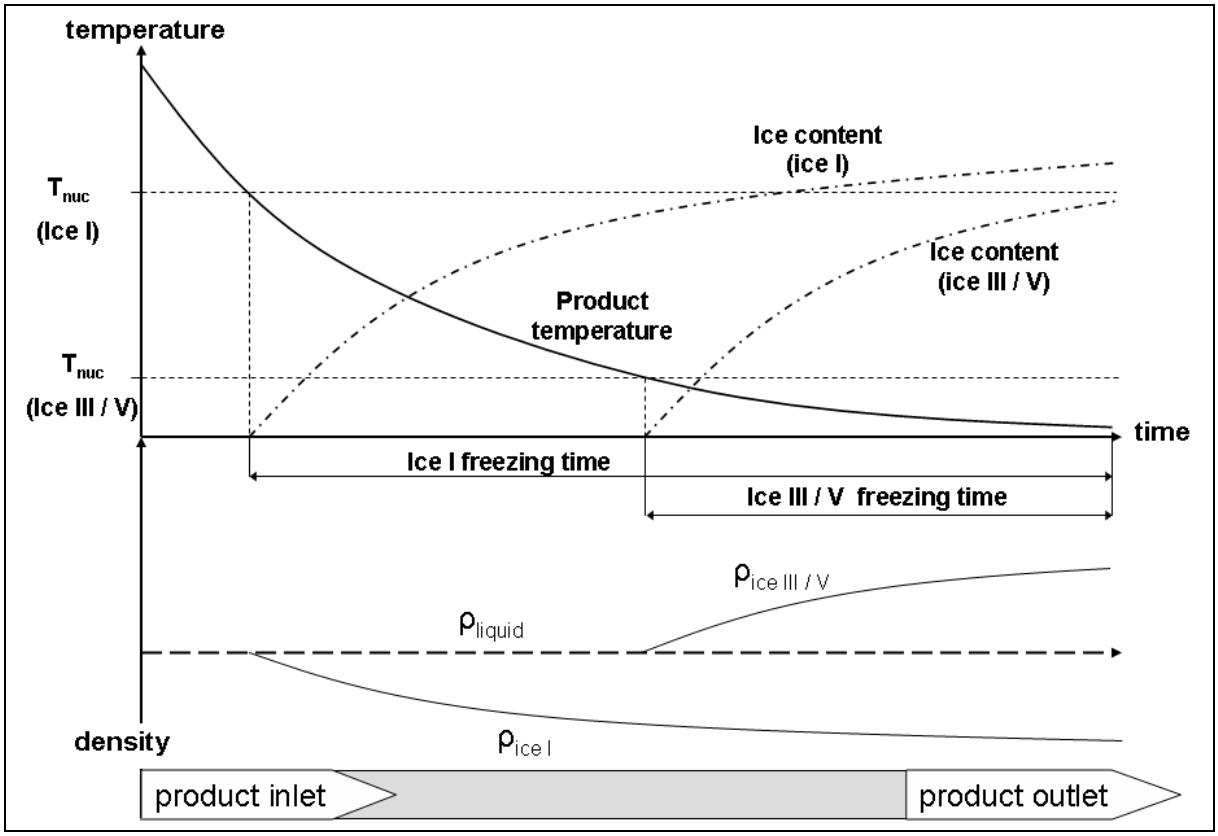

Figure III-17: Schematic process chart of continuous HPLT treatment illustrating the product temperature, freezing time, ice content and density development during PAF to ice I and PAF to ice III / V.

In the continuous PAF III/V treatment a system-pressure drop to the ice I region (< 207 MPa) is especially problematic because of the different nucleation temperatures of ice I and ice III / V. The freezing points of the different ice modifications in the pressure range from 190 to 320 MPa is within the range of 1.8 K but the nucleation temperature of ice I at 190 MPa (about -28°C) is about 12 K higher than the nucleation temperature of ice III or ice V at 320 MPa (-40°C). As a consequence of ice I nucleation, the ice formation is shifted into the supercooling section of the coil and the residence time in the freezing section is extended. The ice content of the product in the coil increases and compared to the PAF III/V treatment the density of the frozen matrix is decreased. Hence, jamming of the coil is promoted.
To provide sufficient system pressure over the freezing coil, the inlet pressure can be increased. A more applicable solution for this process may be a change in the freezing coil design towards higher inner diameter and shorter, straight tubing. As a result internal friction and the total pressure drop would be reduced. However, when changing the design the cooling power of the device has to be considered as with increasing diameter, higher wall thickness and shorter tubing the heat transfer is reduced. The rate of heat transfer trough the HP coil wall can be expressed as:

$$\dot{Q} = A_m \cdot \frac{\lambda}{s} \cdot \Delta T \qquad \textbf{(III-2)}$$

With $\dot{Q}$ = heat transfer rate $\left[W = \frac{J}{s} = \frac{N \cdot m}{s} \right]$; A_m = mean surface area [m^2]; λ = thermal conductivity $\left[\frac{W}{m \cdot k} \right]$; s = wall thickness [m]; ΔT = difference in temperature between the product and the cooling media [K]

4.2.2.2 Continuous PSF and PAF to ice I

During PSF, no ice formation is intended to occur in the freezing coil under pressure. The whole coil functions as a supercooling zone in which the product temperature is lowered under pressure well below the atmospheric freezing point without ice formation. Nucleation is envisaged at the product outlet after passing the expansion valve. For the PSF experiments the cooling bath temperature was set to -20°C. The backpressure vale was adjusted to give an inlet pressure of 200 MPa at a flow rate of 5-10 L/h. In this setup the pressure drop over the coil was <50°MPa, giving rise to the assumption that no nucleation occurred in the cooling coil. However, a partly frozen product flow at the product outlet was not achieved with this setup. Due to the low viscosity of the product the backpressure valve was closed to a minimal gap (10% open) which caused massive heating of the product at the valve outlet. The heat of friction in the passage caused a temperature increase of about 50 K and did fully compensate the PSF effect.

When lowering the product flow rate to (5 L/h), an inlet pressure of about 150 to 200 MPa was achieved when running the system with the backpressure valve 90% open. The outlet pressure in this setup was about 50 MPa and the product temperature at the product outlet below the atmospheric freezing point of the emulsion. In this way a constant flow of partly frozen product was collected at the product outlet. However, the actual process was not only PSF but a combination of PAF I and PSF. Figure III-18 shows a sectional enlargement of a p,t,T chart, recorded during a continuous HPLT treatment of an aerated dairy based emulsion. The product outlet temperature in this chart varies from -7°C to -1.5°C. The PSF batch trials showed that typically the product temperature after pressure release in PSF is higher that -3°C. The low product temperatures that occurred in the continuous treatment (-7°C) prove the occurrence of PAF to ice I to some extend, as they can not be achieved in a PSF without ice formation before pressure release. However, the system pressure was not fully equilibrated over the cooling coil. The remaining outlet pressure of about 50 MPa provides sufficient supercooling for PSF effects at the product outlet as the freezing point of the product at 50 MPa is -9°C.

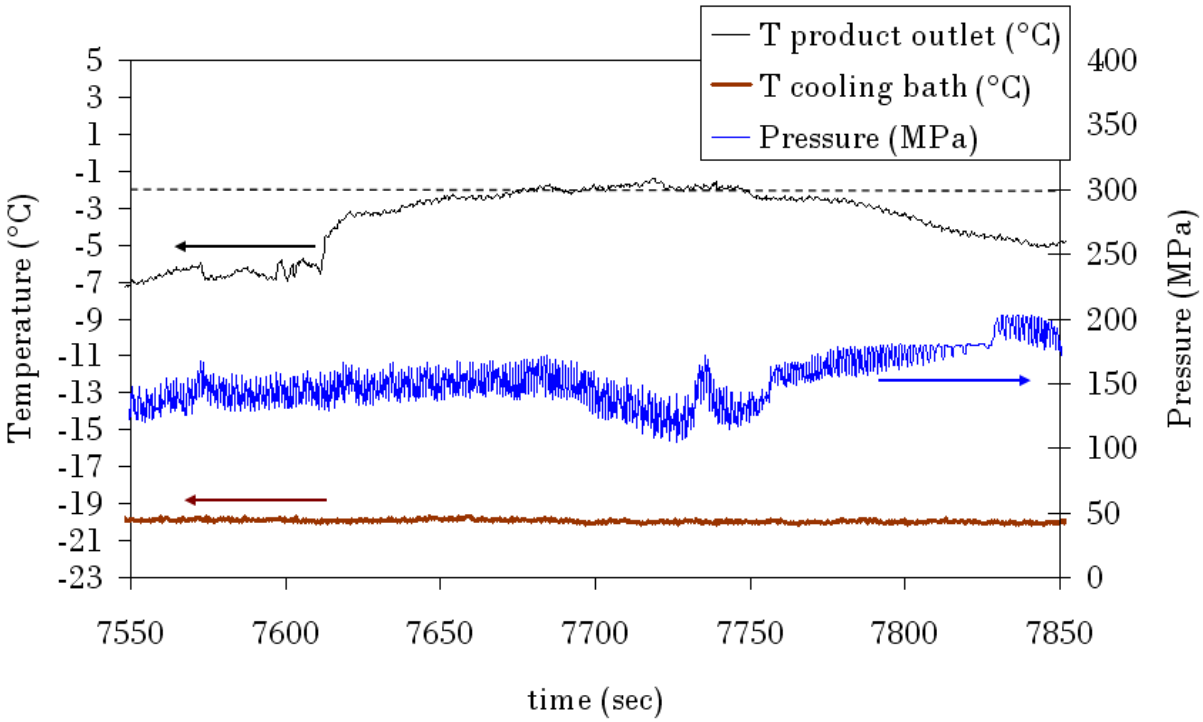

Figure III-18: Sectional p,t,T chart enlargement showing freezing to ice I under pressure, recorded during a continuous HPLT treatment.

4.2.2.3 System pressure control

The results show, that PAF and PSF require different process setups and system designs. In the present study a continuous HPLT treatment that results in a semi frozen product at atmospheric pressure was established. The findings may serve as a base for further research in this field. Of high importance in the continuous HPLT treatment is the balance between pressure and temperature, especially when ice formation is involved. Two basic principles that are particularly relevant for further process design can be identified at this point as they govern the pressure profile in long pipes. The pressure build up in the treatment section can basically be achieved by the following mechanisms:

a) *External pressure control.* The pressure is build up by the means of a backpressure valve. This method is applicable for low viscosity products and a pipe design that does not cause high pressure drops over the treatment section (short, wide and straight tubing). The pressure drop occurs quickly at the backpressure valve outlet, accompanied by high shear forces in the valve gap.

b) *Internal pressure control*. In this case the system pressure is build up by the product in the pipe itself. High viscosity and appropriate pipe design (long, narrow, coiled tubing) supports friction and backpressure in the pipe. A backpressure vale is not required and high internal pressures in the first section of the pipe can be achieved. The pressure release in this design occurs slowly over a long distance in the pipe. The system pressure is not constant over the long pipe but drops progressively from the inlet to the outlet.

5 Conclusion

Temperature plays an important role in HPLT processing. Most treatments require a precise p,T control to control the treatment intensity and in addition temperature serves as the most

relevant indicator for water phase transitions in the product. Producing reliable and conclusive results, especially important in the clarification of cause and effect in scientific research work in the HPLT domain, requires precise temperature measurement. During batch processing the formation of temperature layers in the PTM, caused by the lack of forced convection in the HPLT vessel, and consequently the non-uniform temperatures in the sample material have to be taken into account. Especially when ice formation during the pressure holding phase is involved this becomes a critical aspect, as nucleation does not occur at a certain temperature but within a certain temperature range. With respect to reproducible freezing times, direct temperature measurement in the product is required. One key problem of direct temperature measurement is product contamination with PTM, which is of particular relevance in aerated products. Pressurizing aerated products is accompanied by high volume changes which potentially cause dislocation of specifically located thermocouples. Flexible packaging is required to compensate such effects and minimize the risk of product contamination. With respect to an accurate temperature measurement over the whole treatment cycle, the packaging has to fulfil both, flexibility and shape stability to some extend. With semi-flexible plastic packaging accurate surface region- and core-temperature measurement in pressurized foam was achieved. In addition, a constant sample shape for subsequent texture analysis was obtained. A major problem in batch treatment with respect to uniform treatment conditions is given by the formation of thermal layers in the PTM due to the lack of forced convection. As a consequence, temperature gradients between single samples and in the sample material inside each packaging occur. In a vertically installed treatment chamber these effects equilibrate very slowly. Inhomogeneous temperature distribution leads to inconsistent treatment conditions and process intensities inside the vessel. One critical parameter is the vessel height, which is reduced by the horizontal installation of cylindrical treatment vessels. Nevertheless, with respect to treatment cycle times, the heat conduction remains the limiting factor in HPLT batch processing, irrespective of the vessel orientation. In HPLT treatments this aspect is even more decisive as in conventional HP treatments, since due to ice formation during the process additional latent heat has to be removed over the product surface ad through the vessel wall.

Continuous processing can evade some of the problems that occur in HPLT batch processing, especially in matters of temperature measurement, product contamination and heat transfer. Continuous HPLT treatment of an aerated emulsion without the use of a PTM was achieved with the developed equipment. A major challenge in this process was the pressure control. The backpressure that was required to give a sufficient pressure level in the treatment zone was controlled by two different mechanisms. External pressure control was achieved by the means of a mechanical backpressure valve for liquid product under pressure during PSF treatment. During continuous PAF treatment the system pressure was controlled internally, without the use of a backpressure valve, exploiting the increasing product viscosity and linked to it increasing surface friction and backpressure during freezing. Even though, the developed process setup still needs major improvements as PAF and PSF put different demands on the process design. PSF treatment is less challenging with respect to the continuous product flow, as no ice formation under pressure is involved and only temperature related viscosity changes of the liquid product occur in the cooling section. However, a key problem is the temperature increase caused by rapid expansion of the liquid product through a valve. High shear forces in the small gap result in temperature increases of more that 50 K at the product outlet and fully compensate the PSF related cooling. PSF to temperatures below the atmospheric freezing point of the aerated emulsion was not achieved with the present equipment. A potential solution for this problem can be a stepwise expansion within the cooling zone or a modified valve design.

In contrast, the expansion during the continuous PAF treatment is not accompanied by high temperature changes, as the pressure drop occurs slowly over the cooling/freezing zone. The

key problem in continuous PAF is the pumpability of the progressively freezing matrix, which is directly linked to the resulting ice modification. At same product throughput and temperature conditions, the amount of ice formed in PAF to ice I is higher compared to PAF to ice III or V. Consequently the total backpressure is higher and the system possibly gets jammed. Reducing the surface friction and linked to it the backpressure build up in continuous PAF systems could be achieved by changing the treatment zone design towards straight pipes with higher internal diameter. However, in such modifications, the heat exchange has to be considered as a wider internal diameter reduces product mixing during pumping and requires thicker wall strengths. Microbial inactivation in dairy foams was achieved by HPLT treatments, where in good agreement with literature data the inactivation is highest after PAF treatment, which involves a water phase transition from ice III to ice I. These findings are especially relevant with respect to upstream pasteurization steps, which can be of lesser intensity when replacing the conventional freezing step with a HPLT treatment.

6 References

[1]Bridgman, P. W. (1912). Water, in the liquid and five solid forms, under pressure. *Proceedings of the American Academy of Arts and Sciences*, *47*, 441-558.

[2]Cheftel, J. C. (1995). Review : High-pressure, microbial inactivation and food preservation / Revision: Alta-presion, inactivacion microbiologica y conservacion de alimentos. *Food Science and Technology International*, *1*(2-3), 75-90.

[3]Knorr, D., Schlüter, O. & Heinz, V. (1998). Impact of high hydrostatic pressure on phase transitions of foods. *Food Technology*, *52*(9), 42-45.

[4]Lévy, J., Dumay, E., Kolodziejczyk, E. & Cheftel, J. C. (1999). Freezing Kinetics of a Model Oil-in-Water Emulsion under High Pressure or by Pressure Release. Impact on Ice Crystals and Oil Droplets. *Lebensmittel-Wissenschaft und -Technologie*, *32*, 396-405.

[5]Luscher, C. M. (2008). *Effect of high pressure - low temperature phase transitions on model systems, foods and microorganisms*. PhD thesis, Berlin, Berlin University of Technology, 158.

[6]Otero, L. & Sanz, P. D. (2000). High-Pressure Shift Freezing. Part 1. Amount of Ice Instantaneously Formed in the Process. *Biotechnology Progress*, *16*, 1030-1036.

[7]Otero, L. & Sanz, P. D. (2006). High-Pressure-shift freezing: Main factors implied in the phase transition time. *Journal of Food Engineering*, *72*, 354-363.

[8]Rastogi, N. K., Raghavarao, K. S. M. S., Balasubramaniam, V. M., Niranjan, K. & Knorr, D. (2007). Opportunities and Challanges in High Pressure Processing of Foods. *Critical Reviews in Food Science and Nutrition*, *47*, 69-112.

[9]Reineke, K., Mathys, A. & Knorr, D. (2008). Temperature control for high pressure processes up to 1400 MPa. *Journal of Physics: Conference Series*, *121*, 142012-142016.

[10]Schlüter, O. (2004). *Impact of High Pressure - Low Temperature Processes on Cellular Materials Related to Foods*. PhD thesis, Berlin, Berlin University of Technology, 172.

[11]Thiebaud, M., Dumay, E. M. & Cheftel, J.-C. (2002). Pressure-shift freezing of o/w emulsions: influence of fructose and sodium alginate on undercooling, nucleation, freezing kinetics and ice crystal size distribution. *Food Hydrocolloids*, *16*(6), 527-545.

[12]Urrutia Benet, G., Schlüter, O. & Knorr, D. (2004). High pressure–low temperature processing. Suggested definitions and terminology. *Innovative Food Science and Emerging Technologies*, *5*(4), 413-427.

[13]Urrutia Benet, G., Arabas, J., Autio, K., Brul, S., Hendrickx, M., Kakolewski, A., Knorr, D., Le Bail, A., Lille, M., Molina-García, A. D., Ousegui, A., Sanz, P. D., Shen, T. & Van Buggenhout, S. (2007). SAFE ICE: Low-temperature pressure processing of foods: Safety and quality aspects, process parameters and consumer acceptance. *Journal of Food Engineering*, *83*, 293-315.

[14]Volkert, M., Ananta, E., Luscher, C. M. & Knorr, D. (2008). Effect of air freezing, spray freezing, and pressure shift freezing on membrane integrity and viability of Lactobacillus rhamnosus GG. *Journal of Food Engineering*, *87*, 532-540.

[15]Yaldagard, M., Mortazavi, S. A. & Tabatabaie, F. (2008). The principles of ultra high pressure technology and its application in food processing/preservation: A review of microbiological and quality aspects. *African Journal of Biotechnology*, *7*, 2739-2767.

[16]Yuste, J., Capellas, M., Pla, R., Fung, D. Y. C. & Mor-Mur, M. (2001). High Pressure Processing for Food Safety and Preservation: a review. *Journal of Rapid Methods & Automation in Microbiology*, *9*(1), 1-10.

Chapter IV Nucleation and ice crystal growth in sugar rich dairy based emulsions and solutions under pressure

1 Principles of freezing sugar rich products

Matter can exist in three different classical physical states: solid, liquid and gas. A phase can be defined as a form of matter that is uniform throughout in chemical composition and physical properties, and that can be distinguished from other phases with which it may be in contact by these definite properties and composition. In food related freeze processes, the most relevant phase transition is the water to ice I transition. Ice is a crystalline solid, in which the water molecules are aligned in a lattice, held by molecular forces. The lattice structure of the solid state differs for different ice modifications. For example, ice I shows a hexagonal structure, whereas ice III consist of tetragonal crystals (Chaplin, 2008). Different from pure water, the phase transition of water in the presence of solutes occurs progressively in a certain temperature range. This phenomenon is related to the freezing point depression and freeze concentration. Both effects play an important role in the freezing of complex food systems and become especially relevant at elevated process pressure.

1.1 Supercooling, nucleation and ice crystal growth at atmospheric and elevated pressure

When frozen water is exposed to a constant heat input, the temperature of the ice raises until reaching the melting point. The heat that changes the temperature to this point is known as sensible heat, as it can be sensed as a temperature change. At the melting point, the temperature remains constant until all water is melted. This is because the heat is consumed in overcoming the intermolecular forces in the ice lattice. The heat required to enforce this phase transition is the latent heat and does not cause a quantifiable temperature change, once the freezing point is reached.

In the reverse process (freezing), the phase transition does not occur when the temperature reaches the freezing point. The liquid phase is cooled to temperatures below the melting point without ice formation. This phenomenon is referred to as supercooling. The extend of supercooling depends on different parameters and is reported to reach temperatures of -41°C for pure water under atmospheric conditions (Balibar & Caupin, 2006). At higher pressures the extent of supercooling in aqueous systems is increased (Urrutia Benet, 2005). The cause for supercooling is explained on the molecular level. When ice melts, molecules from the crystal surfaces switch to the liquid state one at a time. Ice crystal growth shows the exact reverse process: individual molecules from the liquid phase join onto the ice crystal lattice. However, crystal growth requires an existing crystal surface. In the event of nucleation in a liquid phase, water molecules accumulate and form tiny ice crystals, referred to as nuclei (Clarke, 2004). When a nucleus is formed, an interface between the solid nucleus and the liquid water phase is created. With occurrence of a first stable nucleus the conditions for ice crystal growth are given and the liquid-solid phase transition takes place. There is an energy gain in the phase transition of water from liquid to the solid state below the equilibrium freezing point. The equilibrium freezing point can be defined as the temperature, at which under constant pressure, the solid-liquid phase transition takes place (Guignon, Otero, Molina-Garcia & Sanz, 2005). However, creating a new interface requires energy. The net energy E of forming a spherical nucleus of radius r is the sum of the energy gain due to change of water to ice and the energy cost due to formation of the interface (equation IV–1).

$$E = \frac{L(T - T_m)}{T} \cdot \frac{4\pi}{3} \cdot r^3 - \gamma \cdot 4\pi \cdot r^2 \qquad \textbf{(IV-1)}$$

The critical radius (r*) that is required to form a stable nucleus is inversely linked to the temperature decrease. Hence, the chance for nucleation is promoted by high degrees of supercooling as illustrated in Figure IV-1.

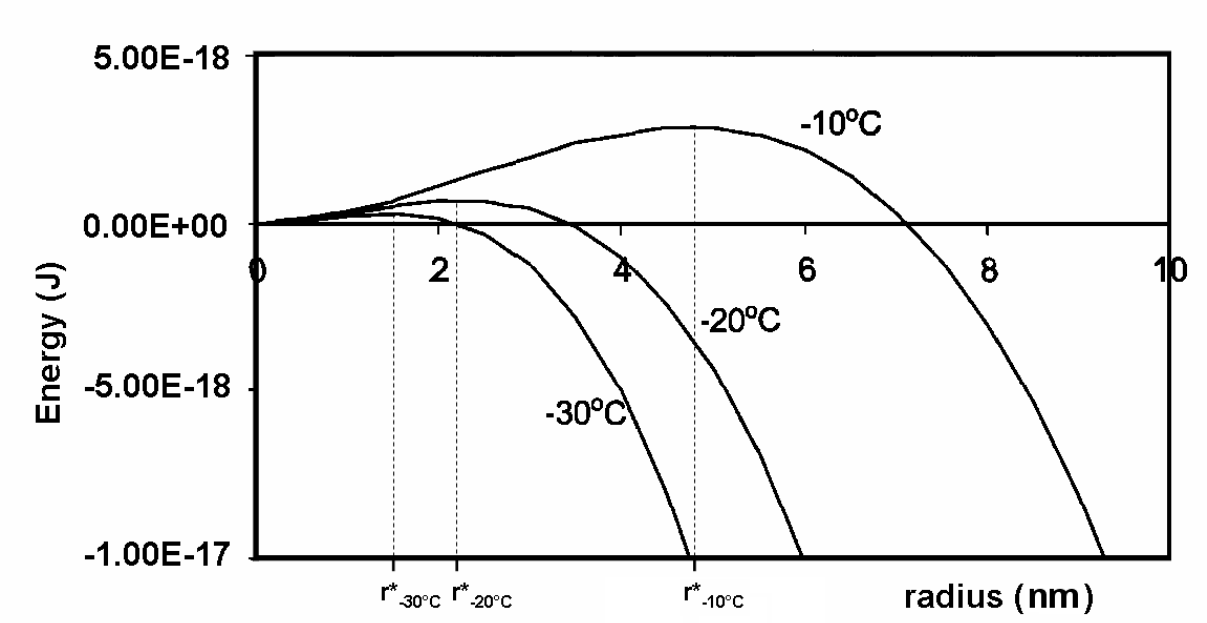

Figure IV-1: Energy required to form a ice crystal nucleus as a function of ice crystal size at -10, -20 and -30°C. The maximum of the curves determines the critical radius (r*). Redrawn from (Clarke, 2004)

Inherently nucleation of ice crystals does not occur at a certain temperature but happens stochastically in a certain temperature range that begins at the freezing point of the matrix at the corresponding pressure and ranges to far lower temperatures. Nucleation can be classified into homogeneous and heterogeneous nucleation. Homogeneous nucleation describes the spontaneous formation of nuclei within the system (Reid, 1998). High supercooling is required (ΔT_{sup}=41 K for pure water) and therefore this phenomenon does hardly ever occur in freezing processes at constant pressure (Janssen, Talsma, van Steenbergen & de Jong, 2004; Balibar & Caupin, 2006). The phenomenon of homogeneous nucleation results in a high number of small ice crystals and is exploited in the PSF process (Lévy et al., 1999; Chevalier, Le Bail & Ghoul, 2000). In conventional freezing and freezing at constant elevated pressure (PAF), ice crystal growth is initiated by heterogeneous nucleation, which occurs as a random process at lower degrees of supercooling (Robinson, Zuh, Singh & Evans, 1996). Heterogeneous nucleation is supported by some form of catalytic surfaces (e.g. tiny particles in the product or irregularities at the packaging wall) that act as nucleation sites on which the water molecules can begin to cluster in a crystalline arrangement. Fewer water molecules are needed to form a stable nucleus and supercooling is reduced (Clarke, 2004). Under high pressure, higher degrees of supercooling occur when freezing to ice III and ice V compared to ice I (Schlüter & Knorr, 2002; Urrutia Benet, 2005; Urrutia Benet et al., 2007). Another factor that affects the formation of stable nuclei is the presence of solutes. Raoult's law (equation IV-2) states that the freezing point depression (ΔT_f) is directly proportional to the molal concentration of the solute (m). K_f is the molal depression constant, which is defined as the depression in freezing point for 1 molal solution. However, this assumption is only true for ideal solutions and is therefore limited applicable in practice.

$$\Delta T_f = K_f \cdot m \qquad \textbf{(IV-2)}$$

As for pure liquids, the absolute viscosity of sugar solutions increases exponentially with pressure (Foerst, Werner & Delgardo, 2002). The chance of nucleation in sugar rich systems at high pressure is reduced, as the nucleation rate decreases with increasing viscosity and supercooling is promoted (Kimizuka, Chotika & Toru, 2007).
High concentrations of solutes in an aqueous product lower the freezing point at atmospheric pressure and cause freeze concentration in the liquid phase during crystallization. In addition, high concentrations of sugar significantly affect ice crystal growth under pressure. Ice crystal growth in sugar rich solutions is slowed down under pressure and "bell-shaped" temperature developments can be observed after nucleation, rather than a rapid temperature increase to the equilibrium freezing temperature (Figure IV-2) (Luscher, 2008). This effect increases with pressure and seems particularly pronounced when approaching the phase transition pressure of a higher ice modification or even entering the metastable region.

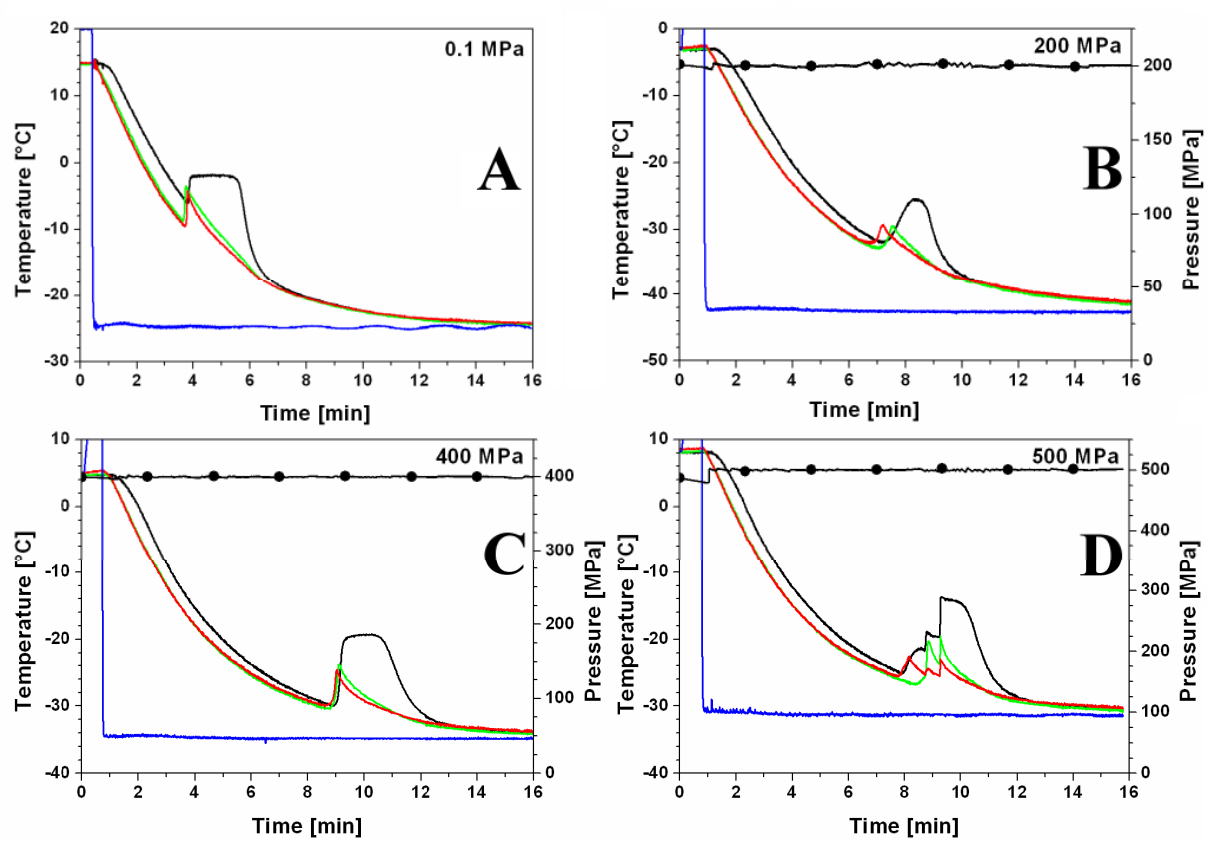

Figure IV-2: Freezing of sucrose solution 23.4% (w/w) at constant pressure to ice I and ice V. Nucleationo to ice I at 0.1 MPa (A), ice I at 200 MPa (B), ice V at 400 MPa (C) and ice V at 500 MPa (C) (Luscher, 2008).

The basic cause for the reduced crystal growth rate is attributed to the increased viscosity of the solutions under pressure. When ice crystals grow into a previously homogeneous solution, water molecules must be transported to the growth centre, displacing solute molecules, which in turn must be transported away. It has to be stated, that even at high solution viscosities and low temperatures water molecules remain very mobile (Reid, 1998). It is the solute molecules which show restricted mobility. However, the phenomenon is not fully understood and especially the decrease in crystal growth rate when approaching the phase boundary of the higher level ice modification is not explained.

2 Experimental Methods

2.1 HPLT setup

The experiments on the freezing behaviour and the equilibrium freezing point determination of the dairy based model system were performed with the laboratory scale HPLT unit and the HPLT pilot scale unit (described in chapter III). According to the HPLT process window defined in chapter III, the investigations focused on the pressure range from 0.1 to 360 MPa. To investigate the freezing behaviour of dairy emulsions and skim milk powder (SMP) solutions during different HPLT freeze processes, pressure shift freezing (PSF), pressure assisted freezing (PAF) and pressure induced crystallization (PIC) was applied.

2.2 Model dairy solutions and emulsions

Different dairy based model emulsions, varying in fat and protein content or composition, and a protein model solution were used to investigate the freezing behaviour under pressure. The protein model solution was reconstituted skim milk, made from skim milk powder (SMP) of defined composition. The 3 model systems used to investigate the freezing behaviour were:

- Sugar rich dairy emulsion (referred to as: “emulsion A”, “emulsion B”)
- reconstituted skim milk (20% w/w aqueous SMP solution)

The detailed ingredient list of all formulations used in this study can be found in the annex. Table IV-1 shows the basic formulation of the dairy based model emulsion that was used for the phase diagram determination (emulsion A). The formulation of the skim milk powder solution is given in Table IV-2. Table IV-3 shows the dry matter composition of emulsion B, which was used for the PSF, PAF and PIC experiments. Emulsion B was designed for improved formability and foam stabilization.

Table IV-1: Dry matter composition of the dairy based model emulsion (emulsion A), divided into MSNF (milk solids no fat), sugar, fat and stabilizers

Ingredient	[%] of total solids
MSNF	11.5
Sugar	18.0
Fat	9.0
Stabilizer	0.5
total solids	**39.0**

Table IV-2: Dry matter composition of skim milk powder (Saliter, Oberguenzburg, Germany)

Ingredient	[%] of total solids
Fat	< 1
Protein	35.5
Lactose	51.7
Ash	7.8
total solids	**> 95**

Table IV-3: Dry matter composition of the dairy based model emulsion (emulsion B), divided into MSNF milk solids no fat), sugar, fat and stabilizers

Ingredient	[%] of total solids
MSNF	9.7
Sugar	19.4
Fat	7.0
Stabilizer	0.7
total solids	**36.8**

2.2.1 Emulsion and solution preparation

All ingredients for the dairy based model emulsions were pre-mixed for 20 min at 65°C followed by a 2 stage homogenization (40 bar / 150 bar) at 72°C. The homogenized emulsion was pasteurized for 30 sec at 85°C and than cooled down in a plate heat exchanger to 5°C. After 24h aging at 5°C the emulsion was frozen in 2.5 litre lots to -30°C.
The emulsion B was aerated to overrun (OR) values of 180% ±20 before HPLT treatment. The aeration of the emulsion was performed with the Minimondo aeration system described in chapter III–3. Prior to aeration, the emulsion was tempered to 3°C in the feed tank of the aeration system, to reach outlet temperatures of about 10°C. The final OR of the liquid foam before treatment was adjusted in the range of 140 to 160% and was determined before the foam was packed for the HPLT treatment.
For the preparation of the dairy based protein solution, SMP was reconstituted in water (20% w/w) and stirred for 2h at 20°C. All protein solutions were prepared in w/w ratio.

2.3 Determination of phase transition temperatures

The determination of the freezing and melting points at different pressures was carried out to obtain data for the generation of phase diagrams for the different model systems. To determine freezing and melting points at atmospheric and elevated pressure DSC analysis at atmospheric pressure and pressure assisted freeze/thaw experiments in the laboratory and pilot scale HPLT units were applied.

2.3.1 Atmospheric DSC analysis

The ice content as a function of temperature was determined via DSC measurement at atmospheric pressure for the model emulsions and the 20% SMP solution. For the analyses a Mettler DSC 30 calorimeter (Mettler Toledo Inc, Columbus, USA) was used. The DSC analyses were carried out in triplets. Enthalpy changes were recorded in a temperature range from 0 to -35°C. STARe Mettler Toledo software was used in order to obtain enthalpy and temperature data.

2.3.2 Freezing and melting point determination under pressure

The phase boundaries of the model systems (emulsion A and SMP solution) under pressure were determined according to the method described by Luscher (Luscher, 2008), which is basically a PAF treatment with subsequent thawing under constant pressure. Figure IV-3 shows the principle of freezing and melting point determination under pressure. When the freezing and melting temperatures in one experiment were not found at the same temperature, the equilibrium freezing point referred to the melting temperature. All experiments were carried out at least in duplicates.

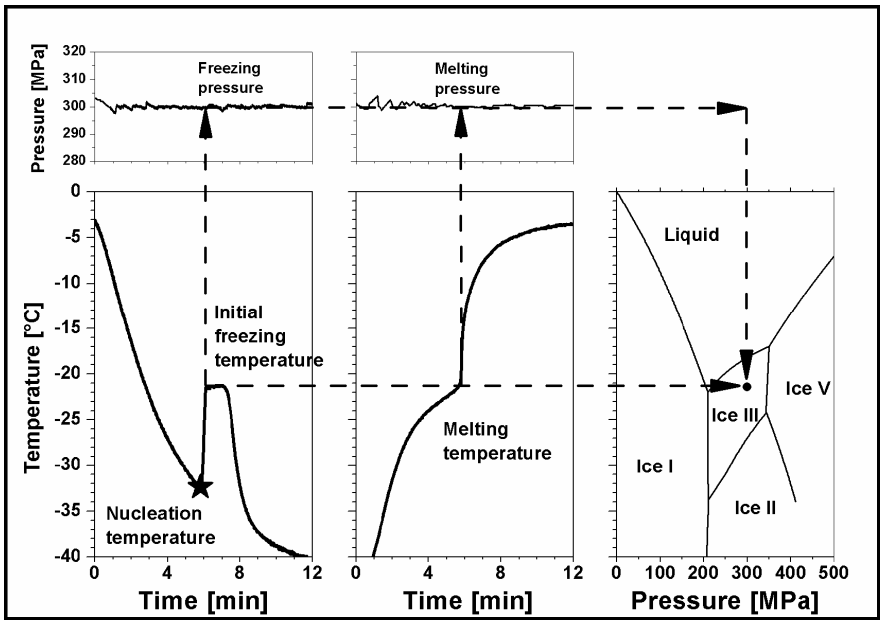

Figure IV-3: Determination of freezing and melting points under pressure, redrawn from Luscher (Luscher, 2008).

2.3.3 Identification of the present ice modification

During pressure shifts the temperature in crystallizing systems shifts along the phase transition line (Schlüter, Benet, Heinz & Knorr, 2004). To identify the ice modification under pressure, the system pressure was varied (ca. ± 50 MPa) when the sample temperature was on the freezing plateau. In the p,T diagram, the temperature line during this pressure change is parallel either to the ice I, ice III or ice V melting line.

3 Results and discussion

3.1 Phase diagrams of dairy emulsions and aqueous SMP solutions

In the field of food science the knowledge of high pressure low temperature phase diagrams of aqueous systems is required to plan and optimize processes, improve treatment results and advance in physical phenomena understanding. HPLT processes are derived from the water phase transition lines, which represent the thermodynamic borders for cooling and freezing aqueous products under pressure. The water phase diagrams describe the thermodynamically stable regions of pure water but do not take into account the occurrence of metastable phases and the effect of freezing point depressing solutes. The phase diagram models in the present study were generated as a basis for product specific HPLT process design. In the pressure range from 0.1 to 350 MPa (ice I and III) the melting lines of two different aqueous systems were experimentally determined and modelled for different ice contents on the base of atmospheric DSC data.

3.1.1 Experimentally determined phase diagrams

The experimentally determined phase diagrams of a 20% w/w SMP solution and a dairy emulsion (emulsion A) are shown in Figure IV-4. Table IV-4 shows the corresponding formulas and statistical data of the regression lines.

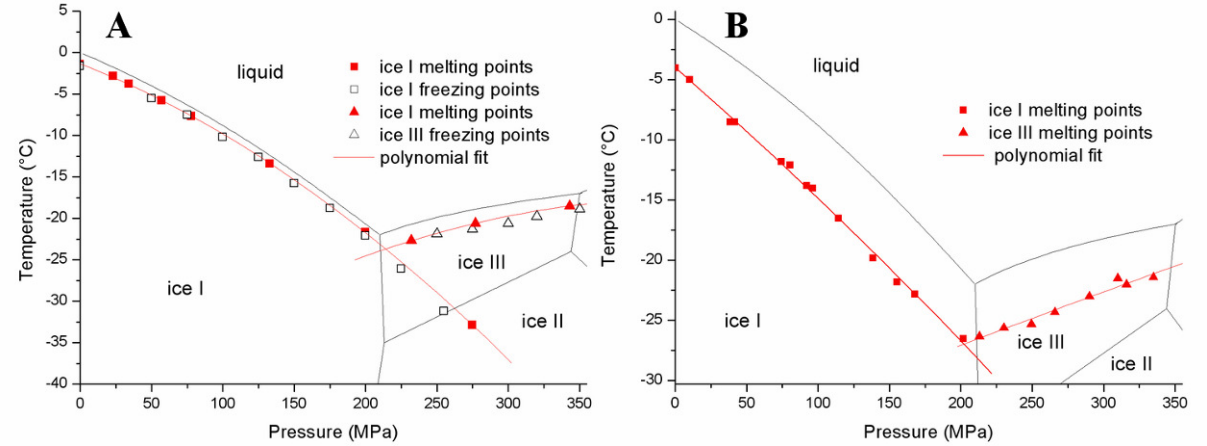

Figure IV-4: Experimentally determined phase diagram of an aqueous 20% w/w SMP solution (A) and a dairy emulsion (B) (emulsion A), showing ice I and ice III freezing and melting points and the polynomial fitted melting lines.

Table IV-4: Polynomial regression of the melting lines for the SMP solution and the dairy emulsion. T_m : temperature at the melting point; p_m: pressure at the melting point

Aqueous SMP solution 20% w/w				Dairy emulsion A			
ice I melting line				**Ice I melting line**			
$T_m = -1.32 - 0.0681 p_m - 1.69843E\text{-}4\ p_m^2$				**$T_m = -3.99175 - 0.10354 p_m - 4.96854E\text{-}5 p_m^2$**			
R^2	SD	N	P	R^2	SD	N	P
0.99997	0.07514	8	<0.0001	0.99752	0.38084	13	<0.0001
ice III melting line				**ice III melting line**			
$T_m = -42.12327 + 0.11476 p_m - 1.3377E\text{-}4 p_m^2$				**$T_m = -36.57208 + 0.04954\ p_m - 1.00764E\text{-}5 p_m^2$**			
R^2	SD	N	P	R^2	SD	N	P
1	0	3	<0.0001	0.98184	0.35655	10	<0.0001

The average melting points obtained by freeze and thaw experiments under pressure are in good agreement with the water melting lines determined by Bridgman (Bridgman, 1912). The slope of the polynomial fitted phase transition lines of the aqueous SMP solution correlate with the slope of the water melting lines (Ice I and ice III). In the determination of the equilibrium freezing points of the dairy emulsion, no significant difference was found between the freezing and melting points. Hence, both temperatures were used for the polynomial regression and no further separation in freezing and melting points was made for emulsion A. Generally, freezing point determination in the dairy emulsion was not as clear as in the SMP solution. Higher deviations with respect to the slope of the water melting lines occurred. In both systems the experimentally determined freezing points show a progressively increasing deviation from the water melting line at lower temperatures. This is accounted to the increasing degree of supercooling and reduced crystal growth rates that occur at higher pressures. In addition, the latent heat of water decreases with increasing pressure. Due to higher supercooling more energy is removed from the water phase before crystallization and the energy costs (latent heat) for the phase transition is reduced. Hence, freeze concentration occurs to a greater extent, as more ice is formed. Metastable ice I was found during pressure assisted freezing point determination above 207 MPa in the SMP solution, resulting in equilibrium freezing points of ice I along the extended ice I melting line of water (Figure IV-4 A). During temperature measurement in the HP vessel, the atmospheric freezing point for the SMP solution was detected at -1.6°C and at -4°C for the dairy emulsion. The mean values of the freezing point depression (FPD) for emulsion A and the SMP solution in the ice I and ice III region are shown in Table IV-5. The freezing point depression (FPD) at constant pressure

can be calculated from experimentally determined melting points of the solution and the corresponding phase transition temperature of water according to:

$$FPD = \vartheta_{Tm,s} - \vartheta_{Tm,w} \quad \textbf{(IV-3)}$$

With $\vartheta_{Tm,s}$ the phase transition temperature of the solution and $\vartheta_{Tm,w}$ the phase transition temperature of water.

Table IV-5: Mean values of the freezing point depression (FPD) and standard deviation (SD) of the experimentally determined ice I and ice III melting lines of the SMP (Saliter, Oberguenzburg, Germany) solution and dairy emulsion A

	20% SMP ice I	20% SMP ice III	Emulsion A ice I	Emulsion A ice III
FPD (mean) [°C]	1.1	1.6	5.6	4.2
SD	0.1492	0.3	0.8250	0.8229

Due to the higher total sugar content, emulsion A shows a higher freezing point depression as the SMP solution. The FPD of the SMP solution increases in the ice III region, whereas the dairy emulsion shows the opposite trend, with higher FPD in the ice I region. A conclusive explanation for this effect can not be given on the base of the present data. However, the present data shows a temperature trend and does not prove a significant difference in the equilibrium freezing point depression of ice I and ice III on a level of significance >95%.

3.1.2 Differential scanning calorimetry based phase diagram models

Differential scanning calorimetry (DSC) represents a precise method for the determination of the ice content in a product as a function of its temperature (Soukoulis, Lebesi & Tzia, 2009). Pure water freezes and changes its phase to 100% at its equilibrium freezing point (0°C at 0.1 MPa). In solutions, freeze concentration occurs with the onset of crystallization. During subsequent freezing, the freezing point is progressively shifted to lower temperatures accompanied by an increase in ice content. Hence, the phase transition of the liquid phase in the system is not properly described by only one phase boundary as it is for water. Only a small percentage of the water changes its phase at the initial freezing point. An appropriate description of the actual state of the system was achieved by modelling the melting curves for different ice contents, taking into account the freezing point depression as a function of ice content, obtained by the atmospheric-pressure DSC data (Figure IV-5).

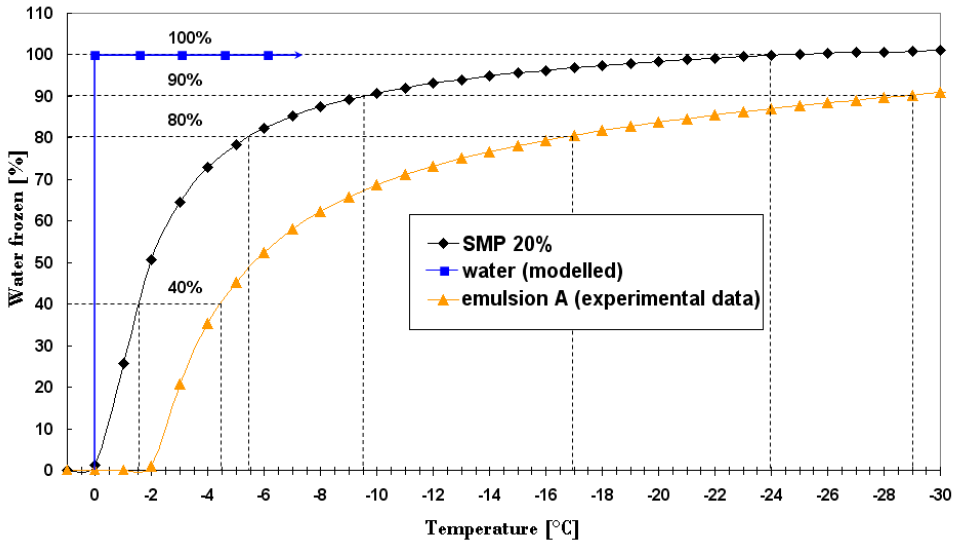

Figure IV-5: Percentage of frozen water as a function of temperature in a dairy emulsion (emulsion A) (▲) and reconstituted skim milk (RSM) 20 % w/w (♦). The

ice content of water as a function of temperature (■) is shown schematically. The dotted lines indicate the freezing points at different ice contents.

The atmospheric freezing point of emulsion A and the SMP solution were found at higher temperatures with the DSC ($T_{m,emulsion\ A}$= -2°C; $T_{m,\ 20\%\ SMP}$= -0.2°C) compared to the conventional freezing point determination in the HP vessel ($T_{m,emulsion\ A}$= -4°C; $T_{m,\ 20\%\ SMP}$= -1.6°C). Table IV-6 shows the average FPD in the ice I and ice III region as found by freezing point measurement in the HP vessel and the correlating ice content according to the DSC data.

Table IV-6: Experimentally determined mean FDP and corresponding ice content in 20% SMP solution and dairy emulsion A according to the DSC data

	FPD (mean) [°C]		Total water frozen [%]	
	Ice I	**Ice III**	**Ice I**	**Ice III**
20% SMP	1.1	1.6	23.0	32.0
Emulsion A	5.6	4.2	45.9	34.8

According to the DSC data, the ice content at the experimentally determined freezing point corresponds to 32.9% at -4°C and 32.8% at -1.6°C for emulsion A and the SMP solution, respectively. The deviation in T_m between experimental determination and the DSC measurement is accounted to the different measuring principles of the two methods. The temperature measurement with a type K thermocouple in the sample centre detects lower freezing and melting temperatures compared to the DSC. This could partly be explained by the general measuring accuracy of the type K thermocouples (±1K) but the basic cause for this seems the location of the thermocouple in the geometrical centre of the sample and the higher sample volume that causes thermal heterogeneity. This assumption is supported by the ice contents at the experimentally determined atmospheric freezing point, which are in good agreement for both systems. A systematic error in the experimental freezing point detection seems most probable. During conventional and pressure assisted freezing, ice crystal growth is triggered by heterogeneous nucleation that causes crystal growth from the surface region of the sample to the core. Water crystals exclude solutes and a concentration gradient from the surface region to the core occurs (Petrenko & Withworth, 1999). As a consequence, the freezing point in the sample centre is shifted below the initial freezing point of the system. The latter effect also affects the temperature measurements under pressure. During DSC this effect does not occur. Because of the small sample volume and high sensitivity, the conditions during DSC measurement are comparable to heterogeneous nucleation without freeze concentration before detecting the initial freezing point.

Phase transition lines can be described by different equations (e.g. Simon equation). A detailed discussion about the mathematical background of water phase boundaries is given by Luscher (Luscher, 2008). As a base for modelling the phase transition lines of the two systems in this study, the water melting lines after Bridgman were described by polynomial regression:

Ice I_{H2O}: $$T_m = 0.02049 - 0.07316\,p_m - 1.52467E-4\,p_m^{\,2} \quad \textbf{(IV-4)}$$

Ice III_{H2O}: $$T_m = -39.42701 + 0.11315\,p_m - 1.40739E-4\,p_m^{\,2} \quad \textbf{(IV-5)}$$

Ice III_{H2O}: $$T_m = -48.79986 + 0.10807\,p_m - 4.86236E-5\,p_m^{\,2} \quad \textbf{(IV-6)}$$

With T_m : melting temperature and p_m : melting pressure. For all equations is $R^2 \geq 0.999$.

Figure IV-6 shows the DSC based phase diagram models of emulsion A and the 20% SMP solution in the pressure range from 0.1 to 350 MPa. The steeper slope of the ice content over temperature in the SMP solution (Figure IV-5) results in a more rapid increase of frozen water with decreasing temperature compared to emulsion A. As a consequence, the iso-

concentration-melting-lines of the SMP solution are closer together as those of the dairy emulsion.

The total frozen water reaches maximum values of about 90% at atmospheric pressure at -29°C. In addition to the higher sugar concentration, the proteins, emulsifiers and stabilizers in the dairy emulsion reduce the amount of free water due to molecular interactions. Due to these interactions, the total amount of freezable water in the system is reduced. According to the results of the DSC analyses, in the SMP solution 100% water is frozen under atmospheric pressure at -24°C. As for the dairy emulsion, freezing of 100% water is not possible in the SMP solution, as a certain percentage of water is non-freezable. However, the method given error is small and does not extensively adulterate the present results.

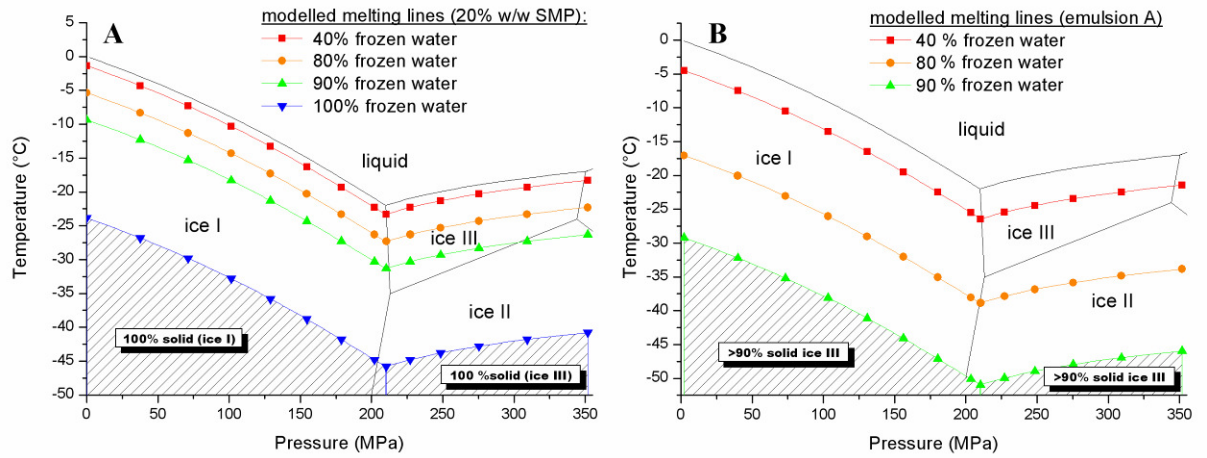

Figure IV-6: Modelled phase transition lines of 20% w/w SMP solution (A) and dairy emulsion A (B). The dotted lines show the modelled phase transition lines, for 40(■), 80(●), 90(▲) and 100%(▼) frozen water according to the atmospheric DSC data. The water phase diagram redrawn after Bridgman is shown in the background (Bridgman, 1912).

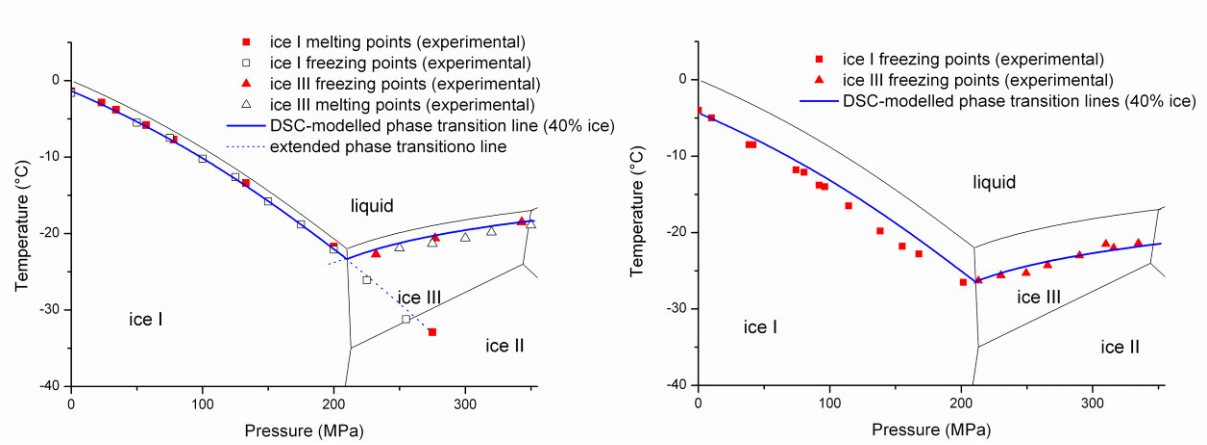

Figure IV-7: Modelled phase transition lines (DSC based) and experimentally determined phase transition points of 20% SMP solution (A) and emulsion A (B).

Figure IV-7 compares the experimentally determined equilibrium freezing points and the DSC modelled melting lines of the SMP solution and emulsion A (corresponding to 40% total water frozen). The phenomenon of higher FPD in the ice III region of sugar rich solutions, as it was reported by Luscher (Luscher, 2008), is confirmed by the results of the SMP solution, which shows an average increase in FPD from ice I to ice III of 0.5K (45% increase). In contrast, the FPD in emulsion A was in average 1.4K lower for ice III than for ice I (33% decrease), which is contrary to the latter assertion. Hence, a general trend to higher FPD in the ice III region of sugar rich products can not be consistently confirmed with the present data. Taking into account the freeze concentration and the progressive phase change of water in

sugar rich systems, it has to be stated that experimentally determined freezing and melting points depend on the experimental setup (sample volume, thermocouple location, cooling rate). The experimentally determined freezing points in sugar rich systems do not necessarily display the experimentally determined freezing point of the system and do not give quantitative information about the actual ice content. However, the freezing points over pressure were well reproducible found in a parallel trend to the water melting lines in the pressure range of 0.1 to 350 MPa.
Evaluating the two applied methods for the phase diagram generation, it is suggested that the freezing behaviour of dairy based solutions and emulsions in the pressure range from 0.1 to 350 MPa can be approximated by transferring the atmospheric ice content as a function of temperature to higher pressures according to the water melting lines after Bridgman.

3.2 Freezing phenomena in sugar rich systems under pressure

In all HPLT experiments, typical quasi-adiabatic heating of the pressure transmitting media (PTM) and the liquid samples occurred. The pressurization causes a temperature increase in the PTM (80% v/v ethanol : water) of 5.3 K/100 MPa and 3.5 K/100 MPa in the liquid dairy emulsions.

3.2.1 Supercooling and metastability

The phenomenon of supercooling and metastability plays an important role in the product specific planning of freezing processes under pressure. Exploiting those effects, processes can be designed beyond the theoretical limits of thermodynamic phase boundaries. Urrutia classified different states of metastability with respect to their periodic change (Urrutia Benet, 2005). In the present study metastability is assumed, independent from the latter classification, when a sample enters a thermodynamic region without changing its phase accordingly. The phenomena of supercooling and metastable liquid and/or solid phases were observed in all HPLT processes (PSF, PAF and PIC)

3.2.1.1 Liquid metastability

Figure IV-8 shows characteristic p,t and p,t,T plots of an initially liquid sample (emulsion B) during PSF treatment. No water phase transition occurred after pressurization to 360 MPa and subsequent cooling to -25°C, as indicated by the constant decrease in temperature. At the time of expansion, the samples were in the metastable liquid state under conditions where the thermodynamically stable state is ice V.

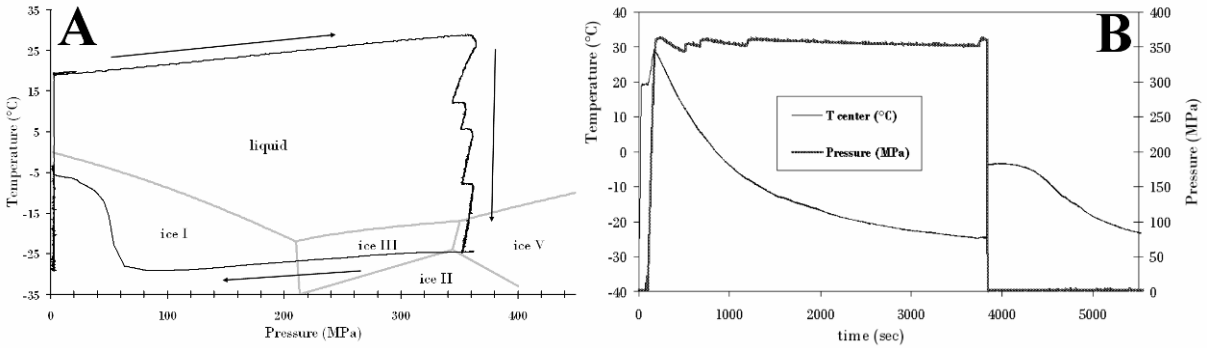

Figure IV-8: Characteristic p,t plot (A) and p,t,T plot (B) of a dairy emulsion (emulsion A) in a PSF cycle with liquid – ice I phase transition. Max. pressure 360 MPa and nucleation pressure 60 MPa. Pressure release rate about 50 MPa/sec. The water phase diagram is in the background, redrawn from (Bridgman, 1912).

During cooling under pressure the water phase of emulsion A enters the metastable region at -18.2°C and 360 MPa (freezing point of water at 360 MPa: -16.2°C; (Bridgman, 1912)). The

degree of supercooling (ΔT_{sup}) of the liquid phase at -25°C is 6.8 K. The emulsion formulation, especially the high level of sugars and stabilizers, is the basic cause for the lowered equilibrium freezing point. In addition, the high sugar content of the emulsion supports the metastability of the liquid phase under pressure. The absolute viscosity of sugar solutions increases exponentially with pressure and with increasing viscosity supercooling is promoted (Foerst et al., 2002; Kimizuka et al., 2007). According to this, the chance of nucleation in sugar rich systems is reduced with increasing pressure.

During controlled pressure release, the metastable liquid phase is shifted from the ice V region to the ice I region (see Figure IV-8). At the point of maximum supercooling in the ice I region homogeneous nucleation is triggered and crystallization throughout the sample occurs, raising the temperature to the ice I equilibrium melting line of the sample. The degree of maximum supercooling in the process can be quantified by the ΔT of the sudden temperature increase from the nucleation temperature to the corresponding freezing point at the nucleation pressure (Thiebaud et al., 2002). In the performed experiments with moderate pressure release rates (20-50 MPa/s) the ice I nucleation typically occurred at pressures between 50 and 100 MPa. However, the nucleation pressure, and linked to it the extent of supercooling, is affected by the pressure release rate. With increasing pressure release rates, the nucleation pressure was lowered and the extent of supercooling increased. During rapid expansion (expansion rate >150MPa/sec), nucleation was reproducibly detected between 0.1 and 40 MPa.

In the PSF process, the metastability of the liquid phase can be exploited to increase the energy removal from the system before freezing. In the PAF process, the high degree of supercooling causes increased process times, and lower process temperatures as thermodynamically expected are required.

During PAF treatment, the nucleation temperatures of the model emulsion (emulsion A) in the ice III region ranged from -38°C to -44°C, resulting in a ΔT_{sup} of 15 to 22 K. In addition to the reduced nucleation temperatures, the nucleation times were not predictable. Maximum supercooling times of 3000s at -38°C were observed before nucleation occurred. Short pressure surges during cooling in the metastable state appeared to induce nucleation and shorten the pressure holding time at constant temperature. In the PSF process design the results of the PAF experiments are of high value, as they show up the limits of supercooling in the matrix, which determine the minimum temperature before pressure release for the PSF process.

Figure IV-9 shows the different nucleation temperatures of emulsion A and the 20% SMP solution in the ice I and ice III region. Higher degrees of supercooling occurred during freezing to ice III compared to ice I. This finding is consistent with results of previous studies ((Schlüter & Knorr, 2002; Urrutia Benet, 2005; Urrutia Benet et al., 2007)). However, the metastable regions described in the latter studies are based on experiments with potato tissue and may not be fully applicable for the model systems that were investigated in the present study. The liquid metastable regions found for the sugar rich model systems exceed those of potato tissue. The emulsion composition reduces the chance of nucleus formation to some extent and the extent of supercooling differs from low sugar products.

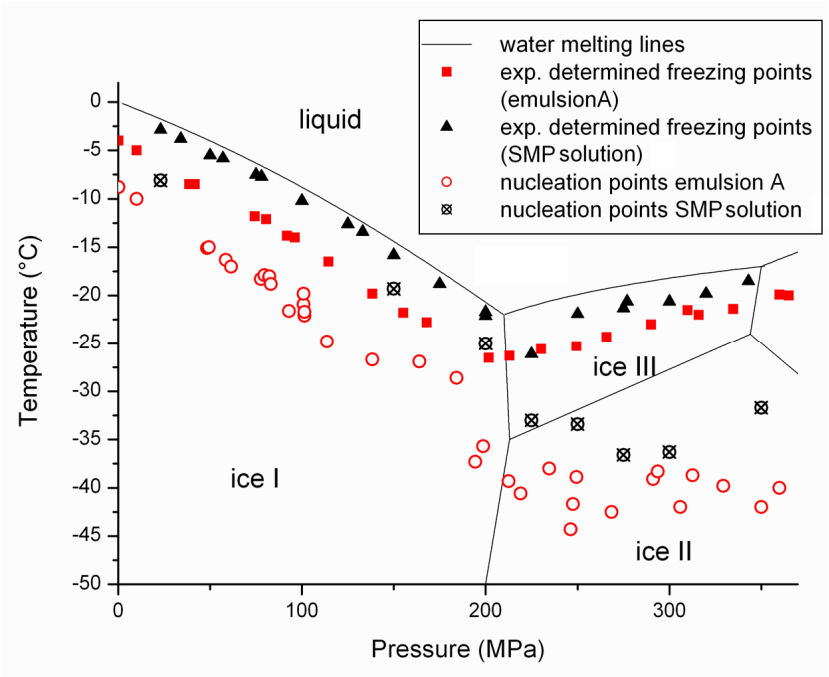

Figure IV-9: Experimentally determined freezing and nucleation temperatures of reconstituted skim milk (20% w/w; SMP A) and a dairy based emulsion (emulsion A).

The occurrence of metastable regions and in particular their dimensions seem affected by the viscosity of the matrix. With an increased sugar content not only the freezing point is lowered but the metastable regions grow and do not just shift to lower temperatures according to the freezing point depression. As a consequence lower process temperatures and higher pressures can be applied.

3.2.1.2 Solid metastability and solid-solid phase changes during pressure induced crystallization

Two effects have to be considered during pressurization of frozen systems:

1) Isochoric compression increases the total energy of the system. The temperature is increased when no phase transition is involved.
2) Pressure induced melting of ice crystals consumes energy.

The results of the pressure induced crystallization (PIC) experiments demonstrate the occurrence of pressure induced metastable solid water phases in the investigated emulsion B. Figure IV-10 shows the p,t and p,t,T plots that describe the characteristic temperature development during the process.

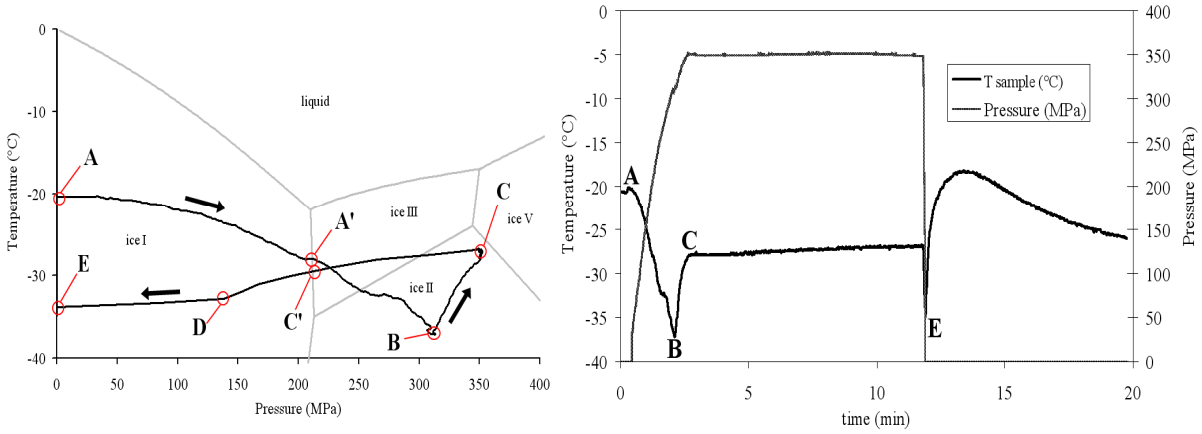

Figure IV-10: Typical p,t (left) and p,t,T (right) chart of frozen aerated emulsion (emulsion B) during PIC treatment. Solid – solid phase transition at 320 MPa and 140 MPa (water phase diagram in the background, redrawn from (Bridgman, 1912)). A→A': temperature passes along the ice I melting line. A'→B: temperature follows the extended ice I melting line in the ice III region (metastable ice I). B→C: recrystallization ice I to ice III. C→C': temperature follows the ice III melting line. C'→D: temperature along the extended ice III melting line in the ice I region (metastable ice III). D→E: quasi-adiabatic cooling of recrystallized ice I.

Upon pressurization the temperature of the frozen sample remains constant up to a certain pressure level (40 MPa in the shown process). In this phase of constant temperature, the heat of compression is equilibrated by the heat uptake of the PTM (T_{PTM}~ -35°C) and the heat of fusion of melting ice crystals. During further pressurization the temperature approaches the melting line of water and enters the metastable region after passing the ice I to ice III phase boundary. Heat of compression (quasi-adiabatic heating) and latent heat in this phase are in equilibrium. The solid – liquid transition is induced by the changing p-T conditions and completely dissipates the heat of compression. Since the energy input due to compression is not sufficient to completely melt the sample, the temperature decreases and keeps approaching the melting line of the system. The gradually increasing freezing point is attributed to partial melting of the sample due to the energy uptake during compression. According to the modelled phase diagram of emulsion A (Figure IV-6), this effect can be described by the passing of different iso-concentration melting lines that correspond to constant ice contents and solute concentrations. The amount of frozen water is reduced during compression. As a result, this melting line is not parallel to the water melting line and shows a decreasing slope. The atmospheric pressure DSC data (Figure IV-5) displays the non linear coherency between ice content and temperature. 45% water is crystallized 3 K below the initial freezing point. To freeze 90% of the total water cooling to 27 K below the initial freezing point (90% water frozen at -29°C) is required. During pressure build up ice I entered the metastable state and the temperature kept approaching the extended ice I melting line to some extent. Ice I occurred metastable in the ice III region (A' → B in Figure IV-10) between 211 and 300 MPa. At higher pressures recrystallization (ice I to ice III) is induced. In this study this point was typically reached at $p > 300$ MPa and $T < -34$°C (B in Figure IV-10). Recrystallization to ice III is followed by the sudden increase of the sample temperature to -28°C at 350 MPa during further pressurization (B→C in Figure IV-10), which represents the corresponding equilibrium freezing point in the ice III region. The subsequent controlled pressure release (C→E in Figure IV-10) causes supercooling of the sample and solid metastability is also observed during pressure release. The recrystallization of ice III to ice I occurred at pressures below 170 MPa. As for nucleation, there is a dependency of recrystallization processes on the rate of pressure change. This is due to the time dependent, instable character of metastable phases, which is discussed in detail by Urrutia, who examined the stability of metastable states of water over time (Urrutia Benet et al., 2007). The

maximum temperature of -18°C after pressure release and recrystallization to ice I indicates that 82% of the total water is frozen at this point.

3.2.2 Ice crystal growth in sugar rich dairy emulsions under pressure

Figure IV-11 shows the temperature development after nucleation at 320 MPa in water and a sugar rich emulsion (emulsion B). With the formation of a stable nucleus in a liquid water phase, crystal growth begins and each water molecule that joins the solid crystal lattice emits energy in the form of latent heat.

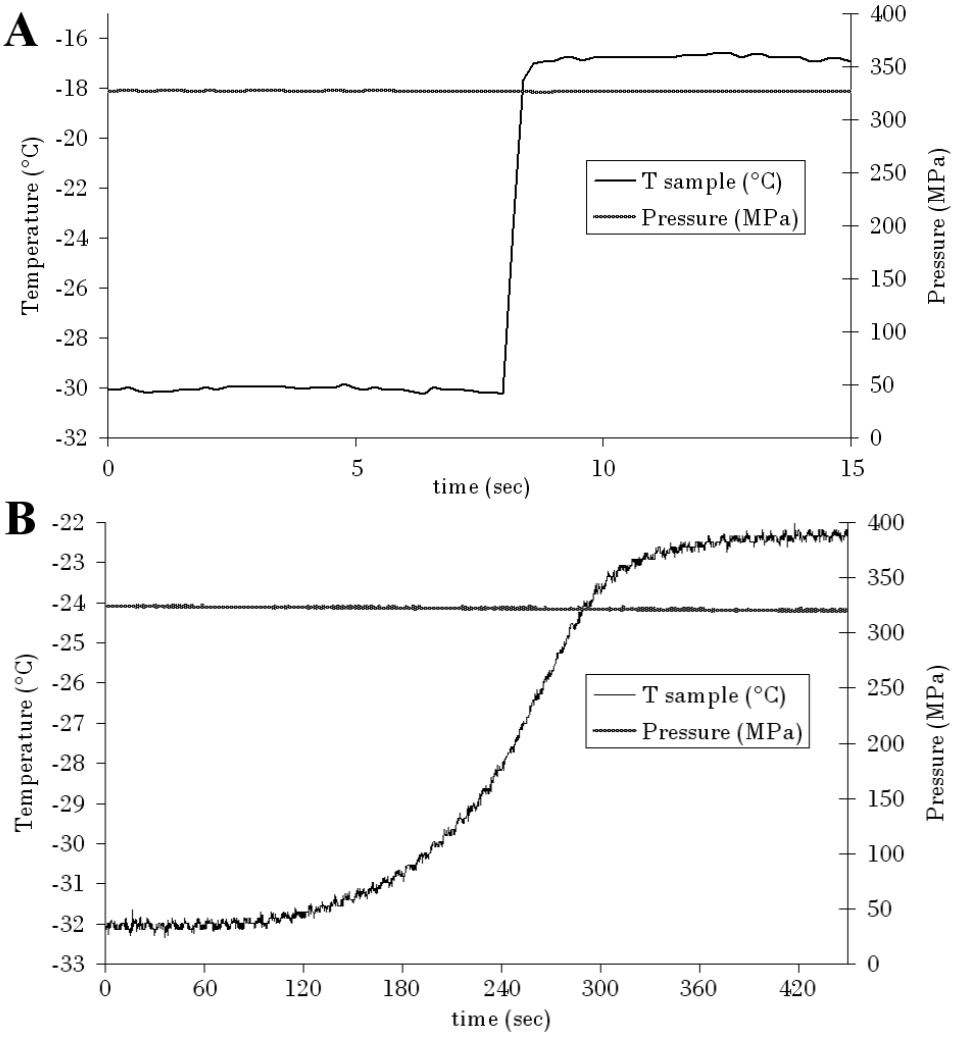

Figure IV-11: Nucleation and core temperature increase to the equilibrium freezing point in water (A) and a sugar rich dairy based emulsion (emulsion B) (B) at 320 MPa. Nucleation to ice V (B) and nucleation to ice III (A).

This energy causes a temperature increase in the crystallizing sample to the equilibrium freezing point according to the present p,T conditions. The higher the crystal growth rate, the faster is the temperature change from the nucleation temperature to the crystallization plateau, as the amount of latent heat released in the system is proportional to the number of molecules that join the solid phase. The crystal growth rate shall here be defined as the number of molecules that join the crystal network ($dV_{crystal}$) per time ($dV_{crystal}$ /dt). During crystallization, the product temperature is limited by the equilibrium freezing point of product. The product temperature remains at this value as long as the amount of latent heat is high enough to compensate the heat removal from the system. In pure water this point is indicated by the end of the freezing plateau. The sudden temperature change after nucleation in water indicates a high crystal growth rate. In the sugar rich emulsion, the temperature change from the

nucleation temperature to the freezing point takes about 300 sec, whereas it takes only 2 seconds in water. The crystal growth rate in the sugar rich emulsion is drastically reduced. Crystal growth after nucleation can be considered a "snowball effect" until the equilibrium freezing point is reached: with increasing crystal surface increases the crystal growth rate. Due o this effect, the temperature in the sugar rich emulsion reaches the plateau temperature with some delay. After 300 seconds the latent heat of crystallization overweighs the heat flow to the cooling media and the maximum temperature after nucleation is reached. The plateau temperature of emulsion B (Figure IV-11) is about -22.2°C at 320 MPa. According to Bridgman, the equilibrium freezing point of water is -17.5°C at 320 MPa for ice III and -19.3°C for ice V (metastable) (Bridgman, 1912). Taking into account the freezing point depression of the sugar rich emulsion of 2K, as it was determined by DSC (Figure IV-5), the equilibrium freezing point of the emulsion at 320 MPa is shifted to -19,5°C for ice III and -21.3°C for ice V.

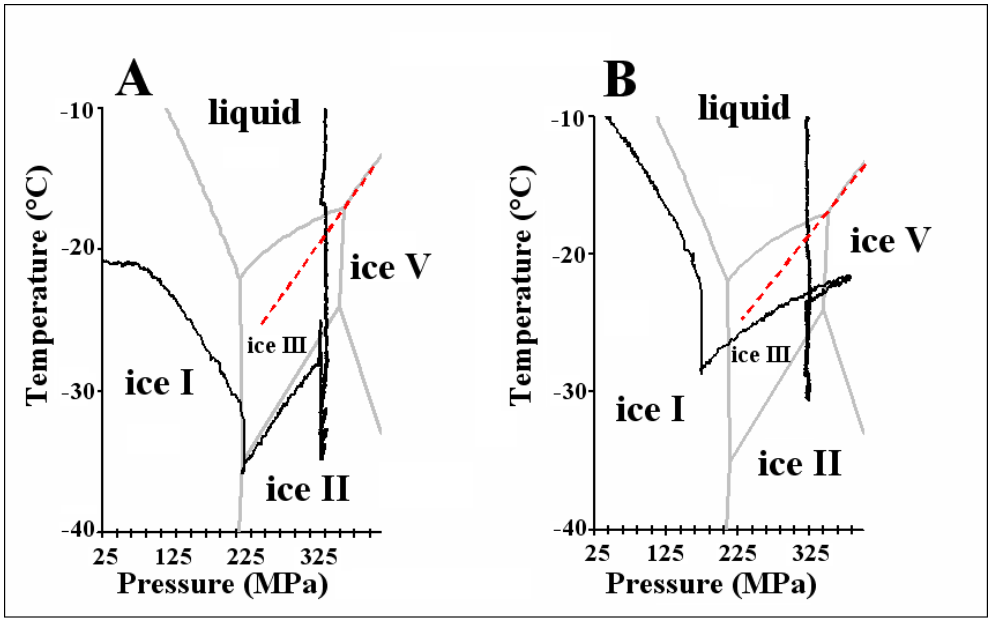

Figure IV-12: Temperature changes during pressure changes in a sugar rich dairy based emulsion. Formation of metastable ice V (A) and ice III (B) at 320 MPa. The dotted red lines show the extended phase transition line of ice V (---).

Pressure changes on the crystallization plateau showed the formation of ice V in the PAF experiment shown in Figure IV-11 B. Accordingly, the equilibrium freezing point at the time of nucleation was at -21.3°C. The ΔT of 0.9K displays the freezing point depression that occurred due to ice crystal growth from the time of nucleation until reaching the plateau temperature. As soon as nucleation occurs, the amount of frozen water in the emulsion increases progressively and before reaching the plateau temperature a certain amount of ice has already caused freeze concentration in the product. According to the DSC data, the freezing point depression of 0.9K caused an ice formation of about 18% (total water). As a consequence, the initial plateau temperature (-22.2°C in the sugar rich emulsion in Figure IV-11 B) is below the actual equilibrium freezing point of the system at the time of nucleation (-21.3°C). The PAF experiments with sugar rich emulsions showed that nucleation to ice V or ice III occurred randomly at pressures around 320 MPa. Predicting the ice formation before nucleation was not possible at 320 MPa ±20 MPa. Figure IV-12 shows two independent PAF treatments of a sugar rich dairy emulsion at 320 MPa and the formation of ice III and metastable ice V. The ice modification is identified by the parallel lines of temperature during pressure shift and the extended phase transition lines of ice I and ice V.

3.3 Process temperatures before and after pressure release during PSF and PAF

In most HPLT freeze processes, i.e. pressure shift freezing, freezing is not completed with the pressure release. Subsequent atmospheric freezing is required to cool the product to the desired temperature. The product temperature after expansion is determined by the total ice content in the product, which can be divided into two basic fractions:

1. Ice formed during freezing under pressure (PAF)
2. instantaneously formed ice during pressure release (PAF and PSF)

Ice formation under pressure occurs only in the PAF treatment and causes freeze concentration analogues to atmospheric freezing. During pressure release in the PAF and PSF process the liquid phase is affected by the sudden supercooling and a certain amount of water crystallizes instantaneously. The latent heat released in this phase transition is consumed by the energy removal due pressure release and supercooling. This energy has not to be removed from the system by the means of heat transfer.

During cooling at constant elevated pressure without ice formation, energy is removed from the system due to supercooling of the liquid phase with respect to the atmospheric freezing point. Crystallization to ice III and further cooling additionally decreases the total energy in the system. During pressure release the liquid phase partly crystallizes and the release of latent heat causes an increase in temperature which results in the atmospheric freezing plateau. The amount of water frozen under pressure and the ice formed during expansion determine the extent of freeze concentration. Hence, the atmospheric freezing plateau is at temperatures below the initial equilibrium freezing point at ambient pressure and depends on the total amount of water frozen after pressure release. During subsequent atmospheric freezing, energy is emitted and the sample temperature progressively decreases.

After PSF at 320 MPa of the dairy emulsion (emulsion B) the plateau temperature was found at -3.3°C, 1.2 K below the freezing point determined with the DSC analysis. The sectional enlargement in Figure IV-13 indicates that 24.5% of the total water is frozen at this point. Deviations of this temperature from the DSC data, as it was found in the experimental freezing point determination, is not expected in this case, since during PSF homogeneous nucleation occurs and freeze concentration in the sample core does not occur.

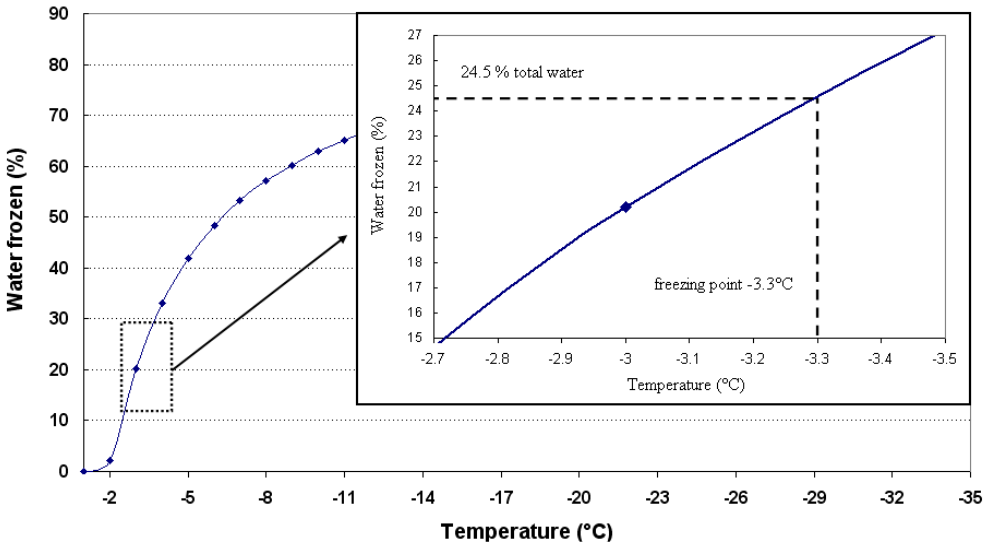

Figure IV-13: Sectional enlargement of the dairy emulsion B DSC plot. The plateau temperature of -3.3°C corresponds to 24.5% total water frozen.

Figure IV-14 shows the product temperature after expansion in a PAF treated dairy foam (emulsion B) as a function of the temperature at the time of pressure release at 320 MPa. The temperature after expansion is determined by the total amount of water frozen in the system.

The temperature trend line correlates with DSC data, showing the total amount of water frozen over temperature (Figure IV-5).

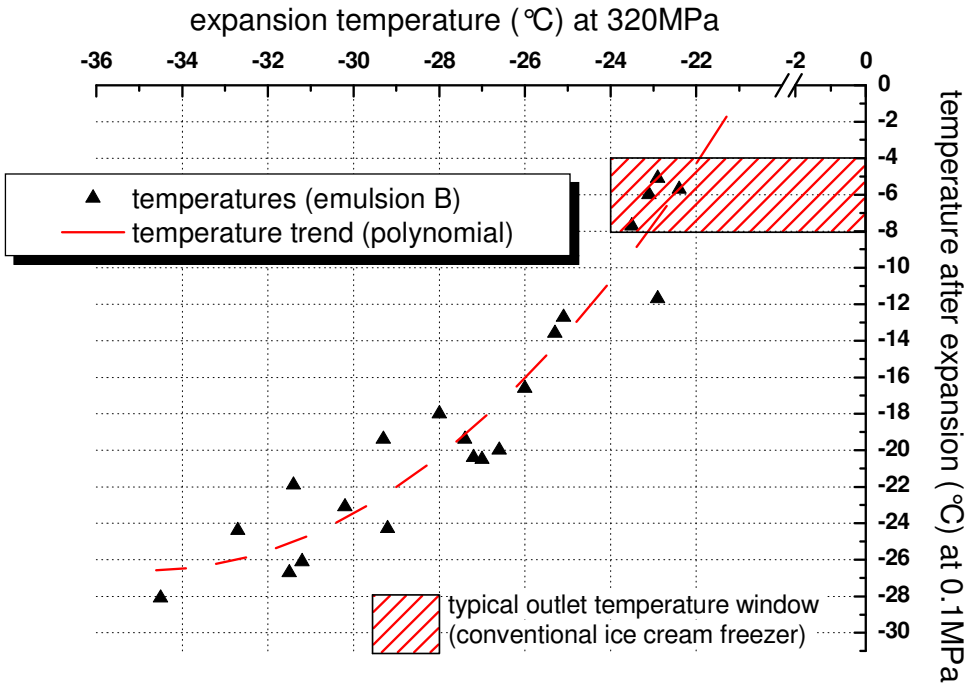

Figure IV-14: Atmospheric product temperature after PAF treatment. Product temperature after expansion as a function of expansion temperature at 320 MPa (▲) in dairy based emulsion (emulsion B).

The dashed window in Figure IV-14 displays the typical outlet temperature range of a conventional ice cream freezer (-4 to -8°C) (Marshall et al., 2003). The end-temperatures after PAF treatment range from -5 to -28°C, which potentially reduces subsequent hardening times or allows leaving out the hardening step.

4 Conclusion

Experimental equilibrium freezing point determination of a sugar rich dairy based emulsion and a 20% SMP solution from 0.1 to 350 MPa showed a parallel trend of the melting lines to the water melting lines of water after Bridgman. In the experimental detection under pressure, the freezing points were progressively found at lower temperatures with increasing pressure. Melting point determination by the means of pressure assisted thawing resulted in more accurate data. The major cause for this effect seems the increased viscosity at increased pressures in sugar rich systems. High viscosity promotes supercooling and reduces the crystal growth rate. As a consequence, freezing point depression in the sample core occurs before the temperature reaches the maximum of the crystallization plateau.

Due to progressive freezing point depression during freezing, the state of a sugar rich system is not properly described with one single melting line. DSC analysis at atmospheric pressure shows the amount of ice as a function of temperature. On the base of this data, a complex phase diagram of a protein model system and a dairy emulsion was modelled, taking into account the freezing point depression with decreasing product temperatures.

Liquid and solid metastability was observed during PSF, PAF and PIC treatments. The extent of liquid metastability was found to be linked to the sugar content. With increasing sugar content supercooling is promoted and metastable regions enlarge. The phenomenon of

supercooling and liquid metastability plays an important role in the product specific planning of freezing processes under pressure. Exploiting these effects, processes can be designed beyond the theoretical limits of thermodynamic phase boundaries. By this means higher amounts of energy can be removed from the system before expansion and the amount of ice that forms during pressure release after PSF can be increased.
Metastable Ice V occurred randomly in PAF treatments with both model systems at pressures around 320 MPa. In the pressure range from 300 to 350 MPa it was not predictable weather freezing the model systems results in the formation of ice III or ice V. This phenomenon has little effect on the overall process but changes the temperature of the product after nucleation, as ice III and V have different equilibrium freezing points in this pressure range.
The product temperature after expansion in the PAF process can be controlled by the temperature at the time of expansion, taking into account the energy reduction in the system during expansion. Compared to conventional freezing processes, e.g. ice cream freezing, very low temperatures can be achieved after PAF. Subsequent cooling steps, e.g. in a hardening tunnel, are not required or hardening times can be shortened. Apart from structural changes in the product that are induced by the treatment, this may be the key advantage of the HPLT technology with respect to the manufacturing of frozen food foams.

5 References

[1]Balibar, S. & Caupin, F. (2006). Nucleation of crystals from their liquid state. *C.R. Physique*, *7*, 988-999.

[2]Bridgman, P. W. (1912). Water, in the liquid and five solid forms, under pressure. *Proceedings of the American Academy of Arts and Sciences*, *47*, 441-558.

[3]Chaplin, M. (2008). Water structure and science, http://www.lsbu.ac.uk/.

[4]Chevalier, D., Le Bail, A. & Ghoul, M. (2000). Freezing and ice crystals formed in a cylindrical food model: part II. Comparison between freezing at atmospheric pressure and pressure-shift freezing. *Journal of Food Engineering*, *46*(4), 287-293.

[5]Clarke, C. (2004). *The Science of Ice Cream*. The Royal Society of Chemistry, Cambridge.

[6]Foerst, P., Werner, F. & Delgardo, A. (2002). On the pressure dependence of the viscosity of aqueous sugar solutions. *Rheologica Acta*, *41*(4), 369-374.

[7]Guignon, B., Otero, L., Molina-Garcia, A. D. & Sanz, P. D. (2005). Liquid water ice I phase diagrams under high pressure: Sodium chloride and sucrose models for food systems. *Biotechnology Progress*, *21*(2), 439-445.

[8]Janssen, A. H., Talsma, H., van Steenbergen, M. J. & de Jong, K. P. (2004). Homogeneous Nucleation of Water in Mesoporous Zeolite Cavities. *Langmuir*, *20*(1), 41-45.

[9]Kimizuka, N., Chotika, V. & Toru, S. (2007). Ice nucleation and supercooling behaviour of polymer aqueous solutions. *Cryobiology*, *56*, 80-87.

[10]Lévy, J., Dumay, E., Kolodziejczyk, E. & Cheftel, J. C. (1999). Freezing Kinetics of a Model Oil-in-Water Emulsion under High Pressure or by Pressure Release. Impact on Ice Crystals and Oil Droplets. *Lebensmittel-Wissenschaft und -Technologie*, *32*, 396-405.

[11]Luscher, C. M. (2008). *Effect of high pressure - low temperature phase transitions on model systems, foods and microorganisms*. PhD thesis, Berlin, Berlin University of Technology, 158.

[12]Marshall, R. T., Goff, H. D. & Hartel, R. W. (2003). *Ice Cream*. Kluwer Academic / Plenum Publishers, New York.

[13]Petrenko, V. F. & Withworth, R. W. (1999). *Physics of ice*. Oxford University Press.

[14]Reid, D. S. (1998). Freezing - nucleation in foods and antifreeze actions. In D. S. Reid. *the properties of waterin foods ISOPOW 6* (pp. 275-286). Blackie Academic & Professional.

[15]Robinson, G. W., Zuh, S. B., Singh, S. & Evans, M. W. (1996). *Water in Biology, Chemistry and Physics*. World Scientific.

[16]Schlüter, O. & Knorr, D. (2002). Impact of the metastable state of water on the design of high pressure supported freezing and thawing processes. In *Proceedings of the ASAE Annual International Meeting / CIGR XVth World Congress*, Chicago, Illinois, USA.

[17]Schlüter, O., Benet, G. U., Heinz, V. & Knorr, D. (2004). Metastable states of water and ice during pressure-supported freezing of potato tissue. *Biotechnology Progress*, *20*(3), 799-810.

[18]Soukoulis, C., Lebesi, D. & Tzia, C. (2009). Enrichment of ice cream with dietary fibre: Effects on rheological properties, ice crystallisation and glass transition phenomena. *Food Chemistry*, *115*(2), 665-671.

[19]Thiebaud, M., Dumay, E. M. & Cheftel, J.-C. (2002). Pressure-shift freezing of o/w emulsions: influence of fructose and sodium alginate on undercooling, nucleation, freezing kinetics and ice crystal size distribution. *Food Hydrocolloids*, *16*(6), 527-545.

[20]Urrutia Benet, G. (2005). *High Pressure Low temperature Processing of Foods: Impact of Metastable Phases on Process and Quality Parameters*. PhD, Berlin University of Technology, 196.

[21]Urrutia Benet, G., Arabas, J., Autio, K., Brul, S., Hendrickx, M., Kakolewski, A., Knorr, D., Le Bail, A., Lille, M., Molina-García, A. D., Ousegui, A., Sanz, P. D., Shen, T. & Van Buggenhout, S. (2007). SAFE ICE: Low-temperature pressure processing of foods: Safety and quality aspects, process parameters and consumer acceptance. *Journal of Food Engineering*, *83*, 293-315.

Chapter V HPLT effects on physicochemical properties of functional ingredients in frozen dairy based foams

Successful product and process development is always linked to profound understanding of the effects occurring during the process, in particular the effects on the physical and biochemical properties of the treated food matrix. The impact of HPLT treatment on the functionality of single ingredients in aerated frozen dairy emulsions is the focus of this chapter. Relevant ingredients were investigated with respect to HPLT induced changes that affect the overall quality of the frozen dairy foams.

1 Functional aspects of relevant ingredients in frozen dairy foams

Commercially available frozen dairy foams, e.g. ice cream and frozen desserts, are comprised of a mixture of water, air, milkfat or vegetable fat, nonfat milk solids (NMS), sweeteners, stabilizers, emulsifiers and flavours. The complex food systems can be subdivided into three major discrete phases:

- Ice crystals
- Air bubbles
- Fat globules

In addition, casein micelles can be present as a minor discrete phase. The continuous phase is comprised of a freeze concentrated unfrozen matrix of dissolved and/or suspended sugars, whey proteins, salts and polysaccharides (Marshall et al., 2003).

The macrostructure of the frozen system is highly dependent upon the functionality and interactions of its single components. Limiting the functionality of one component in the system may cause decisive alterations in the whole product.

1.1 Nonfat Milk Solids

Lactose and milk proteins represent the group of nonfat milk solids (NMS). In frozen dairy foams the NMS aid in giving body and chew resistance and allow increasing gas incorporation without the quality defects associated with high overruns (snowy or flaky textures) (Marshall et al., 2003). Lactose constitutes over one-third of the solid matter in milk and approximately 20% of the carbohydrate in commercially available frozen dairy foams. Lactose is unique in that it is found only in milk. Sugars have two major functions in frozen dairy foams. They make it sweet and contribute to the texture development by controlling the amount of ice in the frozen product. Proteins contribute to develop the structure in frozen dairy foams, including emulsification, foamability and water holding capacity (Schmidt, 1994). Casein networks and whey protein aggregates have a large impact on texture by limiting ice crystal growth (Flores & Goff, 1999). Moreover, they contribute to the typical dairy flavour (Clarke, 2004). Compared to milkfat, NMS are less expensive and therefore an attractive alternative source of total solids (Marshall et al., 2003). The most common source for NMS are skim milk powder (SMP) and whey protein isolates (WPI). The total protein component of milk is composed of numerous specific proteins. The primary group of milk proteins are the caseins. There are 3 or 4 caseins in the milk of most species. The different caseins are distinct molecules but are similar in structure. The proteins that remain in solution after removal of casein are by definition termed whey proteins. The major whey proteins in cow's milk are beta-lactoglobulin (β-lg) and alpha-lactalbumin (α-la). The characteristic

bovine milk protein fractions are shown in Table V-1. The exact composition depends, as for all components in milk, on the breed of cow, the diet and the season.

Table V-1: Characteristics of bovine milk protein fractions

Protein fraction	Molecular weight [Da]	Total protein [%]	Sub fraction [%]
Casein		**83**	
αs1-casein	22.000 – 25.400	37	45
αs2-casein		9	11
β-casein	24.000	21	25
κ-casein	19.000	12	14
γ-casein	20.000	4	5
Whey proteins		**17**	
β-lactoglobulin	18.000	10	58
α-lactalbumin	14.100	2	13
Immunoglobulin	150.000 – 1.000.000	2	12
Serumalbumin	60.300	1	5
Minor proteins	40.000 – 86.000	2	12

1.1.1 Casein

The casein content of milk represents about 80% of the total milk proteins. The distinguishing property of all caseins is their low solubility at pH 4.6. Caseins are conjugated proteins, most with phosphate groups esterified to serine residues. These phosphate groups are important to the structure of the casein micelle. Calcium binding by the individual caseins is proportional to the phosphate content (Cross, Huq, Palamara, Perich & Reynolds, 2005).

The conformation of caseins is much like that of denatured globular proteins. The high number of proline residues in caseins causes particular bending of the protein chain and inhibits the formation of close-packed, ordered secondary structures. Caseins contain no disulfide bonds. An important functional property of caseins is their ability to self associate and to associate with other protein fractions (Merel-Rausch et al., 2007). Most of the casein proteins are present as colloidal particles (casein micelles), typically 40 to 300 nm in size. They are very surface active and stabilize o/w emulsions, as on end of the molecules consists mostly of hydrophilic amino acids, whereas the other end consists mostly of hydrophobic ones (Clarke, 2004). The lack of tertiary structure accounts for the stability of caseins against heat denaturation because there is very little structure to unfold (Marshall et al., 2003). This results in strong association reactions of the caseins and renders them insoluble in water. High pressure causes significant modification of the casein micelles (Fertsch, Mueller & Hinrichs, 2003; Huppertz et al., 2006; Considine, Patel, Anema, Singh & Creamer, 2007a). Dissociation and re-association occurs under pressure and during pressure release and the formation of new casein structures is induced. The pressure induced structure is affected by the protein concentration and may lead to the formation of firm gels (Fertsch et al., 2003; Merel-Rausch et al., 2007).

1.1.2 Whey proteins

β-lactoglobulin

The most relevant protein in whey is β-lactoglobulin (β-lg), which comprises 10% of the total milk protein or 58% of the whey protein. β-lg is pressure sensitive and denaturation is reported to occur at pressures above 100 MPa (Huppertz, Kelly & Fox, 2002).The majority of denatured β-lg in HP-treated milk associates with the casein micelles, although some denatured β-lg remains in the serum phase or is attached to the milk fat globule membrane (Huppertz et al., 2006).

α-lactalbumin

α-lactalbumin (α-la) represents 2% of the total protein in bovine milk which is about 13% of the total whey protein. α-la is a rather baro-resistant protein and denaturation is reported at

pressures >400 MPa (Huppertz, Fox & Kelly, 2004b). The resistance of α-la to pressure can be attributed to the lack of free sulfhydryl groups and to its rigid molecular structure (Lopez-Fandino, Carrascosa & Olano, 1996; Lopez-Fandino & Olano, 1998).

Other whey proteins

Immunoglobulines (Ig), bovine serum albumin (BSA) and other minor proteins play an important role in the functionality and stability of milk in its natural purpose but do not affect the functionality of frozen dairy desserts. However, the immunoactivity of Ig is decreased at pressures >400 MPa (Viazis, Farkas & Allen, 2007).

1.2 Fat

Milkfat is the natural dairy-fat and represents the lipid fraction of the milk. It consist mainly triglycerides, 3 fatty acids bound to 1 glycerol (95.8% w/w). In commercial dairy foams, milkfat may be substituted by non-dairy fats (e.g. palm or coconut oil). Factors in the selection of fat sources are: crystallization rate, temperature dependent melting profile, the content of high melting triglycerides and the flavour and purity of the oil (Marshall et al., 2003). For optimal partial coalescence during freezing of dairy foams, it is important that the droplets contain an intermediate ratio of liquid : solid fat. Fat greatly contributes to stability and quality of frozen aerated dairy products. It plays an important role in the foam formation and stabilization in liquid systems, as well as in frozen products. In the concomitant foaming and freezing step at refrigerated temperatures the partially crystalline fat phase undergoes partial coalescence or fat destabilization (Goff, 1997). As a result, a solid-like structure is created. A network of agglomerated fat develops in the matrix, surrounding the air bubbles and fat clusters partially cover the air interfaces. The model in Figure V-1 describes the basic mechanism of air bubble stabilization in frozen dairy foams. Moreover fat is responsible for a creamy texture, slows down the melting rate and is necessary to deliver flavour molecules that are soluble in fat but not in water (Clarke, 2004). High pressure affects the phase transition of fats and oils. Crystallization in the liquid phase is supported under high pressure (Buchheim & Abou El-Nour, 1992; Huppertz et al., 2006).

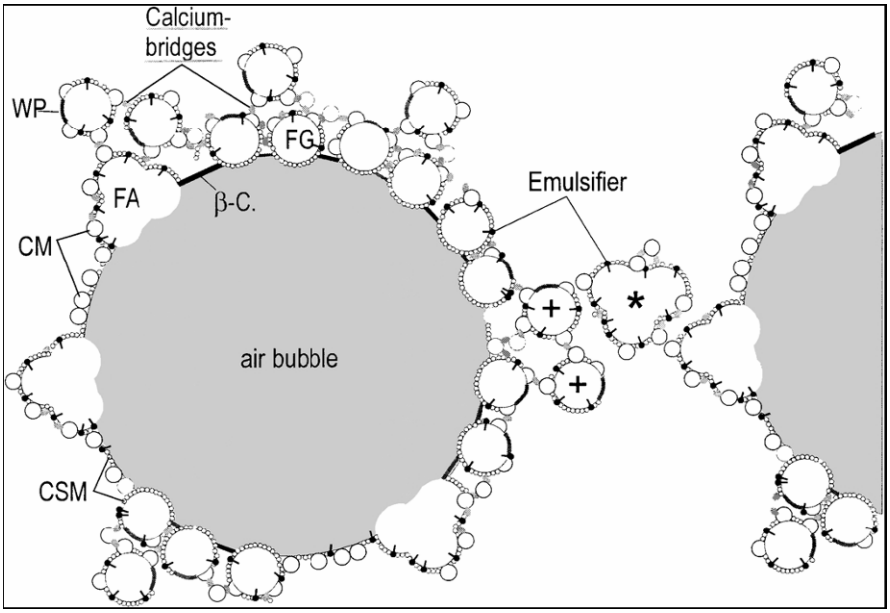

Figure V-1 Model for a stabilized air bubble and the foam lamella during the meltdown of ice cream (FG: intact fat globule; +: intact fat globule attached to the air bubble via calcium bridges; FA: partial destabilized fat agglomerate; ✱: fat agglomerate that blocks the foam lamella; CM: casein micelle; CSM: casein submicelle; β-C.: β-casein; WP: whey protein). Redrawn from (Koxholt, Eisenmann & Hinrichs, 2001).

1.3 Guar Gum

Guar gum is an edible, plant seed polysaccharide extracted from the guar gum bean plant by a series of crushing, sifting and grinding stages. It is used as a common stabilizer in various frozen dairy products. Stabilizers are functional ingredients and important to quality for several reasons (Clarke, 2004):

- Produce smoothness in texture during eating
- Reduce the rate of meltdown
- Prevent shrinkage and slow down moisture migration during storage
- Mask the detection of ice crystals in the mouth
- Allow easier pumping and filling into the packaging
- Support foam formation and increase stability
- Improve heat shock resistance

In combination with other hydrocolloids such as carrageenan and locust bean gum, guar is used as stabilizer in ice cream, sherbets and related products. Its prime function is to bind free water and inhibit crystal growth (Goff, 2002). Guaran, the functional polysaccharide in guar is a chain of (1-4)-linked β-D-mannopyranosyl units with single α-D-galactopyranosyl units connected by (1-6) linkages to, on average, every second main chain unit. The structural integrity of guar gum endosperm cells determines the quality of the raw material and plays an important role in stabilizing air cells and ice crystals (Barniol, 2005). Figure V-2 shows microscopic pictures of hydrated and non hydrated guar gum endosperm cells.

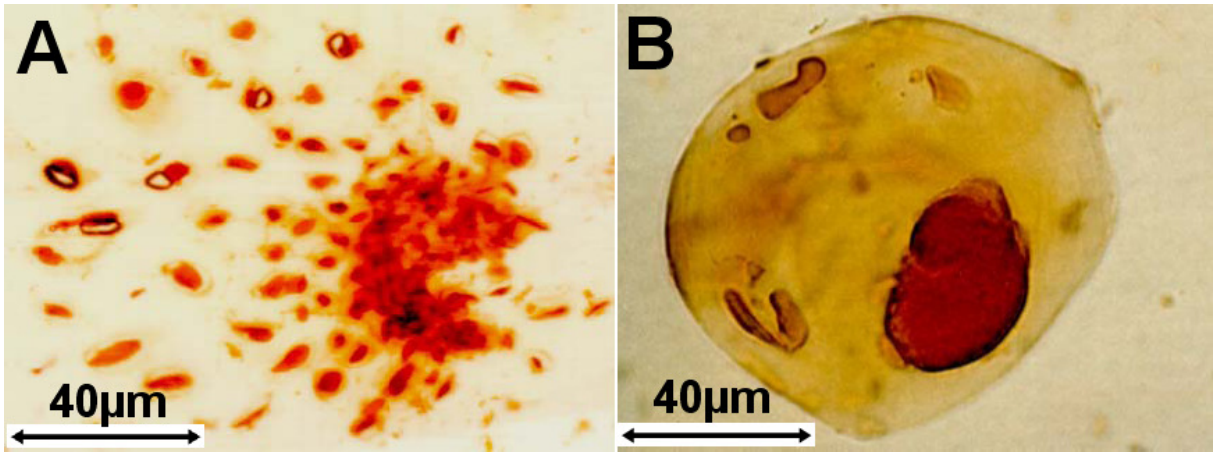

Figure V-2: Microscopic image of non hydrated guar gum endosperm cells (A) and hydrated guar gum endosperm cell (B).

2 Experimental methods

2.1 HPLT setup

To evaluate the effect of HPLT processing on single ingredients and to identify quality defects in HPLT treated frozen dairy foams, PSF and PAF experiments at max. pressures of 320 MPa were performed. For all experiments samples from 50 to 300ml were treated in the pilot scale HPLT unit. A detailed description of the HPLT setup and the sample-packaging is given in Chapter III.

2.2 Sample preparation

2.2.1 Guar gum

Guar gum (Degussa Texturant Systems France SAS, Paris, France) was suspended in water (1% w/w) at 20°C. The dispersion was left for hydration at 20°C for 90 min and filled in PE bags (50 ml) before treatment. The samples were treated at 320 MPa under the same conditions as the foamed dairy emulsion. The structural integrity of the guar gum endosperm

cells was of special interest and characterized by direct optical microscopy before and after treatment.

2.2.2 Skim milk and whey protein solutions

All protein solutions were prepared in w/w ratio. The specifications of the different skim milk powders (SMP) and whey protein isolates (WPI) are attached in the annex. For the preparation of the SMP and WPI solutions the powders were reconstituted in water in concentrations of 2.5%, 10%, and 20% and stirred for 2h at 20°C. Before treatment the solutions were filled into PE bags or pressure resistant polystyrol tubes.

2.2.3 Emulsion aeration

Emulsion A was used as a model for a complex aerated dairy emulsion. The system was used to investigate color changes and the fat coverage on the air interfaces after HPLT treatment. The aeration of the emulsion was performed with the Minimondo aeration system described in chapter III–3. Prior to aeration, the emulsion was tempered to 3°C in the feed tank of the aeration system, to reach outlet temperatures of about 10°C. The final OR of the liquid foam before treatment was adjusted in the range of 140 to 160% and was determined before the foam was packed for the HPLT treatment.
To produce conventionally frozen foam reference products, the model emulsions were frozen in a continuous ice cream freezer (Hoyer KF-80, Tetra Pak Hoyer, Hoejbjerg, Denmark). The OR of the reference foams was typically between 90 and 120%. An exemplary process sheet of the treatment is attached in the appendix. The OR of the reference foams was typically between 90 and 100%.

2.3 Analyses

2.3.1 Direct optical microscopy

The technique allows the characterisation of structural integrity of guar gum endosperm cells and the identification of fat clusters on air cell interfaces. For the microscopic analyses a Nicon Eclipse E400 microscope was used, equipped with a digital camera (JVC, TK-10070E). Images were captured and analysed with AnaliSIS software (Olympus, Hamburg, Germany). The hydrated endosperm cells of guar gum were stained with iodine and investigated after hydration at 20°C before and after HPLT treatment. Of special interest in this respect was the integrity of the endosperm cell plasma membrane.
Fat coverage of air interfaces was examined under 1000-times magnification, transmission mode, using immersion lens, narrowest field depth condenser setting and phase contrast, before and after treatment. At high magnitude the fat clusters on the air bubble surfaces can be identified without staining the sample.
Toluidine blue staining was applied to visualize protein in the aerated emulsion. Protein aggregates are identified as blue “clouds” in the matrix.

2.3.2 Gel electrophoresis

The protein composition of the treated SMP and WPI samples was detected by the discontinuous sodium dodecylsulfate polyacrylamide gel electrophoresis (SDS-PAGE). The treated samples were diluted before loading the gel to obtain optimal color intensity of the single protein bonds. The SDS-PAGE was performed as described by Kuenzel (Künzel, 2009). Minigels were prepared composed of a stacking gel (1 M Tris-HCl buffer at pH 6.8) and a separating gel (1.5 M Tris-HCl buffer at pH 8.8). Two acrylamid concentration ratios between stacking and separation gel were applied (stacking gel: separation gel): 3:6% and 5:12%. Protein samples were loaded onto each well, and electrophoresed in a mini-PROTEAN Tetra Cell (Bio Rad Laboratories GmbH, Munich, Germany) at a starting voltage of 125 volts. 8 µl Roti-Mark 10-150 Plus (Carl Roth GmbH + Co. KG, Karlsruhe, Germany)

was used as a molecular weight marker to identify the electrophoretic mobility of the milk protein fractions in the separation gel. The samples were heat treated at 85°C for 2 min prior to loading onto the gel. Following electrophoresis, gels were stained with Coomassie Blue R-350 (Amersham Pharmacia Biotech, Freiburg, Germany). Dithiothreitol (DTT) (Carl Roth GmbH + Co. KG, Karlsruhe, Germany) reduction (0.8% DTT) was performed to obtain control samples, that indicates disulfide bond aggregates.

2.3.3 Viscosity assessment

Viscosity measurement was performed with a rotary viscosimeter (Rotovisco RV 12, Haake Messtechnik GmbH u. Co, Karlsruhe, Germany). The different protein solutions were analysed at 20°C with the MV I rotor. Reference medium type E7 (Haake Messtechnik GmbH u. Co, Karlsruhe, Germany) was used as a control sample with a defined dynamic viscosity of 5.26 $mPa \cdot s$.

2.3.4 Colour assessment

To estimate the influence on the product color and to identify potential color defects after HPLT treatment, the color of conventionally frozen and HPLT treated dairy foam was measured with a Chromameter (MINOLTA Chroma Meter CR200). The color was determined on the surface of freshly cut samples. The L*a*b values were detected and compared. L value displays the brightness, a and b values the color saturation.

3 Results and discussion

3.1 Product colour

No major color defects were detected in the HPLT treated product. Table V-2 compares the L*a*b values of the conventionally frozen reference and the PSF treated aerated dairy foam.

Table V-2: L*a*b values of frozen aerated dairy emulsion after PSF treatment and conventionally processed reference

	L	a	b
Reference	94.97±0.59	-4.65±0.72	22.01±4.03
HPLT treated aerated emulsion	90.36±0.56	-3.74±0.11	24.02±1.53

The HPLT treated samples significantly differed in color from the conventionally processed reference. However, the treated foam shows only slight differences in the color saturation and brightness. Presumably the reduced OR of the HPLT treated samples and possibly the different crystal size and distribution accounts for the color deviation. The color of dairy products is also affected by the milk proteins. Micellization of casein has been reported to significantly affect the color of HP treated milk, as casein influences the light scattering (Adapa, Schmidt & Toledo, 1997). Reduced L values and higher green values were observed. However, both products were clearly in the same yellowish region of the color spectrum and the color deviations were found within an acceptable range.

3.2 Pressure stability of milk proteins

High pressure induced changes in the structure of milk proteins have been the focus of several research activities. HPLT combines the effects of high pressure with low temperatures, hence pressure and cold denaturation effects potentially occur during treatment.

To investigate the effect of HPLT treatments on the molecular structure of different milk protein, SDS-PAGE analysis of treated and untreated SMP and WPI solutions were

performed. The effect on the macro structure of the systems was evaluated by viscosity measurements. HP reference samples (320 MPa at 20°C, 60 min) were investigated to compare HP and HPLT induced changes and assess the role of ice formation and low temperatures during the HPLT treatment.

3.2.1 Impact of HPLT and HP treatment on the single milk protein fractions

PAF treatment (320 MPa, -35°C, 60 min) and HP treatment (320 MPa, 20°C, 60 min) were applied to investigate the effect on the different protein fractions in WPI and SMP solutions. SDS-PAGE analyses showed changes in the β-lg fraction of all treated samples (HP and HPLT). No effect on α-la and minor whey proteins (Ig and BSA) was detected. The results of a SDS-PAGE analysis with and without DTT, showing the different protein fractions in WPI after HP and PAF treatment, are shown in Figure V-3. After HP and PAF treatment β-lg dimer were found, indicated by the protein bonds above the 30 kDa marker. The molecular weight of monomeric β-lg is 18 kDa. However, β-lg dimerization occurred to a lesser extent after PAF treatment compared to conventional HP treatment. Weak bonds in the region of 72 kDa indicate the formation of β-lg polymers (tetramers) after HP treatment (Figure V-3 B). After DTT reduction, the β-lg dimmer bonds were still present in some gels. This is attributed to an insufficient DDT treatment of the samples, since SH-linked β-lg dimerization should be reversed by DTT addition. All other protein fractions were reduced equally after DDT addition.

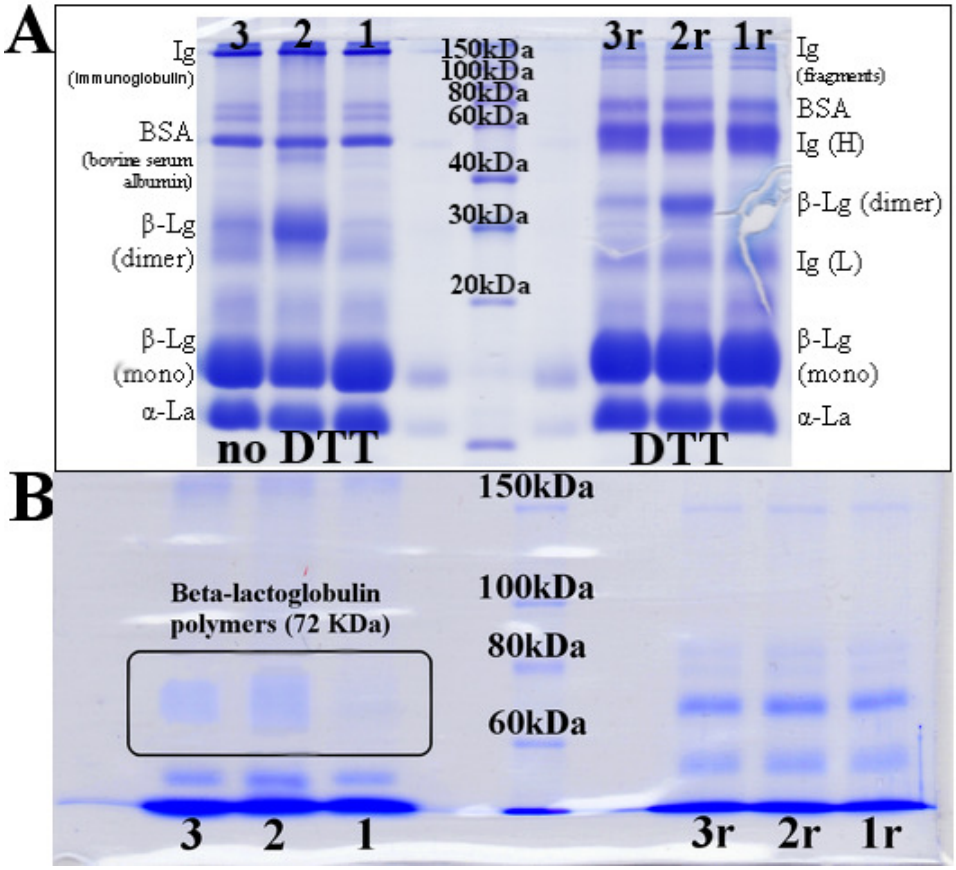

Figure V-3: A: discontinuous SDS-PAGE gel of WPI solution (10% w/w). Untreated reference (1), HP (320 MPa, 20°C, 60 min) treated (2) and PAF (320 MPa, -4 to -35°C, 60 min) treated (3). Lanes 1r, 2r and 3r represent the different samples after DTT reduction. B: discontinuous SDS-PAGE gel of WPI solution (10% w/w) from 60 to 150 kDa. Untreated reference (1), HP (320 MPa, 20°C, 60 min) treated (2) and PAF (320 MPa, -4 to -35°C, 60 min) treated (3). The marked section shows the molecular weight region of β-lg tetramers at 72 kDa. Lanes 1r, 2r and 3r represent the different samples after DTT reduction.

3.2.2 HP and HPLT effects on the casein fraction

Casein plays an important role in dairy products and its micellar structures are sensitive to high pressure. SMP solutions (2.5% w/w) were HP and HPLT treated to investigate changes in the micellar casein. The concentration of the SMP solution was chosen to avoid solidification during high pressure treatment, which occurred at concentrations >2.5% at 320 MPa. The reduction of casein micelle size during HP treatment is well documented in numerous publications (Schrader & Buchheim, 1998; Regnault, Thiebaud, Dumay & Cheftel, 2004). Casein micelles dissociate into smaller submicelles during pressure treatment up to 400 MPa and re-associate during pressure release (Merel-Rausch, 2006). Casein micelles were not detected during SDS-PAGE but the single casein fractions, hence, no difference between untreated and HPLT treated samples was detected (Figure V-4). The SMP solution showed weak β-lg and α-la bonds before DTT reduction. Association of β-lg and α-la with casein occurs during drying of the powder, reducing the amount of detectable monomers. The association of whey proteins with caseins has been reported in previous studies (Considine et al., 2007a).

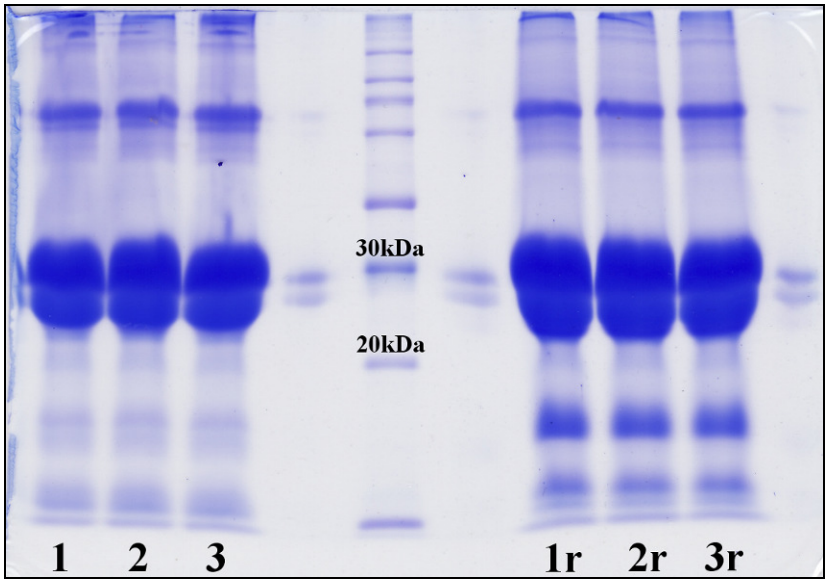

Figure V-4: SDS-PAGE of SMP (2.5% w/w). Untreated reference (1), HP (320 MPa, 20°C, 60 min) treated (2) and PAF (320 MPa, -35°C, 60 min) treated (3). Lanes 1r, 2r and 3r represent the different samples after DTT reduction.

SDS-PAGE as applied in the present study does not give quantitative information about the casein micelle size and aggregation. Transition electron microscopy (TEM), dynamic light scattering analyses or adapted SDS PAGE could be applied to obtain more detailed information in this respect.

3.2.3 HP and HPLT induced β-lg dimerization

Native bovine milk and conventionally dried WPI powders contain β-lg as monomereic molecules. β-lg dimerization occurred in all HP and HPLT treated WPI solutions. However, the effect was poorly developed in PAF treated samples. No significant difference between HP and PSF treatment was found but PAF treated WPI solutions showed very low β-lg dimerization. Figure V-5 shows a sectional enlargement of a SDS PAGE analysis, comparing the β-lg dimerization in HP, PAF, PSF and untreated WPI solution. The β-lg dimers are displayed by the protein bonds between the 30 and 40 kDa markers. After PAF treatment only little β-lg dimerization was detected compared to HP and PSF. The dimerization of β-lg was found equally intense after PSF treatment as it was after HP treatment.

Driving force for the β-lg interactions is the pressure, which is given in all treatment types. Different from HP and PSF treatment, the PAF treatment involves ice formation under pressure. A possible explanation for the poor development of β-lg dimers after PAF treatment is the immobilization of water under pressure. The homodimerization of β-lg requires mobile monomers that interact by formation of disulfide bridges. The mobility of solutes decreases at lower temperatures and increasing viscosities. The formation of ice in the viscous matrix possibly limits β-lg molecule mobility, hence molecular interactions decrease. However, to fully understand the phenomenon of protein interactions under HPLT conditions, further research in this field is required.

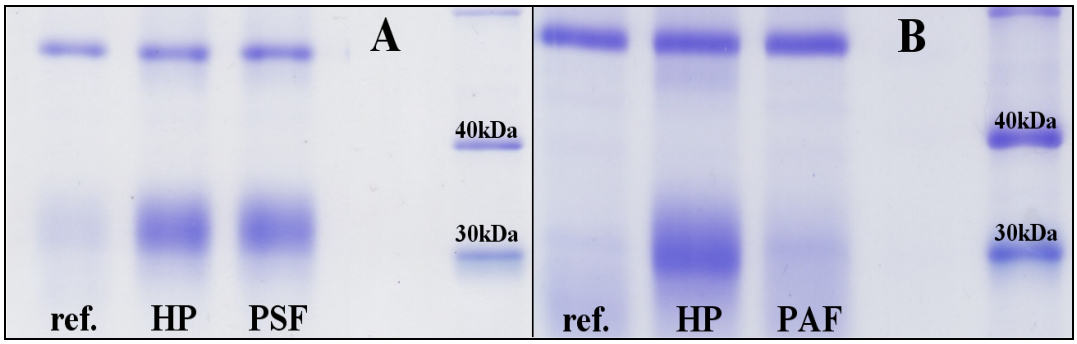

Figure V-5: SDS PAGE of 10% w/w WPI solution. Untreated reference, HP and PSF treated samples (A) and untreated reference, HP and PAF treated samples (B).

3.2.4 Viscosity changes in protein model systems

Protein modification is often linked to changes in the functionality. Changes in the hydration properties are linked to the viscosity of the aqueous system. The viscosity of protein model systems was measured after HP and HPLT treatment at 320 MPa in order to assess changes on a macroscopic level. WPI solution (10% w/w) was used to investigate the whey protein linked viscosity changes after treatments at 320 MPa (Figure V-6). HP and HPLT treated WPI solutions showed a trend to increased viscosities but no significant difference was found between treated samples and the untreated reference.

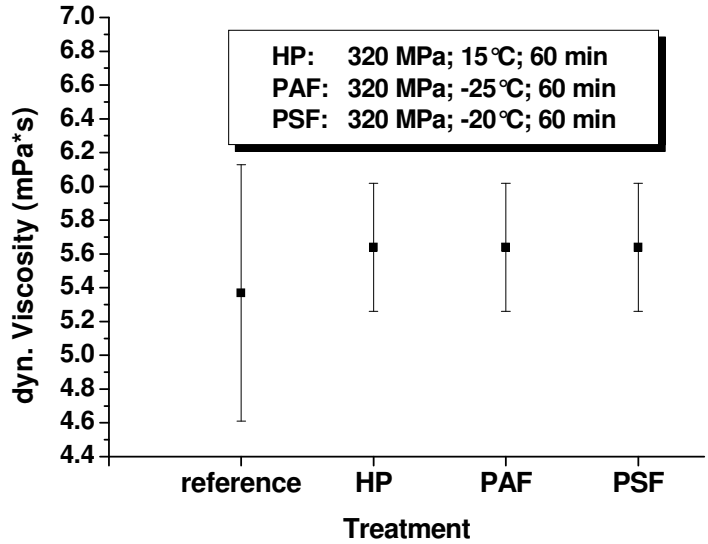

Figure V-6: Viscosity of 10% w/w WPI solution (untreated reference, HP, PAF and PSF treated).

Measurements of viscosity changes after HPLT and HP treatment at 320 MPa in 20% SMP solution was not possible, as partial solidification of the treated SMP solutions occurred at pressures > 190 MPa and pressures > 300 MPa after HPLT and HP, respectively. Figure V-7 shows the viscosity development in 20% w/w SMP solution during PSF and HP treatment in the pressure range from 140 to 300 MPa. During PSF treatment visible aggregation occurred in the SMP solution at pressures > 175 MPa. HP treated samples show a clear trend to increasing viscosities at higher treatment pressure, which is accounted to an increase in protein aggregation. This finding is consistent with previous research on viscosity changes in HP treated milk (Adapa et al., 1997). HP treated SMP solutions were homogeneous without visible aggregates to pressure below 300 MPa. At 320 MPa solidification was observed.

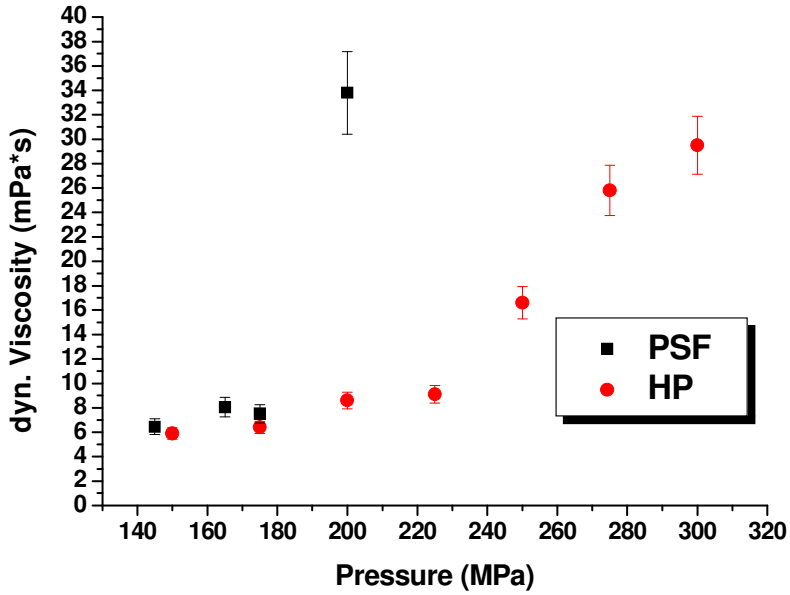

Figure V-7: Viscosity of SMP solution 20% w/w after HP treatment at 320 MPa; 20°C; 1000 sec (●) and PSF treatment at 320 MPa; 1000 - 500 sec at -20°C (■).

With increasing pressure at constant temperatures, the ice content after pressure release is increased during PSF treatment. Aggregation occurs at pressures above 175 MPa, resulting in partial solidification of the matrix. The viscosity data obtained at 200 MPa is not reliable, as particles in the solution disturbed the analyses. Ice formation during PSF is assumed to be the major cause for the detected viscosity increase, rather that pressure induced effects. The present viscosity data indicate protein interactions but do not sufficiently describe the phenomenon. The phenomenon of solidification and gel formation in protein model systems is discussed in detail in chapter VI of this work. Nevertheless, it can be stated that high viscosity and solidification in SMP solutions is promoted by PSF and HP treatment.

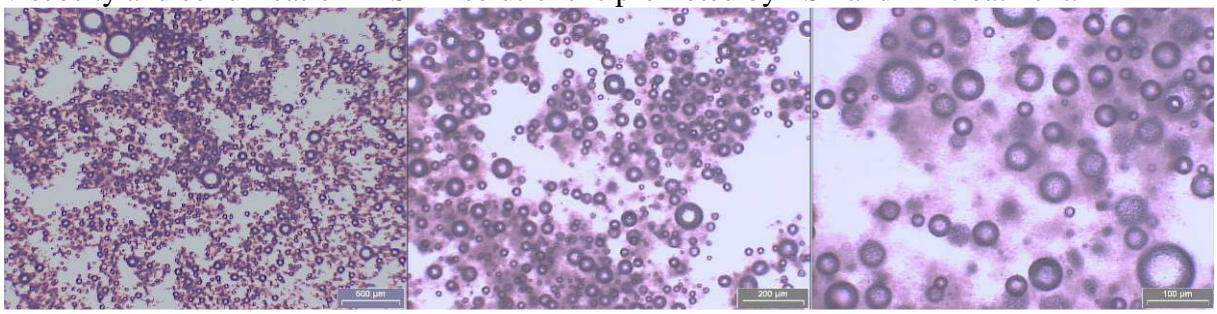

Figure V-8: Microscopic pictures of PSF treated aerated dairy emulsion (toluidine blue stained), containing 5% w/w SMP and 5% w/w WPI powder.

The aggregation of proteins can be observed not only in SMP model systems but also in the aerated dairy emulsion. Figure V-8 shows microscopic pictures of aerated dairy emulsion after PSF treatment at 320 MPa. Good to see are the colored clouds of protein aggregates around the air bubbles after staining with toluidine blue.

3.3 Impact on fat destabilization and fat coverage of air interfaces

Fats play an important role in the stabilization of aerated dairy emulsions. Of central concern in the present study was the fat coverage of air bubble interfaces after HPLT treatment. Fat clusters at the air interfaces can be visually investigated by direct optical microscopy. To evaluate changes in the fat clusters at the interfaces, different foams from emulsion B are investigated:

- Frozen foam after conventional freezing of the emulsion in a scraped surface freezer
- Liquid foam after aeration of the emulsion in the Minimondo aeration system
- Aerated emulsion after PSF treatment in the pilot scale HPLT unit.

Microscopic pictures of the 3 sample types are shown in Figure V-9. Fat clusters at the bubble surface are visible in all three sample types. There is no decrease in the level of fat coverage of the liquid foam (A) after PSF treatment (B). In both samples, small fat droplets are spread over the bubble surface, whereas slightly larger clusters are found in the conventionally frozen foam (C). The major difference between the conventionally frozen foam to the liquid and HPLT treated foam is the temperature, at which the foam formation takes place. In the conventional freezing process, aeration takes place at temperatures around the freezing point of the system. Resultant is the liquid : solid ratio of the fat. The foam formation in the liquid system takes place at higher temperatures (3-4°C), increasing the liquid fraction of the fat at the time of aeration. During HPLT treatment no aeration occurs, but the previously generated foam is pressurized. During pressurization, the air bubble surface is drastically reduced and the air changes its phase to the supercritical state. Under HPLT conditions the fat is fully crystallized. The mechanism of fat re-adsorption to the new created air bubble surface after pressure release can not be conclusively explained on the base of the present data. After visual evaluation of the fat coverage level, no substantial difference between the liquid foam (A) and the PSF treated foam (C) was observed. The adsorption of fat to air interfaces after melting seems not affected by PSF treatment.
The percentage of fat destabilization did not significantly change after HPLT treatment of emulsion B (data not shown). These findings are in good agreement with the pressure induced crystallization of fat during the treatment and indicate that the degree of fat destabilization is not affected by the HPLT treatment.

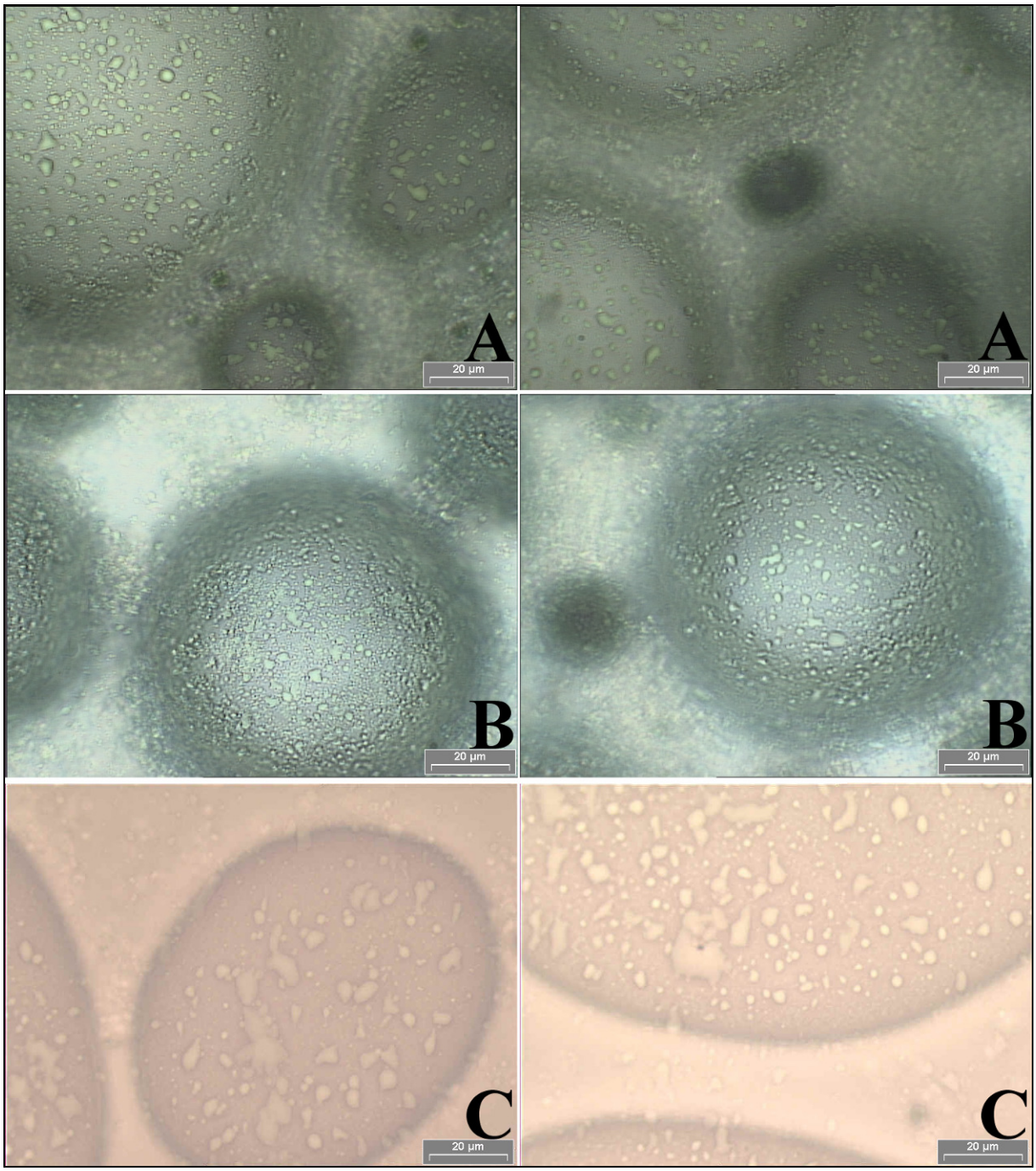

Figure V-9: Microscopic pictures (1000 fold magnitude) of the fat clusters at the air interfaces in liquid dairy foam before HPLT treatment (A), frozen dairy foam after PSF treatment and conventionally (ice cream freezer) frozen dairy emulsion (C). The images show (emulsion B). Different colors of the images result from different filters in the microscope.

3.4 Structural integrity of HP treated guar gum endosperm cells

Guar gum is a common stabilizer in frozen dairy foams. Its primary function is water binding on a molecular level. In addition to the functional properties that are based on the molecular structure, the intact macro structure of the hydrated guar endosperm cells is of high value in frozen dairy foams. Intact endosperm cells act as small "cushions" when hydrated and support the separation of ice crystals and air cells. They support the stability of the frozen foam system by increasing the flexibility of the complex system. Hydrated guar gum endosperm cells before and after PSF treatment at 320 MPa at -25°C are shown in Figure

V-10. Significant cell wall rupture in PSF treated guar endosperm cells was not observed. PSF treatment did not affect the structural integrity of guar endosperm cells.

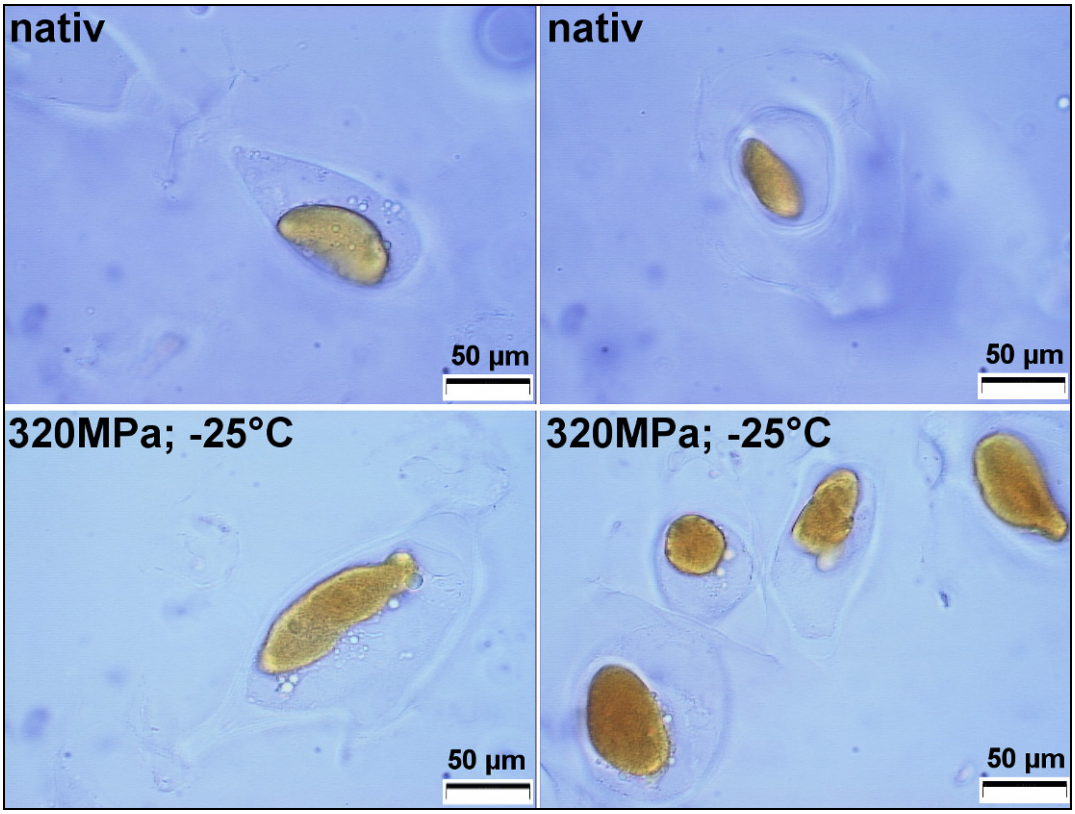

Figure V-10: Microscopic pictures of untreated hydrated guar cells (native) and PSF treated cells (320 MPa, -25°C, 60 min).

4 Conclusion

To gain insight into cause and effect in a complex aerated dairy system after HPLT treatment, single ingredients and complex model systems were HP and HPLT treated. The relevant functional properties of single ingredients in frozen dairy foam were identified and reassessed after treatment. Milk proteins have been identified the most baro-sensitive components with respect to their functionality. Dissociation of casein micelles is reported to occur under pressure but changes on a molecular level in the casein fractions were not observed by SDS-PAGE analyses. In the group of whey proteins, β-lactoglobulin is the only protein that is verifiable affected by HP and HPLT treatment at 320 MPa. Dimerization of β-lg occurs in WPI solution after HP, PSF and PAF treatment, however, to a minor degree after PAF. No difference in the degree of β-lg dimerization was found after PSF and HP treatments at 320 MPa. Hence, the formation of β-lg dimers is assumed to be pressure driven. No evidence for β-lg interactions due to cold denaturation was found with SDS-PAGE. However, viscosity measurements indicate differences in the protein structure after HP and PSF. Aggregation in SMP solutions occurred during PSF at pressures above 175 MPa, whereas HP treated solutions were free of visible aggregates at pressures up to 300 MPa. The early aggregation after PSF treatment seems related to the ice formation involved in the process. Apparently the HPLT treatment induces protein interactions, that can not be directly observed by the applied SDS-PAGE analyses but affect the rheological properties of SMP solutions. Since no aggregation occurred in WPI solutions under the given conditions, casein can be identified as a major cause for HPLT induced solidification. Protein aggregation was also observed by microscopic analyses in PSF treated dairy foams containing 5% SMP and 5% WPI.

HPLT induces changes in the structure and the interactions of milk proteins. The HPLT induced modifications have a higher impact on the rheological properties of milk protein systems as those induced by conventional HP treatment at ambient temperatures. However, a qualitative evaluation of these effects with respect to the overall product quality can not be made at this point.
High pressure supports the crystallization of milkfat and vegetable oils, which was confirmed by the unaffected level of fat destabilization after HPLT treatments. The functionality of fat clusters at the air bubble interfaces after melting seems not affected by HPLT treatments. Microscopic analyses of liquid dairy foams, PSF treated and conventionally frozen dairy foams gave no indication on reduced fat coverage of air cell interfaces after HPLT treatment. The fat coverage generated in the foaming process at 4°C was not reduced after HPLT treatment.
The structural integrity of hydrated guar gum endosperm cells was not affected by PSF treatment at 320 MPa for 60 min at -25°C. No structural differences between untreated reference cells and PSF treated cells were observed, which suggests that the guar endosperm cells maintain their functionality after HPLT treatment.
Minor color changes occurred in aerated dairy emulsions after PSF treatment. However, the color defects were nominal. The basic cause for the color deviation after treatment seems a change in crystal size and distribution and a reduced overrun. In addition, disruption of casein micelles potentially changes the light scattering, resulting in higher green content and reduced brightness. Summarizing, the changes in the final product color after PSF treatment are not rated as critical color defects.
Summarizing, HPLT induced effects in aerated dairy emulsions differ from those induced by conventional HP treatment but no quality defects with respect to the overall structure of the foam system were observed. Rheological properties of HPLT treated SMP solutions were found significantly different from HP treated solutions. Especially relevant is the aggregation of caseins linked to the ice formation during HPLT treatment.

5 References

[1]Adapa, S., Schmidt, K. A. & Toledo, R. (1997). Functional Properties of Skim Milk Processed with Continuous High Pressure Throttling. *J. Dairy Sci.*, *80*(9), 1941-1948.

[2]Barniol, A. (2005). *Interactions of stabilization ingredients in ice cream processes and effects upon durability of microstructure*. master thesis, Technische Universitaet Muenchen, 139.

[3]Buchheim, W. & Abou El-Nour, A. M. (1992). Induction of Milkfat Crystallization in the Emulsified State by High Hydrostatic Pressure. *Fett Wissenschaft Technologie/Fat Science Technology*, *94*(10), 369-373.

[4]Clarke, C. (2004). *The Science of Ice Cream*. The Royal Society of Chemistry, Cambridge.

[5]Considine, T., Patel, H. A., Anema, S. G., Singh, H. & Creamer, L. K. (2007). Interactions of milk proteins during heat and high hydrostatic pressure treatments - A review. *Innovative Food Science & Emerging Technologies*, *8*(1), 1-23.

[6]Cross, K. J., Huq, N. L., Palamara, J. E., Perich, J. W. & Reynolds, E. C. (2005). Physicochemical Characterization of Casein Phosphopeptide-Amorphous Calcium Phosphate Nanocomplexes. *J. Biol. Chem.*, *280*(15), 15362-15369.

[7]Fertsch, B., Mueller, M. & Hinrichs, J. (2003). Firmness of pressure-induced casein and whey protein gels modulated by holding time and rate of pressure release. *Innovative Food Science & Emerging Technologies*, *4*, 143-150.

[8]Flores, A. A. & Goff, H. D. (1999). Ice crystal size distributions in dynamically frozen model solutions and ice cream as affected by stabilizers. *Journal of Dairy Science*, *82*(7), 1399-1407.

[9]Goff, H. D. (1997). Instability and Partial Coalescence in Whippable Dairy Emulsions. *J. Dairy Sci.*, *80*(10), 2620-2630.

[10]Goff, H. D. (2002). Formation and stabilisation of structure in ice-cream and related products. *Current Opinion in Colloid & Interface Science*, *7*(5-6), 432-437.

[11]Huppertz, T., Kelly, A. L. & Fox, P. F. (2002). Effects of high pressure on constituents and properties of milk. *International Dairy Journal*, *12*(7), 561-572.

[12]Huppertz, T., Fox, P. F. & Kelly, A. L. (2004). High pressure treatment of bovine milk: effects on casein micelles and whey proteins. *Journal of Dairy Research*, *71*(01), 97-106.

[13]Huppertz, T., Fox, P. F., de Kruif, K. G. & Kelly, A. L. (2006). High pressure-induced changes in bovine milk proteins: A review. *Biochimica et Biophysica Acta (BBA) - Proteins & Proteomics;Proteins Under High Pressure*, *1764*(3), 593-598.

[14]Koxholt, M. M. R., Eisenmann, B. & Hinrichs, J. (2001). Effect of the Fat Globule Sizes on the Meltdown of Ice Cream. *J. Dairy Sci.*, *84*(1), 31-37.

[15]Künzel, D. (2009). *Veränderung strukturbildender Eigenschaften von Casein und beta-Lactoglobulin in Abhängigkeit verschiedener Prozess- und Produktparameter während der Hochdruck-Niedertemperatur Behandlung*. master thesis thesis, Berlin, Technische Universität Berlin, 110.

[16]Lopez-Fandino, R., Carrascosa, A. V. & Olano, A. (1996). The Effects of High Pressure on Whey Protein Denaturation and Cheese-Making Properties of Raw Milk. *J. Dairy Sci.*, *79*(6), 929-936.

[17]Lopez-Fandino, R. & Olano, A. (1998). Cheese-making properties of ovine and caprine milks submitted to high pressures. *Lait*, *78*(3), 341-350.

[18]Marshall, R. T., Goff, H. D. & Hartel, R. W. (2003). *Ice Cream*. Kluwer Academic / Plenum Publishers, New York.

[19]Merel-Rausch, E. (2006). *Hydrostatic high pressure treatment of casein to generate defined particle and gel structures*. PhD, Universitaet Hohenheim, 95.

[20]Merel-Rausch, E., Kulozik, U. & Hinrichs, J. (2007). Influence of pressure release rate and protein concentration on the formation of pressure-induced casein structures. *Journal of Dairy Research*, *74*(03), 283-289.

[21]Regnault, S., Thiebaud, M., Dumay, E. & Cheftel, J.-C. (2004). Pressurisation of raw skim milk and of a dispersion of phosphocaseinate at 9°C or 20°C: effects on casein micelle size distribution. *International Dairy Journal*, *14*, 55-68.

[22]Schmidt, K. (1994). Effect of milk proteins and stabilizers on ice milk quality. *Journal of Food Quality*, *17*(1), 9-19.

[23]Schrader, K. & Buchheim, W. (1998). High pressure effects on the colloidal calcium phosphate and the structural integrity of micellar casein in milk - II. Kinetics of the casein micelle disintegration and protein interactions in milk. *Kieler Milchwirtschaftliche Forschungsberichte*, *50*(1), 79-88.

[24]Viazis, S., Farkas, B. E. & Allen, J. C. (2007). Effects of High-Pressure Processing on Immunoglobulin A and Lysozyme Activity in Human Milk. *J Hum Lact*, *23*(3), 253-261.

Chapter VI High pressure-low temperature induced changes in the structure of skim milk and whey protein model systems

1 Introduction

Under high pressure milk proteins can be modified, which results in a change of their functional properties (Trujillo, Capellas, Saldo, Gervilla & Guamis, 2002; Fertsch et al., 2003). The functional properties of food proteins are those physicochemical properties that affect the behaviour of proteins in food systems during processing, storage and consumption. The functional properties of food proteins can be classified into three main groups: hydration properties, which are dependent on protein-water interactions (water absorption and retention, wettability, swelling, adhesion, dispersibility, solubility and viscosity); properties that are related to protein-protein interactions (precipitation and gelation); and surface properties (surface tension, emulsification and foaming characteristics) (Messens, VanCamp & Huyghebaert, 1997). Intensive research in the field of HP induced changes in the functionality of milk proteins has proven the potential of HP applications to restructure dairy proteins (Messens et al., 1997; Schrader & Buchheim, 1998; Merel-Rausch et al., 2007). Many studies have reported the usefulness of high pressure to provide gels and pastes with unique properties. As a pre-treatment, high pressure processing appears effective in improving the textural properties of numerous food systems, i.e. the coagulation and gelation properties of milk (Galazka et al., 2000). The Unilever Company has patented a combination of HP processing and freezing for improved consistency and smoothness, and slower melting rates of ice creams (Keenan, Wix & Young, 1998). However, the later patent and most of the data presented in the literature refers to two sequential process steps: heat and high pressure treatment. Combined processes (e.g. high pressure and low temperature) are only rarely investigated so far. Different from the conventional HP treatment, HPLT processing comprises low temperatures, ice formation and pressure effects in one process step. In addition to purely pressure induced changes, effects that are linked to the ice formation under pressure have to be considered, which makes the exploration of cause and effect during HPLT treatment a difficult task.

1.1 High pressure induced aggregation of milk proteins

An introduction into the general effects of high pressure-low temperatures on protein structures is given in chapter II of this study. The different protein fractions in bovine milk and their conformational changes under high pressure and low temperature conditions have been discussed in detail in chapter V.

The major protein component responsible for gelation in bovine milk is casein (Merel-Rausch, 2006). Casein micelle disintegration is reported to be highly involved in the solidification of milk protein solutions under pressure. Sugar concentrations up to 30% support gel formation (Keenan, Young, Tier, Jones & Underdown, 2001). The resultant gel properties are determined by the protein concentration, the p,t,T-regime during treatment and decisively by the rate of pressure release (Merel-Rausch et al., 2007).

Whey proteins, i.e. β-lactoglobulin, are rather barosensitive and the formation of disulfide-linked β-lg aggregates under pressure is well documented in literature (Considine, Patel, Singh & Creamer, 2007b) In addition to the pressure induced dimerization whey protein aggregation occurs mainly through hydrophobic interactions (Gracia-Julia, Rene, Cortes-Munoz, Picart, Lopez-Pedemonte, Chevalier et al., 2008) The fact that whey protein free micellar casein systems form gels under pressure implies that whey protein aggregation is not the basic cause of pressure induced gelation of concentrated milk protein systems. However,

the whey protein aggregation (whether self-aggregation or casein-whey protein aggregation) affects the physical properties of resultant gels (Keenan et al., 2001).
HPLT induced changes in protein confirmation are difficult to interpret since they may be induced by to low temperature, high pressure, mechanical effects due to ice formation and/or freeze concentration. However, it has been explored, that pressure and pressure assisted cold denaturated structures are different from heat denaturated states (Dumay, Picart, Regnault & Thiebaud, 2006). Heat, pressure and cold denaturation is represented by the elliptical Hawley p,T diagram. The Hawley model, however, does not take into account intermediate states of unfolding and aggregation, nor reversible phenomena (Smeller, 2002). Moreover, it is limited to a thermodynamic reflection and does not cover physical effects, e.g. ice formation and freeze concentration. Most freezing damage to proteins are supposed to be induced by cryo concentration effects and adsorption to ice crystals (Franks, 1995; Strambini & Gabellieri, 1996).

2 Experimental Methods

2.1 HPLT setup

All experiments were carried out with the HPLT pilot scale unit as described in chapter III. The aggregation behaviour of the model solutions were investigated in the pressure range from 0.1 to 350 MPa. High pressure (HP), pressure shift freezing (PSF) and pressure assisted freezing (PAF) treatments were applied.

2.1.1 Sample preparation

The different protein model solutions were prepared in w/w ratio. Different skim milk powders (SMP), whey powders (WP), whey protein isolates (WPI) and a casein isolate were used to compose model systems of defined protein content and composition.

Table VI-1: Protein powders used to prepare the protein model solution

Type	Supplier	Comment
SMP	Saliter, Obergünzburg, Germany	High heat SMP
SMP	Laiterie Walhorn, Walhorn, Belgium	Medium heat SMP
SMP	Nestlé, Beauvais, France	High heat SMP
SMP	Nestlé, Beauvais, France	Low heat SMP
WP (Fromy 35)	Nestlé, Beauvais, France	WPI 35% whey protein
WP	Eurosérum, Port sur Saône, France	WP 11.5% whey protein
WPI BiPRO®	Davisco, Foods International, Inc., Eden Prairie, US	WPI >95% whey protein
Casein isolate Promilk 852B	Ingredia, Arras, France	Casein concentrate (>85% casein)

The specifications of all protein powders are attached in the annex. For all protein solutions the powders were reconstituted in water at 20°C and stirred for 60 min prior to treatment.

2.2 Analyses

2.2.1 Water binding capacity

To determine the water binding capacity of differently induced milk protein gels, the gels were stored at 4°C for 24 h prior to analyses. The initial water loss was determined by the amount of drainage that occurred during aging. In addition to the initial drainage, the water loss after centrifugation was measured. After recording the initial water loss the samples were centrifuged at 5858 g (Sorvall® RC-5B Refrigerated Superspeed Centrifuge, Du Pont Instruments, Newtown, US) at 20°C for 10 min. The drainage was measured and the water loss of the gels was calculated as percent of the total water in the gel.

$$\text{water loss} = \frac{m_{darainage}}{m_{sample}} \cdot 100\% \qquad \textbf{(VI-1)}$$

2.2.2 Texture analyses

For the texture analyses a texture analyser (TA) TA-XT2 (Stable Micro Systems Ltd., Surrey, UK) was used. A simple single stroke test was applied to determine the fracture force and fracture distance. A cylindrical probe (d= 0.5cm) was used with a test distance of 15 to 30 mm. The gel hardness was defined by the slope in the force deflection plot. The gel parameters were determined according to Figure VI-1.

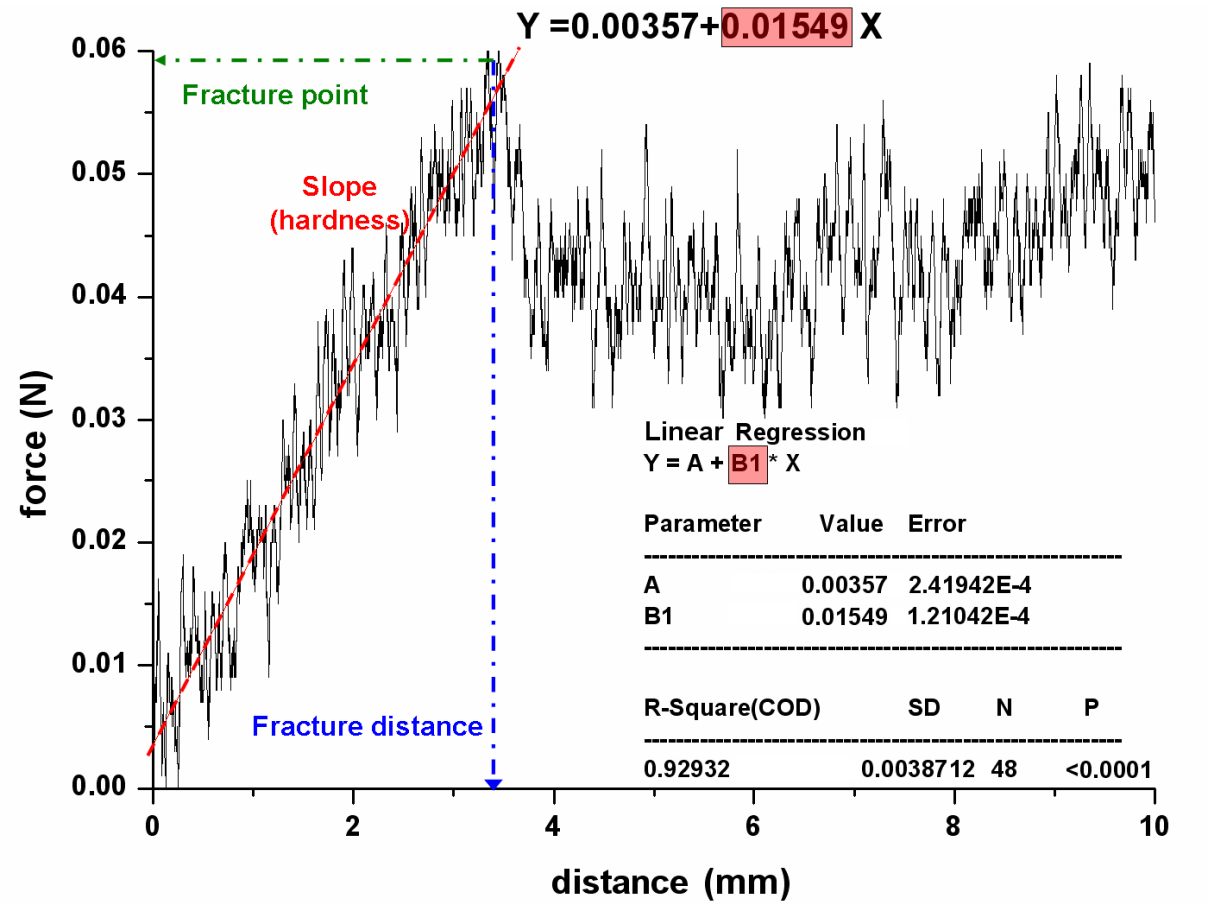

Figure VI-1: Fracture force, fracture distance and linear regression of the slope (hardness) in a force deflection graph.

The single down stroke texture analyses with a cylindrical probe were performed with the following setup:

pre-test speed:	2.0 mm/s
test speed:	1.0 mm/s
post-test speed:	2.0 mm/s
test distance:	15-30 mm
trigger type:	manually
contact surface:	7.85 mm^2

2.2.3 Viscosity measurement

Viscosity measurement was performed with a rotary viscosimeter (Rotovisco RV 12, Haake Messtechnik GmbH u. Co, Karlsruhe, Germany). The different protein solutions were

analysed at 20°C with the MV I rotor. Reference medium type E7 (Haake Messtechnik GmbH u. Co, Karlsruhe, Germany) was used as a control sample with a defined dynamic viscosity of 5.26 mPa · s. Viscosity measurements were performed in samples that contained no visible aggregates.

2.2.4 Ice crystal size and distribution

The method is based on the optical observation of a frozen dairy foam sample mixed with a suitable medium for dispersing the ice crystals and for dissolving fat aggregates. The frozen product is dispersed at -10 °C in paraffin-oil, between two glass slides, and examined with an optical microscope (Olympus, type CX-41), connected to a camera (Sony DC-700) to take black and white pictures. The microscope is set to take pictures with a good contrast, providing a good distinction of the edges of the ice crystals.
Depending on the number of crystals per image, 3 or 5 images were stored. Minimum of 500 crystals was detected. The crystals are analyzed automatically with special software, based on the principle of separation of adjacent crystals. By measurement of the ice crystal size distribution, it is possible to obtain the value of the average diameter (expressed in μm.) of ice crystals, calculated by using image analysis software.

2.2.5 Scanning electron microscopy

For the standard SEM analyses the samples were frozen in liquid nitrogen and freeze dried. Samples were sputter coated with gold and analyzed with a scanning electron microscope (Hitachi S-2700 SEM, Tokyo, Japan). The obtained images were visually evaluated. In addition, selected images were analyzed with image analyzing software ImageJ 1.41 (Wayne Rasband, National Institutes of Health, US).

3 Results and discussion

3.1 Process related effects on milk protein structures

3.1.1 Microstructure

To characterize the microstructure of HP and HPLT induced skim milk gels, HP, PSF and PAF induced gels from 25% w/w SMP (Saliter, Obergünzburg, Germany) solutions were freeze dryed and analysed with a scanning electron microscope. The treatment pressure was 320 MPa for all experiments, with an average compression rate of 6.2 MPa/s and pressure release rate of 200 MPa/s. The process relevant times and temperatures are listed in Table VI-2

Table VI-2: Relevant process times and temperatures during HP, PSF and PAF treatment of 25% w/w SMP solution used for microstructure analyses

Treatment	Pressure holding time [s]	Maximum temperature after compression [°C]	Temp. at pressure release [°C]	Freezing time under pressure [s]
HP	3600	32.9	12.5	0
PSF	1860	26.0	-25.2	0
PAF (short)	4010	24.6	-30.1	500
PAF (long)	5200	23.7	-32.2	2500

SEM images of HP, PSF and PAF induced 25% SMP gels clearly show differences in the microstructure of the gels. Figure VI-2 gives an overview about the gel structure after all treatments. The SEM images of the freeze dried gels show solid regions, which indicate the protein network, and pores that show regions of formally entrapped water.

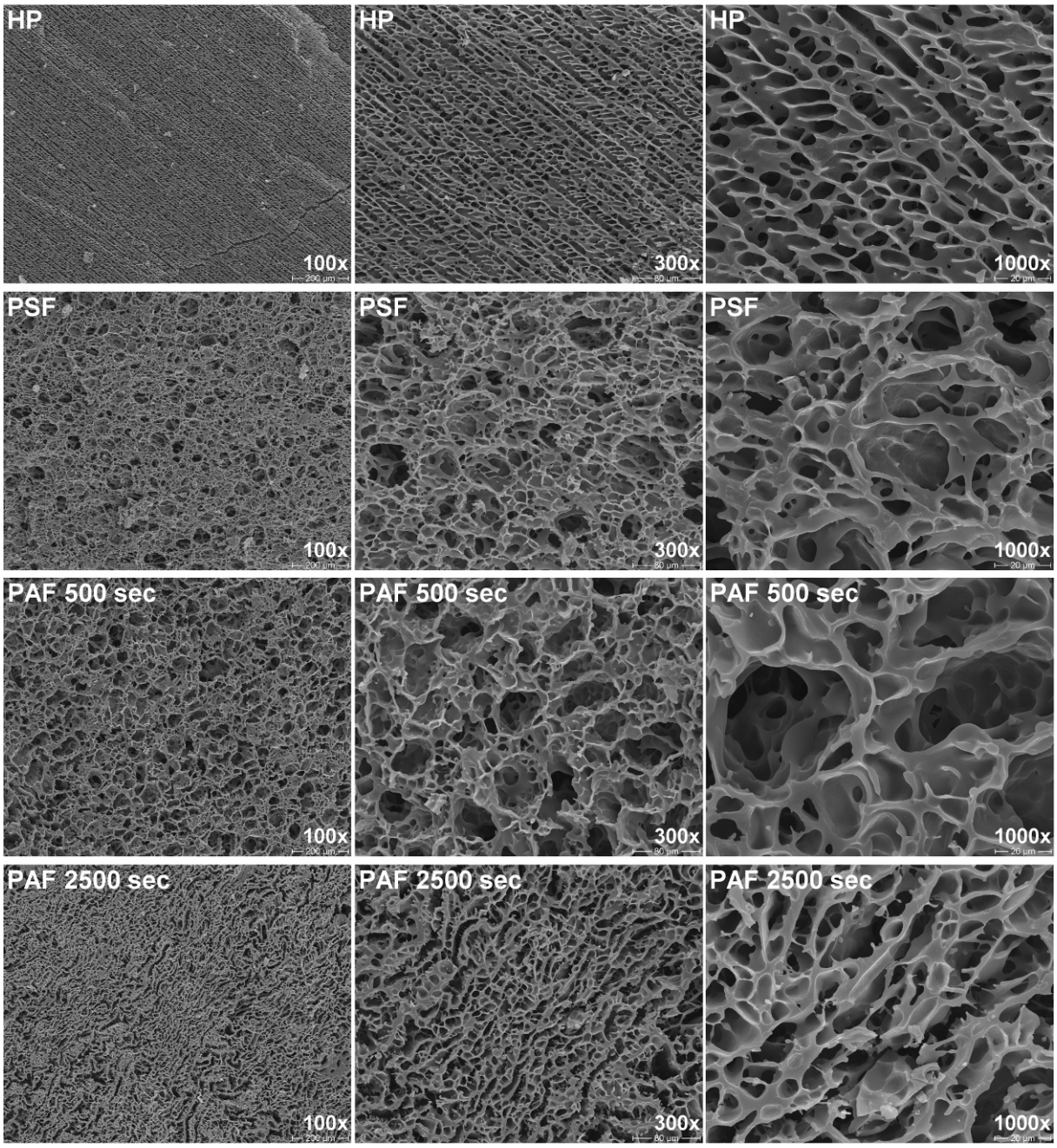

Figure VI-2: SEM images of 320 MPa HP, PSF and PAF induced 25% SMP gels.

3.1.1.1 High pressure induced structure

High pressure treatment of the SMP solution induced a finely pored, homogeneous gel structure. The protein network shows a straight alignment. The gel formation is induced during pressure release (Huppertz et al., 2004b) and small water droplets are immobilized in the matrix.

Figure VI-3 shows an area distribution histogram, the corresponding SEM image and the elliptical pore modulation image of pores in a HP induced 25% SMP gel. The mean pore area was calculated as 7.67 µm² and the maximum pore area detected on the analysed image was 89.81 µm². The narrow area distribution of the pores is indicated by the steep slope of the total pore percentage over pore area.

The straight alignment in the gel structure is supposed to originate from the formation of a mixed casein-serum protein (i.e. denatured β-lg) gel, as hypothesized by Aguilera (Aguilera & Kinsella, 1991).

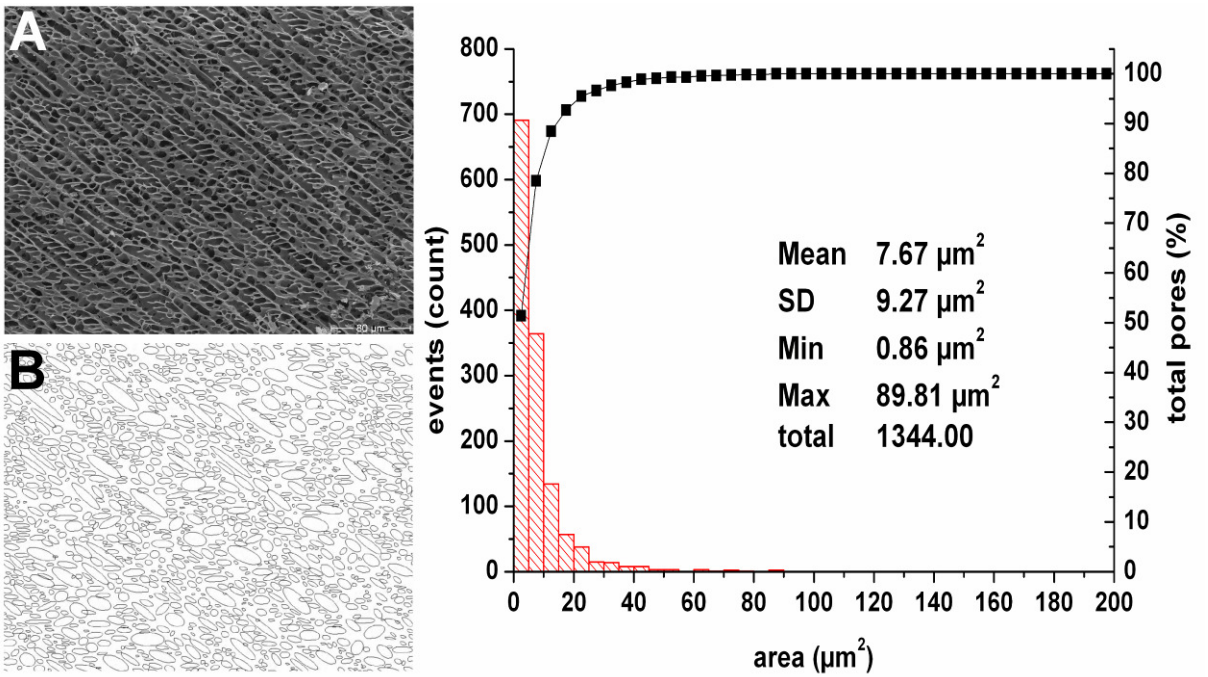

Figure VI-3: Area distribution histogram of pores in HP induced 25% SMP gel (right). The plot data shows mean pore area (Mean), standard deviation (SD) minimum and maximum pore area (min, max) and the total pore count (total). The analysed SEM image at 300x magnitude (A) and elliptical pore modulation image (B) are shown on the left.

3.1.1.2 Pressure shift freezing induced structures

Pressure shift freezing induced gels are rough structured and inhomogeneous with a more widely spread pore size distribution than HP induced gels. Pores are round and closed but vary broadly in size. Figure VI-4 shows the area distribution histogram of a PSF induced gel.

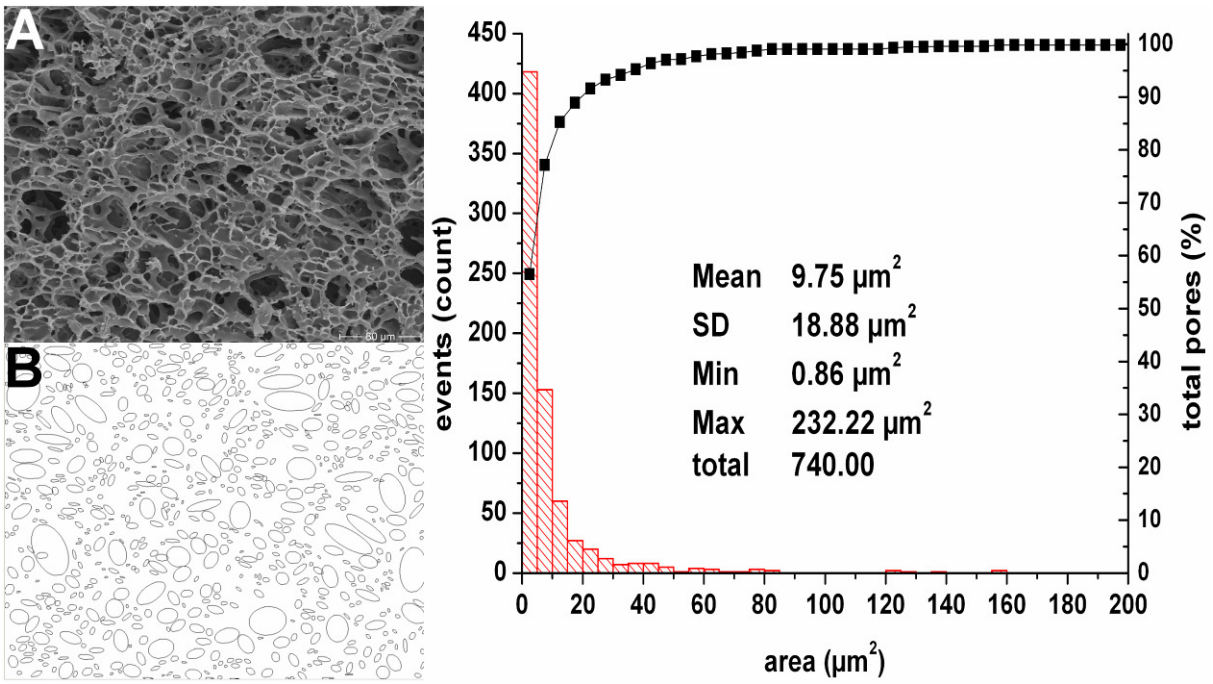

Figure VI-4: Area distribution histogram of pores in PSF induced SMP gel (right). The plot data shows mean pore area (Mean), standard deviation (SD) minimum and maximum pore area (min, max) and the total pore count (total). The analysed SEM image at 300x magnitude (A) and elliptical pore modulation image (B) are shown on the left.

The total number of pores per µm² after PSF treatment is approximately 55% of the number in HP induced gels. The gel structure is massively disordered showing large pores surrounded by areas of fine pored network. The mean pore area detected in the analysed image is 9.75 µm². In Figure VI-4–B large white areas can be identified, which indicate pore free regions. A comparison with the SEM image (A) shows that these areas are not completely free of pores but partly include high numbers of small pores which were not detected by the image analysing software. Accordingly the actual total number of pores per µm² is higher as indicated by the histogram.
During pressure release homogeneous nucleation occurs in the SMP solution and ice crystals grow throughout the generated gel network. The volume increase during freezing in the entrapped water droplets accounts for the disordering of the solid protein network. During subsequent atmospheric freezing crystal growth continues. Hence, further aggregation of ice crystals and network rupture are promoted.

3.1.1.3 Pressure assisted freezing induced structures

To evaluate the impact of PAF treatment on SMP gel structures, PAF induced gels after long freezing time under pressure (2500 s) were investigated. The long freezing time was chosen to clearly point out the effect of ice formation under pressure. Short PAF freezing times involve PSF effects to a great extent. After long freezing times under pressure a high percentage of the water is frozen to ice III and the PSF effect during pressure release is marginal.

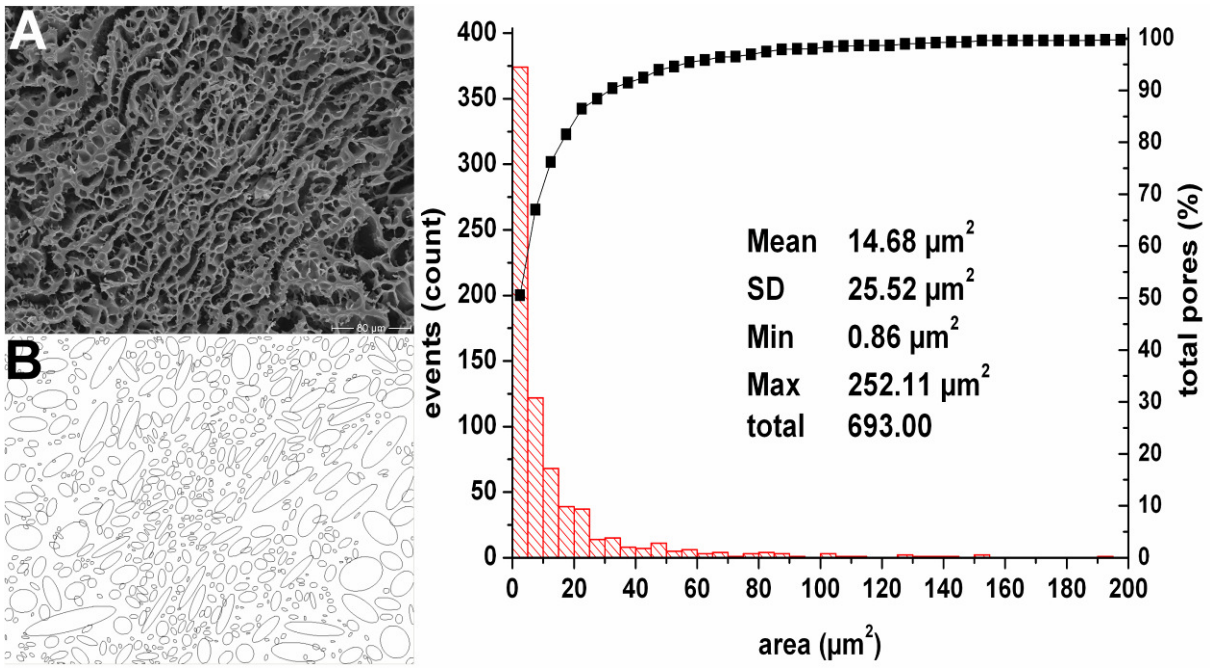

Figure VI-5: Area distribution histogram of pores in PAF (2550 s freezing time) induced SMP gel (right). The plot data shows mean pore area (Mean), standard deviation (SD) minimum and maximum pore area (min, max) and the total pore count (total). The analysed SEM image at 300x magnitude (A) and elliptical pore modulation image (B) are shown on the left.

After PAF treatment the gels are inhomogeneous and have a lamella-like appearance. The relatively fine pored network is interrupted by long slim pores that range far throughout the matrix. Surrounded by thick protein strands, these channels give the gel the typical lamella-like structure. The protein network in between the long pore channels partly consists of broad solid regions.
The basic cause for the formation of long aligned pores in the matrix is assumed to be the ice formation under pressure. Analogous to atmospheric freezing, the ice formation during PAF starts with heterogeneous nucleation. In addition, crystal growth rates under pressure are

reduced as discussed in chapter IV. Hence, large ice crystals grow slowly from the nucleation site through the matrix. Since ice crystal growth excludes any solutes, freeze concentration occurs in the liquid phase around the needle shaped ice crystals. The growing crystals penetrate the increasingly concentrated matrix and form long slim regions which are free from any solutes. Between the crystals high protein concentrations occur, resulting in long slim pores surrounded by thick protein strands upon pressure release. The PSF effect in the liquid matrix possibly accounts for the fine pored structure in the surrounding regions.
Gels induced by short (500 s) PAF treatment lack the characteristic elongated pores. Figure VI-6 compares PAF induced 25% SMP gels after 500 s freezing time (right) and 2500 s freezing time (left). The gel structure after 500 s freezing time under pressure is similar to the PSF induced structure. However, regions of PAF-typical network compression are visible and the pore area distribution is wider.

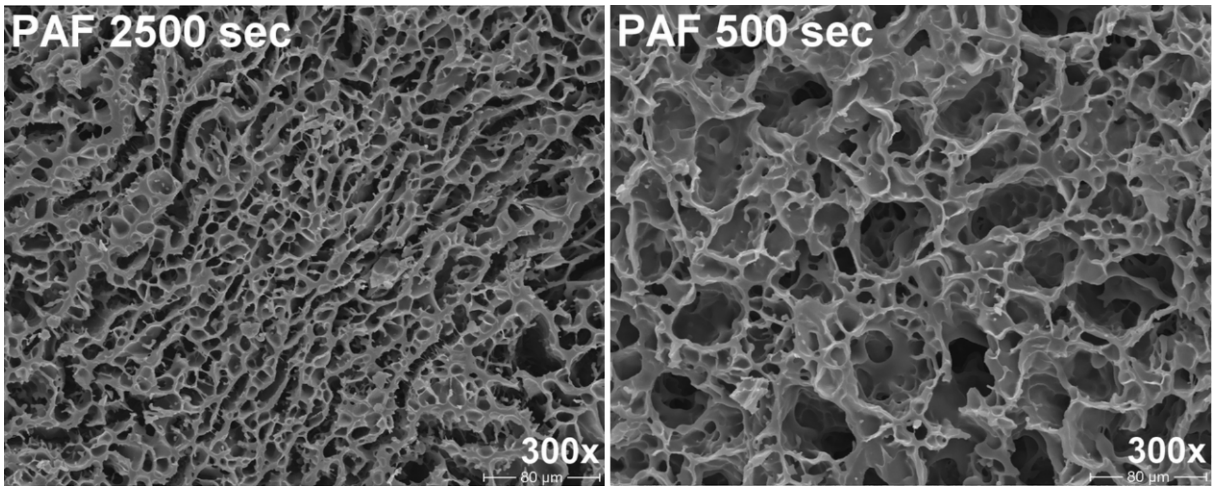

Figure VI-6: SEM images at 300x magnitude of PAF induced 25% SMP gels after 2500 s PAF freezing time (left) and 500 s PAF freezing time (right).

3.1.1.4 Summary

The SEM analyses show significant differences in HP and HPLT induced gels. HP, PSF and PAF treatments induce characteristic structures that differ in the pore number, size and size distribution.

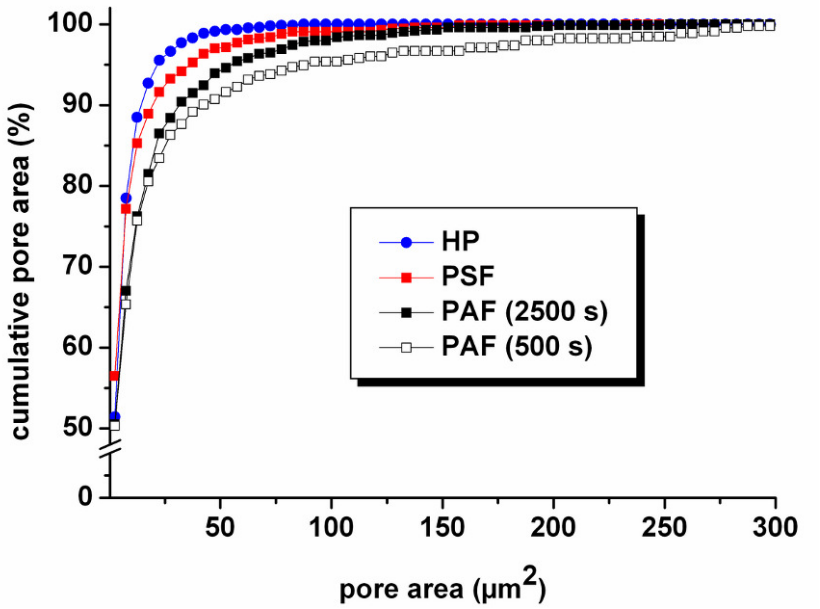

Figure VI-7: Total number of pores as a function of pore area in HP and HPLT induced 25% SMP gels.

Figure VI-7 compares the pore area distribution in HP, PSF and PAF induced gels. According to the present data, the different treatments can be rated with respect to resulting pore structure from fine to rough as: HP > PSF > PAF (long) > PAF (short). An intact gel structure was detected after HP treatment, whereas after PAF treatment massive structural inhomogeneities were observed. This effect seems most pronounced after short PAF treatment (500 s) with high PSF effect upon expansion.

3.1.2 Textural properties of HP and HPLT induced SMP gels

3.1.2.1 Impact of treatment type and SMP concentration

To evaluate the effect of different HP and HPLT treatments on the gel strength, differently concentrated SMP solutions were prepared from SMP (Saliter, Obergünzburg, Germany). HP, PSF and PAF induced gels were compared after treatment at 320 MPa. For the texture analyses, PAF treatment with long freezing times (2500 sec) was applied.

As shown in Figure VI-8, significant differences in the fracture behaviour result from different HP/HPLT treatment setups. At all concentrations, slope, fracture force and fracture distance were detected well reproducible.

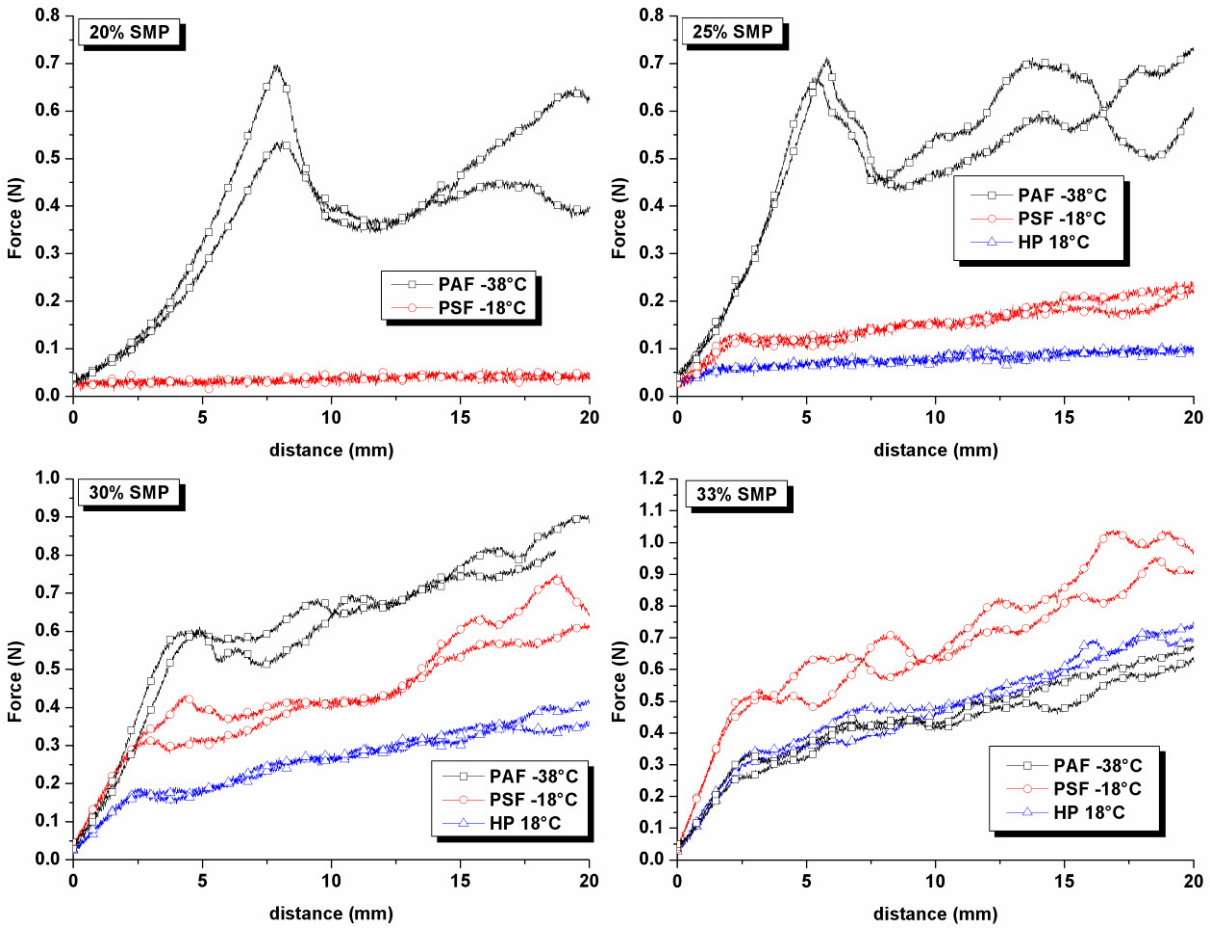

Figure VI-8: Force deflection graphs of HP (Δ), PSF (○) and PAF 2500 sec (□) induced SMP gels (20%, 25%, 30% and 33% w/w) after treatment at 320 MPa for 180 min.

The gel strength or fracture force is most affected by different treatment conditions. HP treatment at 320 MPa and 18°C for 180 min did not induce solidification in 20% SMP solutions. A fracture point was not detected in PSF treated samples at concentrations lower than 25% w/w. High fracture forces (~0.68 N) were found in the single stroke texture analyses after PAF treatment of 25% w/w SMP solutions, whereas fracture forces were 0.12 and 0.05 N after PSF and HP treatment, respectively. The gel hardness in the present experiments

was found to be linked to the fracture force, showing highest values after PAF and lowest after HP treatment at 25% SMP concentration. The high gel strength in 25% SMP gels after PAF treatment is in good agreement with the SEM analyses. The formation of thick stands in the PAF gel causes increased hardness and compression resistance. The volume change in the ice III fraction during pressure release is supposed to cause physical compression of the gel network upon recrystallization to ice I (+ΔV~18%). The proposed mechanism is schematically shown in Figure VI-9. At SMP concentrations above 30%, the fracture force in PAF induced gels is progressively reduced, whereas it is increased in PSF and HP induced gels. At 33% SMP concentration the fracture force of HP and PAF induced gels is about 0.33 N.

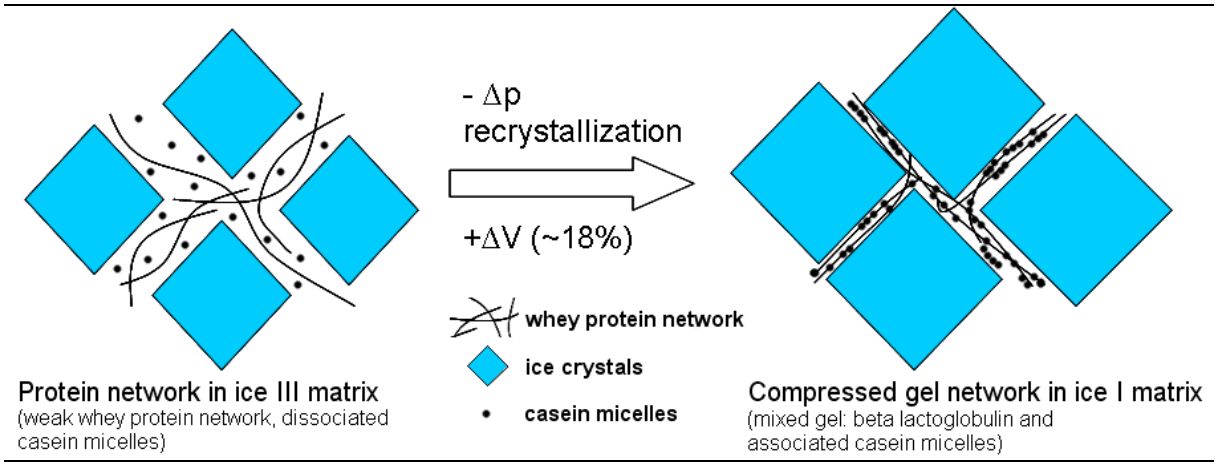

Figure VI-9: Schematic mechanism of physical gel network compression during ice III to ice I recrystallization.

In contrast, the PSF induced gels at the same concentration showed fracture points around 0.5 N. It has been reported, that the pressure induced gel formation in SMP solutions takes place during pressure release (Fertsch et al., 2003). According to this, the hardness reduction in the PAF induced gels is accounted to the high freeze concentration in the matrix. The SMP concentration possibly exceeds a critical level, resulting in weak, brittle gels. In contrast, increasing SMP concentrations increase the hardness of HP and PSF induced gels. A further increase of the SMP concentrations possibly results in reduced gel strength after HP and PSF treatment as well. To confirm this assumption, experiments on the concentration dependency of HP and PSF induced gels are necessary.

3.1.2.2 Pressure holding time (PSF) and freezing time under pressure (PAF)

Dependent on the applied process, the pressure holding time has different effects on the protein system during HPLT treatment. During PSF no water phase transition occurs during the pressure holding time, whereas water crystallization under pressure occurs during PAF and longer pressure holding times result in higher amounts of frozen water. Hence, a critical parameter in the PAF treatments is the freezing time under pressure.

Force deflection plots of 20% SMP gels after PAF treatment with different freezing times under pressure at about -32°C and PSF treatment with different pressure holding times at -18°C are shown in Figure VI-10 A.

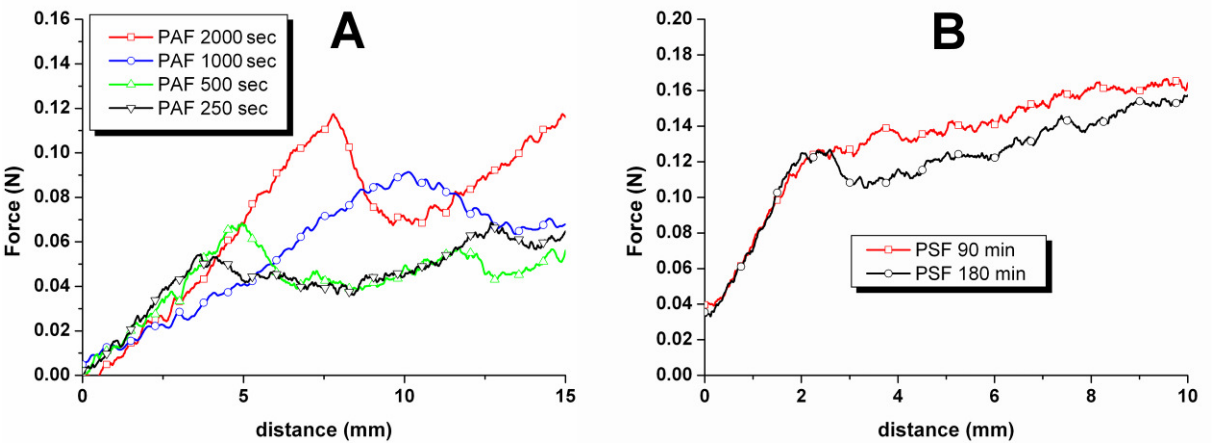

Figure VI-10: Force deflection graph of A: PAF induced 20% SMP gel with different ice contents after 250 sec (▽), 500 sec (△), 1000 sec (○) and 2000 sec (□) freezing time under pressure. B: PSF induced 20% SMP gels after 90 min (□) and 180 min (○) pressure holding time.

The PAF treated 20% SMP gels show an increase in gel strength with increasing freezing time under pressure. The obtained results are in good agreement with the results of the SEM analyses that show the impact of freezing time on the pore size and protein strand formation in PAF induced gels. The higher the ice content under pressure, the lower is the PSF effect during pressure release. Due to progressive freeze concentration, longer PAF freezing times result in firmer gels. The formation of thicker protein strands and a narrow pore size distribution in the gels accounts for increased hardness of the gel network.

In contrast, when no ice formation under pressure is involved (PSF) the effect of longer pressure holding times on the gel strength is negligible. Figure VI-10 B shows the force deflection graph of PSF induced 20% SMP gel after 90 and 180 min pressure holding time at -18°C. No significant difference in hardness (slope) and fracture force occurred after different holding times at 320 MPa.

The pressure induced gel formation is linked to the casein micelle dissociation, which is reported to occur within the first 15 min after pressure build up to a great extent (Fertsch et al., 2003). Hence, for PSF induced SMP gels, that include a high percentage of casein, the pressure holding time is a less critical parameter as for whey protein gels. In contrast, longer treatment times during PAF, that involve ice formation under pressure, significantly affect the gel properties. The ice formation under pressure accounts for the changes in gel structure, rather that the pure pressure effect over time. HPLT experiments with cooling under pressure to -30°C without ice formation and re-heating to 18°C before pressure release support this assumption (schematic process in Figure VI-11).

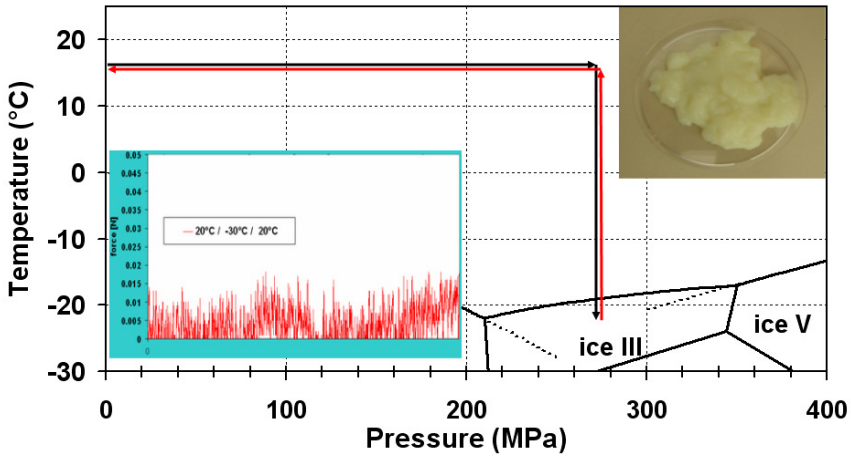

Figure VI-11: Schematic process of cooling and reheating under pressure, the force deflection plot and a picture of a 20% SMP solution after treatment.

No fracture force was detected in 20% SMP solutions that were treated according to the latter process. The protein structure is determined by the conditions at the time of pressure release and a "memory effect" after cooling and re-heating under pressure does not occur. No differences between SMP solutions that were HP treated at constant temperature of 18°C and samples that were cooled and re-heated before pressure release was detected.

3.1.2.3 PSF process temperature

The schematic phase diagram of proteins points out different ways of protein denaturation. Temperature and pressure have an impact on the protein conformation. The results of the previous section imply the important role of the ice content in SMP solutions upon pressure release. This effect becomes especially evident in PAF induced SMP gels with different freezing times under pressure. In the PSF process, ice formation occurs during pressure release and the resulting protein structures differ significantly from those after HP treatment at temperatures above the freezing point. The critical parameter that affects the amount of ice formed during PSF is the temperature upon pressure release (Otero & Sanz, 2006b). To evaluate the effect of different PSF expansion temperatures on the gel strength (fracture force and hardness), 20% SMP solutions (Saliter, Obergünzburg, Germany) were PSF and HP treated at 320 MPa. Pressure was released after different degrees of supercooling (no supercooling for HP treatments). The pressure was released at 18°C in the HP treatment. PSF treatments with different pressure release temperatures (10 K steps from -5°C to -35°C) were performed (see Figure VI-12). HP treated SMP solutions after expansion at 18°C showed no significant fracture point and very low values for hardness of the matrix. Lower temperatures at the point of pressure release during PSF induced stronger gels. As for the PAF treated samples, the gel strength was increased with increasing ice content (lower temperatures).

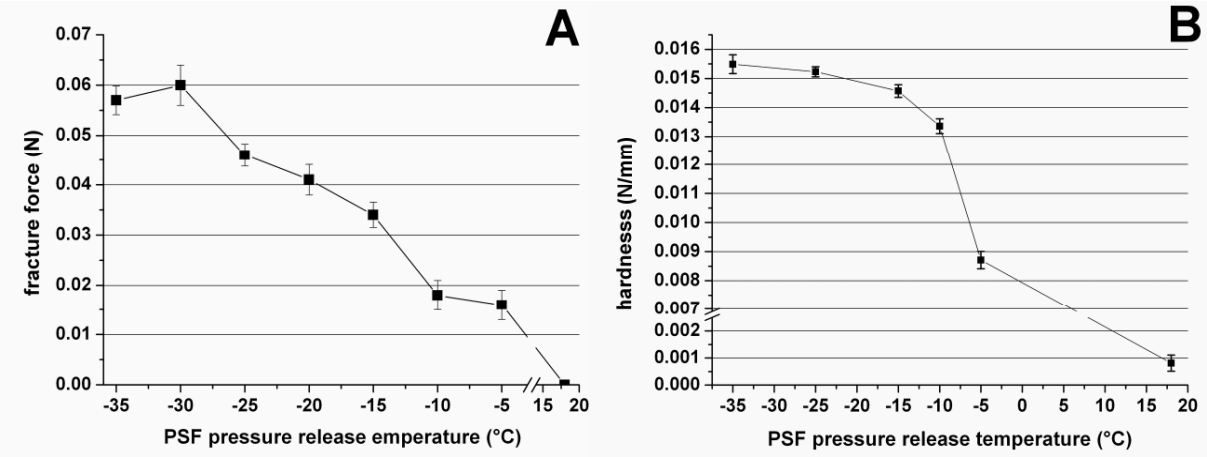

Figure VI-12: Fracture force (A) and hardness (B) of PSF and HP induced 20% SMP gels as a function of temperature upon expansion from 320 MPa.

The results support the assumption that the ice formation during pressure release has a strong impact on the gel properties. Possibly a mechanical compression of the gel network and freeze concentration, similar to the proposed mechanism for the PAF treatment, occurs after homogeneous nucleation in the PSF samples. Sudden ice crystal growth throughout the matrix is associated with freeze concentration and a volume increase of about 9% of the instantaneously frozen water fraction. The higher the percentage of instantaneously formed ice, the higher is the mechanical compression and the protein concentration in the matrix during pressure release and gel formation.

3.1.2.4 Pressure release rate during PAF and PSF treatment

It was reported that the gel formation in SMP solutions is induced during pressure release and that the pressure release rate has a high impact on the properties of high pressure induced gels (Fertsch et al., 2003; Merel-Rausch et al., 2007). To evaluate the effect of fast and slow decompression rates on HPLT induced SMP gels, PAF, PSF and HP treated 20% SMP solutions (Saliter, Obergünzburg, Germany) were investigated after treatment at 320 MPa and pressure release rates of 2 MPa/s and 200 MPa/s.

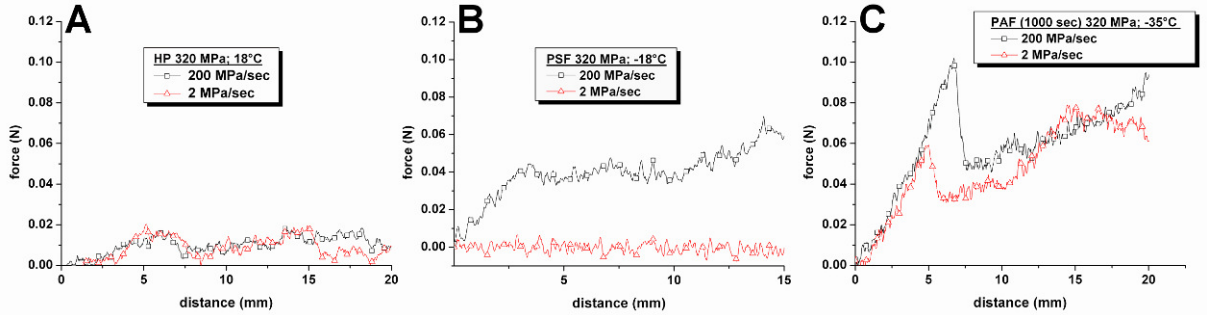

Figure VI-13: Force deflection plots of 20% SMP solution after HP (A), PSF (B) and PAF (C) treatment at 320 MPa and fast pressure release (200 MPa/s) (□) and slow pressure release (2 MPa/s) (△).

The pressure release rate had no significant effect on the hardness and fracture point when 20% SMP solution was HP treated. The SMP content was not sufficient to induce a detectable fracture point, even at high pressure release rates. To get conclusive data, experiments with higher SMP content are required. However, different pressure release rates resulted in different fracture points after PSF and PAF treatment. After fast expansion PSF and PAF induced gels showed significant higher fracture points, whereas hardness was not affected in PAF induced gels. As for the HP treatment, PSF did not induce gels that showed a fracture point at low pressure release rates. The present findings are consistent with literature data about pressure induced SMP gelation (Fertsch et al., 2003; Merel-Rausch et al., 2007). Consequently the hypothesis of casein micelle association in SMP solution subjected to the rate of pressure release after HP treatment (Figure VI-14) is confirmed for the HPLT domain. However, after PAF treatments with long freezing times under pressure, the effect of the pressure release rate is less pronounced, since the mobility of casein micelles is reduced with increasing ice content before expansion.

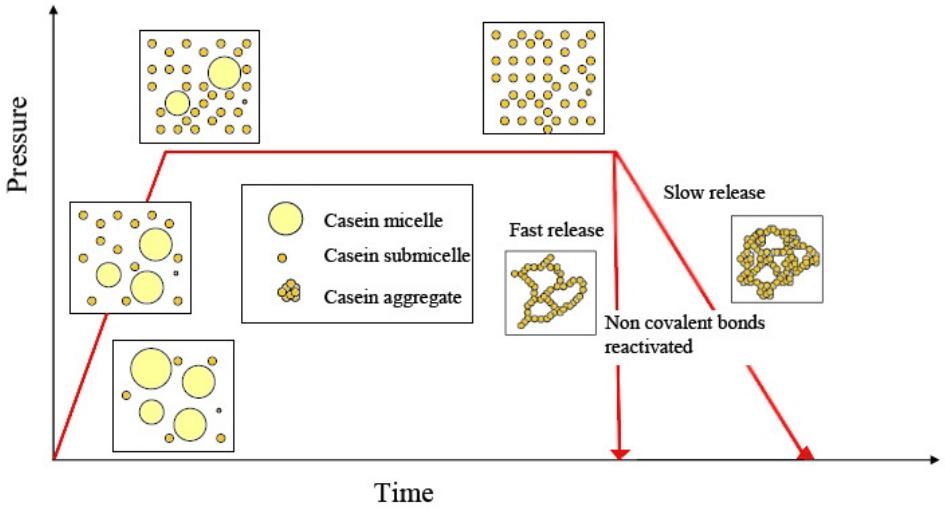

Figure VI-14: Model of the dissociation and aggregation of casein micelles during high pressure treatment of a casein solution, redrawn from (Merel-Rausch, 2006).

In HPLT freeze processes the pressure release is not only responsible for different structures of casein aggregates after expansion but also the ice crystal size and distribution is affected. Figure VI-15 shows the different ice crystal structures in 20% SMP gel after PSF with high and low pressure release rates. The ice crystal size and distribution is strongly affected by the pressure release rate. Large ice crystals form during slow expansion, whereas fast expansion results in small crystals and a narrow size distribution. The low number of ice crystals after slow expansion indicates that ice crystal growth occurred to a great extent, rather than the formation of new crystals.

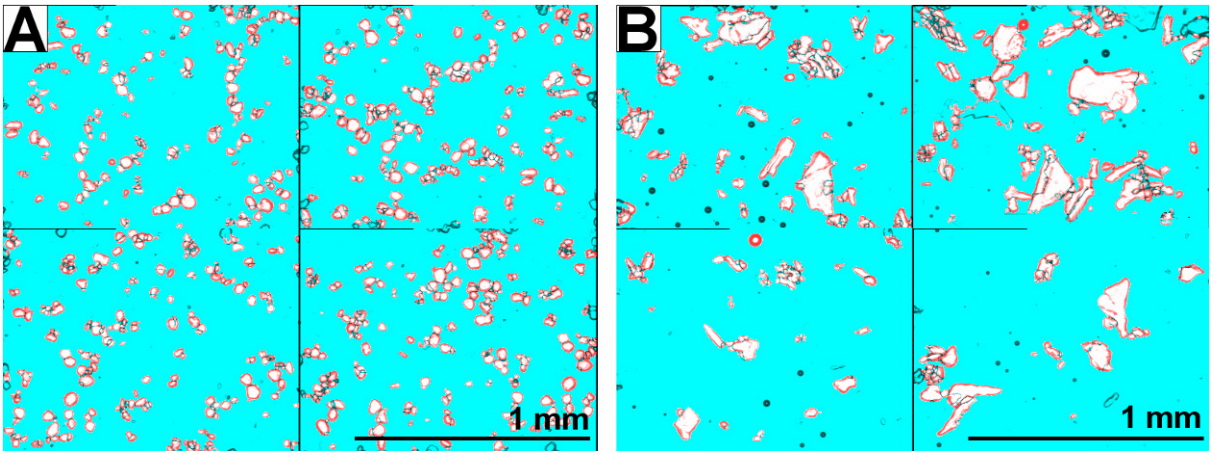

Figure VI-15: Microscopic picture of ice crystals (analytic image) in PSF induced 20% SMP gel after fast pressure release at 200 MPa/s (A) and slow pressure release at 2 MPa/s (B).

Large ice crystals disturb the protein network and immobilize relatively high amounts of water in a small region of the gel. During melting of those large crystals, large water droplets form in the gel. The resultant structure is less homogeneous and relatively soft. The effect of the pressure release rate is also visible on a macroscopic scale. Figure VI-16 shows the inhomogeneous structure after slow pressure release in 20% SMP solution after PSF compared to the homogeneous structure after fast pressure release. After slow expansion the sample shows the typical texture as it is induced by freeze concentration at low freezing rates.

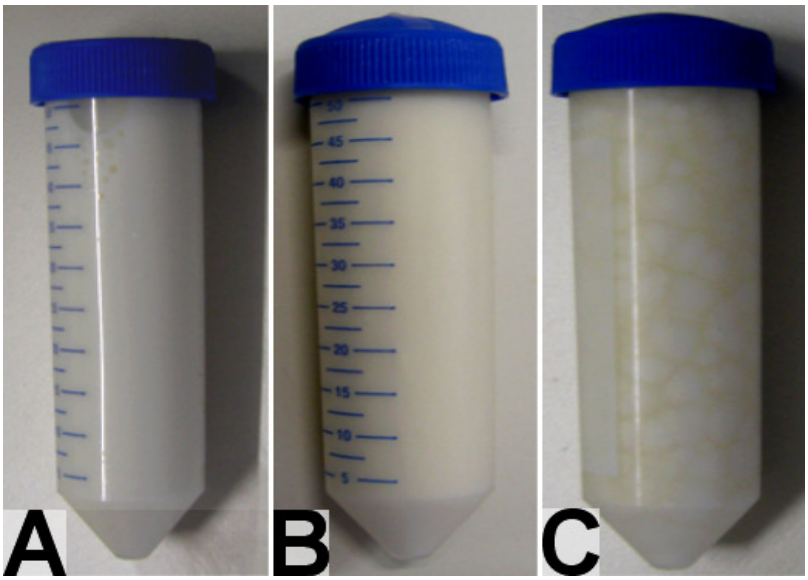

Figure VI-16: 20% SMP solution before HPLT treatment (A) and after PSF treatment with pressure release rates of 200 MPa/s (B) and 2 MPa/s (C).

3.1.2.5 Water binding properties

As for the gel strength, there is a dependency of the water holding capacity of HPLT induced SMP gels on the type of treatment. PSF and PAF induced 20% SMP (Saliter, Obergünzburg, Germany) gels were stored at -27°C and the drip loss was measured after 24 h aging at 4°C (Figure VI-17). The initial drip loss describes the gravitational drainage after 24 h at 4°C and the centrifugal drainage the additional water loss after 10 min centrifugation (5858 rpm at 20°C). Initial drainage is lower after PSF, indicating a more homogeneous and intact gel structure. The initial water loss of PAF induced gels ranges from 34.7 to 37.5% and does not extensively increase after 7 days of storage at -27°C. The PSF induced gels show very low initial drainage of 2.5% after 1 day and 10% after 10 days storage at -27°C. The drainage after centrifugation is higher for both gel types after 7 days storage.

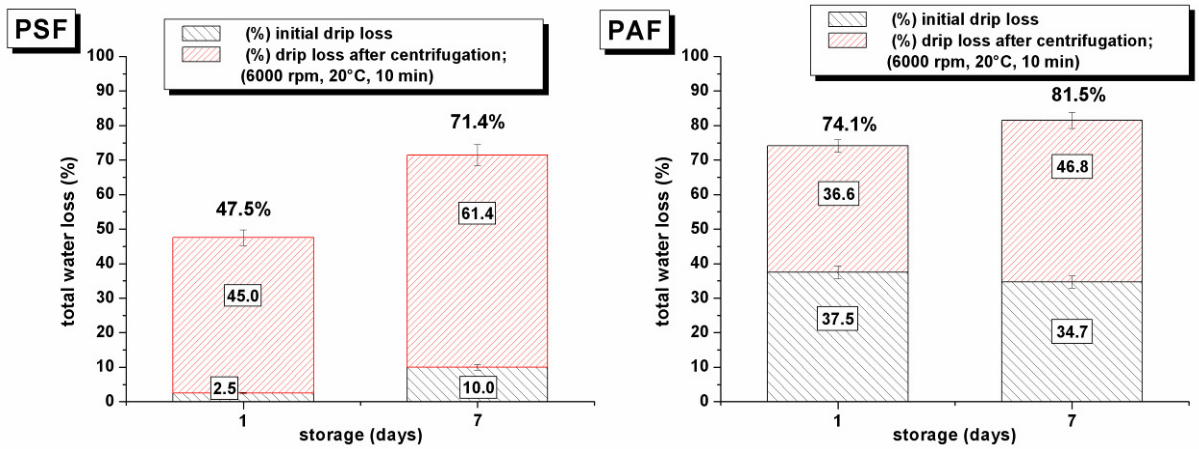

Figure VI-17: Drip loss of 20% SMP gel after 1 and 7 days frozen storage at -27°C. Initial drip loss before centrifugation and drip loss after centrifugation at 5858 g, 20°C for 10 min are shown.

PAF gels suffer from higher total drainage independently of the storage time. The higher ice content at the time of gelation and the high density changes during pressure release (ice III to ice I transition) cause structural damage in the gel network. The mechanical stress partially breaks up the macrostructure and less water is immobilized by the gel network. The long pores that form in the gel may serve as channels for subsiding drainage. In PSF induced gels the structure is more homogeneous. Less mechanical stress occurs during pressure release, since no ice III to ice I transition is involved. However, high gravitational forces during centrifugation result in total drainage comparable to PAF induced gel after 7 days of storage. The reduced water holding capacity over time indicates partial reversibility of the HPLT induced gel structure even during frozen storage.

The high percentage of water loss after centrifugation in the PSF gels, compared to the PAF gels, indicate that most of the water is immobilized as water cells in the intact gel structure, rather than molecular bond. Those structures are intact after PSF treatment, as the initial drainage is low. This assumption is supported by the high initial water loss in PAF induced gels, where macroscopic structures, which are responsible for water holding in PSF gels, are disrupted.

3.2 Product related effects on milk protein structures

As shown in the previous section, the state of proteins is decisively governed by the pressure and temperature conditions during HPLT processing. Changes in conformation that lead to functional changes of single molecules but also to changes on a macroscopic level (e.g. viscosity changes, gel formation) can be induced by various process parameters (time, temperature, pressure). Those external influences determine the structural properties after treatment but it is the properties of the protein system itself that give a limit to the extent of functional changes induced by a certain process. One of these product related properties is the

protein concentration, which has been discussed in connection with the treatment type in section 3.1.2.1 of this chapter. The protein composition and the degree of pre-denaturation in protein powders are two critical parameters that are discussed in the following section.

3.2.1 Pre - denaturation in skim milk powder (WPNI)

The proteins in skim milk powder already suffered from denaturation during drying to some extent. In the early 1960s, the American Dry Milk Institute (ADMI) later to become known as the American Dairy Products Institute (ADPI) published standards for grades of dry milk. A significant feature of these standards was the emergence of a simple heat classification for SMP. The undenaturated Whey Protein Nitrogen Index (WPNI) is a measure of the heat treatment applied to the milk during processing to milk powder. It is expressed as milligrams undenaturated whey protein nitrogen per gram of non-fat milk powder with a moisture content of 3.16% and classifies milk powders in three groups: high heat, medium heat and low heat (Table VI-3).

Table VI-3: Heat treatment classification of skim milk powders

Heat treatment classification	Undenaturated whey protein nitrogen index (WPNI) [mg WPN/g powder]
Low heat	> 6.0
Medium heat	1.5 – 6.0
High heat	< 1.5

The effect of different WPNI on the textural properties of HP and HPLT induced gels was evaluated after treatment of 20% w/w SMP solutions after HP, PSF, and PAF treatment at 320 MPa. High heat and low heat SMP (Nestle, Beauvais, France) was used to prepare the skim milk solutions. For all treatments the maximum pressure was 320 MPa and the pressure release rate 200 MPa/s.

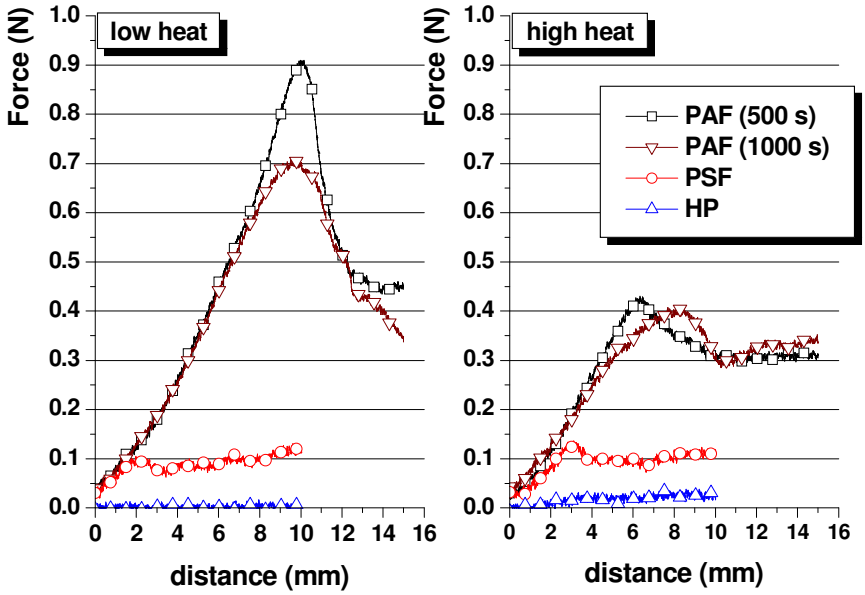

Figure VI-18: Force deflection plots of 20% high heat (right) and low heat (left) SMP after 500 s PAF (□), 1000 s PAF (▽), PSF (○) and HP (△) treatment at 320 MPa.

Table VI-4: Textural gel properties of 20% w/w high heat and low heat SMP solutions after HP, PSF PAF (500 s) and PAF (1000 s) treatment at 320 MPa. The data shows average values. The standard deviation for all measurements was no higher than 10%

Treatment / SMP type	Hardness (N/mm)	Fracture force (N)	Fracture distance (mm)
High Heat			
HP	0.008	0.026	3.76
PSF	0.033	0.149	4.16
PAF 500	0.075	0.426	6.45
PAF 1000	0.05	0.406	8.45
Low Heat			
HP	0	n.d.	n.d.
PSF	0.036	0.1	2.41
PAF 500	0.088	0.91	10.05
PAF 1000	0.056	0.514	9.79

Figure VI-18 shows the force deflection plots of 20% high and low heat SMP solutions after different treatments, the textural gel properties after all treatments are summarized in Table VI-4. For the HP treatment the SMP solutions were pressurized to 320 MPa for 1000 s. Fast pressure release (200 MPa/s) was performed at 25°C sample temperature. For the PSF treatment the samples were cooled to -25°C with a pressure holding time of 1000 s at 320 MPa before fast pressure release (200 MPa/s). Nucleation during PAF treatments was achieved at 320 MPa after an average cooling time under pressure of 4500 s. After crystallization for 500 and 1000 s respectively, pressure was released (200 MPa/s) at temperatures between -30 and -34°C.

Independent from the WPNI, the gels show highest fracture points and hardness after PAF treatment. In contrast to the results obtained in experiments on the impact of the PAF freezing time with high heat 20% SMP solutions (Saliter, Obergünzburg, Germany), short PAF freezing times (500 s) induce stronger gels than long freezing times (1000 s) in the 20% SMP solutions made from low heat SMP (Nestle, Beauvais, France). In turn, the high heat SMP solution (Nestle, Beauvais, France) confirms the formation of stronger gels after longer PAF freezing times. The phenomenon of stronger gel formation after shorter PAF freezing times in low heat SMP solutions can not be conclusively explained on the base of the present data. Possibly the gel formation is supported by the denaturation of native whey proteins during HPLT treatment and promoted by the low temperatures during the PAF treatment. In high heat SMP less native whey proteins are present and β-lg is partially associated with κ-casein. This effect possibly accounts for the reduced gel strengths after PAF but does not conclusively explain the increased gel strength after PSF and HP treatment. In addition, the ice formation which accounts for stronger gels in high heat SMP systems during PAF treatment may has a negative effect in this respect.

HP treatment did not induce gel formation in the low heat SMP solutions under the present conditions. After HP and PSF treatment of high heat SMP solutions a trend to higher fracture points and hardness in the gels is notable, whereas after PAF treatment, gel strength is lowered in high heat SMP solutions. The reverse effect of different WPNI on the gel strength after different treatments indicates different mechanisms behind the structure formation in PAF induced and HP and PSF induced gels. Higher degrees of pre-denaturation support the formation of stronger gels after HP and PSF treatment, whereas after PAF treatment the gel strength is reduced.

3.2.2 Casein to whey protein ratio

High pressure induces gel formation in aqueous casein systems. The proposed mechanism of pressure induced casein gelation is based on the dissociation of casein micelles under pressure and re-association during pressure release (Merel-Rausch, 2006). Whey protein denaturation under pressure is explained by the following mechanism: protein unfolding under pressure exposes the free sulphydryl group in β-lactoglobulin, which, through sulphydryl – disulphide interchange reactions forms aggregates with κ-casein, α-lactalbumin or β-lactoglobulin (Huppertz, Fox & Kelly, 2004a). On pressure release, unfolded whey proteins that have not interacted with other molecules may refold to the native conformation. Furthermore, it is suggested that low temperatures minimize the loss of native structure induced by pressurization and reduce aggregation reactions by the means of a more hydrated state of β-lg under pressure at subzero temperatures (Kolakowski, Dumay & Cheftel, 2001).

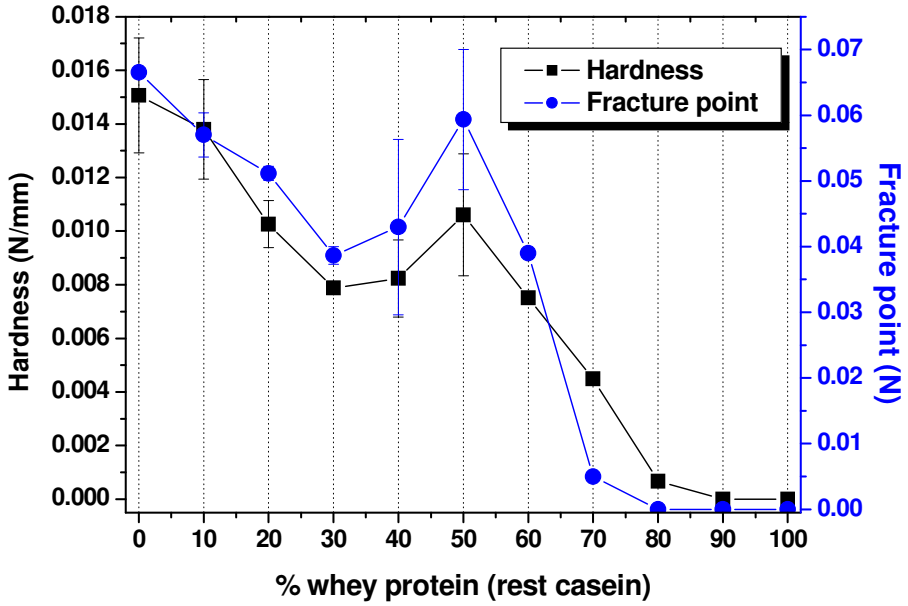

Figure VI-19: Fracture points (●) and hardness (■) of 10% w/w protein solutions of different whey protein to casein ratios after PSF treatment at 320 MPa.

To evaluate the effect of different casein to whey protein ratios on the textural properties of protein gels after HPLT treatment, 15% w/w protein solutions (total protein > 98%) with casein to whey protein ratios (c/w ratios) from 1:0 to 0:1 were PSF treated at 320 MPa, pressure release rate 200 MPa/s and -25°C expansion temperature. The different protein ratios were achieved by blending casein isolate powder (Promilk 852B) and whey protein isolate powder (BiPRO®). The fracture point and hardness of PSF induced gels as a function of the protein composition is shown in Figure VI-19. Hardness and fracture points of the gels correlate reproducible over the full range of different casein to whey protein ratios. WPI solutions with casein percentages below 20% did not show solidification after PSF treatment as indicated by the lack of a fracture point. With increasing casein content the gel strength increased to a local maximum at a c/w ratio of 1:1. The maximum hardness and fracture point were found at a c/w ratio of 1:0.

According to literature data and results that were obtained in the present study, β-lg is the only whey protein that contributes to gel formation in the investigated pressure and temperature range (max. pressure 320 MPa). The non-linear development of hardness and fracture force over different c/w ratios indicates the contribution of β-lg–β-lg and/or β-lg–casein interactions to the gel formation in mixed protein solutions. In the absence of sufficient amounts of casein, whey proteins do not cause solidification after PSF treatment.

Hence, β-lg interactions alone do not induce solid gels under the investigated conditions. This finding supports the assumption that β-lg – casein aggregates form during PSF treatment, which is consistent with data given in the literature (Aguilera & Kinsella, 1991; Huppertz et al., 2006). A c/w ratio of 1:1 results in fairly high gel strengths. In solutions with only casein isolate, the mechanism of gel formation is clearly linked to the association of casein micelles during expansion. The whey protein aggregation, i.e. the β-lg aggregation, occurs before expansion during the pressure holding time (Anema, 1998). Presumably β-lg associates with casein micelles before pressure release and prevents casein micelle interactions during expansion to some extent and weakens the gel structure. This effect may account for the reduced gel strength between 60 and 90% casein content in the solution and the peak at c/w ratio of 1:1. However, to develop a conclusive hypothesis about the mechanism behind gel formation in casein-whey protein mixtures during HPLT treatment further research is required. The key finding with respect to the present data is the non-linear coherency between gel strength and c/w ratio, which implies that whey proteins contribute to the gel formation in the presence of casein micelles and increase hardness and fracture points under p,T conditions where pure whey protein solutions do not form solid gels after PSF treatment.

3.3 Impact of pressure and the amount of instantaneously formed ice during pressure shift freezing on the liquid to gel transition in SMP solutions

3.3.1 Amount of instantaneously formed ice during PSF

In the high pressure shift freezing process the freezing point depression of water at increasing pressures can be exploited to induce sudden supercooling and instantaneous ice formation in the product during fast pressure release. The results presented in the previous sections emphasize the important role of ice formation under pressure and during pressure release in HPLT induced SMP gels. The pressure at the time of expansion and the degree of supercooling during PSF determine the amount of ice that is instantaneously formed during pressure release (Otero & Sanz, 2006b). Different approaches used to calculate the amount of ice instantaneously produced after quasi-adiabatic expansion in high-pressure shift freezing processes have been reviewed by Otero et al. (Otero & Sanz, 2006b):

$$m_w \cdot cp_w \cdot \Delta T = L \cdot m_i \qquad \textbf{(Le Bail, Chourot, Barillot \& Lebas, 1997)} \qquad \textbf{(VI-2)}$$

$$L \cdot m_i = \left[m_i \cdot cp_i \cdot \Delta T\right] + \left[(1 - m_i) \cdot cp_w \cdot \Delta T\right] \qquad \textbf{(Barry, Dumay \& Cheftel, 1998)} \qquad \textbf{(VI-3)}$$

$$\bar{c}p_w \cdot \Delta T \cdot m_w + \bar{c}p_i \cdot (1 - m_w) = (1 - m_w) \cdot T \qquad \textbf{(Otero \& Sanz, 2000)} \qquad \textbf{(VI-4)}$$

With m_w the mass of water; cp_w the specific heat capacity of water; ΔT the degree of supercooling; L the latent heat; m_i the mass of ice; cp_i the specific heat capacity of ice; $\bar{c}p_i$ is the specific heat capacity of ice at atmospheric pressure (mean value of the specific heat capacity at the minimum temperature reached after expansion and the specific heat capacity at the melting point); $\bar{c}p_w$ is the specific heat capacity of liquid water at atmospheric pressure (mean value of the specific heat capacity at the minimum temperature reached after expansion and the specific heat capacity at the melting point).

Equations VI–2 and VI–3 do not take into account the pressure and temperature dependency of the latent heat and specific heat capacities at the nucleation point. Equation VI–4 includes mean values for cp but still lacks a pressure dependent latent heat value.

A more precise estimation of the amount of ice formed during expansion is possible by including the dynamic properties of water and the latent heat at the nucleation pressure (p_N). The following equation combines the three equations above, taking into account pressure and temperature dependency of cp and L. Accordingly, the percentage of instantaneously frozen water at p_N can be determined with the following heat balance (Otero & Sanz, 2006b):

$$m_i \cdot L_{PN} = \left(m_i \cdot \bar{c}p_i + (1 - m_i) \cdot \bar{c}p_w\right) \cdot \Delta T \qquad \textbf{(VI-5)}$$

Accordingly the amount of ice is given by

$$m_i = \frac{\bar{c}p_w \cdot \Delta T}{L_{PN} - \bar{c}p_i \cdot \Delta T + \bar{c}p_w \cdot \Delta T} \qquad \textbf{(VI-6)}$$

cp_w and cp_i can be calculated according to:

$$cp_w = \frac{cp_{T\,min} + cp_{Tf}}{2} \Leftrightarrow cp_i = \frac{cp_{T\,min} + cp_{Tf}}{2} \qquad \textbf{(VI-7)}$$

Pressure release causes cooling of the sample until nucleation occurs at the minimum temperature T_{min} and the nucleation pressure p_N. T_f defines the freezing point at the present conditions. Pressure and Temperature before expansion are described by T_0 and p_0. The relevant process parameters during PSF are pointed out in Figure VI-20.

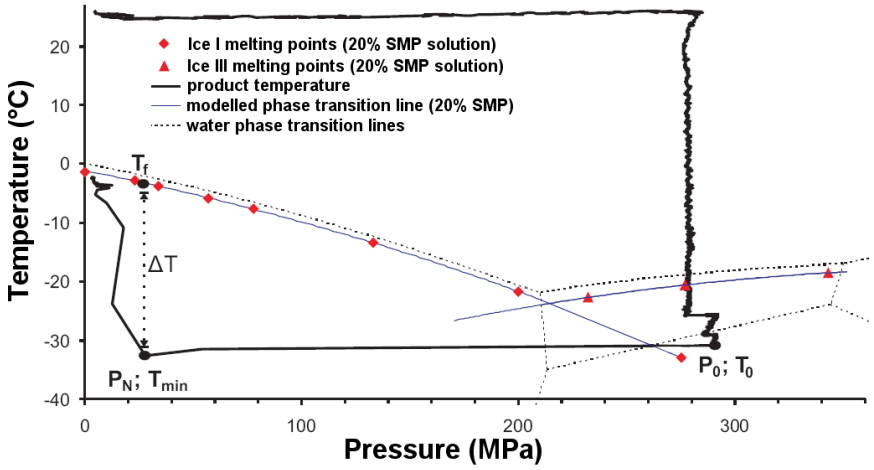

Figure VI-20: PSF cycle of 20% SMP solution showing the relevant pressures and temperatures before and during pressure release.

Table curve 2D regression of characteristic values for ice and water was performed to approximate the water and ice heat capacities at p_N and T_f (supercooled, metastable region). Figure VI-21 shows the heat capacity of ice and water as a function of temperature at atmospheric pressure and the temperature span that was relevant for the polynomial (water) and linear (ice) regression.

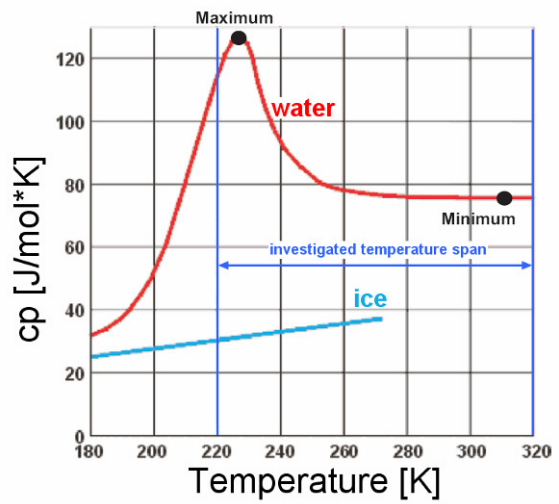

Figure VI-21: Specific heat capacity of water and ice as a function of temperature, redrawn from (Chaplin, 2008). Temperature span for polynomial and linear regression from 220 to 320 K.

According to the regression of the heat capacity over time of water and ice, the specific heat capacities of ice and water at atmospheric pressure can be calculated as

$$\mathrm{cp_w} = \frac{a + c \cdot T^{0.5} + e \cdot T}{1 + b \cdot T^{0.5} + d \cdot T + f \cdot T^{1.5}} \qquad \textbf{(VI-8)}$$

(a=4.1989022; b=-0.13257539; c=-0.5552019; d=0.0044045513; e=0.018366738; f=-5.6709768E-7); r^2>0.999

$$\mathrm{cp}_i = a + b \cdot T$$

(a=-0.024683283; b=0.0077200289); r^2>0.99

The temperature dependency of the latent heat along the melting curve is expressed as a function of pressure (MPa) obtained from Hobbs' data by linear regression (Hobbs, 1974; Otero & Sanz, 2000).

$$L_P = 3.114 \cdot 10^{-3} \cdot p^3 - 1.292 \cdot p^2 - 3.379 \cdot 10^2 \cdot p + 3.335 \cdot 10^5 \qquad \textbf{(VI-9)}$$

The latent heat values at different nucleation pressures obtained by the above equation strongly influence the calculated amount of ice formed during expansion. To narrow down the nucleation pressure range, experiments on the dependency between nucleation pressure and expansion rate were performed. Figure VI-22 shows nucleation pressures in 20% SMP solution after fast (200 MPa/s) and slow (2 MPa/s) expansion from different temperatures at 320 MPa.

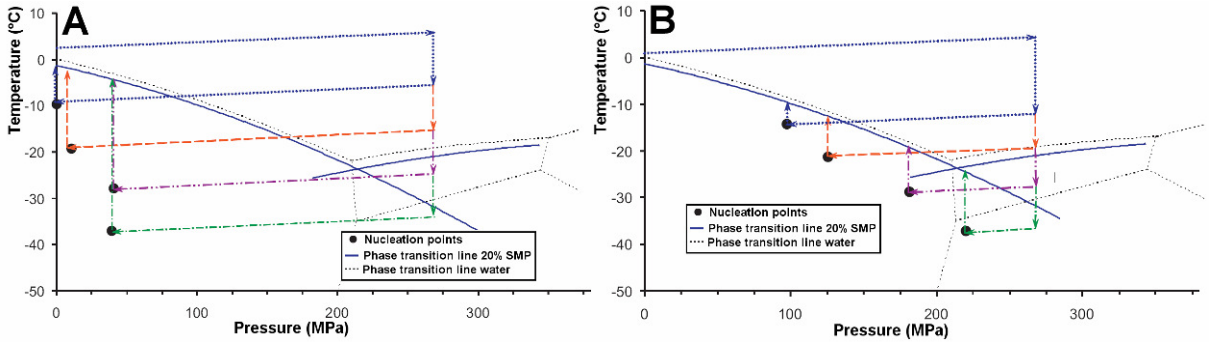

Figure VI-22: Nucleation temperatures in 20% SMP solution in a PSF cycle at 200 MPa/s pressure release rate (A) and 2 MPa/s pressure release rate (B).

It shows that the nucleation pressure depends on the rate of pressure release. At fast pressure release rates nucleation occurs after expansion from -8 to -35°C at low pressures between 40 and 0.1 MPa. In contrast, at low pressure release rates nucleation occurs at significantly higher pressures. The extent of supercooling during pressure release, which can be described as a shift of the metastable supercooled phase from the ice III region to the ice I region, is affected not only by the extend of supercooling but also by the residence time in the metastable state. In this respect, nucleation occurs as a delayed effect, which allows high degrees of supercooling at fast pressure release rates. The described phenomenon has been reported before by Thiebaud et al (Thiebaud et al., 2002). The amount of ice that is instantaneously formed during pressure release at p_N can be calculated according to equation VI–6. Calculating the percentage of ice that crystallized from p_N to p_{atm} is more complex and follows from (Otero, Sanz, de Elvira & Carrasco, 1997; Otero & Sanz, 2000):

$$\left(\frac{\partial \mathrm{V}}{\partial \mathrm{p}}\right)_S = (1-Z)\cdot\left[\left(\frac{\partial V_i}{\partial p}\right)_T + \frac{2\cdot T_K}{L}\cdot\left(\frac{\partial V_i}{\partial T}\right)_T \cdot (V_w - V_i) - \frac{cp_i \cdot T_K}{L^2}\cdot(V_w - V_i)^2\right] + Z\cdot\left[\left(\frac{\partial V_w}{\partial p}\right)_T + \frac{2\cdot T_K}{L}\cdot\left(\frac{\partial V_w}{\partial T}\right)_T \cdot (V_w - V_i) - \frac{cp_w \cdot T_K}{L^2}\cdot(V_w - V_i)^2\right] \quad \textbf{(VI-10)}$$

where V is the specific volume (m^3/kg), p is the pressure in Pa, T_K is the temperature in K, cp is the specific heat capacity in J/kg·K, L is the latent heat in J/kg and Z is the liquid water percentage in a mixture of ice and water in %, which can be calculated as

$Z = (1 - m_i)$; with m_i calculated according to equation VI–6. **(VI-11)**

In the present study the nucleation pressure during fast pressure release is assumed to be 0.1 MPa. Hence the amount of instantaneously formed ice during PSF at high pressure release rates is approximated by equation VI–6. This calculation does not take into account the amount of ice formed after nucleation, if nucleation occurs at pressures above 0.1 MPa. However, the maximum Δp between nucleation and atmospheric pressure at fast pressure release rates during PSF of 20% SMP solution was found no higher than 40 MPa and is therefore neglected.

3.4 Sol-gel transition of SMP solution in the pressure shift freezing process

Pressure shift freezing experiments with 20% SMP solution resulted in different macroscopic structures after treatment, depending on the treatment pressure and the amount of ice instantaneously formed during pressure release. For a structure based categorization the induced structures were classified into three states:

- *Liquid (sol):* dynamic viscosity < 30 mPa·s; no visible aggregates
- *Sol – gel transition:* dynamic viscosity > 30 mPa·s; visible aggregation; no fracture force detectable
- *Gel:* fracture force > 0.2 N; visible solidification

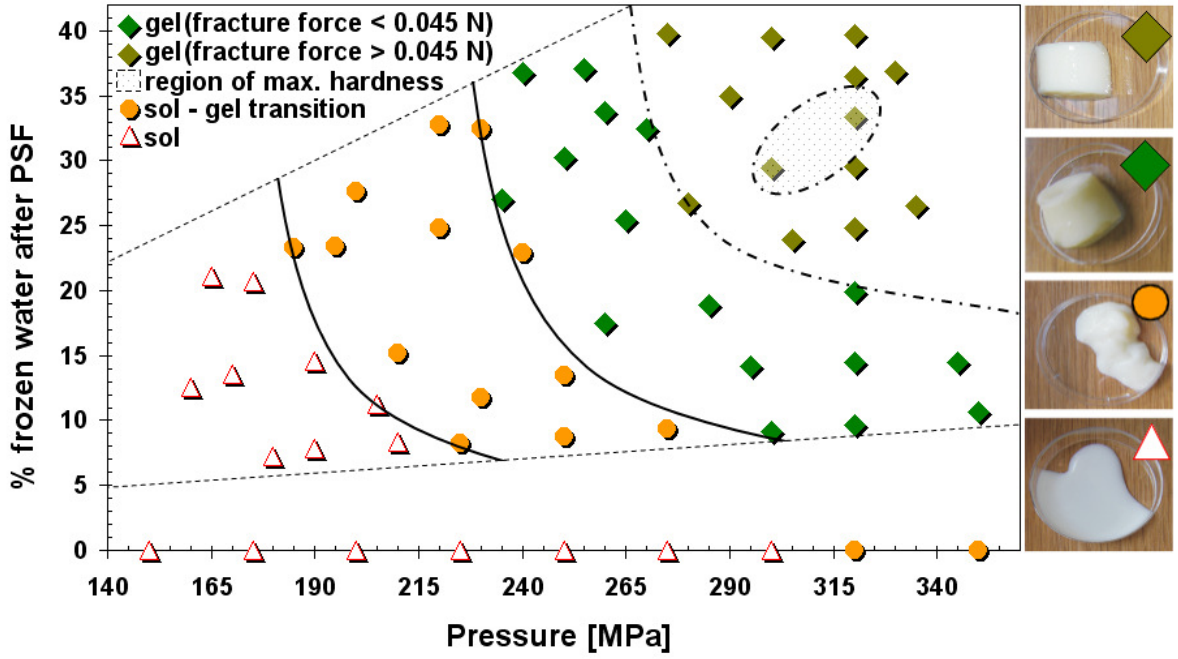

Figure VI-23: State diagram of 20% SMP solution after PSF treatment, pointing out the sol state (△), the sol – gel transition state (●) and the gel state (◆). The images on the right show product examples corresponding to the different states in the diagram.

The state diagram in Figure VI-23 subdivides the gel state into two classes of different gel strengths, which are separated by the dashed line. The dark green markers indicate gels with a fracture force between 0.2 and 0.045 N, the light green markers indicate fracture points > 0.045 N. The dotted area shows the region of maximum hardness detected in the experiments.
The state diagram shows that the formation of aggregates and gel structures during PSF strongly depends on the amount of water that freezes during pressure release. HP treatment without ice formation did not cause gel formation at pressures up to 350 MPa. HP treatment at 320 MPa induced the sol – gel transition structure, whereas PSF at the same pressure induced firm gels when 8 to 38% of the total water was frozen during pressure release. The present data further supports the hypothesis of ice crystal driven gel formation during pressure release in HPLT freeze processes. The gel formation is induced by a complex mechanism, involving thermodynamic effects (pressure and temperature driven protein denaturation) and physical effects related to the water phase transition during pressure release (freeze concentration, mechanical compression).

To evaluate the effect of higher protein concentrations due to freeze concentration in the partly frozen matrix after expansion, SMP solutions with adapted protein content were HP treated and compared with the 20% SMP solutions after PSF. The protein concentration was increased according to the freeze concentration during PSF. Table VI-5 shows the amount of ice instantaneously formed during pressure release during PSF treatments with different expansion temperatures (calculated according to equation VI–6) and the correspondingly increased concentrations for the HP treatments.

Table VI-5: Expansion temperatures and resulting ice content in 20% SMP solution during PSF treatment at 320 MPa. The "increased SMP concentration" displays the SMP concentration in the solution after pressure release

Expansion temperature [°C]	Nucleation temperature [°C]	Frozen water [%]	Increased SMP concentration [%]
-5	-10.7	10.6	21.86
-10	-14.2	14.5	22.61
-15	-19.2	20.0	23.79
-20	-23.6	24.8	24.96
-25	-27.8	29.5	26.18
-30	-31.8	33.9	27.47
-35	-36.9	39.7	29.31

The textural properties of 20% SMP solutions after PSF treatment at 320 MPa and different expansion temperatures vs. the textural properties of SMP solution with increased solid content according to the freeze concentration in the PSF samples are shown in Table VI-6. The HP induced gels show lower fracture forces and hardness at all adapted concentrations. Most obvious is this effect at 29.3% SMP concentration during HP treatment, which results in a fracture force of 0.047 N, whereas the corresponding PSF treatment results in a fracture force of 0.061 N in 20% SMP solution. Hence, a simple concentration effect as the basic cause for increased gel strengths at higher percentages of frozen water after expansion in the PSF treatment can be ruled out. Fracture force and hardness of the HP treated gels increase with concentration but do not reach the values of PSF induced gels.

Table VI-6: Textural properties of 20% w/w SMP gels after PSF and the corresponding solutions for HP treatment (320°MPa) at increased concentration. The data shows average values. The standard deviation for all measurements was no higher than 10%

SMP concentration [%] / Treatment	Hardness (slope)	Fracture force (N)	Fracture distance (mm)
20.0 (PSF; -5°C)	0.009	0.027	1.91
21.86 (HP; 18°C)	n.d.	n.d.	n.d.
20 (PSF; -15°C)	0.014	0.042	2.67
23.79 (HP; 18°C)	0.004	0.028	3.74
20 (PSF -25°C)	0.0147	0.055	3.49
26.18 (HP; 18°C)	0.007	0.044	5.34
20 (PSF; -35°C)	0.015	0.061	3.45
29.31 (HP; 18°C)	0.005	0.047	5.36

Since the increased concentrations after HP treatment did not induce comparable gel properties to PSF with 20% SMP, it is supposed that the temperature before pressure release plays an important role in the gel formation. The temperature upon expansion can not be regarded as a simple parameter in this respect, though. Temperature changes affect the system in two ways. They affect the equilibrium of the system and possibly induce unfolding of the protein molecules. In addition, lower temperatures upon expansion increase the amount of ice formed during pressure release. Hence, the total volume change during expansion and linked to it during gel formation is increased. On the base of the present data none of the proposed mechanisms can be ruled out. Clearly the increased solute concentration after expansion is not the only cause for higher gel strengths after PSF. The temperatures before and after expansion certainly affect the gel formation. In addition to the shift of the thermodynamic equilibrium, the ice formation seems involved.

4 Conclusion

The formation of pressure induced protein structures during HP, PSF and PAF treatments in the range from 150 to 350 MPa has been investigated with respect to different process and product related parameters. SEM analyses of HPLT and HP induced 25% SMP gels showed clearly process related structural changes in the induced gels. HP treated gels are homogeneous with a finely pored gel network. After PSF the structure is disordered and the protein network shows a wider pore size distribution. With increasing freezing time under pressure (PAF) the formation of long pores and thick protein strands in the network is promoted. Texture analyses confirm the formation of different structures and demonstrate the effect on the gel fracture forces and hardness values. Highest gel strengths are induced after PAF with long freezing times under pressure. The gel strength in PSF induced gels is higher compared to HP induced structures and increases at lower temperatures upon expansion.

In good agreement with the microstructure, differences in the water holding capacity of PSF and PAF induced gels were observed. PAF gels suffer from initial water loss of about 37% after 1 day storage at 4°C. In contrast, the PSF induced gels show drainage of only 2.5% after the same time. During frozen storage the water loss in PSF induced gels is increased and reaches 10% after 1 week storage at -27°C. In PAF gels the drainage is slightly reduced under the same conditions. This indicates partial reversibility of HPLT induced gel structures during frozen storage, which reduces the water holding capacity after PSF treatment and slightly increases it in PAF induced gels.

When no ice formation is involved, an increase of the pressure holding time from 90 to 180 min during PSF treatment does not affect the gel strength, whereas longer freezing times during PAF significantly increase the gel strength. A mechanism of physical protein network compression in SMP solutions during HPLT freeze processes is proposed. According to this, the ice formation under pressure and during pressure release accounts for an increase in the gel strength in HPLT induced SMP gels. The physical compression is linked to the volume changes that occur during the water phase transitions. The effect is more pronounced during PAF treatment as the total volume change in this process results from the ice III to ice I transition ($\Delta V \sim +18\%$) and the liquid to ice I transition ($\Delta V \sim +8.6\%$) during pressure release. The PSF process involves only the water phase transition from liquid to ice I, which causes less volume changes than the ice III to ice I transition.

Gel strength after HPLT treatment is promoted by high pressure release rates. Hence, the hypothesis of casein micelle association in SMP solution subjected to the rate of pressure release after HP treatment is confirmed for the HPLT domain. In addition to the casein association, the pressure release rate affects the HPLT induced ice crystal size in SMP gels, which affects the structure of the protein network. Large crystals locally immobilize higher amounts of liquid water than small crystals. During melting, large water droplets form and the resultant gel structures are less homogeneous and relatively soft.

Experiments with different SMP qualities indicate a strong dependency of the gel strength after HPLT treatment on the WPNI of the raw material. Low heat SMP results in higher gel strengths after PAF treatment compared to high heat SMP, whereas fracture points and hardness are higher after HP and PSF treatment of high heat SMP solutions. A conclusive mechanism of this phenomenon can not be developed on the base of the present results. However, the results support the assumption that whey proteins contribute to the gel formation in the presence of casein during HPLT, as the WPNI is a measure for the degree of whey protein denaturation during drying.

Experiments on different casein to whey protein ratios showed a non-linear coherency between gel strength and the c/w ratio. This implies that whey proteins contribute to the gel formation in the presence of casein micelles and increase hardness and fracture points by supporting the casein based gel formation under p,T conditions where pure whey protein solutions do not form solid gels after PSF treatment. The highest gel strengths were found at

c/w ratios of 1:0, at a c/w ratio of 1:1 a local maximum in the hardness and fracture points occurred.
Based on the calculations of the amount of water that freezes instantaneously during pressure release in the PSF process, a state diagram of a 20% SMP solution was generated. The diagram shows the impact of pressure and the ice content after expansion on the progressive solidification of the SMP solution. In this respect three different states were identified: sol state, sol – gel transition state and the solid gel state. The state diagram highlights the importance of ice formation during pressure release in the structure formation in SMP solutions during HPLT treatment.
Concentration effects during HPLT treatment as the basic cause for changes in the gel structure were ruled out by HP treatment of SMP solutions with concentrations, adapted to the freeze concentration during PSF. Accordingly increased concentrations did not induce comparable gel strengths after HP treatment. Consequently the temperature upon pressure release was identified as a critical parameter, where it is not clarified whether temperature linked protein unfolding or temperature induced ice formation is responsible for the induced structures. However, since gel formation is strongly affected by the casein micelle association and casein micelles are not pressure denaturated, the role of the physical effect of ice formation seems of higher relevance in this respect.
Summarizing it can be stated that unique milk protein structures are induced by HPLT treatment, which differ significantly in their properties from HP induced structures. In this respect, the ice formation under pressure and during pressure release has a major impact on the induced structures.

5 References

[1]Aguilera, J. M. & Kinsella, J. E. (1991). Compression Strength of Dairy Gels and Microstructural Interpretation. *Journal of Food Science*, *56*(5), 1224-1228.

[2]Anema, S. G. (1998). Effect of Milk Concentration on Heat-Induced, pH-Dependent Dissociation of Casein from Micelles in Reconstituted Skim Milk at Temperatures between 20 and 120 °C. *Journal of Agricultural and Food Chemistry*, *46*(6), 2299-2305.

[3]Barry, H., Dumay, E. M. & Cheftel, J. C. (1998). Influence of pressure-assisted freezing on the structure, hydration and mechanical properties of a protein gel. In N. S. Isaacs. *High pressure food science, bioscience and chemistry* (pp. 343-353). Royal Society of Chemistry, London.

[4]Chaplin, M. (2008). Water structure and science, http://www.lsbu.ac.uk/.

[5]Considine, T., Patel, H. A., Singh, H. & Creamer, L. K. (2007). Influence of binding conjugated linoleic acid and myristic acid on the heat- and high-pressure-induced unfolding and aggregation of beta-lactoglobulin B. *Food Chemistry*, *102*(4), 1270-1280.

[6]Dumay, E., Picart, L., Regnault, S. & Thiebaud, M. (2006). High pressure-low temperature processing of food proteins. *Biochimica Et Biophysica Acta-Proteins and Proteomics*, *1764*(3), 599-618.

[7]Fertsch, B., Mueller, M. & Hinrichs, J. (2003). Firmness of pressure-induced casein and whey protein gels modulated by holding time and rate of pressure release. *Innovative Food Science & Emerging Technologies*, *4*, 143-150.

[8]Franks, F. (1995). Protein destabilization at low temperatures. *Adv. Prot. Chem.*, *46*, 105-139.

[9]Galazka, V. B., Dickinson, E. & Ledward, D. A. (2000). Influence of high pressure processing on protein solutions and emulsions. *Current Opinion in Colloid & Interface Science*, *5*(3-4), 182-187.

[10]Gracia-Julia, A., Rene, M., Cortes-Munoz, M., Picart, L., Lopez-Pedemonte, T., Chevalier, D. & Dumay, E. (2008). Effect of dynamic high pressure on whey protein aggregation: A comparison with the effect of continuous short-time thermal treatments. *Food Hydrocolloids*, *22*(6), 1014-1032.

[11]Hobbs, P. V. (1974). *Ice Physics*. Oxford university Press, USA.

[12]Huppertz, T., Fox, P. F. & Kelly, A. L. (2004a). High pressure-induced denaturation of -lactoglobulin in bovine milk and whey: a possible mechanism. *Journal of Dairy Research*, *71*(04), 489-495.

[13]Huppertz, T., Fox, P. F. & Kelly, A. L. (2004b). High pressure treatment of bovine milk: effects on casein micelles and whey proteins. *Journal of Dairy Research*, *71*(01), 97-106.

[14]Huppertz, T., Fox, P. F., de Kruif, K. G. & Kelly, A. L. (2006). High pressure-induced changes in bovine milk proteins: A review. *Biochimica et Biophysica Acta (BBA) - Proteins & Proteomics;Proteins Under High Pressure*, *1764*(3), 593-598.

[15]Keenan, R. D., Wix, L. & Young, D. (1998). *Method for the preparation of a foodstuff*. patent, (PCT/EP1997/005917).

[16]Keenan, R. D., Young, D. J., Tier, C. M., Jones, A. D. & Underdown, J. (2001). Mechanism of Pressure-Induced Gelation of Milk. *Journal of Agricultural and Food Chemistry*, *49*(7), 3394-3402.

[17]Kolakowski, P., Dumay, E. & Cheftel, J. C. (2001). Effects of high pressure and low temperature on beta-lactoglobulin unfolding and aggregation. *Food Hydrocolloids*, *15*(3), 215-232.

[18]Le Bail, A., Chourot, J. M., Barillot, P. & Lebas, J. M. (1997). Congélation-décongélation par haute pression. *Revue Générale du Froid*, *7*(2), 51-56.

[19]Merel-Rausch, E. (2006). *Hydrostatic high pressure treatment of casein to generate defined particle and gel structures*. PhD, Universitaet Hohenheim, 95.

[20]Merel-Rausch, E., Kulozik, U. & Hinrichs, J. (2007). Influence of pressure release rate and protein concentration on the formation of pressure-induced casein structures. *Journal of Dairy Research*, *74*(03), 283-289.

[21]Messens, W., VanCamp, J. & Huyghebaert, A. (1997). The use of high pressure to modify the functionality of food proteins. *Trends in Food Science & Technology*, *8*(4), 107-112.

[22]Otero, L., Sanz, P. D., de Elvira, C. & Carrasco, J. A. (1997). Modelling thermodynamic properties of water in the high pressure assisted freezing process. In K. Heremans. *High Pressure Research inthe Bioscience and Biotechnology* (pp. 347-350). Leuven University Press, Leuven.

[23]Otero, L. & Sanz, P. D. (2000). High-Pressure Shift Freezing. Part 1. Amount of Ice Instantaneously Formed in the Process. *Biotechnology Progress*, *16*, 1030-1036.

[24]Otero, L. & Sanz, P. D. (2006). High-pressure-shift freezing: Main factors implied in the phase transition time. *Journal of Food Engineering*, *72*(4), 354-363.

[25]Schrader, K. & Buchheim, W. (1998). High pressure effects on the colloidal calcium phosphate and the structural integrity of micellar casein in milk - II. Kinetics of the casein micelle disintegration and protein interactions in milk. *Kieler Milchwirtschaftliche Forschungsberichte*, *50*(1), 79-88.

[26]Smeller, L. (2002). Pressure-temperature phase diagrams of biomolecules. *Biochimica Et Biophysica Acta-Protein Structure and Molecular Enzymology*, *1595*(1-2), 11-29.

[27]Strambini, G. B. & Gabellieri, E. (1996). Proteins in frozen solutions: Evidence of ice-induced partial unfolding. *Biophysical Journal*, *70*(2), 971-976.

[28]Thiebaud, M., Dumay, E. M. & Cheftel, J.-C. (2002). Pressure-shift freezing of o/w emulsions: influence of fructose and sodium alginate on undercooling, nucleation, freezing kinetics and ice crystal size distribution. *Food Hydrocolloids*, *16*(6), 527-545.

[29]Trujillo, A. J., Capellas, M., Saldo, J., Gervilla, R. & Guamis, B. (2002). Applications of high-hydrostatic pressure on milk and dairy products: a review. *Innovative Food Science & Emerging Technologies*, *3*(4), 295-307.

Chapter VII Air cell development in high pressure-low temperature treated dairy foams

1 Introduction

The impact of HPLT processing on single ingredients in aerated dairy emulsions was discussed in chapter V of this work with focus on the dry matter components of the system. The two major components of frozen dairy foams were left out in these investigations. Water (ice) and air comprise more that 80% of the total volume of the investigated foamed emulsions. The present chapter focuses on the effects related to these two fractions during and after HPLT processing.

In the manufacture of frozen dairy foams the overrun (the increase in volume of the frozen foam over the volume of the liquid fraction) is produced by the incorporation of air into the matrix. The amount of incorporated air highly influences the quality of the product and is involved in meeting legal standards (e.g. in ice cream) (Marshall, Goff & Hartel, 2003). In this respect, maintaining the targeted uniform amount of incorporated air is an essential prerequisite. In the conventional processing of frozen aerated dairy products the air is incorporated in the concomitant freezing and mixing step in the freezer. In the present study two different approaches on the incorporation of air in dairy emulsions with respect to the HPLT freezing process were investigated.

1. HPLT induced aeration
2. Aeration prior to HPLT treatment.

The air cell development during and after HPLT processing was investigated and fundamental effects related to process and product parameters were identified.

2 Experimental Methods

2.1 Emulsion formulations

A series of model emulsions was developed to highlight effects related to the absence or presence of single components in the system. The complete list of all emulsion formulations that were used in this study is attached in the annex. An overview about the main characteristics of the developed formulations that are relevant for the present chapter is given in Table VII-1.

Table VII-1: Labeling and basic characteristic parameters of dairy based model emulsions

Labeling	Total solids [%]	Fat content [1] [%]	SMP/WP/ content [2] [%]	Sugar content [3] [%]
emulsion A	38.7	8.8	2.1 / 9.4	17.9
emulsion B	36.8	7	4.9 / 4.8	19.4
emulsion C	17.3	2.4	7.7 / 0	7

[1] additional fat (milkfat or vegetable oil); [2] skim milk powder and whey powder formulation attached in the appendix; [3] additional sucrose and/or sugar corn syrup

All ingredients of the dairy based model emulsions were pre-mixed for 20 min at 65°C followed by a 2 stage homogenization (40 bar / 150 bar) at 72°C. The homogenized emulsions were pasteurized for 30 sec at 85°C and than cooled down in a plate heat exchanger to 5°C. T he emulsions were frozen in 2.5 liter lots to -30°C. To produce a conventionally frozen foam reference, the model emulsions were frozen in a continuous ice cream freezer (Hoyer KF-80,

Tetra Pak Hoyer, Hoejbjerg, Denmark). The OR of the reference foams was typically between 90 and 100%.

2.2 HPLT setup

For all experiments the pilot scale HPLT unit, as described in chapter III, was used. Pressure assisted freezing (PAF), pressure shift freezing (PSF) and pressure induced crystallization (PIC) treatments were performed. The standard treatment pressure was 320 MPa. The process time was adjusted according to the respective process. For all experiments that involved overrun measurements, the semi flexible plastic shell packaging was used (see chapter III). Pressure release rates for all experiments was 200 MPa/s. Nucleation during expansion typically occurred between 0.1 and 40 MPa.

2.3 Product aeration

For the controlled aeration of the different dairy emulsions the aeration system Minimondo A-05 P13774 (Haas Mondomix, Almere, Netherlands) was used as described in chapter III–3.1. The standard aeration setup is shown in Table VII-2. For experiments on the impact of the liquid foam OR the air flow was varied to obtain the target foam OR (60 to 185%). Depending on the emulsion formulation, the overrun of the liquid emulsions at the outlet of the aeration system after foaming with the standard setup was between 140 and 180% at temperatures between 10 and 12°C.

Table VII-2: Standard aeration setup for the aeration of model emulsions in the Minimondo A-05 P13774

Feed pump frequency [Hz]	Mixing head [rpm]	Backpressure [bar]	Air flow [L/h]	Jacket temperature [C°]
50	1500	2	10L/h	3

2.4 Analyses

2.4.1 Consistency measurement (Bostwick)

The consistency of a sample can be measured by its resistance to flow under specific conditions, for a specified time. As a control analysis, in addition to the overrun measurement, Bostwick-consistency measurements of the liquid aerated emulsions were performed after aeration in the Mondomix aeration system. For the measurements a Bostwick consistometer (Cenco Scientific Co., Chicago, U.S.A.) was used. The flow properties of the foams were measured at 10°C and the Bostwick scale was read after 30 seconds.

2.4.2 Overrun and density measurement

The amount of air incorporated into aerated products is commonly expressed as percent overrun (OR). The overrun is the increase in volume of the foam (V_{foam}) over the volume of the liquid phase (V_{liquid}). It is expressed as percent of the volume of the non aerated mix.

To determine the overrun of frozen samples, frozen product of known mass was immersed into a beaker of water at 4°C. The low temperature of the water prevents quick melting of the samples during the measurement and assures a water density of 1 g/ml. According to the Archimedes Principle the buoyant force exerted by a fluid on an object is equal to the weight of the fluid displaced by the object. The weight of the displaced water during immersion of the sample (in g) was recorded and corresponds to the sample volume (in ml).

The density of the model emulsion was determined with a Calculating Density Meter DMA 55 (Chempro / PAAR, Graz, Austria). The Overrun and shrinkage were calculated according to equation VII–1 and equation VII–2, respectively.

$$\text{overrun} = \frac{V_{foam} - V_{liquid}}{V_{liquid}} \cdot 100\% \qquad \text{(VII-1)}$$

The OR of liquid foam was determined by volume and weight measurement in a scaled measuring cylinder (1L foam). To describe the percentage of OR loss during the process the "shrinkage index" is introduced. The shrinkage index is defined as:

$$\text{shrinkage index}\,[\%] = 1 - \frac{OR_B}{OR_A} \cdot 100\% \qquad \text{(VII-2)}$$

With OR_A: OR of the sample before treatment and OR_B: the OR of the sample after treatment. All analyses were carried out at least in triplets for each sample. The final OR was calculated as the mean value of the single analyses.

2.4.3 Scanning electron microscopy

Cryo-SEM

For the cryo-SEM analyses, the frozen foam samples were directly transferred from frozen storage (-27°C) to a cryo-holder and transferred into liquid nitrogen and into the preparation chamber. An Alto 2500 cryotrans system (Gatan, Inc., Warrendale, US) attached to a Quanta 200F (FEI Company, Oregon, US) scanning electron microscope was used for the analyses. The frozen samples were first etched at -105°C and then cooled down to -120°C. Samples were sputter coated with gold. The coated samples were transferred from the preparation chamber to the cold stage within the column. The images were obtained at 10 kV. The pressure in chamber was $3\text{-}4 \cdot 10^{-6}$ torr.

SEM

For the standard SEM analyses, the samples were frozen in liquid nitrogen and freeze dried. The samples were prepared for microscopic analysis according to the cryo-SEM procedure. The samples were analyzed with a scanning electron microscope (Hitachi S-2700 SEM, Tokyo, Japan). The SEM method is described in detail by Künzel (Künzel, 2009). The obtained images were visually evaluated. In addition, selected images were analyzed with image analyzing software ImageJ 1.41 (Wayne Rasband, National Institutes of Health, US).

3 Results and discussion

3.1 High pressure-low temperature induced aeration

Following the fundamentals of gas-liquid interactions, the amount of air dissolved in a fluid is proportional to the pressure of the system (Henry's Law). The potential of HPLT processing to induce mixing of two initially separated phases (gas and liquid) under pressure was evaluated by PSF treatment of a liquid dairy emulsion (emulsion A) in the presence of air (volume ratio 1:1) for 60 min at -25°C and 320 MPa. After PSF treatment, the samples were phase separated into a gaseous phase and a partially frozen phase which did not show a foamy appearance. No formation of air cells in the emulsion could be validated by overrun measurements. There was no significant difference in density of the melted emulsion after treatment in comparison to the untreated non-aerated reference. It is unclear if the absence of a detectable air volume fraction in the samples is the result of a compressed mass fraction that passed out during melting or the actual absence of air enclosure at all.

Any pure substance whose pressure and temperature exceed those of its critical point is a supercritical fluid (Chester & Haynes, 1997). In addition to the volume reduction during pressure build up the air phase of the dairy foam undergoes the phase change from gaseous to the supercritical state when exceeding the critical pressure and temperature (p_{crit}= 3.7860

MPa; T_{crit}= 132.5 K) (Lemmon, Jacobsen & Penoncello, 2000; Cazenave Gassiot, 2007). The supercritical fluid region in the phase diagram of a pure fluid is shown in fig Figure VII-1.

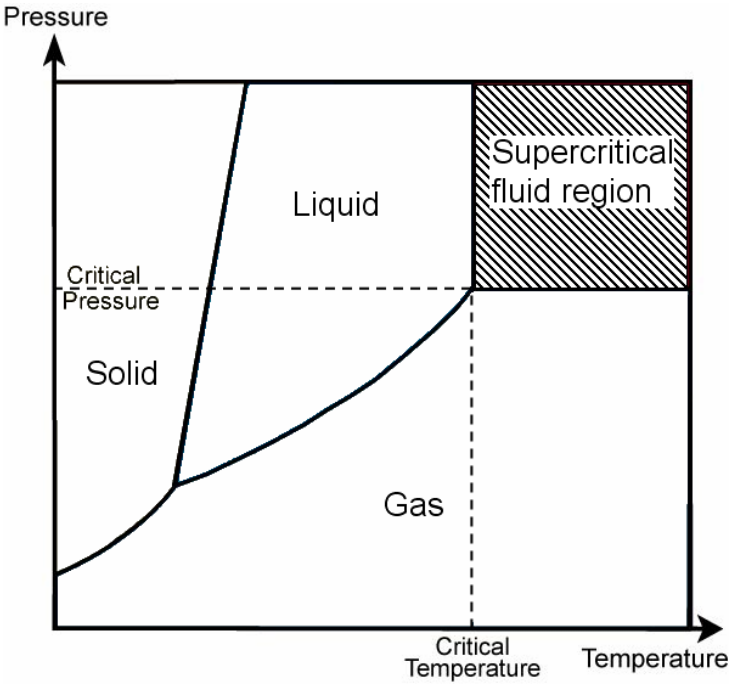

Figure VII-1: Schematic drawing of the supercritical region in the phase diagram of a pure fluid.

Assuming that a certain amount of gas is dissolved in the liquid phase under pressure, a possible mechanism of gas loss is the pass out of gas bubbles after their reformation during pressure release, promoted by a lack of interfacial stabilization. During conventional aeration (e.g. mixing of air and ice cream mix in a continuous freezer), complex stabilization mechanisms take place that ensure the creation of homogeneously distributed and stable air cells. Fat destabilization and interactions with proteins are major effects in this context (Marshall et al., 2003). Since the applied HPLT treatment lacks any kind of mechanical energy input, the conventional mechanisms of foam formation are not induced by this treatment. However, taking into account the instantaneous ice formation during pressure release, it is unclear if the mechanism of simple pass out (channeling) of air through the partially frozen, high viscous matrix occurs. In spite of the uncertainty about the mechanism behind this phenomenon, it can be stated that replacing a mechanical aeration step of the product with the HPLT technology is currently not an option.

3.2 Impact of HPLT processing on the air volume fraction in dairy foams

In preliminary experiments with melted ice cream (data not shown) it was found that after HPLT treatment of stable liquid foam a certain percentage of the initial liquid foam overrun is maintained in the frozen product. Since aeration under pressure does not induce detectable overrun, the liquid dairy emulsions were aerated prior to the HPLT treatments.

3.2.1 Impact of the initial liquid foam overrun

To investigate the influence of the initial overrun in the liquid system before HPLT treatment on the overrun of the final product, model emulsion B was HPLT treated at 320 MPa with initial overrun ranging from 60 to 185%. The overrun of the liquid foam was measured prior to PSF and PAF treatment. The pressure was released (200 MPa/s) when the sample core

temperature reached -25°C during PSF and after 3000 s freezing time at about -34°C after PAF treatment. The OR of the treated emulsions was measured after 24 h storage at -27°C.

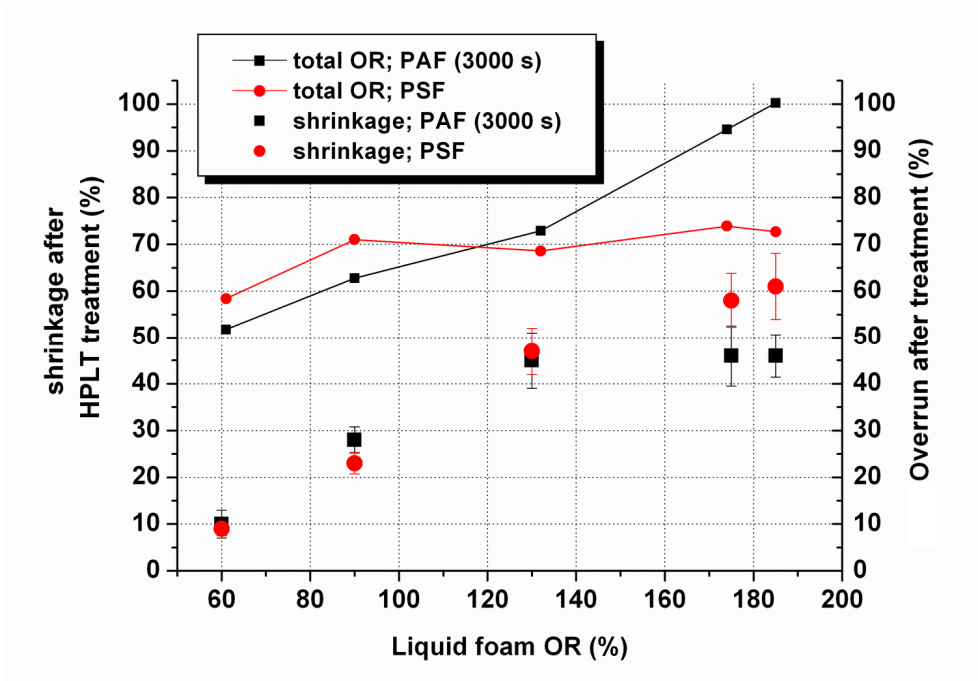

Figure VII-2: Shrinkage (overrun reduction) and overrun after 24 h storage at -27°C in PSF (■) and PAF (●) treated dairy emulsion (emulsion B) as a function of the initial liquid foam overrun before treatment.

As shown in Figure VII-2 the OR after treatment is influenced by the OR of the initial liquid foam OR. At low initial OR the HPLT induced shrinkage is low after PSF and PAF treatment. With increasing start OR, the final OR reaches maximum values of about 70% after PSF treatment (~10% shrinkage at 60% OR). Accordingly, the shrinkage after PSF increases at higher OR values before treatment. In contrast, the shrinkage after PAF treatment approximates a maximum of about 45% when liquid foam OR values are higher than 130%. In a liquid foam OR range from 130 to 185% the OR after PAF treatment increases proportional with the liquid foam OR. This finding suggests two different mechanisms behind the air cell stabilization during and after PAF and PSF.

3.2.2 Overrun development in HPLT treated pre-aerated dairy emulsions

Storage time

During HPLT treatment the air phase is exposed to pressure levels that drastically affect its physical properties. Following the law of Boyle Mariotte, at constant temperature the volume of an ideal gas is reduced proportional with increasing pressure. At low pressures, this law is approximately applicable to air (Agassi, 1977). As a consequence, the characteristic foam structure is disintegrated during the pressure holding time in HPLT treatments. During and after pressure release the air cells reform and grow, driven by the pressure gradient between the compressed bubbles and the surrounding matrix. As the partly frozen matrix counteracts the pressure induced bubble growth, the foam structure is not instantaneously restored after pressure release. The air cell development is governed by two basic parameters: time and temperature, where the temperature indirectly affects the gas expansion as it decisively determines the hardness and viscosity of the matrix.

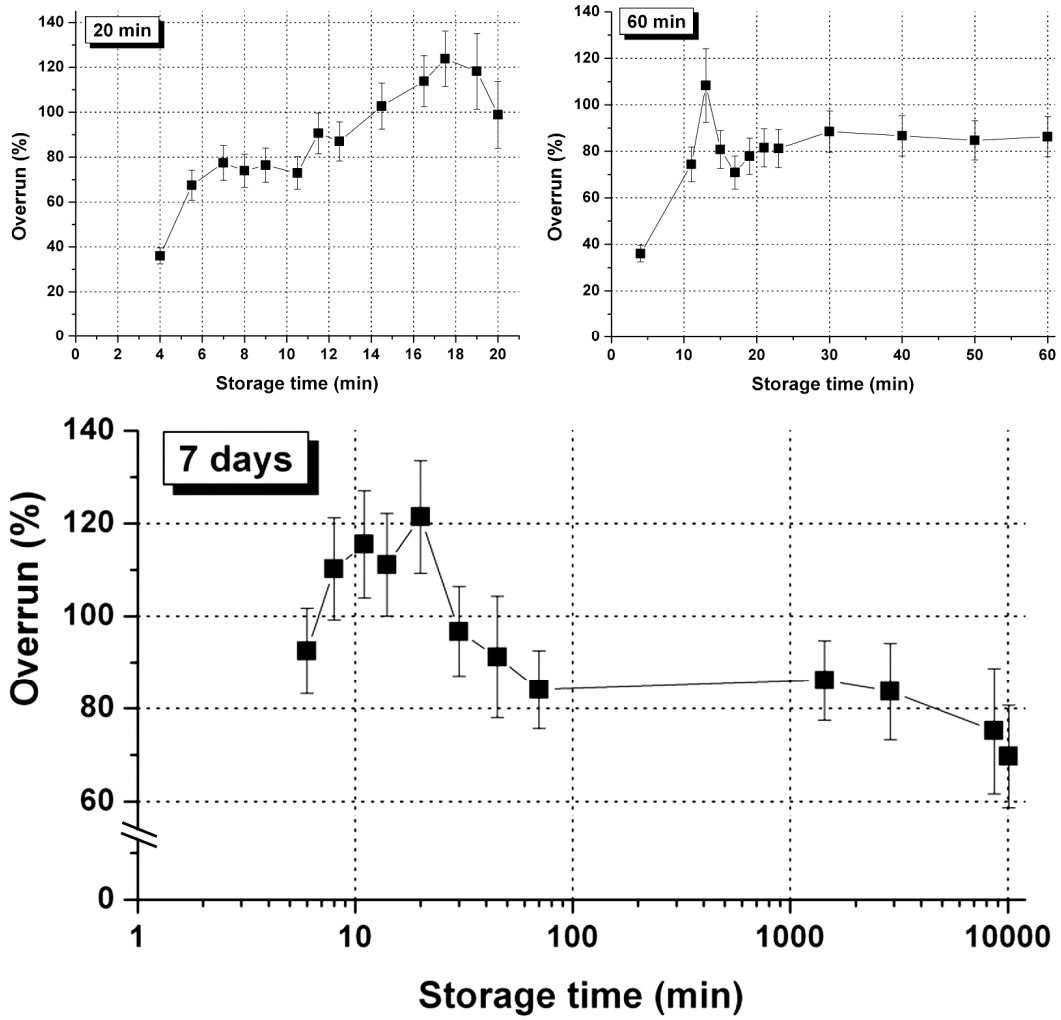

Figure VII-3: Overrun development over time in PAF treated aerated dairy emulsion (emulsion B) during storage at -27°C. The three charts show the OR development in three independently treated emulsions.

Figure VII-3 shows the overrun development in PAF treated pre-aerated emulsion B during storage at -27°C. The liquid foam OR before treatment in this experiments was 160 ±15%. During the first 20 min after treatment the OR increased from about 40 to 100% with a maximum of 120% after 17 min. Directly after treatment the air cells are highly compressed and expand slowly in the partly frozen, high viscous matrix. After reaching a local maximum, the OR decreased and equilibrated to about 80% within the first 60 min. During further storage for 7 days the OR is slightly decreased to minimum values of about 70%. The results in the previous section showed that the OR of the liquid foam is decreased after HPLT treatment. Average shrinkage of 50% occurred after PAF treatment with initial liquid OR above 120%. Figure VII-3 indicates that after treatment a high percentage of air is entrapped in the matrix and the major gas loss does not occur during the treatment. Two effects occur after the HPLT treatment, driven by the high internal pressure of the entrapped air cells: air cell expansion (volume gain) and gas loss (volume reduction). The expansion of bubbles lowers the internal pressure, which is accompanied by an increase in volume. The OR increases in the first minutes after treatment. After reaching the maximum OR, progressive gas loss causes OR reduction in the treated emulsions. The migration of gas from the entrapped bubbles to the product surface also lowers the pressure gradient. Presumably the gas loss starts concurrently with the bubble expansion after treatment but the air cell expansion compensates the air volume loss to some extent. The air cell expansion is limited

by the progressively decreasing pressure gradient between bubbles and the surrounding matrix. After reaching the maximum OR the air loss dominates the OR development and the OR decreases. As the air cell expansion, the gas loss is driven by the high internal pressure of the air cells. Besides these two effects, the formation of new air cells due to previously dissolved gas that is released from the matrix after pressure release may additionally increase the OR. However, to validate this assumption further investigation on the number and distribution of air cells after treatment is needed. In experiments with air and emulsion as two separated phases (non-aerated) this effect was not validated.

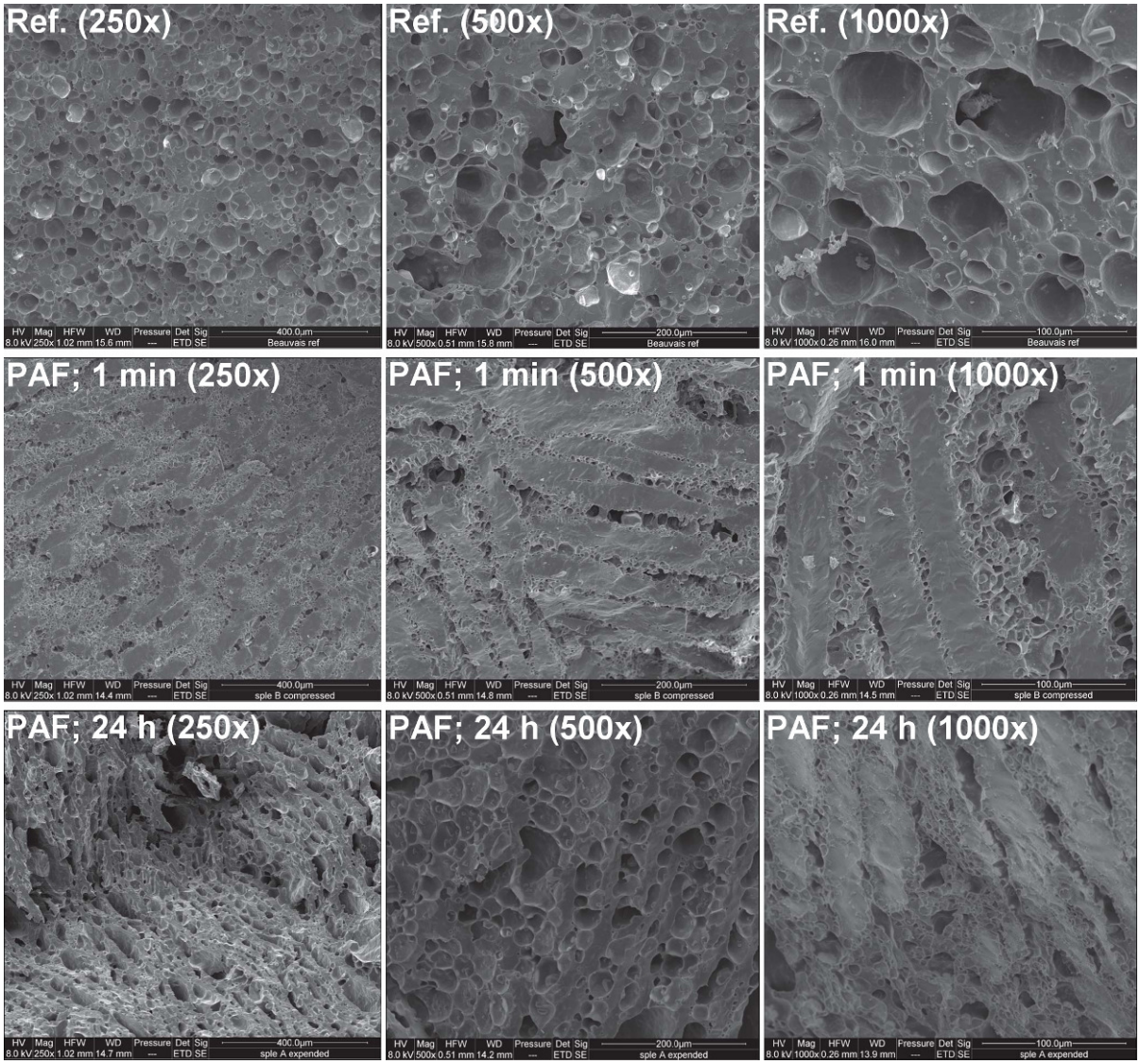

Figure VII-4: Cryo-SEM images of aerated dairy emulsion after conventional freezing (Ref.) and pre - aerated dairy emulsions after PAF treatment (2500 s freezing time), frozen in liquid nitrogen 1 min and 24h after treatment.

Cryo-SEM analyses of the PAF treated emulsions confirm the hypothesis of air cell expansion after HPLT treatment. Figure VII-4 shows SEM pictures of a conventionally processed reference (continuous ice cream freezer) and PAF treated pre-aerated emulsion B that was frozen in liquid nitrogen directly after treatment and after 24 h storage at -27°C. To preserve the microstructure the frozen samples were kept at -80°C until the cryo-SEM pictures were taken. The freezing step in liquid nitrogen possibly causes additional changes in the foam structure but as the freezing rate is very high and the matrix is entirely frozen at -80°C, it is assumed that the actual structure of the samples after treatment is well preserved.

The conventionally processed reference samples show a homogeneous air bubble distribution with gas bubbles of about 50 µm average diameter. There is little coalescence of air bubbles and gas-free regions are small. An ordered alignment of air bubbles or gas-free regions is not noticeable.
Images of samples 1 min after treatment sought to show the state of the emulsion right after the HPLT treatment. At this stage the samples have little OR (~30%) and a high internal pressure in the gas bubbles that causes further expansion over time as shown by the OR development during storage (Figure VII-3). The SEM images show small air bubbles in a non uniform distribution and large air-free regions. The average air cell size in these samples is small compared to the reference, indicating that the air cell development was not completed at this point. The air cells are aligned to channel-like structures, which are separated by thick strands of air free matrix. The structure is similar to the typical lamella-structure that was found in PAF treated SMP solutions (see Chapter VI). Higher magnitude (Figure VII-5) highlights the alignment of air cells between broad regions without air cells. The porous appearance of the narrow aligned air cells between the air free regions suggests the formation of air channels that promote the gas loss after treatment. The thin white films in the air-free areas between the channels are possibly membrane components of air cells that merged into the channels during and after expansion.

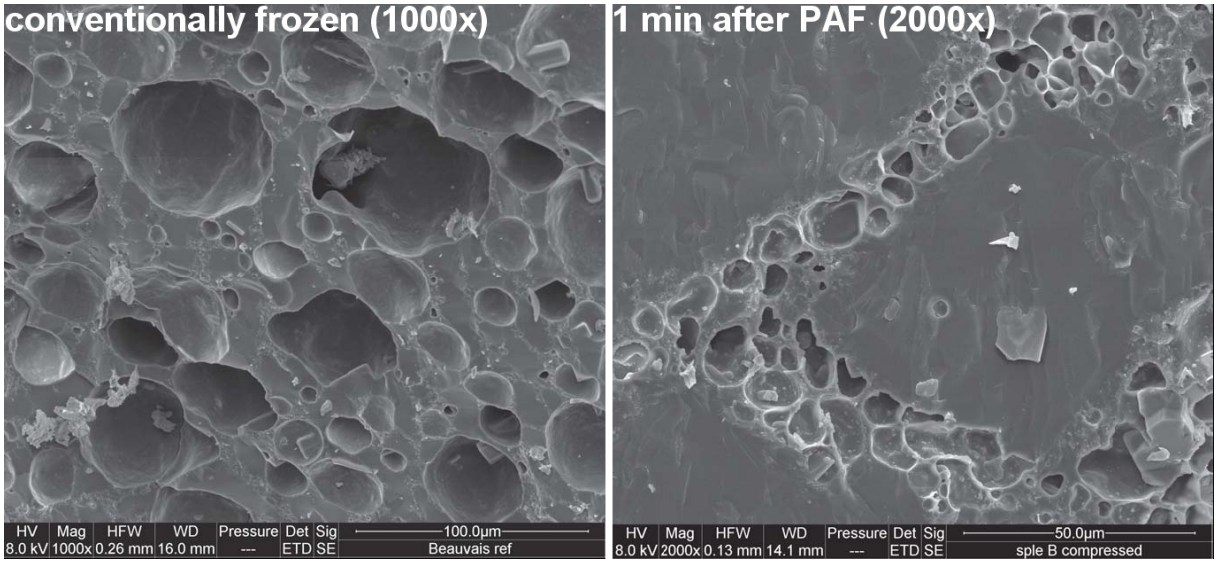

Figure VII-5: Conventionally frozen aerated dairy emulsion (left) at 1000x magnitude and PAF treated pre-aerated dairy emulsion (right) 1 min after treatment.

After 24 h storage at -27°C the foam structure in the PAF treated emulsions differs significantly from the structure of the samples 1 min after treatment. The pictures of the samples at low magnitude in Figure VII-4 suggest a fairly homogeneous air bubble distribution throughout the matrix. During storage the bubbles expanded and the OR developed to about 80%. Higher magnitudes indicate that as in the PAF samples that were taken 1 min after treatment, the air cells after 24 are aligned in a lamella-like structure. The number of bubbles after 24 h storage appears higher than 1 min after treatment, which may be due to the release of gas from the matrix and the nucleation and growth of new bubbles during storage. However, to validate this assumption further analysis with focus on the air cell size and distribution are required. Generally, the number of bubble seems comparable to the reference sample but the distribution is less homogeneous. As in the pictures that show the PAF treated emulsions directly after treatment, long air free regions can be found throughout the matrix after 24 h storage.

Storage temperature

In the previous section it was stated that the OR of HPLT treated dairy foams develops over storage time after treatment. The matrix hardness counteracts the air cell expansion and limits OR development. The viscosity and hardness of frozen foams are decisively determined by the temperature (Marshall et al., 2003; Muse & Hartel, 2004). With increasing ice content at lower temperatures the hardness of the matrix, and linked to it the resistance against bubble expansion, increases. To validate this hypothesis, the OR values of PAF treated pre-aerated emulsions (emulsion B) were compared after 24 h storage at different temperatures.

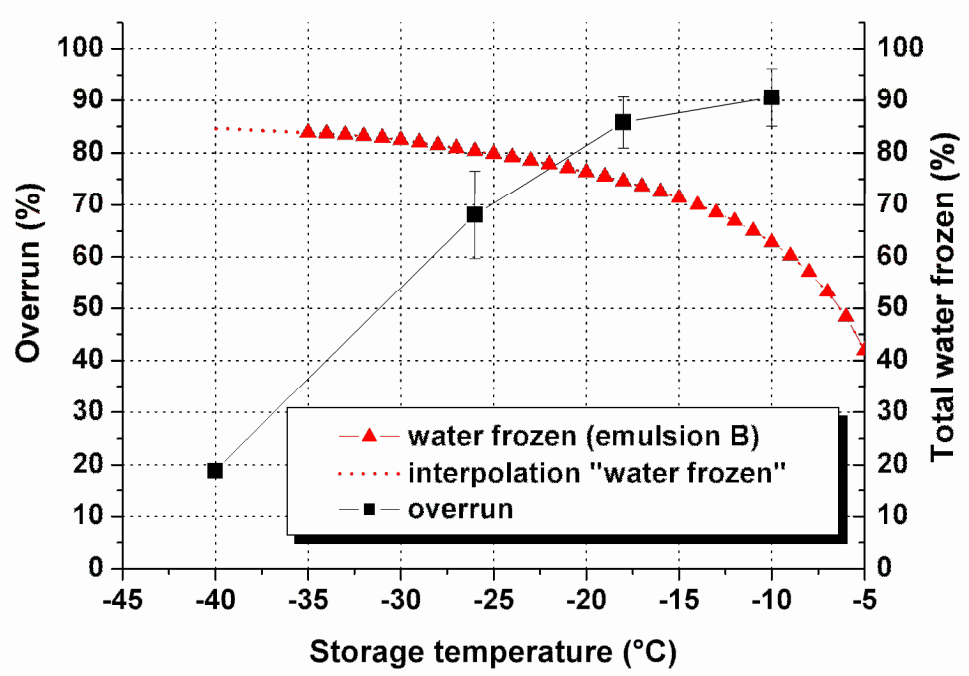

Figure VII-6: Overrun (■) and total amount of frozen water (▲) as a function of storage temperature in PAF treated dairy emulsion (emulsion B).

Figure VII-6 shows the OR of pre-aerated emulsion B after PAF treatment and subsequent storage for 24 h at -40, -26, -18 and -10°C. The corresponding amount of frozen water in the emulsions as a function of temperature is assigned to the right ordinate. Supporting the hypothesis of hardness-related gas expansion in the frozen foams, the OR after 24 h storage is higher at lower temperatures. During storage at -40°C approximately 80% of the water in the foam is frozen and no significant expansion occurs. The OR remains at about 20%, which corresponds to the OR right after treatment. At higher storage temperatures the ice content in the frozen foam is lower and air cells in the matrix can expand. At a typical storage temperature of -18°C the OR develops to about 85%. All samples were stored in PE bags that fitted closely to the frozen sample surface after treatment. During storage the PE bags detached from the samples and gas enclosures outside the sample material developed. When the frozen samples were exposed to higher temperatures after 24 h frozen storage, no additional expansion occurred during melting. This indicates that the internal bubble pressure was equilibrated at this stage. According to this, the gas loss in the frozen samples occurs within the first 24 h after treatment and OR development is limited to this period. A schematic description of the air cell development in pre-aerated dairy emulsions during and after HPLT treatment is shown in Figure VII-7.

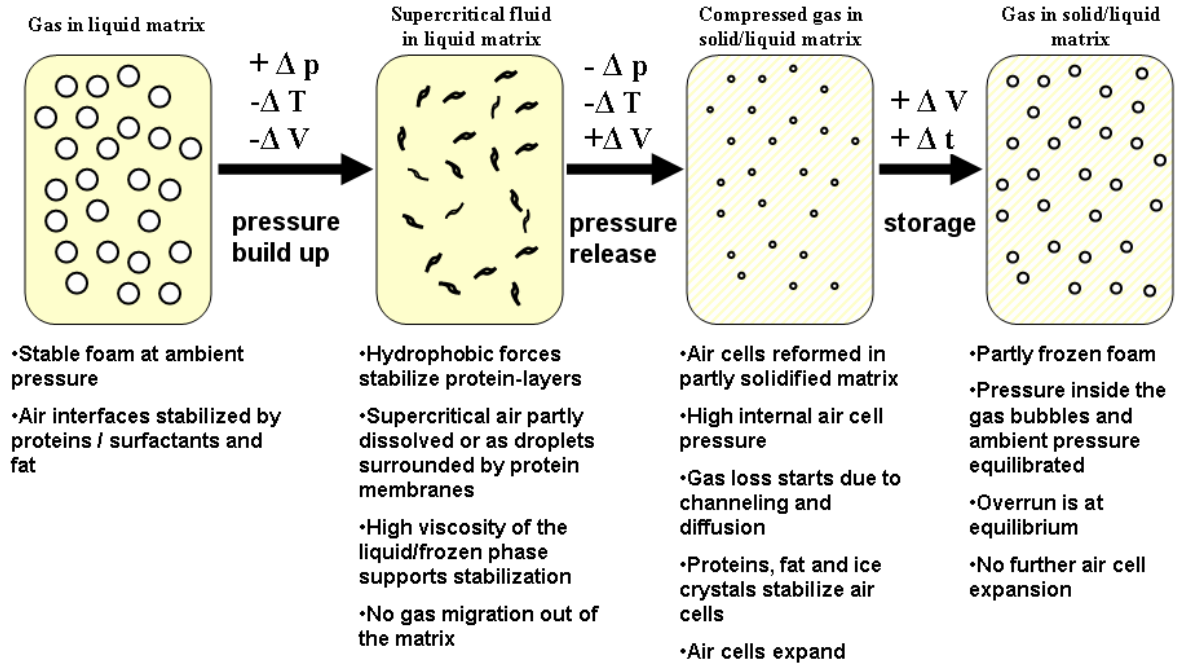

Figure VII-7: Hypothesis of Overrun development in pre-aerated dairy emulsions during and after HPLT treatment.

3.2.3 Freezing time under pressure

The ice content in aqueous products after HPLT treatment results from two effects: ice formation during pressure release (PSF-effect) and ice formation under pressure (PAF-effect). With increasing ice content, the product hardness and viscosity are increased (Muse & Hartel, 2004). Assuming that OR development and gas loss after HPLT treatment begin during pressure release and the air cell expansion is linked to the hardness and viscosity of the matrix, as indicated by the results of the previous section, the freezing time under pressure is an important parameter with respect to the final OR of the product. The product temperature after expansion equates to the freezing point of the system and is determined by the ice content at atmospheric pressure. The amount of water that freezes instantaneously during pressure release (PSF effect) is limited by the degree of supercooling and the pressure before expansion (Otero & Sanz, 2000). According to the ice content calculation (chapter VI–3.3.1), the total amount of ice in the treated dairy emulsions is no higher than 41% after PSF treatment at 320 MPa and typical nucleation temperatures of about -38°C close to atmospheric pressure. As shown in Figure VII-6, this corresponds to storage temperatures of about -5°C for emulsion B. With increasing freezing times under pressure the difference between the product temperature after HPLT treatment and the target storage temperature can be reduced as more water is frozen under pressure. Hence, downstream freezing times (e.g. in a hardening tunnel) are reduced. The effect of the freezing time under pressure on the final product temperature has been discussed in detail in chapter IV-3.3.

To evaluate the effect of higher freezing times under pressure on the OR of pre-aerated dairy emulsions, 200 ml lots of model emulsion B were HPLT treated at 320 MPa with freezing times under pressure ranging from 0 seconds (PSF) to 9360 seconds (long PAF). The freezing time is defined by the time span between nucleation in the sample and the pressure release. The OR in emulsion B as a function of freezing time is shown in Figure VII-8. The OR was measured after 24 h storage at -27°C.

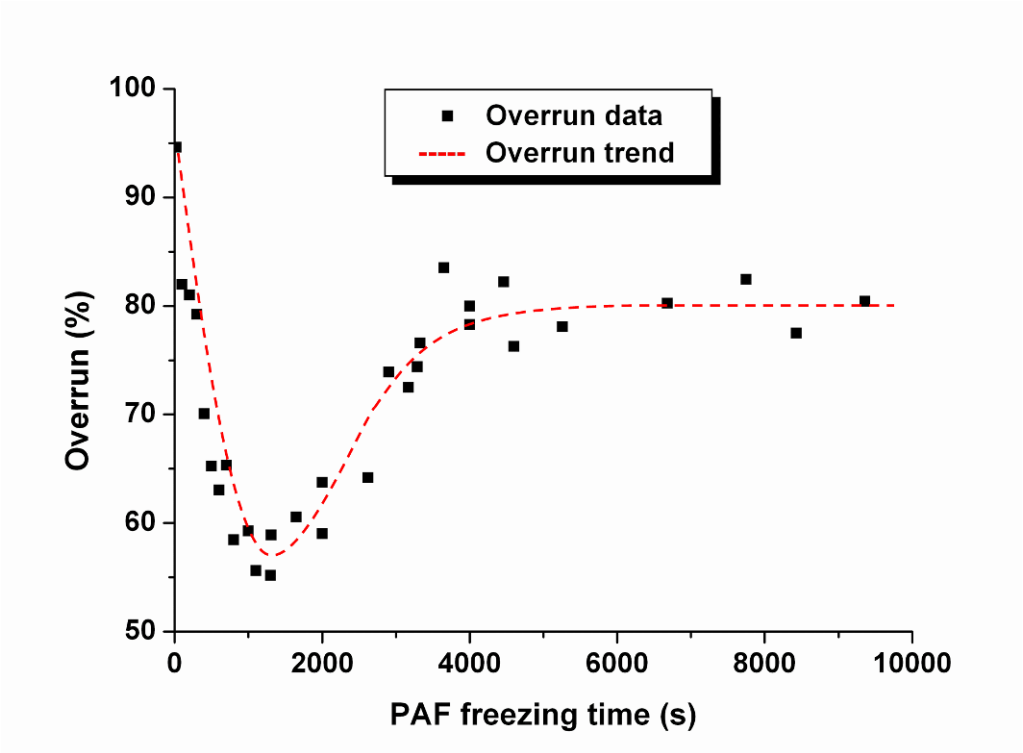

Figure VII-8: Measured overrun (■) and overrun trend (---) in pre-aerated dairy emulsion (emulsion B) after PAF treatment at 320 MPa with different freezing times under pressure. The data point at 0 seconds freezing time results from PSF at 320 MPa at -25°C. The OR was measured after 24 h storage.

A maximum OR of 95% was reached after PSF treatment, when no ice formation occurred before pressure release. With increasing freezing times under pressure the OR was progressively reduced and reached a minimum of about 55% after 1250 s freezing under pressure. Beyond this point the OR progressively increased and reached maximum values of about 80% after 4000 s. With a further increase of the freezing time no significant OR change was observed. As discussed in chapter IV of this work, the final temperature and ice content after PAF treatment are linked to the product temperature before pressure release. The more water is frozen under pressure, the higher the resultant percentage of frozen water after expansion and the lower the final temperature. On the base of the DSC data of emulsion B, the ice content at different temperatures can be approximated. After 4000 s freezing at 320 MPa the temperature after expansion was in average -28°C, which equates to about 81% of frozen water in the sample. Figure VII-9 shows the ice content in the dairy emulsion B after pressure release versus the freezing time under pressure at 320 MPa and the corresponding OR values. The graph shows the OR development from the minimum OR at about 1000 s freezing time to the equilibrium at >4000 s. The ice content was calculated on the base of the corresponding DSC data, taking into account the product temperature after expansion. The OR was measured after 24 h storage at -27°C. In the investigated period the OR correlates with the ice content and reaches its maximum of about 80% after 4000 s freezing time. With a further increase of the freezing time, the ice content is not considerably increased and approximates a maximum of about 85% when exceeding a sample temperature of -30°C. A possible explanation for the phenomenon of higher OR at higher ice content is the stabilization of air cells due to ice crystals in the matrix. The ice crystals possibly function as physical barriers that prevent bubble coalescence and resulting channel formation in the matrix. However, after shorter freezing times the ice content is low and the OR has a maximum at the point of minimum ice content (PSF) (Figure VII-8). Hence, the ice formation

is not the only stabilizing effect during HPLT treatment and furthermore, seems to have a detrimental effect on the OR development in the first period of freezing under pressure.

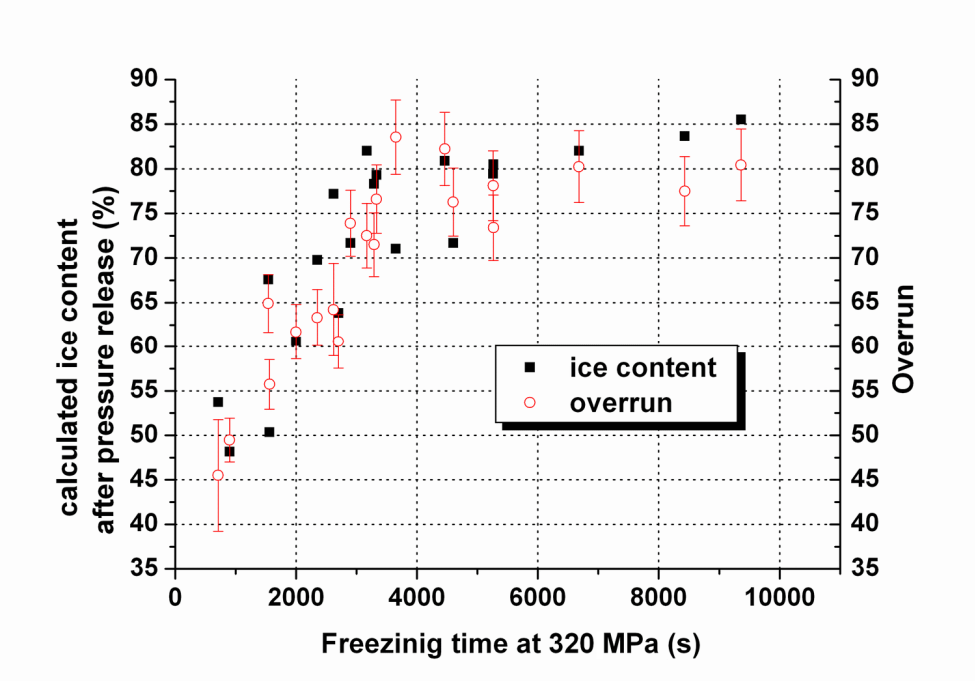

Figure VII-9: Calculated ice content (■) and overrun (○) of PAF treated dairy emulsion (emulsion B) versus the freezing time at 320 MPa.

To visualize the structural changes in the matrix cryo-SEM pictures were taken at the critical points of the HPLT treatment. Figure VII-10 shows the microstructure of the pre-aerated emulsion B after PSF, and PAF treatment with 500, 1250, 2500 and 4000 s freezing time under pressure after 24 h storage at -27°C. The cryo-SEM images show air cells as “holes” in the surrounding matrix, which consists of ice crystals and the high viscous serum phase, including the 3-D protein and fat network. Different from the conventional SEM analysis, the water is not removed from the product before cryo-SEM analysis.

Microstructure

After PSF treatment the partly frozen foam shows a high number of evenly distributed, mostly round air cells. The OR at this stage is about 90 to 95%. A structured alignment of air cells is not recognizable. The structure is similar to the conventionally processed reference foam in Figure VII-4. With increasing freezing time under pressure (PAF 500 s) the homogeneous structure is disrupted and the samples show an inhomogeneous air cell distribution. The OR is reduced to about 70%. Large air cells developed and the surrounding matrix shows broad regions that are free of any air enclosures. The overall structure is highly disordered, air cell expansion is reduced and gas loss promoted.

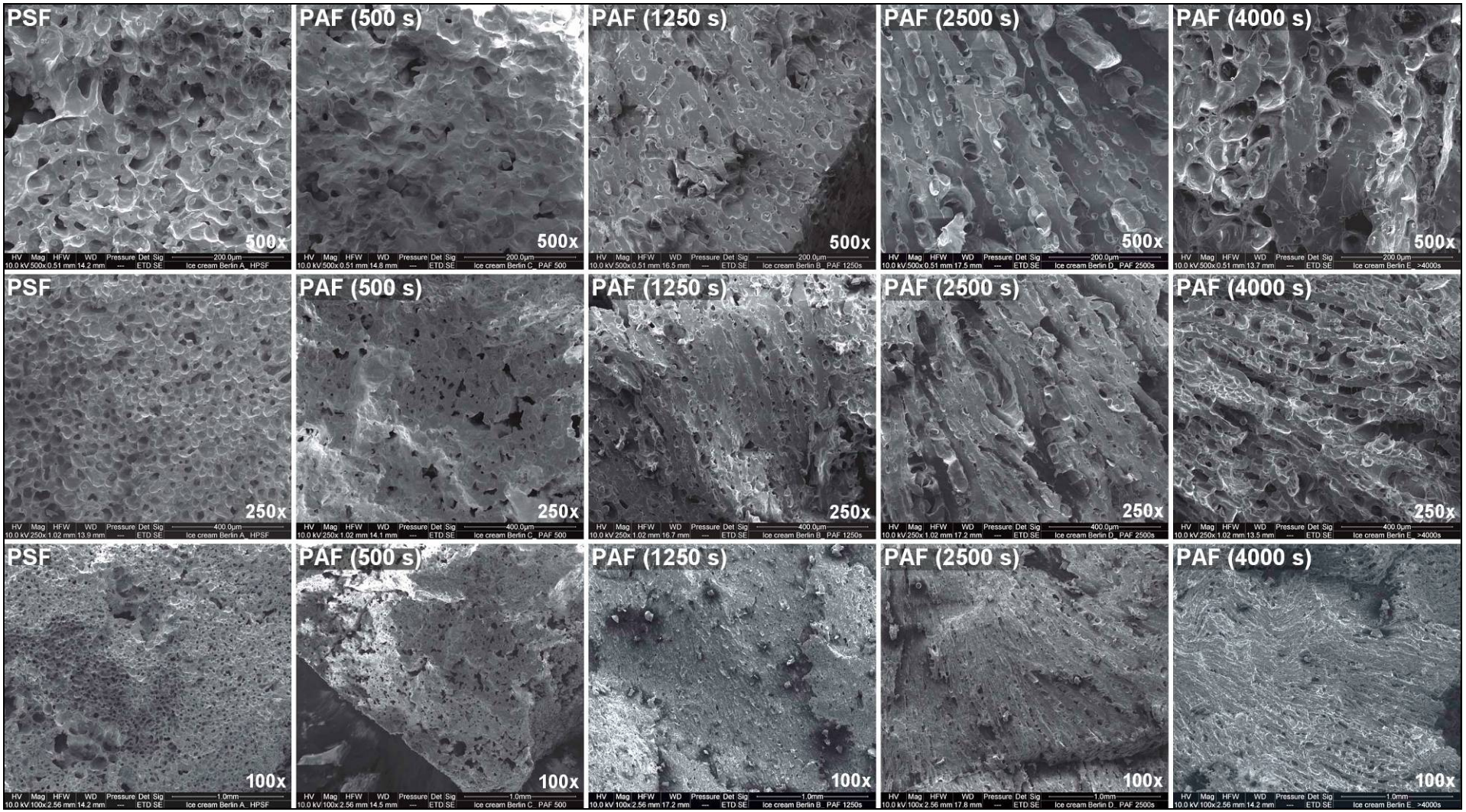

Figure VII-10: Cryo-SEM images of HPLT treated pre-aerated dairy emulsion (emulsion B) after different freezing times under pressure (no ice formation under pressure (PSF), 500 s, 1250 s, 2500 s and 4000 s) at different magnitudes.

After freezing for 1250 s under pressure, the PAF-typical lamella-structure as it was observed in the PAF treated SMP solutions in chapter VI is induced. At this stage, the frozen foam OR is close to the total minimum (about 55%). In contrast to the "PAF 500 s" samples, relatively small air cells are lined up to long channels which are surrounded by thick air free strands. After freezing under pressure for 2500 s the OR is about 70%, which is equivalent to the OR after freezing for 500 s. However, the foam structure has significantly changed. The PAF typical structure developed and the ordered air cell alignment is pronounced further. After 4000 s freezing time, the lamella-structure is maintained but the average air cell size seems increased. The matrix strands in between the air cell channels appear thinner and the air cells within the channels are more closely packed, which is in agreement with the increased OR that reached 80 to 85% in these samples.

Stabilizing mechanisms

The SEM-pictures show a clear structure development that is linked to the OR in the foam after different freezing times under pressure. It is assumed that two mechanisms that are associated with the ice formation under pressure govern the OR development in HPLT treated dairy foams. The structure development indicates that the initial stabilization mechanism that dominates after PSF treatment at low ice contents is impaired by the formation of ice crystals in the matrix during PAF. In turn, the growing ice body provides air cell stabilization when a certain percentage of frozen water in the foam is reached. With respect to the structural integrity of SMP gels after HPLT treatment, the initial stabilizing mechanism is assumed to be protein network based. The occurrence of protein network based and ice crystal based stabilization of air cells over freezing time after HPLT treatment of pre-aerated dairy emulsions is schematically shown in Figure VII-11.

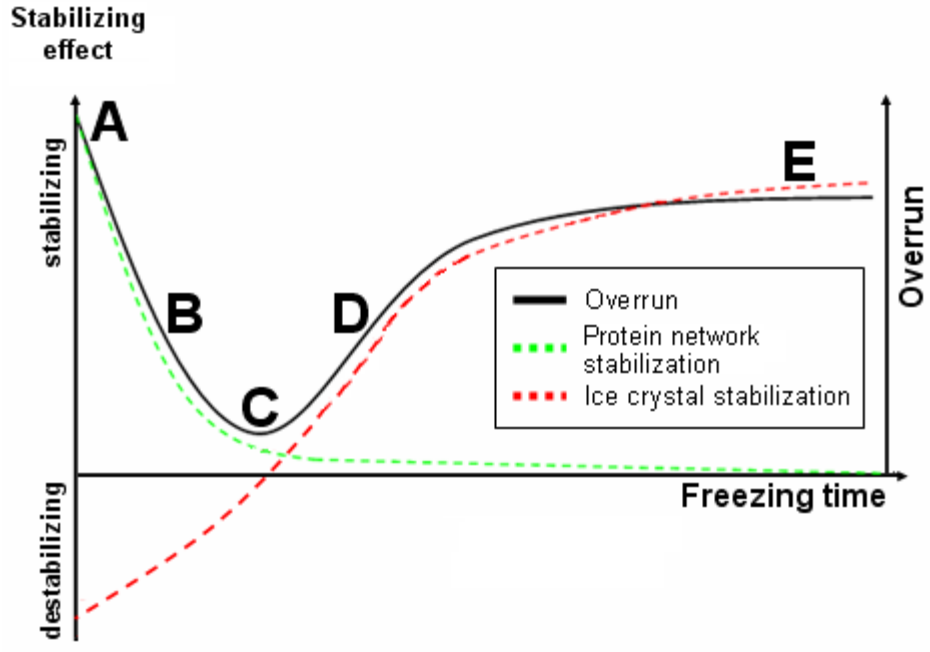

Figure VII-11: Hypothesis of protein network and ice crystal based air cell stabilization during PAF treatment in aerated-dairy emulsions (highly schematic). Maximum OR after PFS (A), decreasing OR after short PAF times (B), minimum OR (C), increasing OR with increasing ice content (D), equilibrated OR after long PAF times (E).

At low ice content after PSF the OR is at its maximum and the samples show a homogenous structure. As shown in chapter VI, the protein network exhibits maximum structural integrity

at this point. The air cells are stabilized by the homogeneous protein network (A). With increasing freezing times and ice content the protein network is gradually disintegrated. Air cell coalescence and channel formation is promoted. The OR is reduced as the protein network breaks up (B). Increasing ice formation causes further disintegration of the protein network and results in an OR minimum. The extent of overall air cell stabilization after pressure release is at its minimum (C). The growing ice crystal network in the matrix does not yet provide sufficient stabilization to compensate the detrimental effect on the protein network. The protein network at this stage shows the widest pore size distribution, which possibly accounts for the high gas loss after expansion. With increasing freezing times the OR increases and the foam progressively assumes an aligned structure, similar to the structure found in PAF treated SMP solutions (D). The ice crystal network develops with increasing freezing times and progressively stabilizes the air cells. After exceeding a certain ice content after pressure release (about 80% in emulsion B), the OR equilibrates (E). Figure VII-12 compares the microstructure of dairy emulsion B and a 25% SMP solution after different PAF freezing times and highlights the structure development in both model systems.

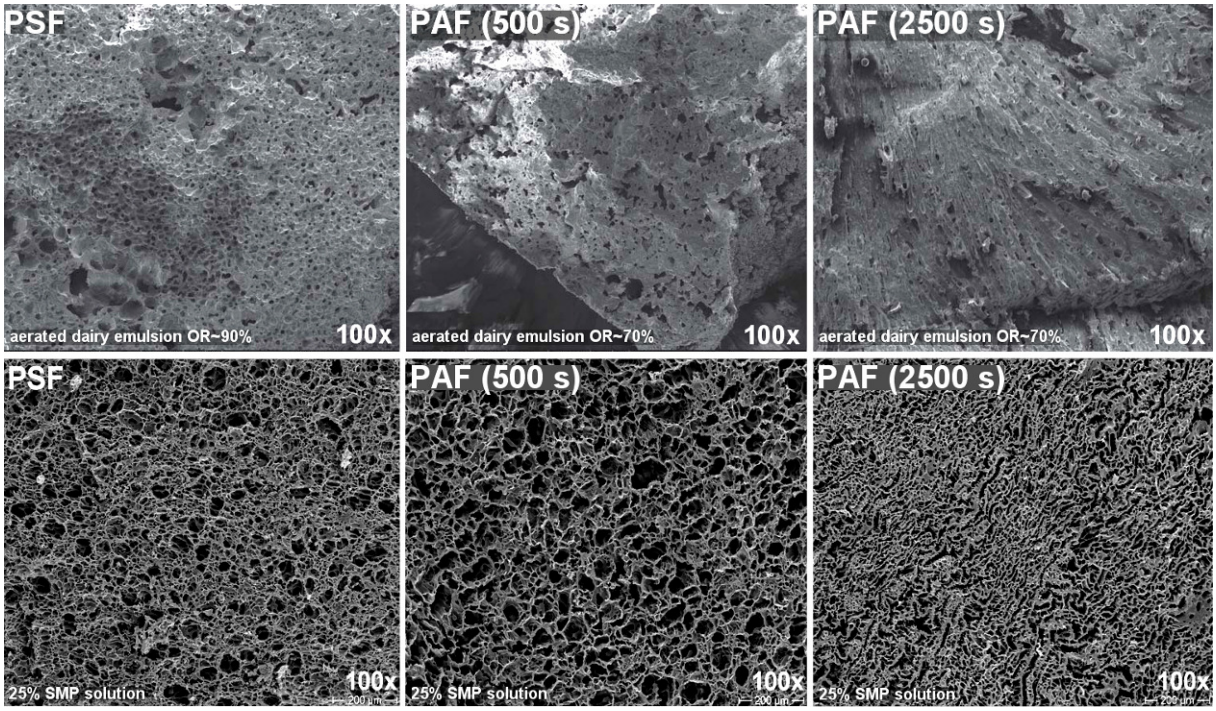

Figure VII-12: Cryo-SEM pictures of dairy emulsion B and SEM pictures of 25% SMP solution after PSF and PAF treatment at 320 MPa.

Both systems show comparable structural changes over freezing time under pressure. The structure and alignment of pores in the SMP gel is similar to the air cell development in the pre-aerated emulsion. The gel formation takes place during pressure release from 320 to 0.1 MPa, whereas considerable air cell development occurs at very low pressures and the air cells grow into the protein network. According to this, the structural integrity of the protein network plays an important role in the air cell stabilization. In this respect, air cell coalescence and channel formation is promoted by a wide pore size distribution.

3.2.4 Impact of the freezing point depression and solid content on the air cell development in pre-aerated emulsions after HPLT treatment

The typical development of the OR over freezing time under pressure, as is was observed after PAF treatment of emulsion B, was not validated after PAF treatment of a low fat and sugar emulsion (emulsion C) with a sugar content of 7% and total solids of 17.3% compared to total sugar content of 19.4% and total solids of 36.8% in emulsion B. The OR of

emulsion C after HPLT treatment at 320 MPa with different freezing times under pressure is shown in Figure VII-13. As after HPLT treatment of emulsion B, the OR maximum occurs at the ice content minimum after PSF treatment of the aerated emulsion. With increasing freezing times the OR is progressively reduced and approaches an equilibrium value of about 35% after 2000 s. It is assumed that the low sugar content (low freezing point depression) and the low total solid content in the emulsion account for the absence of the typical OR increase after reaching the minimum, as it occurs after PAF treatment of emulsion B.

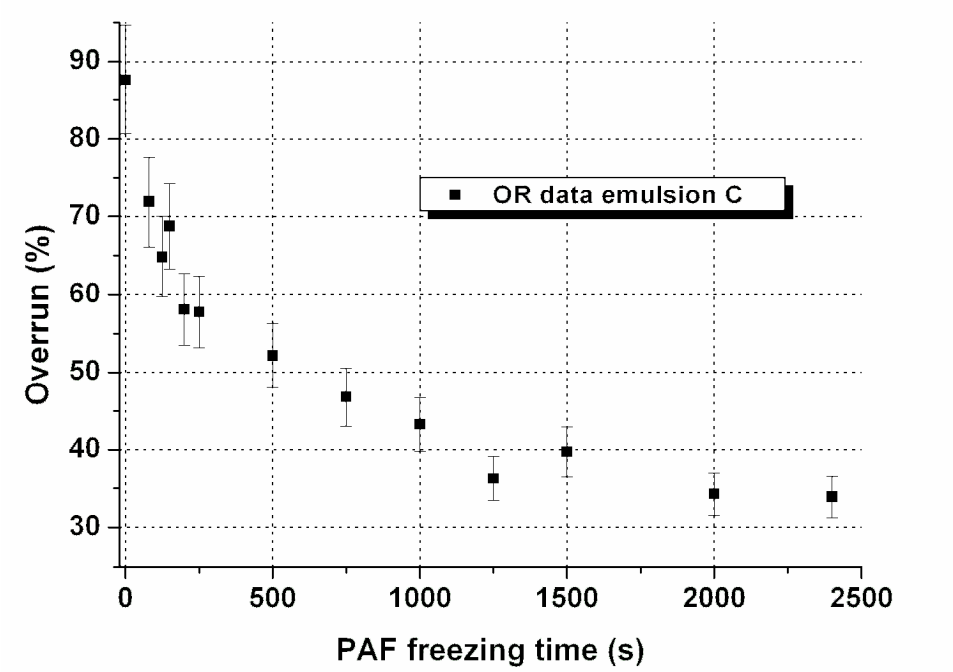

Figure VII-13: Measured overrun (■) in pre-aerated low fat and sugar dairy emulsion (emulsion C) after PAF treatment at 320 MPa after different freezing times under pressure.

The freezing point depression (FPD) describes the phenomenon that occurs when the freezing point of a liquid is lowered by adding another compound to it, such that the solution has a lower freezing point than the pure solvent. The freezing of complex foods occurs over a range of temperature and not at a fixed point as with a pure solvent (Lacey & Payne, 1991). The FPD of a solution is a specific property and is determined by the number of molecules in solution (Wolfe, Bryant & Koster, 2002). Due to increasing ice content and solute concentration in the matrix during freezing, the viscosity and hardness increase over freezing time. The important role of ice crystals in the development of air cells in dairy foams after HPLT treatment has been pointed out in the previous sections. OR measurement after HPLT treatment of pre-aerated emulsions with different sugar and total solid content indicated the importance of the FPD on the expansion of air cells after pressure release. To validate these findings, different model emulsions were PAF treated at 320 MPa with freezing times under pressure from 0 to 2000 s. For the treatment emulsion C was used in the standard formulation, with additional glucose (5, 10 and 15%) and additional glycerol (0.5, 1, 1.5, 2 and 3%). The overrun of the different emulsions after HPLT treatment is shown in Figure VII-14. To produce comparable results, the start OR for all foams was about 160%.

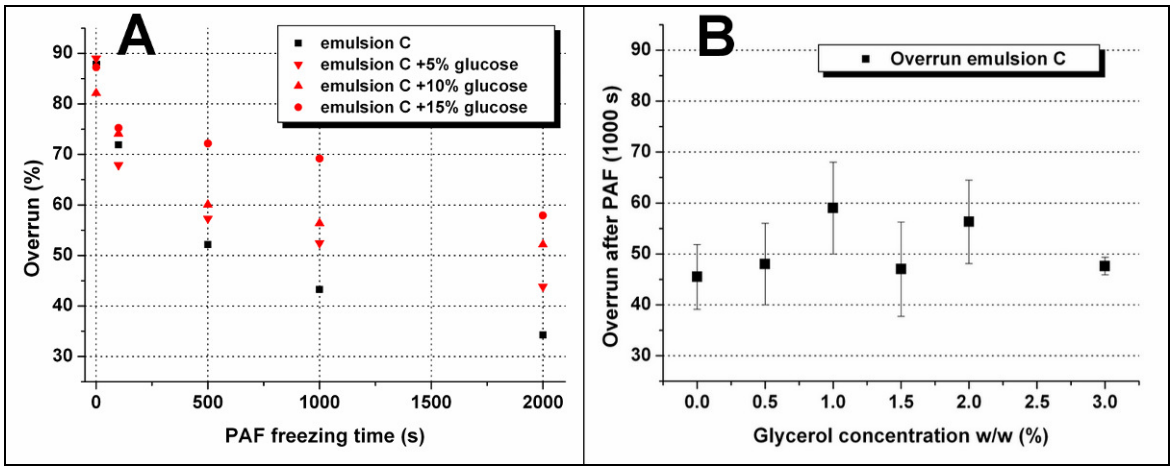

Figure VII-14: A: Overrun as a function of freezing time after PAF treatment at 320 MPa and different freezing times in emulsion C (■) and emulsion C after sucrose addition of 5 (▼), 10 (▲) and 15% (●). Standard deviation for all measurements was no higher than 10% (data not shown in the diagram). B: Overrun as a function of glycerol concentration (■) after PAF treatment at 320 MPa with 1000 s freezing time under pressure.

It shows that sugar addition promotes the OR development after HPLT treatment. No significant increase in the OR after PSF occurs but with increasing freezing times under pressure the OR of the high sugar formulations increases compared to the low sugar emulsions. This effect is marginal after short PAF times (100 s) and increases with increasing freezing times under pressure. After 2000 s freezing under pressure the OR in HPLT treated emulsion C with 15% additional glucose is about 25% higher than in emulsion C without additional glucose. In contrast, the addition of glycerol did not significantly increase the OR after PAF treatment, even though the initial freezing point was decreased.

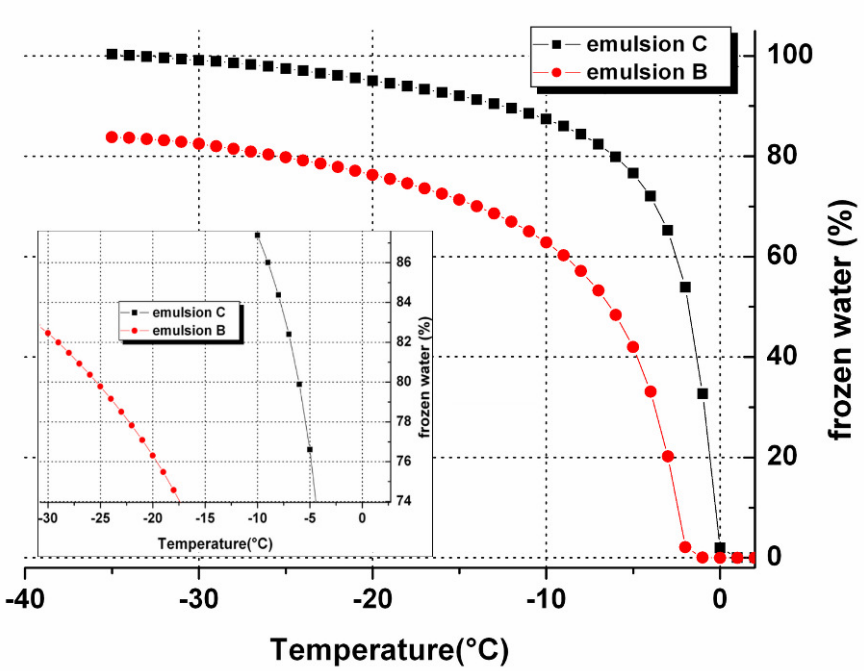

Figure VII-15: Ice content as a function of temperature in emulsion B (●) and emulsion C (■). The sectional enlargement highlights the temperature difference at 80% frozen water.

The results indicate that the FPD alone does not account for improved air cell development after PAF treatment of dairy foams. With the addition of glycerol to emulsion C the freezing

point of the system was lowered but the total dry matter was not affected. In contrast, addition of glucose is directly linked to an increase in dry matter.
The important role of the dry matter content is further supported by the DSC results of emulsion B (36.8% TS) and emulsion C (17.3 TS). Figure VII-15 highlights the different slopes of the ice content vs. temperature of the two emulsions. The ice content increases faster over temperatures in emulsion C as in emulsion B. 80% of the water in emulsion C is frozen 6 K below the initial freezing point, whereas in emulsion B cooling of -23.3 K below the initial freezing point is required to freeze 80% water. In addition to the different slopes, the total amount of water that freezes in the investigated temperature range is different for both emulsions. At -30°C, 82.4% water are frozen in emulsion B. At the same temperature 99.1% water are frozen in emulsion C. The effect becomes especially obvious when taking into account the total solid content of both emulsions. At -30°C emulsion B and emulsion C have a total ice content of 52.1% and 81.8% respectively. Concluding, the OR development is promoted by the FPD of the system but it is the dry matter content that governs the ice content over temperature, hence, determines the matrix hardness, which is the key parameter in the expansion of air cells after pressure release.

4 Conclusion

Air as the major component in dairy foams undergoes drastic physical changes during HPLT treatment. During pressure build up the air is compressed and enters the supercritical state. Upon pressure release the supercritical air expands and re-enters the gaseous state. HPLT induced aeration of a dairy emulsion under pressure by exploiting the high solubility of gases under pressure was investigated. After pressure shift freezing of an initially liquid dairy emulsion at 320 MPa in the presence of a non-dispersed air phase no detectable overrun was produced. In contrast, in pre-aerated emulsions, 40 to 90 % of the initial liquid foam overrun was maintained after PSF and PAF treatment. The shrinkage after HPLT treatment was found to be linked to the initial liquid foam overrun and the applied treatment. Shrinkage was low at low initial foam overrun and highest shrinkage occurred after PSF treatment of high overrun dairy emulsions. When exceeding liquid foam overrun of 120%, the shrinkage was constant at about 45% after PAF treatment, whereas the shrinkage after PSF treatment progressively increased with increasing start overrun.
The overrun in pre-aerated HPLT processed frozen dairy emulsions is a dynamic parameter that develops as a function of different external and internal factors. Once a dispersed air phase is created in the foaming step, the air phase undergoes significant changes. To what extent the air volume fraction is altered depends on factors that can be characterized as internal parameters, which are linked to the properties of the aerated product (e.g. fat content, protein content and composition, bubble size and distribution and solid content) and external parameters, which relate to the manufacturing process and subsequent storage conditions (e.g. process pressure and temperature, storage time and temperature). External parameters always affect the properties of the product as they directly affect the properties and interactions of single ingredients, especially in complex food systems. Hence, a clearly separated investigation with respect to cause and effect of internal and external parameters is only possible on a limited scale.
The obtained results imply that in addition to the stabilizing effects that are induced during aeration, the air volume fraction in HPLT treated dairy foams is stabilized by two process-induced mechanisms: protein network formation and ice crystal growth. During the HPLT treatment the air volume fraction of the liquid foam is compressed and the initial foam structure disintegrates until the pressure is released. No significant gas loss occurs in the pressurized foam. Upon pressure release casein micelles and whey proteins associate and form a gel network, which serves as a stabilizing barrier to air bubbles that reform throughout

the matrix at relatively low pressure. The protein network prevents air cell coalescence and channel formation to some extent. It was shown that gas loss and air cell expansion begin with the reformation of air cells after pressure release. The protein network structure is affected by the formation of ice crystals that grow under pressure (PAF) and during pressure release (PSF). The ice crystals cause destabilization of the foam and promote gas loss after treatment until a certain amount of ice has formed. Beyond this point, the ice crystals limit gas loss and provide air cell stabilization. The ice crystal based stabilization possibly originates from a direct stabilization by means of an ice crystal network that functions as a physical barrier to air cell coalescence and channel formation. Furthermore, it was shown that a hardening of the protein network occurs at high ice contents. The latter mechanism is supported by the freeze concentration that occurs during freezing under pressure. HPLT treatments that involve the formation of high amounts of ice under pressure (long PAF) induce solidification in SMP solutions that do not form a gel after PSF, when the amount of ice in the product is low after pressure release.
However, the ice formation does not necessarily promote overrun development and inhibits air cell development when the total ice content in the matrix is too high. In this respect the matrix hardness and viscosity are supposed to be the key parameters in the air cell development, as not only the freezing point depression but also the dry matter content of the emulsions affect the final overrun. Aerated dairy emulsions showed increased air cell expansion after HPLT treatment at higher total solid contents and high dry matter contents caused a slow increase of the ice content with decreasing temperatures.

5 References

[1]Agassi, J. (1977). Who discovered Boyle's law? *Studies In History and Philosophy of Science Part A*, *8*(3), 189-250.

[2]Cazenave Gassiot, A. (2007). *Prediction of Retention for Pharmaceutical Molecules in Supercritical Fluid Chromatography. The Synthesis of a Library of Sulfonamides.* Ph.D., University of Southampton.

[3]Chester, T. L. & Haynes, B. S. (1997). Estimation of pressure-temperature critical loci of CO2 binary mixtures with methyl-tert-butyl ether, ethyl acetate, methyl-ethyl ketone, dioxane and decane. *The Journal of Supercritical Fluids*, *11*(1-2), 15-20.

[4]Künzel, D. (2009). *Veränderung strukturbildender Eigenschaften von Casein und beta-Lactoglobulin in Abhängigkeit verschiedener Prozess- und Produktparameter während der Hochdruck-Niedertemperatur Behandlung*. master thesis thesis, Berlin, Technische Universität Berlin, 110.

[5]Lacey, R. E. & Payne, F. A. (1991). A Model to Estimate Thermodynamic Properties of Biological-Materials During Freezing. *Transactions of the Asae*, *34*(4), 1836-1842.

[6]Lemmon, E. W., Jacobsen, R. T. & Penoncello, S. G. (2000). Thermodynamic Properties of Air and Mixtures of Nitrogen, Argon, and Oxygen From 60 to 2000 K at Pressures to 2000 MPa. *Journal of Physical and Chemical Reference Data*, *29*, 331-385.

[7]Marshall, R. T., Goff, H. D. & Hartel, R. W. (2003). *Ice Cream*. Kluwer Academic / Plenum Publishers, New York.

[8]Muse, M. R. & Hartel, R. W. (2004). Ice Cream Structural Elements that Affect Melting Rate and Hardness. *Journal of Dairy Science*, *87*, 1-10.

[9]Otero, L. & Sanz, P. D. (2000). High-Pressure Shift Freezing. Part 1. Amount of Ice Instantaneously Formed in the Process. *Biotechnology Progress*, *16*, 1030-1036.

[10]Wolfe, J., Bryant, G. & Koster, K. L. (2002). What is 'unfreezable water', how unfreezable is it and how much is there? *Cryoletters*, *23*(3), 157-166.

Chapter VIII Texture and rheology properties of HPLT treated dairy based foams

1 Introduction

In the food industry the word 'quality' has a variety of meanings. At the very simplest level 'quality' may stand for basic consumer acceptance (Moskowitz, 1995; Aguilera & Stanley, 1999). However, there may be different expectations about the food, such as nutritional value, storage stability or microbial safety but certainly the impressions involved in consuming the product are among the most relevant. On a scientific level, these impressions are described by the sensory properties of a product (van Vliet, 2002). The sensory properties are the characteristics of foods perceived by the senses of sight, smell, taste, touch and hearing, such as flavour, texture and appearance (Clarke, 2004). However, sensory assessment of food quality is time consuming and expensive and the results are dependent on the observers' preferences unless highly trained people are used (Rhodes, Jones, Chrystall & Harries, 1972; Granitto, Biasioli, Endrizzi & Gasperi, 2008). Frozen dairy foams have many attributes that contribute to the overall sensorial appearance. With respect to HPLT treatment and characteristic effects on food structure that are associated with this technology, such as protein denaturation and the formation of small ice crystals, textural properties of pre-aerated frozen dairy emulsions after HPLT treatment are the focus of this chapter. The closeness of structure-texture relationship is indicated by the following definition:

> "Texture is the sensory and functional manifestation of the structural and mechanical properties of foods, detected through the senses of vision, hearing touch and kinesthetics (Szczesniak, 1998)."

In this study, the results of subjective texture assessment were compared with instrumental measurements but the present work does not claim a precise quantification of the induced changes in texture. It rather aims for revealing the basic phenomenon of textural changes after HPLT treatment on a qualitative level.

One important consumer attribute of frozen food foams is the creaminess (Richardson-Harman, Stevens, Walker, Gamble, Miller, Wong et al., 2000; de Wijk, Terpstra, Janssen & Prinz, 2006), which is not a primary attribute in technical tasting but a characteristic which originates among others from a combination of the attributes smoothness and mouth coating or thickness (van Vliet, 2002). The latter attributes were of central concern as they were found to be most influenced in dairy foams after HPLT treatment in preliminary tests. Another central texture attribute of frozen dairy foams is the chewiness, which is affected by the amount of stabilizers in conventionally processed frozen food foams and relates to the primary attributes hardness and elasticity (Bourne, 2002; Clarke, 2004). The chewiness of different pre-aerated dairy emulsions was evaluated after HPLT treatment by technical tasting and compared with results obtained by Texture Profile Analyses (TPA). Furthermore the melting behaviour of HPLT treated pre-aerated dairy emulsions was investigated, particularly with regard to low fat formulations.

In previous chapters the gel formation in milk protein model systems after HPLT and HP treatment was investigated. However, it stays unexplained if the molecular changes that are induced in the protein systems during HPLT treatment can be transferred to conventionally processed product that contains pre-treated protein.

It is economically advantageous if a process involves only the ingredients that are positively affected by process, rather that applying the treatment to the whole product. Moreover, a pre-treatment of a single ingredient potentially results in a tailor made ingredient, which can be

introduced to a variety of other products that benefit from the unique and new properties. To evaluate the effect of HPLT pre-treated milk proteins on the textural properties of frozen dairy foam, SMP solutions were HPLT treated and used as an ingredient for the dairy emulsion in the conventional freezing process.

2 Materials and Methods

2.1 HPLT setup

All samples were treated at 320 MPa with the pilot scale HPLT unit, as described in chapter III. Pressure assisted freezing (PAF), pressure shift freezing (PSF) and pressure induced crystallization (PIC) treatments were performed. The process times were adjusted according to the respective process.

2.2 Model recipes and dairy emulsion preparation

The complete list of all emulsion formulations that were used in this study is attached in the appendix. An overview about the main characteristics of the formulations that are relevant for the present chapter is given in Table VII-1.

Table VIII-1: Labeling and basic characteristic parameters of investigated dairy based model emulsions

Labeling	Total solids [%]	Fat content [1] [%]	SMP/WP content [2] [%]	Sugar content [3] [%]
emulsion A	38.7	8.8	2.1 / 9.4	17.9
emulsion B	36.8	7	4.9 / 4.8	19.4
emulsion C	17.3	2.4	7.7 / 0	7.0
emulsion D	16.5	0.38	7.7 / 0	8.2
emulsion E	17.5	2.3	0 / 0	12.8
emulsion F	36.9	7.0	0 / 9.7	19.4
emulsion G	32.5	6.0	8 / 0	18.0

[1] additional fat (milkfat or vegetable oil); [2] skim milk powder and whey powder formulation attached in the appendix; [3] additional sucrose and/or sugar corn syrup

All ingredients were pre-mixed for 20 min at 65°C followed by a 2 stage homogenization (40 bar / 150 bar) at 72°C. The homogenized emulsions were pasteurized for 30 s at 85°C and than cooled down in a plate heat exchanger to 5°C. After aging for 24h at 5°C the emulsions were frozen in 2.5 liter lots to -30°C.

2.3 Conventional freezing

To produce conventionally frozen foam reference products, the model emulsions were frozen in a continuous ice cream freezer (Hoyer KF-80, Tetra Pak Hoyer, Hoejbjerg, Denmark). The OR of the reference foams was typically between 90 and 120%. An exemplary process sheet of the treatment is attached in the appendix. The OR of the reference foams was typically between 90 and 100%.

2.3.1 Skim milk pre-treatment

To investigate the impact of HPLT pre-treated SMP solutions as ingredient for the conventional freezing process, 20% SMP solutions were PSF treated for 30 min at -20°C and 320 MPa. The treated emulsions were stored at -27°C before addition to the emulsion.

2.4 Analyses

2.4.1 Technical Tasting

The effect of HPLT treatment on the textural attributes smoothness, creaminess mouth coating and chewiness of pre-aerated dairy foams was evaluated.

Discriminative test

A discriminative test was applied to evaluate the impact of HPLT treatments on the smoothness, creaminess, mouth coating and chewiness of pre-aerated dairy emulsions. In this study the attribute smoothness was defined as the absence of particles (i.e. ice crystals) and the mouth coating as the amount and persistence of the film that coats mouth and palate after swallowing. Chewiness was defined by the resistance of the product to bite with the molars and the effort required preparing the sample for swallowing. Creaminess as a very complex attribute was defined according to de Wijk et al. as a range of sensations typically associated with fat content, such as full sweet taste, compact, smooth, not rough and dry with a velvety coating (de Wijk et al., 2006).

For the analyses a consumer panel of 13 persons was briefed by a trained person in the assessment of the three attributes in frozen food foam systems. Focus of the tasting was the differentiation of the attribute characteristics in: higher, equal and lower compared to the reference. The actual rating scale ranged from much less to much more, as shown in Figure VIII-1.

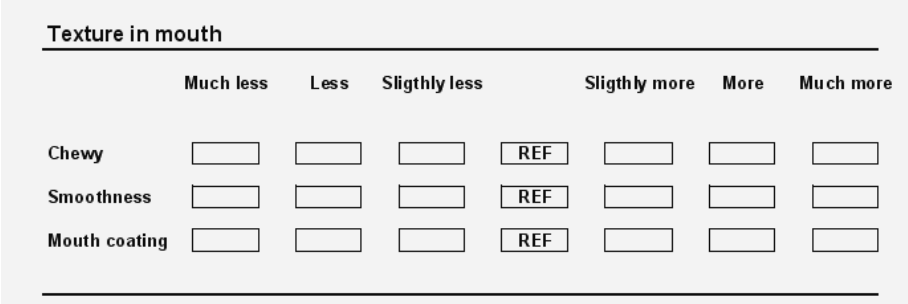

Figure VIII-1: Evaluation sheet for the discriminative consumer test .

Each panellist independently rated the treated samples according to the latter procedure. All samples were taken for technical tasting at -18°C.

2.4.2 Texture Analysis

Texture Profile Analysis (TPA) was performed to obtain instrumental data for the chewiness of the treated products. For the texture analyses a texture analyser (TA) TA-XT2 (Stable Micro Systems Ltd., Surrey, UK) with the analysing software Texture Expert (Stable Micro Systems Ltd., Surrey, UK) was used. The texture analyser was located in a cooling chamber at -18°C for time of analyses.

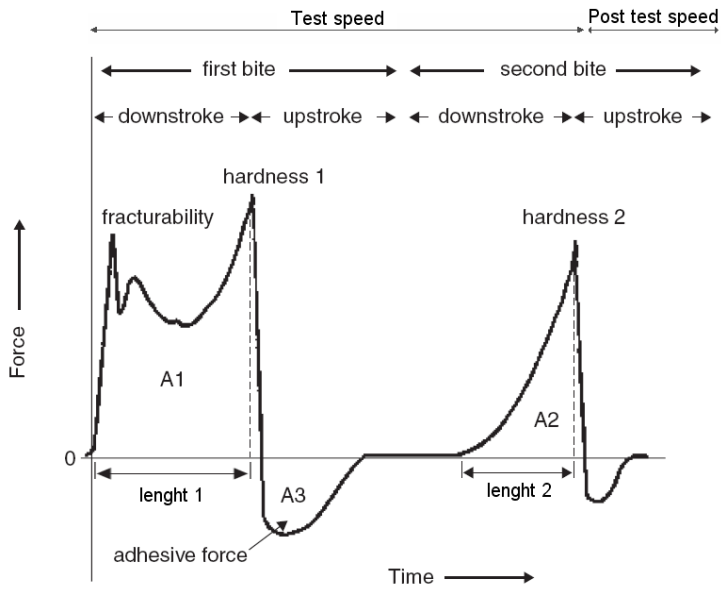

Figure VIII-2: Generalized texture profile analysis curve. Redrawn from (Pons & Fiszman, 1996).

Frozen cylindrical samples were prepared with a diameter of 0.8 cm and a length at 1.5 cm. The TPA analyses compression tests were performed with a pre-cooled cylindrical probe (d= 30 mm) and the following setup:

pre-test speed:	2.0 mm/s
test speed:	1.0 mm/s
post-test speed:	5.0 mm/s
test distance:	10 mm
trigger type:	manually
wait:	5 sec

Chewiness was calculated as:

$$Chewiness = \left(\frac{A2}{A1} \cdot hardness1\right) \cdot \left(\frac{lenght1}{lenght2}\right) \quad \textbf{(VIII-1)}$$

All values were obtained by the Texture Expert analysing software and displayed according to Figure VIII-2.

2.4.3 Drip Test

The aim of the comparative drip test is to evaluate the structural stability of frozen foams at room temperature. For the analyses a sample is placed on a drip test device (wire mesh support) with 3 mm mesh size and 0.9 mm mesh thickness. The measurement was performed at 20°C, starting with a sample temperature of -27°C. Cylindrical samples of about 4 cm diameter and 2 cm height were placed on the drip test device. The amount of liquid that drips during the melting of the product was monitored by weighing at regular time intervals. The evolution of the product appearance was evaluated visually. The drip loss is expressed in % w/w and was calculated according to:

$$DripLoss = \frac{m_2}{m_1} \cdot 100\% \quad \textbf{(VIII-2)}$$

With m_1 the mass of the frozen foam before the test and m_2 the mass of the dripped product at a given time in grams.

2.4.4 Ice crystal size and distribution

The ice crystal size and distribution was determined by direct optical microscopy and digital image analysis. A full description of the applied method is given in chapter VI.

2.4.5 Air cell size and distribution

The method, like the one for ice crystal size, is a destructive method where the air bubbles are dispersed, in this case in a glycerol-acetic acid solution. The frozen foam is sliced from a central part of the sample in a freezer at a temperature of about -20 °C. Cubes (1 cm^3) were prepared with a razor blade and cut in 1 mm thick slices. The samples were dispersed at room temperature with a mixture of glycerol and acetic acid. Two aliquots of the dispersion were spread on a microscopic slide with a ring and investigated under the microscope (CX 41 Olympus). Images of the dispersions are captured with a video camera (JVC TK-C1381). The quantitative analysis is carried out automatically. For each sample 10 images were analyzed (min. 2000 bubbles per batch).

2.4.6 Rheology

Oscillation rheology measurement

For the determination of the storage and loss moduli and the complex viscosity a rheometer Physica MCR 300 (Physica Messtechnik GmbH, Ostfildern, Germany) was used. Temperature sweep (-10 to 10°C at 1 Hz) and frequency sweep (0.03 to 1 Hz) were performed. The samples were cut in cylinders of 25 mm diameter and about 5 mm thickness and tested at a starting temperature of -10°C. The method was adapted from Wildmoser (Wildmoser, 2004). The frequency sweep was performed right after the temperature sweep with the same sample.

Brookfield viscosity

Brookfield viscosity of the emulsion before freezing was measured with a Brookfield Viscometer. The samples were tested directly after the emulsion preparation at about 5°C with 30 rpm rotation speed.

Quenelle weight

The quenelle describes the pieces of frozen foam that tears off the continuously extruded frozen foam at the freezer exit. The determination of the quenelle weight is a correlated measurement that gives indirect information about the elongation at yield stress and linked to it the cohesion of the product.

3 Results and discussion

3.1 Structural properties of pre-aerated low fat and sugar diary emulsions after HPLT treatment

3.1.1 Ice crystal size and distribution

Several studies have described the formation of small ice crystals in aqueous products after pressure shift freezing (Lévy, Dumay, Kolodziejczyk & Cheftel, 1999; Chevalier, Le Bail & Ghoul, 2000; Fernández, Otero, Guignon & Sanz, 2006).

Microscopic ice crystal size analyses of aerated dairy emulsions were performed after PSF and PAF treatment of pre-aerated dairy emulsions and PIC treatment of a conventionally frozen sample. The treatment pressure for all experiments was 320 MPa. The PAF treatments involved crystal growth under pressure for 2000 s. The pressure release rate for all HPLT

experiments was 200 MPa/s. HPLT treated samples were compared with a conventionally frozen reference (Figure VIII-3).
A significant lower ice crystal diameter was found after PSF and PIC treatment. The average ice crystal diameter after PAF treatment was reduced in emulsion G, whereas the ice crystal size was not significantly changed in emulsion B. The results are in good agreement with the before mentioned literature data. The formation of small ice crystals during HPLT treatment is linked to the high freezing rates after expansion and the homogeneous nucleation during fast pressure release. In the PAF treatments that involve long freezing times under pressure, the PSF effect is low, as the amount of liquid water during expansion is reduced by the formation of ice under pressure. The ice crystals that develop under pressure grow during static freezing after heterogeneous nucleation and their size and shape is governed by the p,T conditions before pressure release. The impact of the recrystallization during PIC treatment can not be conclusively evaluated on the base of the present results, as the pressure was released immediately after reaching the maximum treatment pressure of 320 MPa. During pressure build up the ice phase undergoes partial melting and the amount of liquid water before pressure release is increased. Presumably the reduced ice crystal size after PIC treatment results from the PSF effect that occurs in the liquid phase during expansion. However, it can not be ruled out, that the solid-solid phase changes during pressure build up and pressure release has an impact on the ice crystal size as well. Figure VIII-4 displays the ice crystal size distribution after conventional processing and after PSF treatment and confirms the formation of small ice crystals during PSF treatment.

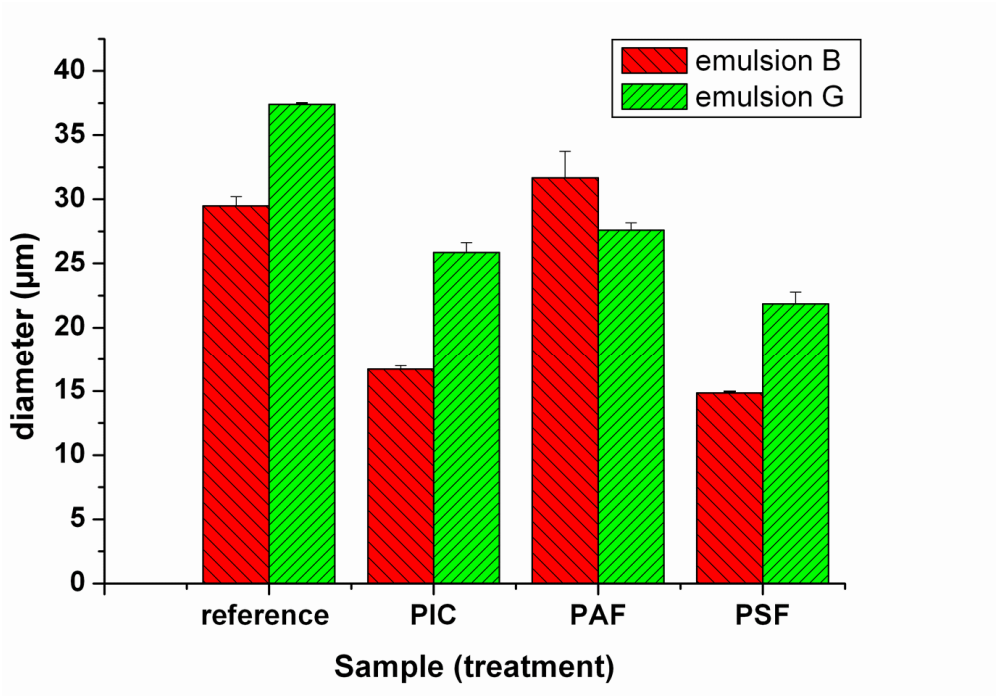

Figure VIII-3: Average ice crystal diameter in aerated dairy emulsions after freezing in a continuous freezer (reference) and after HPLT treatment (PIC, PAF and PSF).

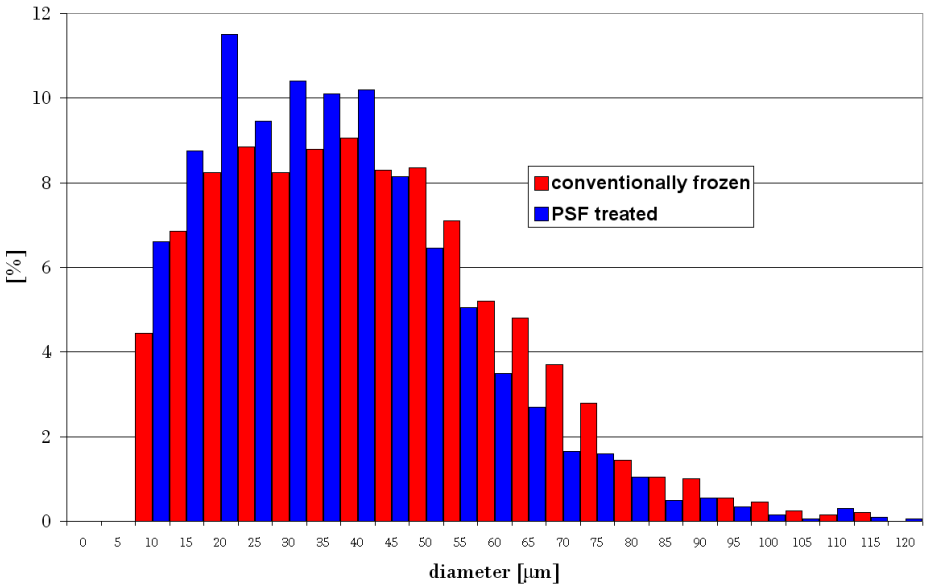

Figure VIII-4: Ice crystal size distribution in frozen foam (emulsion A) after conventional processing and PSF treatment at 320 MPa with 200 MPa/s pressure release rate.

3.1.2 Air cell size

The air cell size in frozen food foams has a significant impact on the sensorial properties of the product (Marshall, Goff & Hartel, 2003; Clarke, 2004). To evaluate the impact PAF treatment on the average air cell size, conventionally frozen emulsion D and PAF treated emulsion D were analyzed by direct optical microscopy. The obtained data for the average air cell size after both treatments is shown in Table VIII-2.

Table VIII-2: Average air cell diameter in emulsion D after conventional freezing and after PAF treatment at 320 MPa with 2000 s freezing after pressure

	Average air cell diameter* [µm]
Conventionally frozen	24.8 ± 6.9
PAF treated	42.4 ± 7.9

*average diameter at 50% cumulated volume

In the investigated emulsion, the average air cell diameter increased significantly after PAF treatment. This trend was confirmed after PAF treatment of other pre-aerated dairy emulsions (data not shown). The mechanism behind the air cell formation during pressure release after HPLT treatment is still unclear and investigations that involve different HPLT treatments (i.e. PSF) remain to be done. For a profound understanding of impact of HPLT treatment on the air cell size and distribution in pre-aerated dairy emulsions more detailed investigations are needed.

3.1.3 Rheology

The rheology of food systems is a highly complex field and accurate measurement of the rheological properties of a multiphase physicochemical system, such as aerated frozen dairy foam, is not an easy task (Wildmoser, 2004). With respect to the results obtained by HPLT treatment of milk protein model systems (chapter VI), the protein related changes in the dairy foam were of special interest in the present chapter. To evaluate whether significant rheological differences are induced by HPLT treatment (i.e. gel formation), the storage modulus (G´), the loss modulus (G´´) and the complex viscosity (η*) of conventionally frozen reference samples and pre-aerated HPLT treated dairy emulsions were compared.

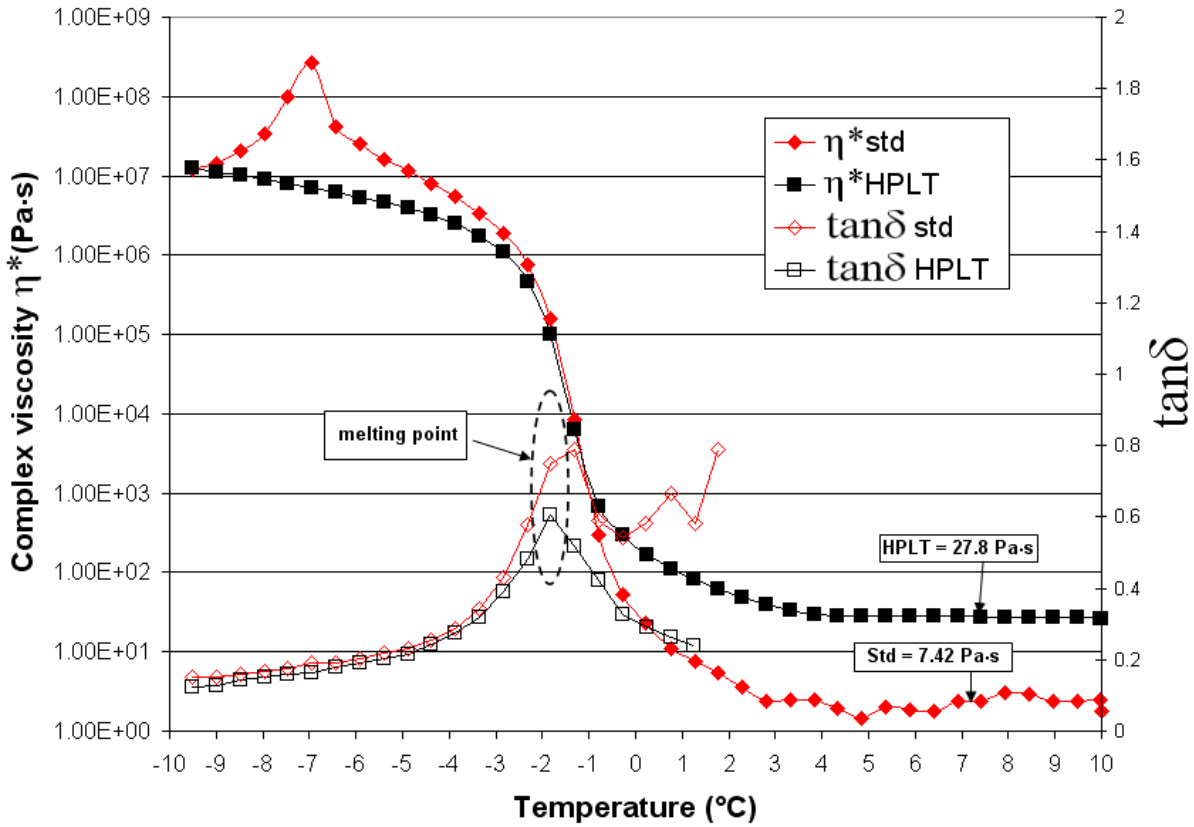

Figure VIII-5: Oscillation thermo rheometry (temperature sweep) of emulsion B. Complex viscosity (solid symbols) after conventional freezing (η *std) and PAF treatment (η *HPLT) and the corresponding values for tanδ (blank symbols).

Figure VIII-5 shows the complex viscosity and the tanδ as a function of temperature in a temperature sweep of emulsion B after conventional freezing and PAF treatment at 320 MPa and 2000 s freezing time under pressure. The complex viscosity of the HPLT treated emulsion remains higher after melting compared to the conventionally frozen reference. This is in good agreement with the gel structure formation in protein model systems after HPLT treatment. The high complex viscosity at temperatures above the freezing point indicates that the structural changes are not linked to the presence of ice crystals, even though the ice formation is involved in the structure formation.
The tanδ values of the HPLT treated foams support the hypothesis of HPLT induced structure formation in pre-aerated dairy emulsions. Values for tanδ are calculated from the storage and loss modulus as follows (Mezger, 2006):

$$\tan\delta = \frac{G''}{G'} \qquad \textbf{(VIII-3)}$$

Above the freezing point of -2°C, the small values for tanδ in the HPLT treated samples indicate the solidification of the sample. The products show solid-like characteristics after melting. The liquid solid transition is characterized by tanδ values as follows (Mezger, 2006):

Liquid state:	tanδ > 1 (G´ < G´´)
Solid state:	tanδ < 1 (G´ > G´´)
Sol-gel transition	tanδ = 1 (G´ = G´´)

In the frequency sweep (Figure VIII-6), the HPLT treated samples show a tanδ much lower than the conventionally frozen samples. G' is higher than G", which indicates solid character and the gel formation in the HPLT treated samples.

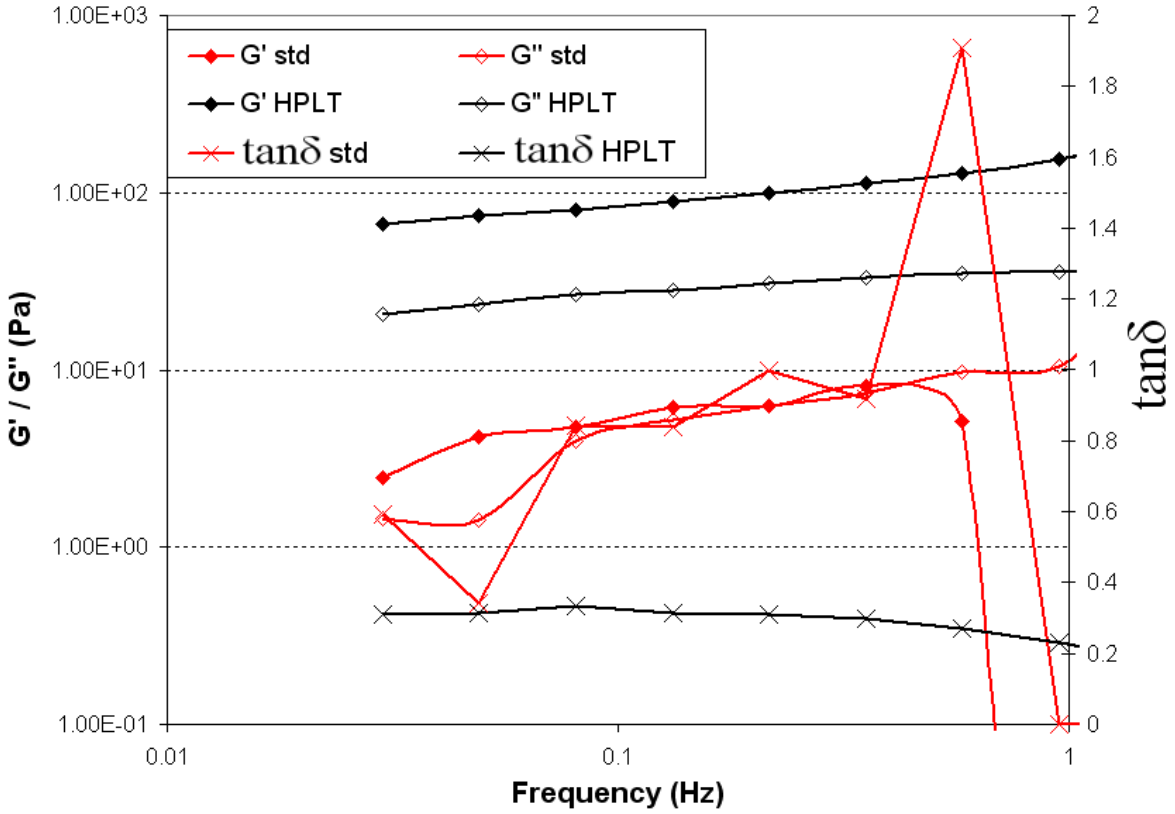

Figure VIII-6: Oscillation rheometry (frequency sweep) of emulsion B. Storage modulus G´ (solid symbols) and loss modulus G´´ (blank symbols after conventional freezing (G´std and G´´std) and PAF treatment (G´HPLT and G´´HPLT)) and the corresponding values for tanδ (✕).

3.2 Subjective texture after HPLT treatment

Particularly useful to the investigator dealing with complex foods are direct difference tests, because they can provide a quick decision about whether or not a sensory difference of any kind has resulted from some treatment or change in production (Harries, 1973). To evaluate the effect of HPLT treatment on the smoothness, creaminess, chewiness and mouth coating, technical tasting of HPLT treated pre-aerated emulsions and conventionally frozen foams was performed by a consumer panel of 13 panelists.

3.2.1 Smoothness and creaminess

Independent from the process setup, the smoothness and creaminess of HPLT treated pre-aerated dairy emulsions was rated higher by all panelists compared to the smoothness and creaminess of conventionally frozen emulsions with comparable or higher overrun. Smoothness is defined by the absence of particles in the product during compression and melting between tongue and palate in the mouth. Typically, a non-smooth (sandy) texture is caused by large ice crystals or lactose crystals in frozen food foams. However, lactose related sandiness in frozen dairy foams does not occur at storage temperatures below -15°C (Marshall et al., 2003). Hence, the absence of detectable ice crystals in pre-aerated HPLT treated dairy emulsions most probably accounts for the high smoothness. This assumption is supported by the results of the ice crystal size and distribution analyses of HPLT treated emulsion and the conventionally processed references, which showed significantly reduced average ice crystal diameter after PSF treatment and a clear trend to smaller ice crystals after PAF treatment.

Creaminess is an important determinant of the perceived quality of foods and is, therefore, of great interest for the food industry (de Wijk et al., 2006). Creaminess is of high importance to the consumer, especially in dairy products. In a study of ice creams, the least liked sample was also the sample perceived to be the most different from consumers ideal level of creaminess (Lähteenmäki & Tuorila, 1994). Although creaminess may be a familiar term to consumers, its bases are complex, involving multiple texture and favour components (Richardson-Harman et al., 2000). The creaminess of o/w emulsions was found to be linked to the fat content and the viscosity of the emulsions (Akhtar, Stenzel, Murray & Dickinson, 2005). Untrained consumers think of creaminess as a multimodal percept, which combines texture and taste sensations (van Vliet, 2002). However, the sensation of creaminess does not change much with training. Highly trained panelists and naive consumers agreed on the foods that were creamy and those were not (van Vliet, 2002), which supports the reproducibility of the present results.
13 panelsits performed a discriminative test, comparing conventionally frozen and HPLT treated emulsions. Creaminess was tested for a rich emulsion (emulsion B) and a low fat and sugar emulsion (emulsion G). The HPLT treated samples were PSF and PAF treated at 320 MPa. The PAF freezing time was 2000 s and for both treatments the pressure release rate was 200 MPa/s. The samples were tested after 24 hAll panelists rated the creaminess of HPLT treated pre-aerated dairy emulsions superior to the creaminess in conventionally processed products. Since creaminess is a rather complex attribute, a clear link to the structural properties of the frozen foams is difficult. Most probable cause for the high perception of creaminess in HPLT treated products seems the structural changes in the matrix that are related to the protein denaturation and gel formation. Many liquid products, e.g. water or lemonade, are commonly associated with low creaminess (de Wijk et al., 2006). In this respect, aggregation of proteins in the dairy emulsion during HPLT treatment or moreover, a partial solidification of the matrix, is expected to account for the increased creaminess.

3.2.2 Chewiness and mouth coating

In the sensory assessment of frozen dairy foams the mouth coating is a measure of how the melting product coats the inside of the mouth on or right after swallowing (Clarke, 2004). Chewiness is defined by the effort needed to masticate the sample to a consistency suitable for swallowing (Pons & Fiszman, 1996). Thus, both attributes contribute to a rich texture and mouthfeel of frozen food foams. Typically, low fat products suffer from a low chewiness and poor mouth coating (Schaller-Povolny & Smith, 1999).
The chewiness and mouth coating of a low fat and sugar emulsion (emulsion G) were tested after conventional processing in a continuous freezer and after PAF and PSF treatment at 320 MPa. In a first test the conventionally frozen foam served as the reference and was compared with the PSF and PAF treated pre-aerated emulsions, respectively. The results of this test are shown in Figure VIII-7. Figure VIII-8 shows the results of a second test that compared the PAF treatment with the PSF treatment, whereas the PSF treated sample served as the reverence. Compared to the conventionally frozen reference, both HPLT treated foams showed a higher chewiness and mouth coating in technical tasting. Comparing the two differently treated HPLT samples it shows that mouth coating and chewiness are higher after PAF treatment. As for the creaminess, the HPLT induced changes in the protein fraction of the pre-aerated dairy emulsion is assumed to account for the changes in chewiness and mouth coating. For the chewiness, the results of the technical tasting are consistent with the TA analyses that were performed with HPLT treated protein model systems (chapter VI).

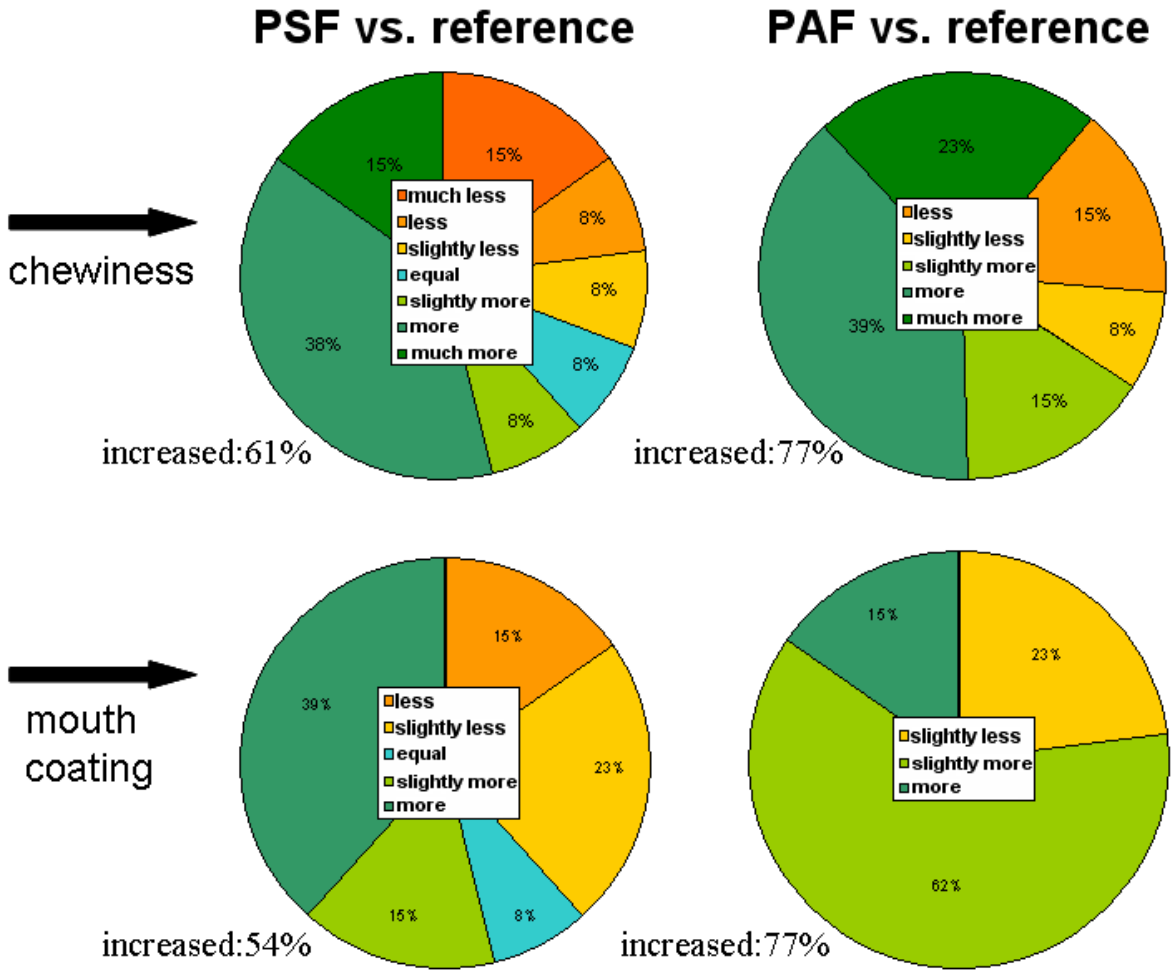

Figure VIII-7: Mouth coating and chewiness of pre-aerated dairy emulsions after PSF and PAF treatment versus a conventionally processed reference. The general increase in perception of the attributes is summarized in percent below the diagrams.

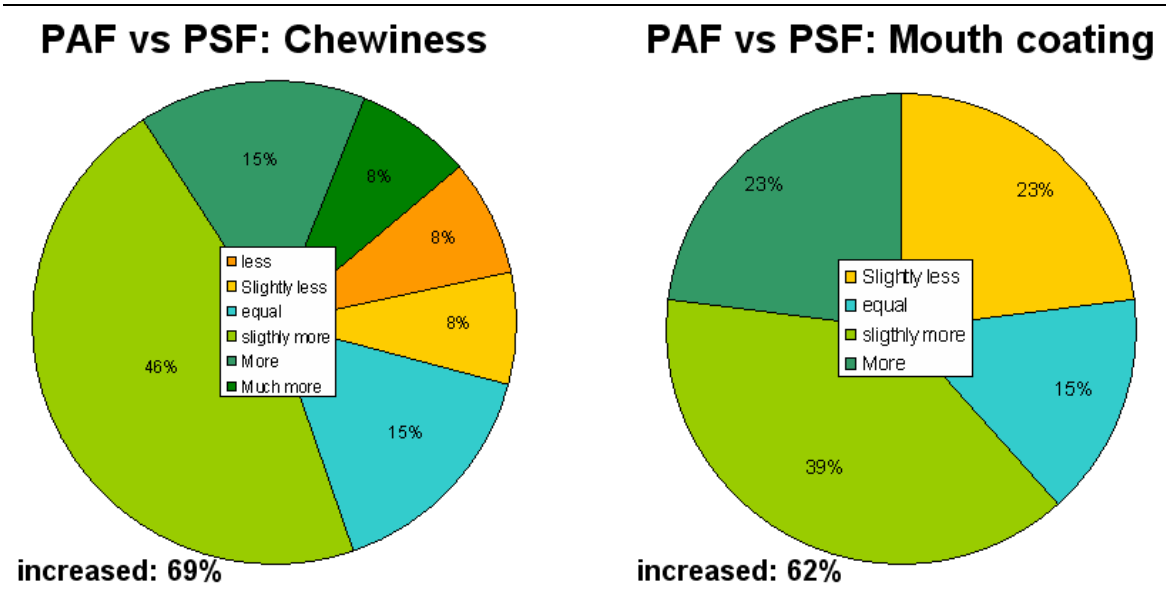

Figure VIII-8: Mouth coating and chewiness of pre-aerated dairy emulsions after PSF and PAF treatment.. The general increase in perception of the attributes is summarized in percent below the diagrams.

PAF treatments induced higher gel strengths in SMP solutions than PSF treatments, which correlates with the higher chewiness of the PAF treated dairy foams. On the base of these results the increased chewiness can be attributed to the HPLT induced protein aggregation in the matrix.

3.3 Instrumental texture profile analysis of chewiness

The development of objective methods to describe the mechanical properties of food systems has been an important target for food technology in recent decades. The texture profile analysis has turned out to be a good tool to assess textural properties of semisolid foods (Pons & Fiszman, 1996). The TPA of the frozen diary foams was performed in addition to the technical tasting with focus on the chewiness of the products. Figure VIII-9 shows the TPA results for chewiness of the conventionally processed reference and two HPLT treated foams. The freezing time under pressure for the PAF sample was 2000 s. All measurements were carried out at -18°C.

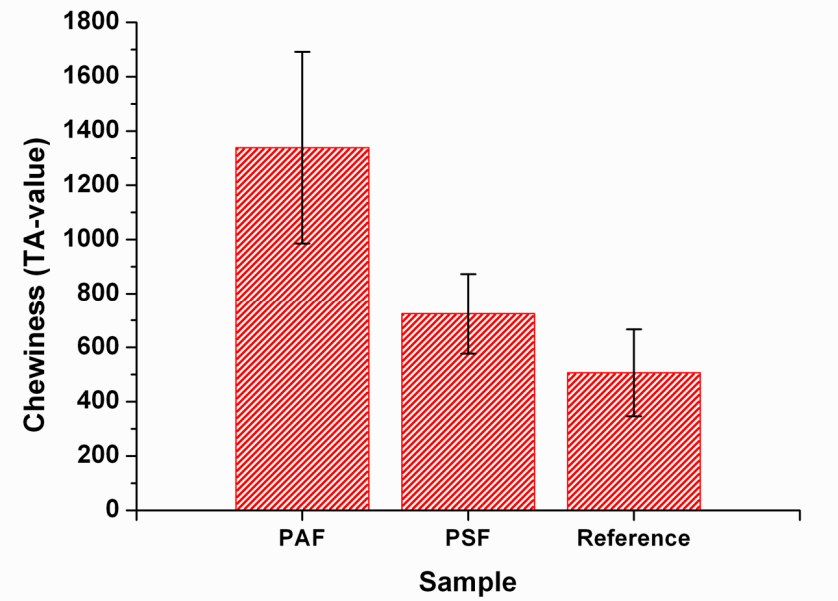

Figure VIII-9: Chewiness of aerated low fat dairy emulsion (emulsion G) after conventional freezing (reference) and HPLT treatment (PAF, PSF) at 320 MPa, determined by texture profile analysis.

The instrumentally obtained results are in good agreement with the results obtained by subjective technical tasting. Highest chewiness was detected after PAF treatment of the emulsions and lowest chewiness was detected in the conventionally frozen product. The TPA presents a good addition to the technical tasting, which was done by an untrained consumer panel and the consistence of the results further supports the hypothesis of protein based texture changes after HPLT treatment of pre-aerated dairy emulsions.

3.4 Melting behaviour

Consumer acceptance of frozen dairy foams depends largely on its textural quality any temperature fluctuation or abuse between manufacture and consumption can cause detrimental effects on ice cream quality (Alvarez, Wolters, Vodovotz & Ji, 2005). The melt-down rate of ice cream is affected by many factors, including the amount of air incorporated and the network of fat globules formed during freezing (Muse & Hartel, 2004). Since air cells act as insulators, low overruns promote quick melting, whereas high overruns support a good melting resistance (Sakurai, Kokubo, Hakamata, Tomita & Yoshida, 1996; Marshall et al.,

2003). Supporting the foam structure, the fat network plays a significant role. Increasing levels of destabilized fat increase the fat network and slows down melting. Melting as such is not a texture defect of frozen foams. Unlike other thermal properties, meltdown is not a uniquely defined standard physical parameter but an empirical measure that can indicate, for example, the effect of changing the formulation or process on the properties of the product (Clarke, 2004).
The melting behavior of different frozen dairy foams was investigated after conventional freezing and HPLT treatment. Of central concern was the impact of the HPLT treatment on the drip loss during melting of fat and sugar rich formulations and emulsions with reduced fat and sugar content.

Treatment related drip loss
The drip loss of foamed emulsion B after conventional freezing, and HPLT treatment at 320 MPa is shown in Figure VIII-10. It clearly shows that the melting behavior is decisively influenced by the freezing process. After conventional freezing in a continuous ice cream freezer the frozen dairy foam melts slowly and loses 30% of its initial mass after 200 min at 20°C. Comparable melting behavior was observed after PAF treatment at 320 MPa and 2000 s freezing time under pressure. The foam structure is relatively stable at room temperature and the drip loss after 200 min only slightly higher compared to the reference. After PAF treatment the pre-aerated dairy emulsion suffers from massive drip loss as soon as melting begins. 45 min after the first drip loss was detected, 94% of the detected mass loss occurred. The rapid melting of the PSF sample indicates poor water binding in the matrix and insufficient foam stability at temperatures above the freezing point.

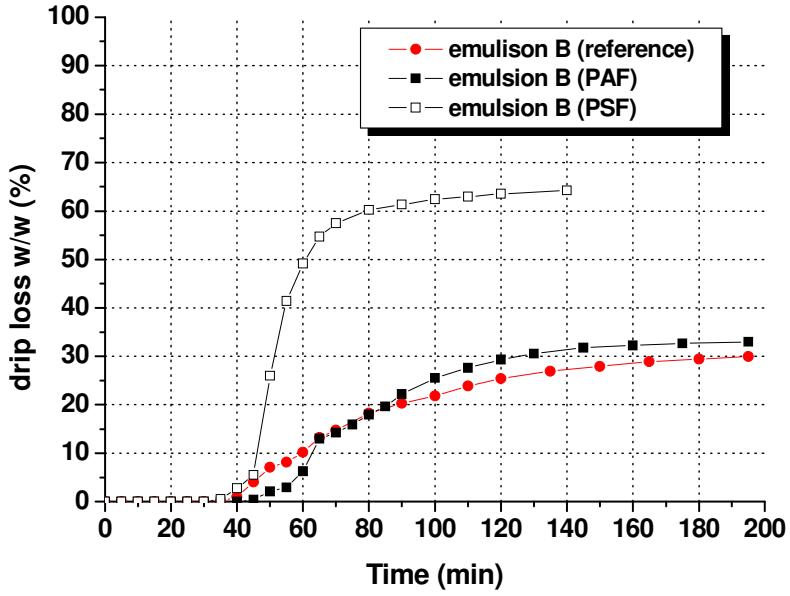

Figure VIII-10: Drip loss during melting at 20°C in conventionally frozen (●), PAF treated (■) and PSF treated (□) foamed dairy emulsion (emulsion B).

The results indicate two different mechanisms for HPLT treated and conventionally frozen dairy foams that contribute to the stabilization of the liquid foam after melting. The fat phase in the matrix undergoes partial coalescence in the concomitant whipping and freezing step during conventional freezing and provides air cell stabilization in the partially frozen system (Marshall et al., 2003). This mechanism probably accounts for the slow melt down of the reference foam. During long PAF treatment a firm gel network develops in solutions that contain caseins and whey proteins in a suitable ratio, even at low initial protein concentrations

(see chapter VI). This effect is supposed to provide the slow pass out of the serum phase during melting in the PAF treated samples, even though the conventional mechanism of fat stabilization is not induced by this treatment. During PSF treatment, neither mechanical energy input induces fat destabilization and partial coalescence, nor is the formation of firm protein networks induced at low protein concentrations. Consequently foam stabilization and water immobilization is provided by the ice crystals to a great extend. Upon melting the ice crystal network breaks down and the serum phase drains off the product due to a lack of additional stabilization.

Formulation related drip loss

Along with the impact of different freezing processes the structural changes related to different emulsion formulations were investigated. Of special interest were the fat content and the protein content and composition. Figure VIII-11 shows the drip loss after conventional freezing and PAF of four different emulsions that vary in fat content, protein content and composition and total solids.

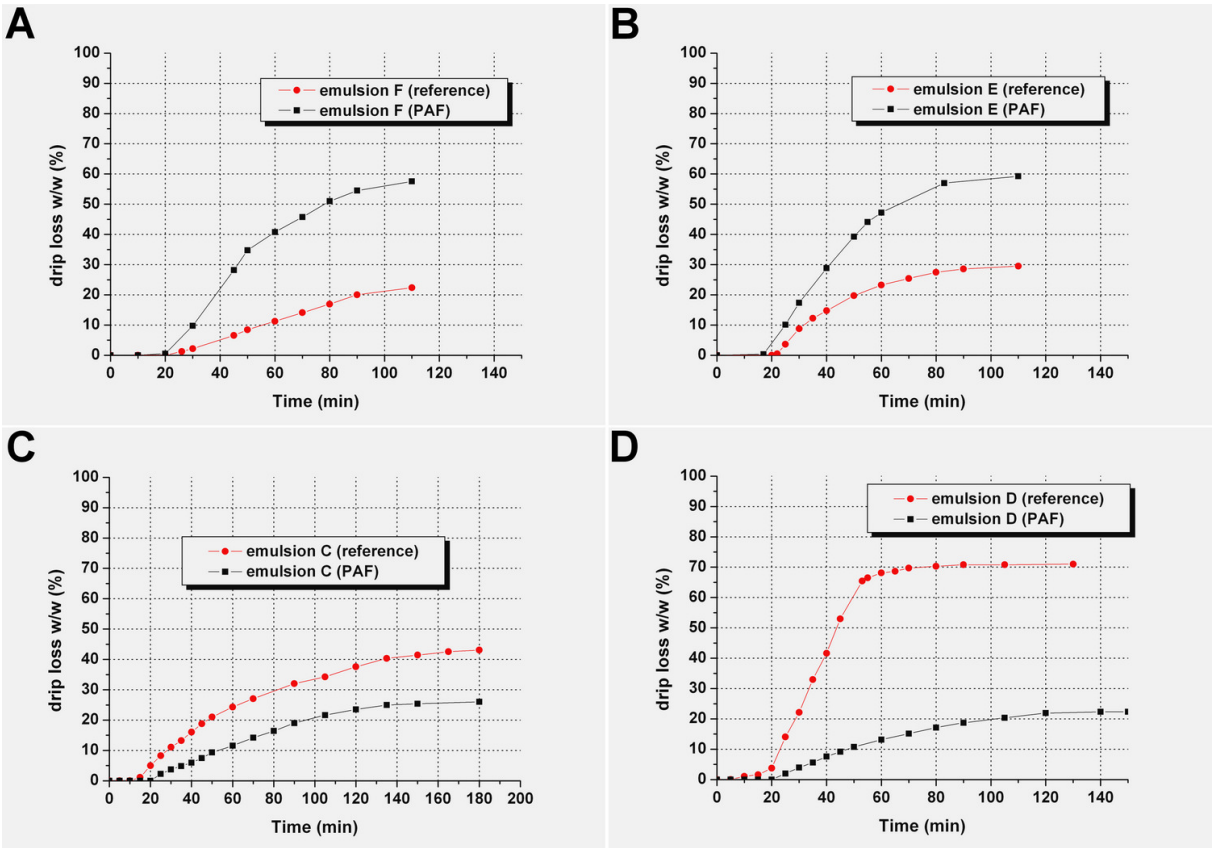

Figure VIII-11: Drip loss over time at 20°C of conventionally frozen reference foams (●) and pre-aerated dairy emulsions after PAF treatment at 320 MPa and 2000 s freezing time under pressure (■).
A: 36.9% total solids; 7% fat; 9.7% WP. B: 17.5% total solids; 2% fat; no protein. C: 17.3% total solids; 2% fat; 7.7% SMP. D: 16.5% total solids; no fat; 7.7% SMP.

It shows that the fat content and the protein composition of the emulsions have a strong impact on the melting behaviour after conventional freezing and after PAF treatment. In agreement with the results of the previous section, fat reduces the drip loss in aerated emulsions after conventional freezing, whereas high drip loss occurs in emulsion F and B after HPLT treatments, which have a fat content of 7 and 2% respectively. In contrast to the conventional freezing, fat does not prevent drip loss during melting in HPLT treated samples. After HPLT treatment the drip loss is significantly reduced when proteins, i.e. caseins, are present. This phenomenon is most obvious in the frozen emulsion D, which is a no fat recipe

with 7.7% SMP. The conventionally frozen emulsion D is highly instable and suffers from massive drip loss of about 70% after 60 min. In contrast the HPLT treated sample reaches a maximum drip loss of about 22% after 140 min. Figure VIII-12 shows the conventionally frozen foam and the HPLT treated dairy foam (emulsion D) after the drip test. After 140 min the HPLT sample is slightly deflated, whereas the conventionally frozen sample is flattened.

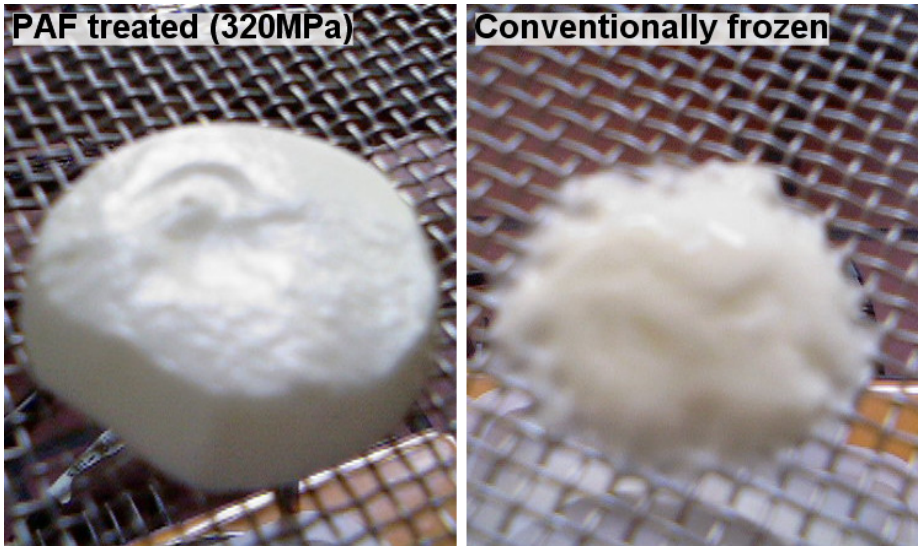

Figure VIII-12: PAF treated (left) and conventionally frozen (right) no-fat dairy foam with 7.7% SMP after drip test for 140 min at 20°C.

The major stabilization mechanism in conventionally processed frozen dairy foams, that provides foam stability and affects melt down during holding at temperatures above the freezing point is the destabilization of fat and migration of partially coalesced fat globules towards the air cell interfaces (Marshall et al., 2003). This mechanism is induced by the shearing action in the freezing step. The pre-aerated dairy emulsions are stabilized by comparable effects during foam formation in the aeration step. During the HPLT treatment the foam structure breaks down and the formally interfaces disappear. Upon reformation of the air cells during pressure release the fat is fully crystallized and migration to the air interfaces additionally hindered by the partially frozen matrix. Consequently the initial mechanism of fat based air cell stabilization is not fully restored after pressure release. Although, microscopic analyses of the melted foams show melted fat clusters on the air cell interfaces. However, during the HPLT treatment a second stabilizing structure is induced. Caseins and whey proteins associate during pressure release and form a 3D-network that immobilizes water and stabilizes air cells that grow into the network during pressure release. The resulting structures are rather temperature-stable and the stabilizing properties maintained at temperatures above the freezing point of the system.

3.5 Pre-treated milk protein in conventionally frozen dairy emulsions

HPLT treatment as a manufacturing process for frozen dairy foams has proven to induce unique textural properties in the product. To evaluate the effect of HPLT-pre-treated milk proteins in the conventional freezing process, emulsion G was conventionally frozen under addition of native SMP and PSF treated SMP solution as a source of milk proteins.

Table VIII-3: Viscosity and average "quenelle" weight of emulsion G after conventional freezing with native SMP and PSF-pre-treated SMP at 320 MPa

Sample	Sample age	Sample temperature [°C]	Viscosity [mPa·s]	Average "quenelle" weight [g]
Native protein	0 min	5.3	97	55.3
	24 h	3.7	101	n.d.
Pre-treated protein	0 min	5.4	238	77.6
	24 h	4.5	239	n.d.

It shows that the pre-treated SMP causes increased viscosity in the emulsion before freezing. This implies that the functional properties of the HPLT treated protein are transferred to the mix to some extend. Most probably the change in casein micelle size and the dimerization of β-lg, which was found in the SDS-PAGE analyses account for the increased viscosity. The quenelle weight is linked to the elongation at yield stress and correlates with the cohesion of the product. After conventional freezing the weight of the quenelle was increased by about 33%. This indicates that there is a transfer of HPLT induced protein structures to the conventionally frozen emulsion to some extent. However, the unique textural properties of HPLT treated dairy foams were not found in the conventionally frozen emulsions after addition of pre-treated protein. This indicates that the texture of SMP gels after HPLT treatment are based on structures that are irreversibly destroyed by the mixing or freezing step during conventional processing. Further analyses of the protein fraction before and after conventional freezing is required to get insight into the texture giving parameters in HPLT treated protein solutions.

4 Conclusion

The microstructure of ice crystals, air cells, fat droplets and proteins is central to the textural properties of frozen dairy foams. Considering these components separately gives valuable information about the mechanisms behind texture formation and is supportive in the conclusive interpretation of the complex system.

Oscillation rheology measurements have proven the gel formation and increased complex viscosity in pre-aerated dairy emulsions after HPLT treatment that contain whey proteins and caseins. No gel formation was detected in conventionally frozen emulsions. In technical tasting the chewiness and mouth coating of HPLT treated pre-aerated dairy emulsions was perceived superior to the conventionally frozen reference products. Taking into account the gelling behaviour of milk protein solutions during HPLT treatment, it is assumed that the basic texture of pre-aerated dairy emulsions after treatment stems from the gelling and aggregation properties of milk proteins in the partially frozen foam. The aggregated proteins account for higher chew resistance and are perceived as a coating film in the mouth. The increased chewiness was well reproducible found in TPA analyses. Chewiness increases analogous to the gel strength in protein model systems after HPLT treatment and furthermore with ice formation under pressure.

Previous studies have documented the formation of small ice crystals during HLT treatment of aqueous products, which is confirmed by the present results and assumed to be the basic cause for the higher perception of creaminess and smoothness of dairy foams after HPLT treatment. However, since PAF treatment does not significantly result in smaller ice crystals compared to conventional freezing, it can not be ruled out that the HPLT induced protein aggregation contributes to an increase in perceived smoothness and mouth coating as well.

Drip tests with HPLT treated and conventionally frozen reference samples showed that the melting rate and structural changes in the foam during melting are affected by the freezing

process and also depend on the emulsion formulations. Fat content and protein content and composition were identified as the key parameters that affect the melting behaviour.
Fat stabilization, as it occurs in the conventional freezing of aerated dairy products, is not induced by HPLT treatment but supports the foam formation and stabilization in the pre-aeration step. During HPLT treatment the fat stabilization loses effect as no shear activity is provided during the reformation of the foam. The fat globules are highly crystallized and do not provide sufficient air cell stabilization. In turn, the role of milk proteins changes from mainly surface active components to highly structure generating aggregates. In HPLT treated pre-aerated dairy emulsions the major stabilizing mechanism is based on the aggregation of casein and whey proteins, which limits the meld down at temperatures above the freezing point to a great extent, even in the absence of fat that provides stabilization in conventional processing.
HPLT treatment of the protein fraction prior to conventional freezing of the dairy emulsions is a promising alternative to HPLT processing of the whole product. Pre-treated ingredients are beneficial from an economic point of view, as the total processing costs can be reduced and moreover, the unique properties of HPLT treated proteins could be introduced into the formulation of numerous different products.
The properties of HPLT treated proteins affect the rheological properties of dairy emulsions before conventional freezing and of the frozen foam after treatment. Treated proteins caused increased viscosity in the emulsion before freezing and the frozen foams showed increased cohesion, as the average weight of the "quenelle" was 50% higher compared to those of dairy foam that was produced with untreated protein. However, the induced changes are not as distinct as they were after HPLT treatment of the whole pre-aerated emulsion and technical tasting did not show significant differences. It is assumed that the HPLT treatment changes the functional properties of milk proteins on a molecular level, which contributes to the product properties of the pre-aerated emulsions after HPLT treatment and, to some extent, after conventional freezing. In the conducted experiments the unique properties of HPLT treated pre-aerated dairy emulsions could not be fully transferred to conventionally frozen products by the incorporation of HPLT treated proteins. However, the results of protein pre-treatments prior to conventional freezing highlight the importance of further research in this area. Significant changes of some instrumentally determined parameters of the conventionally frozen emulsion in presence of pre-treated proteins were found (quenelle weight, mix viscosity) but the induced structures did not affect the sensory properties of the product. Gaining profound understanding of the protein denaturation mechanisms during HPLT treatment and the transferability of HPLT induced properties to create and modify texture of conventionally processed products remains to be done.

5 References

[1]Aguilera, J. M. & Stanley, D. W. (1999). *Microstructural Principles of Food Processing and Engineering, Second Edition*. Springer.

[2]Akhtar, M., Stenzel, J., Murray, B. S. & Dickinson, E. (2005). Factors affecting the perception of creaminess of oil-in-water emulsions. *Food Hydrocolloids*, *19*(3), 521-526.

[3]Alvarez, V. B., Wolters, C. L., Vodovotz, Y. & Ji, T. (2005). Physical Properties of Ice Cream Containing Milk Protein Concentrates. *J. Dairy Sci.*, *88*(3), 862-871.

[4]Bourne, M. C. (2002). *Food Texture and Viscosity Second Edition:Concept and Measurement*. Academic Press, New York.

[5]Chevalier, D., Le Bail, A. & Ghoul, M. (2000). Freezing and ice crystals formed in a cylindrical food model: part II. Comparison between freezing at atmospheric pressure and pressure-shift freezing. *Journal of Food Engineering*, *46*(4), 287-293.

[6]Clarke, C. (2004). *The Science of Ice Cream*. The Royal Society of Chemistry, Cambridge.

[7]de Wijk, R. A., Terpstra, M. E. J., Janssen, A. M. & Prinz, J. F. (2006). Perceived creaminess of semi-solid foods. *Trends in Food Science & Technology*, *17*(8), 412-422.

[8]Fernández, P. P., Otero, L., Guignon, B. & Sanz, P. D. (2006). High-pressure shift freezing versus high-pressure assisted freezing: Effects on the microstructure of a food model. *Food Hydrocolloids*, *20*, 510-522.

[9]Granitto, P. M., Biasioli, F., Endrizzi, I. & Gasperi, F. (2008). Discriminant models based on sensory evaluations: Single assessors versus panel average. *Food Quality and Preference*, *19*(6), 589-595.

[10]Harries, J. M. (1973). Complex sensory assessment. *Journal of the Science of Food and Agriculture*, *24*(12), 1571-1581.

[11]Lähteenmäki, L. & Tuorila, H. (1994). Liking for Ice Cream Measured with three Procedures: Side-by-Side, after Consumption and Single Samples. *Journal of Sensory Studies*, *9*(4), 455-465.

[12]Lévy, J., Dumay, E., Kolodziejczyk, E. & Cheftel, J. C. (1999). Freezing Kinetics of a Model Oil-in-Water Emulsion under High Pressure or by Pressure Release. Impact on Ice Crystals and Oil Droplets. *Lebensmittel-Wissenschaft und -Technologie*, *32*, 396-405.

[13]Marshall, R. T., Goff, H. D. & Hartel, R. W. (2003). *Ice Cream*. Kluwer Academic / Plenum Publishers, New York.

[14]Mezger, T. G. (2006). *The Rheology Handbook, for users of rotational and oscillatory rheometers*. Vincentz, Hannover.

[15]Moskowitz, H. R. (1995). Food quality: Conceptual and sensory aspects. *Food Quality and Preference,The Definition and Measurement of Quality*, *6*(3), 157-162.

[16]Muse, M. R. & Hartel, R. W. (2004). Ice Cream Structural Elements that Affect Melting Rate and Hardness. *Journal of Dairy Science*, *87*, 1-10.

[17]Pons, M. & Fiszman, S. M. (1996). Instrumental Texture Profile Aanalyses with Particular Rreference to Gelled Systems. *Journal of Texture Studies*, *27*(6), 597-624.

[18]Rhodes, D. N., Jones, R. C. D., Chrystall, B. B. & Harries, J. M. (1972). MEAT TEXTURE: II. The Relationship Between Subjective Assessments and a Compressive Test on Roast Beef. *Journal of Texture Studies*, *3*(3), 298-309.

[19]Richardson-Harman, N. J., Stevens, R., Walker, S., Gamble, J., Miller, M., Wong, M. & McPherson, A. (2000). Mapping consumer perceptions of creaminess and liking for liquid dairy products. *Food Quality and Preference*, *11*, 239-246.

[20]Sakurai, K., Kokubo, S., Hakamata, K., Tomita, M. & Yoshida, S. (1996). Effect of production conditions on ice cream melting resistance and hardness. *Milchwissenschaft*, *51*(8), 451-454.

[21]Schaller-Povolny, L. A. & Smith, D. E. (1999). Sensory Attributes and Storage Life of Reduced Fat Ice cream as Related to Inulin Content. *Journal of Food Science*, *64*(3), 555-559.

[22]Szczesniak, A. S. (1998). Sensory Texture Profiling - historical and scientific perspectives. *Food Technology*, *52*(8), 54-57.

[23]van Vliet, T. (2002). On the relation between texture perception and fundamental mechanical parameters for liquids and time dependent solids. *Food Quality and Preference*, *13*(4), 227-236.

[24]Wildmoser, J. (2004). *Impact of Low Temperature Extrusion Processing on Disperse Microstructure in Ice Cream Systems*. PhD, Swiss Federal Iinstitute of Technology Zurich, 133.

Chapter IX Final conclusion

High pressure is a relatively new technology in the food industry that carries great potential in the production of foods and food supplements of unique properties and superior quality. Fundamental knowledge about the effects and mechanisms that occur during HP treatment of food systems at moderate and high temperatures has been established in the last decades, especially in the inactivation of microorganisms and enzymes. However, the potential of high pressure applications is far from being fully utilized. In the high pressure research, high pressure low temperature treatments represent a novel field that involves various process options, as it combines thermal and pressure effects with water phase transitions and interrelated effects.

In this study, a first approach to utilizing the HPLT technology as a production process for frozen dairy foams was performed and its effects on textural and technological properties, taking into account different compositions of the food matrix, have been revealed. Furthermore, HPLT induced structures in protein model systems were investigated with respect to different process conditions and product parameters. The HPLT process has been found to induce unique properties in complex dairy systems and simple protein models. Different structural and technological effects were observed and fundamental mechanisms that seem unique to this technology are proposed.

Serious hurdles to the HPLT technology are technical limitations in the construction of high performance equipment. Adopting HP batch process concepts, as they are implemented in the food industry for several years, involves long process times and temperature inhomogeneities in the product, which result in inhomogeneous treatment conditions during cooling and freezing under pressure. The importance of homogeneous cooling and precise temperature control of the product during HPLT treatments is demonstrated by the results of this study and makes an approach to continuous processing an even more relevant requirement as it is for standard HP processes. Accurate pressure and temperature control are essential to benefit from the metastable character of aqueous products under pressure and to realize maximum heat consumption before pressure release, which allows efficient HPLT processing beyond the theoretical limits of thermodynamic phase boundaries. It has been shown that continuous HPLT freezing is technically feasible, without the use of a pressure transmitting media by direct pressurization of the liquid product. In this way, sample packaging is not required and problems associated with the volume changes of aerated products during HPLT treatment, such as insufficient temperature measurement or contamination of the product with pressure transmitting medium, can be eliminated. A major challenge in the continuous HPLT processing is the pressure control, which was found to be possibly realized by the means of a backpressure valve for PSF treatments or by the partly frozen product in the tubing, exploiting the increased product viscosity during PAF. However, high shear forces in the backpressure valve cause sudden temperature peaks that fully compensate the previously induced supercooling and long thin tubing tend to jam during PAF. To overcome this problem, further research effort on the development of expansion systems and the design of treatment sections is required.

As a tool for specific HPLT process planning, complex phase diagrams of a dairy emulsion and a protein model system were modeled, taking into account the progressive freezing point depression with increasing ice content. The metastability of dairy emulsions was found to be promoted by increasing sugar contents, which can be exploited by extensive supercooling in the PSF process. During PAF in the pressure range from 300 to 350 MPa the ice modifications III and V occur randomly, which does not concern the general process but affects the process temperature after nucleation, as ice III and metastable ice V have different equilibrium freezing points in the given pressure range. The product temperature after expansion is governed by the ice content and the temperature at the point of pressure release.

By this means product outlet-temperatures between -5 and -28°C were achieved in the PAF process. This effect highlights the technological advantages of HPLT freezing, since compared to conventional freezing a downstream hardening step is not necessarily required.
The milk proteins were identified as the most affected component in HPLT treated dairy emulsions. SDS-PAGE analyses indicated dimerization of β-lactoglobulin in whey protein solutions after HPLT treatment at 320 MPa and minimum temperatures of -25°C, especially pronounced after PSF. Viscosity measurements of HP and HPLT treated protein model solutions indicated significant differences in the protein structure after HPLT and HP treatment. Aggregation in protein solutions occurred in the presence of caseins after PSF treatment at pressures above 175°MPa, whereas HP treated solutions were free of visible aggregates after treatment at pressures up to 300 MPa. The results imply that the ice formation is a critical parameter to the aggregation behavior and that crystal growth during HPLT treatments is involved in the protein structure formation. Very little destabilization of fat occurred in dairy emulsions during HPLT treatments, which is in good agreement with literature data. It is assumed that the fat is highly crystallized during the process. Guar gum endosperm cells that serve as stabilizers in frozen dairy foams were not affected in their structural integrity after treatment at 320 MPa at -25°C, nor were any critical color defects observed in the treated emulsions.
The structural properties of protein solutions after HPLT treatment are governed by numerous process and product related parameters. Caseins contribute decisively to the solidification of milk protein solutions after HPLT treatment and a non-linear coherency between gel strength and the casein to whey protein ratio was found. This suggests the contribution of whey proteins, i.e. β-lactoglobulin, to the gel formation and indicates synergistic effects between whey proteins and casein micelles during HPLT treatment. The ice formation under pressure and during pressure release is suggested to have a key impact on the induced structures, which makes HPLT induced gels significantly different in their textural properties from HP induced gels. In this respect freeze concentration and volume changes of the water phase seem to be the most relevant effects. A mechanistic approach to the phenomenon is given by the proposed hypothesis of ice crystal based mechanical compression of protein structures under pressure and during pressure release. SMP gel strengths after HPLT treatments are promoted by higher pressure release rates, which confirms the hypothesis of casein micelle association subjected to the rate of pressure release, as it was proposed for HP treatments at moderate temperatures, for the HPLT domain. However, after PAF the effect lowers with increasing ice content before pressure release. It is assumed that the gel strength is no further increased when the freeze concentration exceeds a certain level. This assumption is in good agreement with PAF and PSF experiments with differently concentrated SMP solutions, which showed reduced gel strength of PAF treated samples at SMP concentrations higher than 25%.
HPLT treatments of pre-aerated dairy emulsions have shown that the liquid foam once aerated, maintains 40 to 90% of the initial overrun after HPLT treatment, strongly depending on the treatment conditions and the initial overrun. However, compared to conventional freezing an increase in the average air cell size was detected. It is proposed that during compression the air volume fraction disappears and changes its state from gaseous to supercritical. Upon expansion, a reformation of air cells occurs in the partially frozen matrix. Oscillation rheometry has proven the gel formation in HPLT treated dairy foams that contain SMP. In addition, SEM analyses of HPLT treated SMP solutions and HPLT treated dairy foams show comparable microstructures after treatment. Two basic mechanisms are suggested to contribute to the air cell stabilization after treatment. The HPLT induced protein network stabilizes the air cells at low ice contents and is progressively disordered with increasing ice content. With increasing amounts of frozen water after expansion the stabilization is shifted to the growing ice crystal network, which is supposed to functions as a physical barrier to air cell coalescence and channel formation. Since most of the fat is

crystalline, the role of fat as a stabilizing component after HPLT treatment is supposed to be marginal. However, the air cells show relatively high fat coverage after melting of the treated foams, which implies that upon melting the liquid to solid ratio of the fat phase increases and liquid fat resumes its stabilizing function on the air cell interfaces to some extent.

In good agreement with the micro-structural changes that were found in dairy foams and protein solutions after HPLT treatment, the rheological and textural properties of treated foams were found significantly different from conventionally frozen dairy foams. Creaminess, mouth coating and chewiness of frozen dairy foams were perceived higher after HPLT treatment. The protein structures that are induced by the process are supposed to account for the higher perception of the latter attributes. The increased smoothness is related to the formation of small ice crystals during HPLT freezing. The formation of superior textural properties in dairy foams after HPLT processing is especially pronounced in low fat formulations. The melting behavior of HPLT treated and conventionally frozen no-fat and low-fat foams indicated that the texture formation and foam stabilization after HPLT treatments is protein based and the fat fraction does not contribute to stabilization after treatment. Conventionally frozen dairy foams showed different rheological properties when HPLT treated milk proteins were incorporated in the formulation. Higher average weights of the quenelles were found at the freezer outlet, which implies increased cohesion of the frozen foam.

HPLT processes have proven their potential as manufacturing processes for frozen dairy foams of unique properties and high sensorial quality. Pressure assisted freezing and pressure shift freezing are flexible freezing process that allow the specific product parameter control (e.g. overrun, outlet-temperature, texture) of frozen dairy foams. During HPLT treatments that involve a water phase change from ice III to ice I microbial inactivation is achieved, which is beneficial in the gentile production of foods as thermal processing intensities in the pasteurization step can be reduced. The present study has revealed key problems in the HPLT batch process (i.e. long process times and insufficient process control due to inhomogeneous treatment conditions) and introduces first approaches to the continuous HPLT processing of dairy foams. To make the HPLT process attractive to the food industry, further research and development towards the implementation of continuous systems is required. In this respect the key challenges are the pressure control over the HPLT tubing and product temperature peaks due to high shear forces that occur during expansion by means of a backpressure valve.

Furthermore this work has shown that HPLT processing is a promising tool in the production of pre-treated milk proteins that offer unique properties and, introduced as food supplements, potentially contribute to the textural properties of a variety of conventionally processed foods. This approach is of special potential as it suggests the HPLT treatment not only as a manufacturing process for one end-product to the consumer but reveals the potential to produce food supplements of unique properties and a variety of possible applications.

Annex

Annex 1: Emulsion Formulations

EMULSION A

Code Loc.	Nom ingrédient	Réfer. externe	Qté. brut Pourcent	Mat.sèche Pourcent	Qté. brut kg(*)
000527	EAU FROIDE RESEAU NGF		54.876	0.020	38.413
007057	EMULSTAB LYGOMME FM 3601 (827365)		0.500	0.485	0.350
008737	PROTEINES SERIQUES 15%		9.640	9.351	6.748
000798	LAIT ECREME EN POUDRE SPRAY EN SACS		2.160	2.074	1.512
001472	SUCRE CRISTALLISE N 2 VRAC USINE		8.920	8.915	6.244
005591	SIROP DE GLUCOSE DE 36-40 (MS 60%) MI-FAB.		15.000	9.000	10.500
008420	GRAISSE (COCO) RAFFINEE 24-26°		8.800	8.799	6.160
000243	COLORANT CAROTENE BETA 10% CWS E160A		0.002	0.002	0.001
002600	COLORANT JAUNE E101 RIBOFLAVINE 5 PHOSPHAT		0.002	0.002	0.001
008790	VANILLE AROME NATUREL		0.100	0.077	0.070
Total ingrédient			100.000	38.724	70.000

EMULSION B

Local Code	Ingredient name	Batch load Percent	Solids Percent	Batch load kg(*)
000527	WATER COLD FROM NGF FACTORY	56.199	0.020	56.171
008737	WHEY PROTEINS 15%	5.000	4.850	4.997
000798	MILK SKIMMED POWDER SPRAY BAGS	5.000	4.800	4.997
001472	SUGAR SUCROSE CRYS EEC N2 BULK	9.500	9.494	9.495
005591	SUGAR CORN SYRUP DE 36-40 DM 60%	16.500	9.900	16.491
009246	FAT BLEND PALM/COCONUT 60/40	7.000	7.000	6.996
006880	GUM GUAR INS412	0.150	0.136	0.150
006873	CMC INS466	0.050	0.046	0.050
006257	CARRAGEENAN INS407A	0.020	0.018	0.020
007776	MONOGLYCERIDES INS471	0.200	0.200	0.200
008775	EMULSIFIER PGMS	0.300	0.300	0.300
006741	SORBITAN TRISTEARATE INS492	0.030	0.030	0.030
006742	MONOGLYCERIDES INS471	0.050	0.050	0.050
000243	COLOR CAROTINE BETA 10% CWS INS160A	0.001	0.001	0.001
002600	COLOR YELLOW RIBOFLAVINE 5 INS101(ii)	0.001	0.001	0.001
Total ingredient			100.000	
36.845	99.950			

EMULISON C

Local Code	Ingredient name	Batch load Percent	Solids Percent	Batch load kg(*)
000527	WATER COLD FROM NGF FACTORY	82.405	0.030	82.405
000798	MILK SKIMMED POWDER SPRAY BAGS	8.000	7.680	8.000
001472	SUGAR SUCROSE CRYS EEC N2 BULK	7.000	6.996	7.000
008420	COCONUT OIL REFINED FAT 24-26°	2.000	2.000	2.000
006257	CARRAGEENAN INS407A	0.015	0.014	0.015
006115	CAROB POWDER (INS410) LBG	0.150	0.135	0.150
005724	GUM GUAR INS412	0.050	0.044	0.050
007749	EMUL INS471	0.300	0.297	0.300
006267	FLAVOR VANILIN PURE CRISTALLISED	0.050	0.050	0.050
005126	XANTHAN GUM	0.030	0.028	0.030
Total ingredient		100.000	17.273	100.000

EMULSION D

Local Code	Ingredient name	Batch load Percent	Solids Percent	Batch load kg(*)
000527	WATER COLD	83.175	0.030	41.588
000798	MILK SKIMMED POWDER SPRAY BAGS	8.000	7.680	4.000
001472	SUGAR SUCROSE CRYS EEC N2 BULK	8.210	8.205	4.105
006257	CARRAGEENAN INS407A	0.015	0.014	0.008
006115	CAROB POWDER (INS410)	0.150	0.135	0.075
005724	GUM GUAR INS412	0.050	0.044	0.025
007749	EMUL INS471	0.300	0.297	0.150
006267	FLAVOR VANILIN PURE CRISTALLISED	0.050	0.050	0.025
005126	XANTHAN GUM	0.050	0.046	0.025
Total ingredient		100.000	16.501	50.000

EMULSION E

Local Code	Ingredient name	Batch load Percent	Solids Percent	Batch load kg(*)
000527	WATER COLD	82.405	0.030	41.203
001472	SUGAR SUCROSE CRYS EEC N2 BULK	12.800	12.792	6.400
008420	COCONUT OIL REFINED FAT 24-26°	2.000	2.000	1.000
006257	CARRAGEENAN INS407A	0.015	0.014	0.008
006115	CAROB POWDER (INS410)	0.150	0.135	0.075
005724	GUM GUAR INS412	0.050	0.044	0.025
007749	EMUL INS471	0.300	0.297	0.150
006267	FLAVOR VANILIN PURE CRISTALLISED	0.050	0.050	0.025
008853	CORN FIBERS SOLUBLE	2.180	2.093	1.090
005126	XANTHAN GUM	0.050	0.046	0.025
Total ingredient		100.000	17.500	50.000

EMULSION F

Local Code	Ingredient name	Batch load Percent	Solids Percent	Batch load kg(*)
000527	WATER COLD	56.199	0.020	56.171
008737	WHEY PROTEINS 5%	10.000	9.700	9.995
001472	SUGAR SUCROSE CRYS EEC N2 BULK	9.500	9.494	9.495
005591	SUGAR CORN SYRUP DE 36-40 DM 60% (NGF)	16.500	9.900	16.491
009246	FAT BLEND PALM/COCONUT 60/40	7.000	7.000	6.996
006880	GUM GUAR INS412	0.150	0.136	0.150
006873	CMC INS466	0.050	0.046	0.050
006257	CARRAGEENAN INS407A	0.020	0.018	0.020
007776	MONOGLYCERIDES INS471	0.200	0.200	0.200
008775	EMULSIFIER PGMS	0.300	0.300	0.300
006741	SORBITAN TRISTEARATE INS492	0.030	0.030	0.030
006742	MONOGLYCERIDES INS471	0.050	0.050	0.050
000243	COLOR CAROTINE BETA 10% CWS INS160A	0.001	0.001	0.001
002600	COLOR YELLOW RIBOFLAVINE 5 INS101(ii)	0.001	0.001	0.001
Total ingredient		100.000	36.895	99.950

EMULSION G

	Percent	Solids
WATER COLD	66.960	0.024
MILK SKIMMED POWDER SPRAY	8.330	7.997
GLUCOSE SYRUP DRIED DE 40 BAG	4.210	4.000
SUGAR SUCROSE CRYS EEC	14.000	13.992
EMULSIFIER PWDR INS471	0.300	0.300
GUM GUAR INS412	0.080	0.070
CAROB POWDER (INS410)	0.050	0.045
CARRAGEENAN INS407A	0.020	0.018
FLAVOR VANILIN PURE CRISTALLISED	0.050	0.050
COCONUT OIL REFINED FAT 24-26°	6.000	5.999
Total ingredient	100.000	32.495

Annex 2: Milk powder and protein isolate specifications

*Bi*PRO®

Whey Protein Isolate

Product Description

*Bi*PRO is manufactured from fresh, sweet dairy whey that is concentrated and spray dried. The product is a homogenous, free flowing, semi-hygroscopic powder with a clean, bland flavor.

Product Functionality

*Bi*PRO is a unique, natural and pure dairy protein comprised of beta-lactoglobulin and alpha-lactalbumin. *Bi*PRO's functional protein groups have valuable gelling, water binding, emulsification and aeration properties. *Bi*PRO replaces larger quantities of other functional ingredients providing improved flavor and mix efficiency. *Bi*PRO is not denatured and is fully soluble over the pH range 2.0 to 9.0. *Bi*PRO is lactose-free.

Analysis*	Specification	Typical Range	Test Method
Moisture (%)	5.0 max.	4.8 ± 0.2	Vacuum Oven
Protein, dry basis (N x 6.38) (%)	95.0 min.	97.8 ± 0.2	Leco Combustion
Fat (%)	1.0 max.	0.4 ± 0.2	Mojonnier
Ash (%)	3.0 max.	2.0 ± 0.2	Residue on Ignition
Lactose (%)	1.0 max.	<0.5	By Difference
pH	6.7 - 7.5	7.0 ± 0.2	10% Sol. @ 20°C.
Scorched Particles	15 mg/25g max.	7.5mg	ADPI

Microbiological Profile	Specification	Typical Range	Test Method
Aerobic Plate Count	10,000/g max.	<2,500	Standard Methods**
Coliform (MPN)	10/g max.	<10	FDA/BAM
E. coli (MPN)	Negative/g	Negative	FDA/BAM
Yeast & Mold	10/g max.	≤10	Standard Methods**
Coag. Pos. Staph (MPN)	<10/g	<10	FDA/BAM
Salmonella sp.	Negative/1500 g	Negative	AOAC / ELISA
Listeria sp.	Negative/25 g	Negative	AOAC / ELISA

* All results reported on "AS IS" basis except where noted.
** Standard Methods for the Examination of Dairy Products, 16th Edition.

Storage and Packaging

Dried dairy products can absorb odors and moisture. Therefore, adequate protection is essential. Shelf life will be enhanced through ideal storage conditions which include temperatures below 25°C., relative humidity below 65%, and an odor free environment. Avoid less than ideal storage conditions.

Packaged in Kraft multiwall bags incorporating a polyethylene bag liner, individually closed.

Net wt: 33 Lbs. version 07L-0103

Davisco Foods International, Inc.
11000 West 78th Street, Suite 210, Eden Prairie, MN 55344
PHONE 952-914-0400 FAX 952-914-0887
www.DaviscoFoods.com

Sailer

Natürlich aus dem Allgäu.

Seite: 1
von: 1
Abschnitt: 3

Spezifikation: Instant Magermilchpulver

Spezifikationsnummer: SP032D05.DOC

1.	**Beschreibung**	Instant Magermilchpulver ist ein freifließendes Pulver, das aus frischer Milch durch Eindampfen und Sprühtrocknung gewonnen und durch Agglomeration instantisiert wird.			
2.	**Pulver-Charakteristik**				
	Aussehen	weißes, leicht gelbliches Pulver			
	Geruch, Geschmack	reiner Milchgeschmack, ohne Fremdnote			
	Analyse	**Methode**	**Anforderungen**		
3.	**Chemische Kriterien**				
	Wassergehalt	VDLUFA C 35.6	<	4,0	%
	Fettgehalt	VDLUFA C 15.3.9	<	1,0	%
	Eiweiß	VDLUFA C 30.2		35,5	%
	Lactose	LMBG § 35 L01.00-17		51,7	%
	Asche	VDLUFA C 10.2		7,8	%
4.	**Physikalische Kriterien**				
	Reinheit (ADMI)			A - B	
	Erhitzungsgrad			high heat	
	Schüttgewicht			500-550 g/l	
5.	**Mikrobiologische Kriterien**				
	Gesamtkeimzahl	VDLUFA M 6.3.1	max.	5.000 / 1,0	g
	Coliforme Keime	VDLUFA M 7.2.2.1	neg.	/ 1,0	g
	E-Coli	VDLUFA M 7.2.2.4	neg.	/ 1,0	g
	Hefen/Schimmel	VDLUFA M 7.7.2	max.	10 / 1,0	g
	Enterobacteriaceae	VDLUFA M 7.14.2	max.	10 / 1,0	g
	Koagulasepositive Staphyloc.	LMBG L02.07-2	neg.	/ 1,0	g
	Hemmstoffe	BR-Test	neg.		
		Die Abwesenheit von Salmonellen wird durch laufende Analysen in einem zertifizierten Institut überprüft.			
6.	**Sonstige Kriterien**				
	Nährwert	1519 KJ/100g (356 kcal/100g)			
7.	**Verpackung**	Karton mit Alu-Innensack a 250 g netto			
8.	**Mindesthaltbarkeit und Lagerung**	**18 Monate Kühl und trocken lagern**			

Die angegebenen Werte sind Durchschnittsangaben; geringfügige Abweichungen sind jahreszeitlich bedingt!

Dateiname: Sailer Spezifizierung.DOC
Stand:13.08.07

Reg-Nr.: 004916 IFS

J.M.Gabler-Sailter, Milchwerke
Postfach 1162
87630 Obergünzburg
Telefon: 0 83 72 - 703-0
Telefax: 0 83 72 - 703-144

REF : 8K02

BBA LACTALIS INDUSTRIE

FROMY 35
Concentré de protéines sériques à 35 %

DESCRIPTION

FROMY 35 est un concentré de protéines sériques obtenues par ultrafiltration, concentration et séchage de lactosérum.

VALEUR NUTRITIONNELLE /100g

1609 KJ / 380 Kcal

SPÉCIFICATIONS PHYSIQUES

Couleur	Blanc crème
Goût et Odeur	Neutres, francs.
Épreuve de filtration	Disque A / B (ADPI)
pH	6.4 ±0.3 (ITSV Chimie III-24)
Solubilité	99% mini (IDF129A – ISO8156)

SPÉCIFICATIONS CHIMIQUES					MÉTHODES
Protéines (N x 6.38) (%)			min	35	IDF 20 B – ISO 8968-1
Humidité (%)			max	4	IDF 26 A – ISO WD 5537
Matière grasse (%)			max	3.5	IDF 9 C – ISO 1736
Lactose (%)			max	52	IDF 79 B – ISO DIS 5765-2
Matières minérales (%)			max	7.5	NF V04 208
Calcium	*(%)*	*Ca*	*approx*	*0.6*	Indicatif
Sodium	*(%)*	*Na*	*approx*	*0.75*	"
Potassium	*(%)*	*K*	*approx*	*2*	"
Chlorure	*(%)*	*Cl*	*approx*	*1.8*	"
Phosphore	*(%)*	*P*	*approx*	*0.75*	"
Magnésium	*(%)*	*Mg*	*approx*	*0.17*	"
Activité de la phosphatase				Négative	IDF 63 – ISO 3356
Nitrites				Absence	IDF 97A – ISO 14673-1
Nitrates				50 ppm	IDF 97A – ISO 14673-1
Acidité titrable (%)				0.15	ADPI

SPÉCIFICATIONS BACTÉRIOLOGIQUES			MÉTHODES
Germes totaux	/ 1 g	< 30 000	IDF 100 B – ISO 6610
Levures / moisissures	/ 1 g	< 50	IDF 94 B – ISO 6611
Streptocoques fécaux	/ 1 g	< 100	SLANETZ BARTLEY
Coliformes	/ 0.1 g	Absence	IDF 73 B – ISO 5541-1
E. coli	/ 0.1 g	Absence	IDF 170 A – ISO 11 866
Clostridium perfringens	/ 1 g	< 1	ISO 7937
Listeria	/ 25 g	Absence	IDF 143 A – ISO 10560
Salmonelles	/ 375 g	Absence	VIDAS ICS
Staphylocoques à coag. +	/ 1 g	Absence	IDF 145 B – ISO 5944

CONDITIONNEMENT

Sacs papier, multiplis, doublés polyéthylène réglés à 25 Kg net sur palettes houssées. (Big bag 1000 Kg sur demande)

STOCKAGE ET DURÉE DE CONSERVATION

12 mois (HR < 65 % ; 5°<T< 25° C)
Eloigné de toute source de goûts et odeurs parasites.

DÉCLARATION DES INGRÉDIENTS

Protéines de lait

POSITION DOUANIÈRE

NC 04.04.10.14

RECOMMANDATIONS

L'utilisation alimentaire de ce produit pouvant varier d'un pays à l'autre, la législation locale devra être consultée.

IMPORTANT : AVERTISSEMENT

Notre responsabilité contractuelle consiste à fournir une marchandise conforme aux spécifications ci-dessus et dans le cadre de nos conditions générales de vente. Notre responsabilité ne saurait être engagée en cas d'utilisation erronée de notre produit. L'acheteur doit se conformer à la réglementation en vigueur dans les pays d'utilisation.

09 / 07 / 2004
Annule et remplace la fiche du 09 / 06 / 2004

Lactalis Industrie S.N.C. au capital de 8 649 584 € - Siège Social : Les Placis – 35230 Bourgbarré – France
Siren 402 737 936 – RCS Rennes – Ets BBA : 5, les Placis, 35230 Bourgbarré.
Tel 00 33 (0) 2 99 26 63 33 Fax 00 33 (0) 2 99 26 66 84
site web www.bba-lactalisindustrie.com

Fax reçu de
Fax émis par : A4->A4 03/02/99 13:49 Pg: 1/1

euroserum

BP 17 • 70170 PORT SUR SAONE
☎ 03 84 96 11 11 • Fax 03 84 96 11 10

LACTOSERUM DOUX
Consommation Humaine

(SP.F/CL/03/003 Rév.0 du 01/02/1994)

I) Description -Utilisation :

Lactosérum doux de première qualité, déshydradé par séchage spray.
Remplaceur de lait, il est utilisable en biscuiterie, panification, chocolaterie, crème glacées, fromages fondus etc...

II) Caractéristiques physiques :

- Couleur blanche à légèrement crème.		
- Odeur franche, goût légèrement salé.		
- Propreté (ADMI)	A	maxi B
- Indice de solubilité (ADMI)	0.5 ml	maxi
- Absence de colorants et conservateurs.		

III) Caractéristiques chimiques :

- Humidité	4 %	maxi
- Matières grasses	1.5 %	maxi
- Protéines (Nx6.38)	11.5 %	mini
- Matières minérales	8 %	maxi
- Lactose	72 %	mini
- Acidité	2 %	maxi
- pH (solution à 10%)	6	mini
- Nitrates	50 ppm	maxi
- Nitrites	1 ppm	maxi

IV) Caractéristiques bactériologiques :

- Germes aérobies mésophiles	20.000/g	maxi
- Coliformes	absence	dans 0.2 g
- E.Coli	absence	dans 1 g
- Spores de Sulfito- Réducteurs	10/g	maxi
- Levures et Moisissures	100/g	maxi
- Salmonelles	absence	dans 50 g

V) Méthodes d'analyses :

Les analyses sont effectuées suivant les protocoles utilisés par le laboratoire Eurosérum. Elles sont disponibles sur demande.

VI) Conditionnement :

- Sacs de 25 kg
- Big bag de 1000 à 1250 kg
- Vrac pour citerne pneumatique.

Télécopie
Fax n°: 03.44.05.13.75
A: Mr QUENNESSON
De: MYRIAM CAPRETTI
Date: 3/02/99 Nb de Pages: 1
Meilleures Salutations

S.A. au capital de 70 850 000 F
RCS VESOUL TGI B 400 869 977 • TVA CEE : FR 00 400 869 977 • APE 155 D • SIRET 400 869 977 00014

LACTALIS ingredients

Les Placis, 5
35230 BOURGBARRE FRANCE

MOULINS LAITERIE WALHORN

Chemin de la Laiterie, 14
4711 WALHORN BELGIUM

L-263-I

ANALYSIS CERTIFICATE

DATE : 09/05/2008
PRODUCT : SKIMMED MILK POWDER (0% FAT) LOW HEAT
DESTINATION : CENTRE R & D NESTLE BEAUVAIS
CALL OFF NR : 11700156
QUANTITY : 75 kg
PACKING : BAGS 25 KG

LOT NUMBERS		S1-02-173
PRODUCTION DATE		04/2008
QUANTITY / LOT		75 kg
PHYSICAL AND CHEMICAL ANALYSIS		
- Moisture	: in %	3.6
- Fat	: in %	0.9
- Filtration	: disque ADPI	A
- Titrable acidity	: in ° D	14.9
- Antibiotic	:	ABS.
BACTERIOLOGICAL ANALYSIS		
- Total plate count	: /g	2000
- Yeast & Moulds	: /g	< 50
- Bacillus cereus	: /g	< 100
- Coliform bacteria	: /0.1g	NEG.
- Escherichia Coli	: /0.1g	NEG.
- Clostridium perfringens	: /g	< 1
- Listeria	: /25g	NEG.
- Salmonellae	: /375g	NEG.
- Stap. aureus	: /g	NEG.
CONTROLLED		*W. HEYEN (QA)*

NESTLE PRODUCT TECHNOLOGIE CENTRE BEAUVAIS
LAIT ECREME LOW HEAT
No lot 017814 (Article: 006181)
Location MP J12
Péremption 10 OCT 2009
Livré le 15 MAI 2008

Warning : Marchandise sold are in conformity with the commited specifications of which present certificate of analysis is in compliance with.
The fragility of the product against some external elements (temperature - humidity - odeurs etc.) compels the user, on receipt of the marchandise, to thoroughly comply with the storage conditions such as they are stipulated in our specification sheets.

FICHE TECHNIQUE

PROMILK 852 B

DEFINITION

Isolat de Protéines de lait .

APPLICATIONS

PROMILK 852 B est une protéine de lait concentré naturellement en micelles de caséines natives pour enrichir et standardiser la fraction protéique des laits de fromagerie.

CONDITIONNEMENT

20 kg net : sacs kraft multiplis, enveloppe polyéthylène intérieure

STOCKAGE

A utiliser de préférence dans les 12 mois à compter de la date de fabrication.

A conserver dans un local frais et sec, à une température inférieure à 25°C avec une humidité relative inférieure à 70%.

NOMENCLATURE DOUANIERE DU PRODUIT (N.D.P.)

Code douane 35 04 00 0080 90 N (Union Européenne) – Autre : nous consulter
(Au 01/03/2005 - sous réserve de modification)

COMPOSITION TYPE

Caractéristiques physiques

	composition type	normes garanties cc 3000
Acidité (ADMI)	0,15 %	
Propreté (ADMI)	A	B
Couleur	blanc crème	
Goût et odeur	francs, légèrement lactés	
Aspect	poudre fine homogène	

Caractéristiques chimiques

Humidité	5 %	6 % maximum
Matière grasse	1,5 %	2 % maximum
Matières azotées/matières sèches	85,5 %	85 % minimum
Matières minérales	8,5 %	9 % maximum
Lactose	4 %	
Matières azotées (sur poudre)	81 %	
Micelles de caséines/Matières azotées	92 %	
Ca	2,6 %	
P	1,5 %	
K	0,3 %	
Na	0,1 %	
Mg	0,1 %	

Caractéristiques microbiologiques

Germes totaux	10.000/g	50.000/g maximum
Entérobactéries	absence/g	absence/0,1g
E.Coli	absence/10 g	absence/g
Clostridium perfringens	absence/g	absence/g
Staphylococcus aureus	absence/g	absence/0,1g
Salmonelles	absence/50 g	absence/50 g
Levures - Moisissures	< 10/g	30/g maximum

En l'absence de spécifications particulières, cette fiche technique tient lieu de cahier des charges.

Siège Social : 51 - 53 Avenue F Lobbedez – B.P. 946 – 62033 ARRAS Cedex – France
Tél. : 33(0) 3.21.23.80.00 – Fax : 33(0) 3.21.23.80.01 – Site Web : www.ingredia.com

03/05

REMS : 0798

BBA

LAIT ECREME EN POUDRE SPRAY

TYPE NIRO

MEDIUM / HIGH HEAT

FICHE DE SPECIFICATIONS N° 8 B10

FABRICANT :

Usine de PONTIVY	**56300 PONTIVY**	**(Medium/High Heat)**
Usine de WALHORN	**Belgique**	**(Medium Heat)**
Usine de MAYENNE	**53101 MAYENNE**	**(Medium Heat)**
Usine de CHATEAUBOURG	**35220 CHATEAUBOURG**	**(Medium Heat)**
Usine de CANELIA	**08 150 ROUVROY-SUR-AUDRY**	**(Medium/ High Heat)**

1 - CARACTERISTIQUES ORGANOLEPTIQUES

- Aspect	: poudre fluide	- Goût	: lacté
- Couleur	: blanc crème	- Odeur	: neutre

2 - CARACTERISTIQUES CHIMIQUES ET PHYSIQUES

		MÉTHODES
Humidité, maximum	: 4 %	IDF 26A/ 1993
Matières grasses, maximum	: 1,5 %	IDF 9C/ 1987
Protéines (N x 6.38)	: 34 % ± 1	IDF 20B/ 1993
WPN, maximum	: 5.99 mg/g	NIRO A 21 a DOC 4ème Ed. 1978
Acidité titrable maximum	: 0.17 %	IDF 86/ 1981
Insoluble ADPI, maximum (Solubilité volumétrique 99 % minimum)	: 1 ml	ADPI
Matières minérales, maximum	: 8.5 %	NFV/ 04208
Lactose, maximum	: 54 %	IDF 79B/ 1991
Epreuve de la phosphatase	: Négative	IDF 82A/ 1987
Epreuve de filtration (ADPI)	: Disque A	ADPI
Acide lactique + lactates, maximum	: 200 mg % d'ESD	IDF 69B/ 1987

BBA

FICHE DE SPECIFICATIONS N° 8 B 10 (SUITE)

3 - CARACTERISTIQUES BACTERIOLOGIQUES

		MÉTHODES
Flore totale revivifiable maximum	: 10.000 / g	IDF 100B/ 1991
Levures, maximum	: 10 / g	IDF 94B/ 1990
Moisissures, maximum	: 10 / g	IDF 94B/ 1990
Bactéries coliformes	: absence dans 0.1 g	IDF 73A/ 1985
Clostridiums perfringens	: absence dans 1 g	DOC MICR II 2ème groupe B
Salmonelles	: absence dans 25 g	IDF 93A/ 1985
Staphylococcus Aureus	: absence dans 1 g	IDF 60B/ 1990
Escherichia Coli	: absence dans 0.1 g	IDF 73A/ 1985 et test de Mackenzie

VALEUR ENERGETIQUE : par 100 g : 1 510 KJ/360 KCal.

4 - CONDITIONNEMENT / LIVRAISON

Sacs grande contenance de 25 Kg, multiplis, kraft, doublés polyéthylène.
Livraison sur palettes EURO-ECHANGE 80 x 120 cm, houssées.

5 - STOCKAGE ET DUREE DE CONSERVATION

18 mois dans un local propre, sec et tempéré (25° C maximum) ; éloigné de toutes sources de goûts et odeurs parasites.

6 - POSITION DOUANIERE : NC : 04.02.10.19

7 - IMPORTANT : AVERTISSEMENT

Notre responsabilité contractuelle consiste à fournir une marchandise conforme aux spécifications ci-dessus ou, sur demande, à des spécifications complémentaires. En cas de manquement à ces spécifications, reconnu par nous et notifié dans les délais d'usage, notre garantie se limitera au seul remplacement de la marchandise défectueuse. Notre responsabilité ne saurait être engagée en cas d'utilisation erronée de notre produit. L'acheteur doit se conformer à la réglementation en vigueur dans le pays d'utilisation.

19 SEPTEMBRE 1997

Annule et remplace fiche du 20 FEVRIER 1997

Annex 3: exemplary process sheet of conventional emulsion freezing

Date: 15/04/08	TRIAL REPORT				berlin	
Operator: AP						
PASTEURISATION / HOMOGENIZATION						
Parameters	**3277-31**	**3277-30**				
Contre pression [bar]	11	11				
Cooling / Temp.Refroid. [°C]	3,9	3,9				
Pasteurisation Temp. [°C]	86,1	85,9				
Preheating / Temp.Préchauff. [°C]	71,9	71,9				
Homogenisation P_1 [bar]	40	40				
Homogenisation P_{TOTAL} [bar]	150	150				
Total solids [%] - MS (theoretic)	32,49	32,49				
Fat [%] - MG (theoretic)	6,38	6,38				
Total solids [%] - MS	32,19	32,35				
Fat [%] - MG	6,04	6,24				
Total solids [%] - MS (difference)	-0,3	-0,14	0	0	0	0
Fat [%] - MG (difference)	-0,34	-0,14	0	0	0	0
Observations:	treated milk	no treated milk				
	en poches					
ordre de glacage	2	1				
[illegible]						
Date: 16/04/08	Operator: DP					
Consignes Essai						
Temp. Consigne CG [°C]	-5°C (FPD : -2,23°C)					
OR Consigne [%]	100%					
Densité	1,10	1,10				
Paramètres d'affichage						
Débit affiréel [l/h]	80					
OR affiréel [%]	98 / 98	98 / 96				
Viscosité affiréel [ ]	50 à 55	35 à 42				
P cylinder affiréel [bar]	3,0 / 3,03	3,0 / 3,02				
Temp. Évapo affiréel [°C]	-21,8 / -19,0	-20,3 /- 18,0				
Temp. Crème affiréel [°C]	-5,0 / -5,1	-5,0 / -5,2				
Moteur Principal	88					
Taux Pompe	1,06 / 1,34	1,06 / 1,22				
Mesures début d'essai						
Temp. réelle [°C]	-4,7	-4,7				
OR réel [%]	100	100				
Mesures fin d'essai						
Temp. réelle [°C]	-4,7	-4,6				
OR réel [%]	99	102				
Poids Quenelles						
1	78,5	54,35				
2	78,5	55,7				
3	78,2	55,7				
4	74,4	54,6				
5	77,9	56,14				
	77,2					
Moy	77,617	55,298	#DIV/0!	#DIV/0!	#DIV/0!	#DIV/0
Stdev	1,747	0,778	#DIV/0!	#DIV/0!	#DIV/0!	#DIV/0
Conf	1,532	0,682	#DIV/0!	#DIV/0!	#DIV/0!	#DIV/0
Observations:	lisse	lisse				
	un peu mousseux	un peu mousseux				
aspect CG	qq bulles ext	qq bulles ext				
	quenelles lisses	quenelles lisses				
	sucré	plus crémeux				
	vanilline	plus présent				
	froid	moins froid				

Curriculum vitae

Marcus Volkert, Dipl.-Ing
Department of Food Biotechnology
and Food Process Engineering
Koenigin - Luise - Str. 22
14195 Berlin
Phone: +49 30 314 71248
email: marcus.volkert@gmx.net

BIOGRAPHY:

07/05-04/09	Research associate (PhD student), Berlin University of Technology; Department of Food Biotechnology and Food Process Engineering in cooperation with the Néstle PTC, Beauvais, France.
08/04-04/05	Research associate, Fonterra, Palmerston North, New Zealand, in cooperation with Danisco Deutschland GmbH, Niebuell, Germany
06/2004	Dipl.-Ing. (Master) in Food Technology, Technische Universität Berlin, Germany Master thesis title: "Evaluation of the feasibility of spray-processes as preservation methods for probiotic bacteria, using *Lactobacillus rhamnosus* GG as a model strain"
10/03-04/04	Research Fellow, Danisco Deutschland GmbH, Niebuell, Germany, in cooperation with the Berlin University of Technology, Berlin, Germany.
1996-2004	Studies of Food Technology, Berlin University of Technology, Berlin, Germany

Research activities:

HIGH PRESSURE – LOW TEMPERATURE (HPLT) PROCESSING
• complex emulsions and foam structures
• HPLT induced protein denaturation
• impact of HPLT treatment on single ingredients: air, fat, protein, polysaccharides
• Freezing behaviour of complex food systems under pressure and phase transition in the ICE III / ICE V region.

PRESERVATION OF PROBIOTIC BACTERIA
• improvement of viability and stability of probiotic bacteria
• identification of process related protection/inactivation mechanisms occurring during fermentation, preservation (i.e. spray-drying, spray-freezing) and storage.
• screening different preservation methods in order to evaluate their use as preservation methods for probiotic bacteria

Peer-reviewed publications:

Ananta, E., Volkert, M. and Knorr, D. (2004). "Cellular injuries and storage stability of spray dried probiotic bacterium Lactobacillus rhamnosus GG." International Dairy Journal 15: 399-409.

Volkert, M., E. Ananta, C. M. Luscher and D. Knorr (2008). "Effect of air freezing, spray freezing, and pressure shift freezing on membrane integrity and viability of Lactobacillus rhamnosus GG." Journal of Food Engineering 87: 532-540.

Knorr D., Balasa A., Boll D., Jaeger H., Mathys A., Oba E., Richter J. & Volkert M. (sumitted). Alternative processing methods for functional foods. In: H. R. Moskowitz, S. Saguy & T. Straus. *An integrated approach to new food product development*. Taylor & Francis, London.

Knorr D., Jaeger H., Janositz A., Mathys A. & Volkert M. (submitted). Process induced generation of tailor made foods. Trends in Food Science and Technology.

Volkert M., Schössler K., Schulz A. & Knorr D. (accepted). Preservation Strategies for Probiotic Bacteris: Stress Responses, Preservation Processes, and Protective Media. In: D. Heldman, A. Bridges, D. Hoover and M. Wheeler. *Encyclopedia of Biotechnology in Agriculture and Food (EBAF)*. Taylor & Francis, London.

Other publications:

Ananta, E., Bauer, B., Volkert, M. und Knorr, D. (2005). Sprühtrocknung von probiotischen Bakterien Deutsche Molkerei Zeitung – dmz 2 52-55

Puaud, Max; Wille, Hans-Juergen Erich; Knorr, Dietrich; Volkert, Marcus
HIGH PRESSURE FREEZING OF FROZEN DESSERTS (WIPO Patent Application WO/2007/128826). Patent record available from the World Intellectual Property Organization (WIPO) and from the European Patent Office.

Eidesstattliche Erklärung

Ich erkläre an Eides statt, dass die vorliegende Dissertation in allen Teilen von mir selbstständig angefertigt wurde und die benutzten Hilfsmittel vollständig angegeben sind.

Veröffentlichungen von irgendwelchen Teilen der vorliegenden Dissertation sind von mir wie folgt vorgenommen worden.

Weiter erkläre ich, dass ich nicht schon anderweitig die Promotionsabsicht angemeldet oder ein Promotionseröffnungsverfahren beantragt habe.

Berlin, den 27.03.2009

Marcus Volkert